

# **Development of an engineered tissue designed for pelvic floor repair**



**Thesis submitted to the University of Sheffield for  
the degree of Doctor of Philosophy**

**Department of Materials Science and Engineering**

**Sabiniano Román Regueros**

**August 2014**





## Acknowledgments

I would firstly like to thank both my supervisors Prof Sheila MacNeil and Prof Christopher Chapple because they believed in me since they interviewed me for the position of this PhD. They gave me the opportunity to carry out this project and they made me feel since the beginning I was able to do a good job. Their support encouraged me to give my best and at the same time they knew when to give good advice.

I would like to thank everybody from University of Sheffield who contributed to improve my work by technical help, training, advice, or just cheering me up when I needed it.

I would like to show my gratitude particularly to Dr Anthony Bullock and Altaf Mangera who introduced me to the tissue engineering field and the complicated environment of the “pelvic floor”; and, together with them, to all the members of the “pelvic floor mafia” including Nadir Osman, Julio Bissoli and Giulia Gigliobianco.

As a big part of the work of this thesis, I would like to thank Dr Gwendolen Reilly and Dr Robin Delaine-Smith for teaching and advising about the use of the BOSE tensiometer.

I would like to thank the help received from Karen Heard for administrative support, Claire Johnson and Mark Wagner for technical support, Dr Pallavi Deshpande for immunostaining procedures, Dr Ilida Ortega for scanning electron microscope preparations and Dr Nicola Green for technical assistance regarding the fluorescence microscopy, among many others.

I would like to show special gratitude for everybody from University of Leuven who helped me with the animal work of this thesis as a collaborative work between the two Universities. I did a stay of only 2 months in Leuven but it was enough to make me feel at home and sad when leaving. It was amazing how friendly everybody was and the amount of work they did for this project since working with animals was something new for me. In particular, I would like to thank Prof Jan Deprest, the head of the department, Silvia Zia, Stefano Manodoro and Dr Maarten Albersen.

I would also like to thank my main PhD financial sponsor, a European Marie Curie Framework Programme 7, under the project title Training for Urology Scientist to develop new Treatments (TRUST). The TRUST project allowed me to conduct this research, but also gave me the opportunity to visit the people in Leuven and present my work for scientific networking in many conferences around Europe. However, the best thing about this programme was the interaction with all the other TRUST fellows. We all attended several meetings only for the TRUST fellows involving recognized researchers of this field to ensure the gain of the aptitudes needed to become a professional. In addition, a TRUST family was created and this led to a continuous relation between the fellows for specific advice, support and, why not say it, a lot of fun. Therefore, a big thank for all of them including Jen Tidman and Michelle Battye, Chris Chapple's secretary and EU manager respectively.

Finally, I would really like to thank my family and friends. It was very difficult for all of them to see me go to another country; however, they were understanding and incredibly supportive from miles away. Without their support I would have not been able to start a new life away from them.

From my point of view, this thesis is an achievement that belongs to all of them; and particularly to my parents because what I am and what I have got today is thanks to them, as well as, to Emma because she always believed in me and also left her country and family to stay with me.

# Contents

<b>Acknowledgements</b> .....	2
<b>Contents</b> .....	4
<b>Publications</b> .....	9
<b>Presentations</b> .....	10
<b>Abbreviations</b> .....	13
<b>List of figures</b> .....	17
<b>Abstract</b> .....	23
<b>Chapter 1 – Introduction</b> .....	25
<b>1.1 Stress urinary incontinence (SUI)</b> .....	26
1.1.1 Epidemiology.....	26
1.1.2 Aetiology.....	27
1.1.3 Risk factors.....	31
1.1.4 Treatments.....	32
<i>1.1.4.1 Non surgical treatments</i> .....	32
<i>1.1.4.2 Surgical treatments</i> .....	35
<i>1.1.4.3 Surgical complications</i> .....	38
<i>1.1.4.4 Surgical outcomes</i> .....	40
<b>1.2 Pelvic organ prolapse (POP)</b> .....	40
1.2.1 Epidemiology.....	40
1.2.2 Aetiology.....	42
1.2.3 Risk factors.....	44
1.2.4 Treatments.....	45
<i>1.2.4.1 Non surgical treatments</i> .....	45
<i>1.2.4.2 Surgical treatments</i> .....	46
<i>1.2.4.3 Surgical complications</i> .....	49
<i>1.2.4.4 Surgical outcomes</i> .....	50
<b>1.3 Comparison of SUI and POP</b> .....	51
<b>1.4 Histology of the supportive tissues of the pelvic floor</b> .....	53
1.4.1 Connective/fascial tissue of the pelvic floor.....	54
<i>1.4.1.1 Collagen</i> .....	56

1.4.1.2 Elastin.....	58
1.4.1.3 Fibroblasts.....	59
1.4.1.4 Estrogens.....	60
1.4.2 Muscles of the pelvic floor.....	61
<b>1.5 Prostheses used for the surgical treatment of SUI and POP.....</b>	<b>66</b>
1.5.1 Non-degradable synthetic prostheses.....	67
1.5.2 Degradable synthetic prostheses.....	69
1.5.3 Autologous prostheses.....	70
1.5.4 Allograft prostheses.....	71
1.5.5 Xenograft prostheses.....	73
1.5.6 Tissue engineered prostheses.....	74
<b>1.6 Aims.....</b>	<b>80</b>
 <b>Chapter 2 - Material and Methods.....</b>	 <b>82</b>
<b>2.1 Electrospinning of Poly-(L)-lactic acid (PLA) scaffolds.....</b>	<b>83</b>
<b>2.2 Isolation and culture of human oral fibroblasts (OFs) and rat and human adipose-derived stem cells (ADSCs).....</b>	<b>84</b>
<b>2.3 ADSCs characterization.....</b>	<b>86</b>
2.3.1 Flow cytometry.....	86
2.3.2 Adipogenic and osteogenic differentiation assays.....	88
2.3.3 Immunostaining for specific antigens.....	89
<b>2.4 Culture of OFs and/or ADSCs on PLA scaffolds.....</b>	<b>90</b>
2.4.1 PLA scaffold preparation.....	90
2.4.2 Cell seeding.....	90
2.4.3 Metabolic activity assessed by AlamarBlue® staining.....	90
2.4.4 4',6-Diamidino-2-phenylindole (DAPI) staining.....	91
2.4.5 Total collagen production assessed by Sirius red staining.....	91
2.4.6 Mechanical testing using BOSE electroforce tensiometer.....	91
2.4.7 Contraction.....	93
2.4.8 Immunostaining of extracellular matrix components.....	93
2.4.9 Histology and Haematoxylin and Eosin staining (H&E).....	94
2.4.10 Scanning electron microscope (SEM).....	95
<b>2.5. Rapid extraction of ADSCs.....</b>	<b>95</b>

2.5.1 GentleMACS® Dissociator.....	95
2.5.2 MACS® Separation.....	96
<b>2.6 Animal studies.....</b>	<b>96</b>
2.6.1 Implantation.....	97
2.6.2 Sacrifice and sample fixation.....	99
2.6.3 Histology.....	100
2.6.2.1 <i>Fresh frozen section</i> .....	100
2.6.2.2 <i>H&amp;E</i> .....	100
2.6.2.3 <i>Immunohistochemistry and Sirius red staining</i> .....	101
<b>2.7 Statistical analysis.....</b>	<b>104</b>
 <b>Chapter 3 - Production of candidate scaffolds.....</b>	 <b>105</b>
3.1 Introduction.....	106
3.2 Comparison between PLA and thermo-annealed PLA (Th-PLA) scaffolds....	108
3.3 <i>In vitro</i> degradation of Th-PLA scaffolds.....	112
3.4 Discussion.....	113
 <b>Chapter 4 – Exploring cell candidates for a tissue engineered repair material (TERM).....</b>	 <b>116</b>
4.1 Introduction.....	117
4.1.1 Fibroblasts.....	117
4.1.2 Adult stem cells.....	118
4.2 Isolation, culture and characterization of OFs and ADSCs.....	121
4.3 Comparison of OFs and ADSCs cultured on Th-PLA scaffolds.....	128
4.3.1 Cell attachment and proliferation.....	128
4.3.2 Extracellular matrix (ECM) production.....	130
4.3.3 Contraction.....	134
4.3.4 Mechanical properties.....	135
4.4 Discussion.....	136
 <b>Chapter 5 - Optimizing culture conditions for the TERMS.....</b>	 <b>140</b>
5.1 Introduction.....	141
5.1.1 Mechanical stimulation.....	141

5.1.2 Chemical stimulation.....	142
<b>5.2 Mechanical stimulation of TERMS.....</b>	<b>144</b>
5.2.1 Restrained and intermittent stress conditions.....	144
5.2.2 Dynamic conditions.....	154
<b>5.3 Chemical stimulation of TERMS.....</b>	<b>156</b>
<b>5.4 Optimal number of cells and period of culture.....</b>	<b>158</b>
5.4.1 ADSCs seeded on Th-PLA scaffolds at different cell concentrations.....	159
5.4.2 Culture of ADSCs on Th-PLA scaffolds for different periods.....	162
<b>5.5 Discussion.....</b>	<b>166</b>
 <b>Chapter 6 - <i>In vivo</i> assessment of TERMS.....</b>	 <b>169</b>
<b>6.1 Introduction.....</b>	<b>170</b>
6.1.1 Animal models to assess materials used to treat SUI and POP.....	172
<b>6.2 Integration into host tissues.....</b>	<b>174</b>
<b>6.3 Acute inflammatory response.....</b>	<b>178</b>
<b>6.4 ECM remodelling.....</b>	<b>180</b>
<b>6.5 Discussion.....</b>	<b>185</b>
 <b>Chapter 7 -Mechanical properties of TERMS.....</b>	 <b>189</b>
<b>7.1 Introduction.....</b>	<b>190</b>
7.1.1 Mechanical properties of the native tissues and the prosthesis used to treat SUI and POP.....	191
7.1.2 Correlation between mechanical properties and outcomes of the prosthesis used to treat SUI and POP.....	191
7.1.3 Mechanical properties for our TERMS.....	193
<b>7.2 Increasing mechanical properties of PLA scaffolds.....</b>	<b>195</b>
7.2.1 Description of the different setups for the electrospinning rig.....	196
7.2.2 Physical and mechanical properties of PLA scaffolds with different fibre configuration.....	200
<b>7.3 Effect of fibre configuration on cell behaviour.....</b>	<b>202</b>
<b>7.4 Suture retention test, wettability and degradation.....</b>	<b>206</b>
<b>7.5 Discussion.....</b>	<b>213</b>

<b>Chapter 8 - Exploring methodologies of extracting and culturing ADSCs</b>	218
<b>8.1 Introduction</b>	219
<b>8.2 Donor variability</b>	220
<b>8.3 One stage “in theatre” approach</b>	224
8.3.1 Rapid ADSCs isolation	224
8.3.2 Seeding the stromal vascular fraction (SVF) on PLA scaffolds	228
<b>8.4 Discussion</b>	229
 <b>Chapter 9 - Conclusions and future directions</b>	233
<b>9.1 Scaffold candidates</b>	236
<b>9.2 Cell candidates</b>	236
<b>9.3 Culture conditions</b>	237
<b>9.4 Host response to TERM</b>	238
<b>9.5 Mechanical properties of the TERM</b>	238
<b>9.6 Potential of ADSCs</b>	239
<b>9.7 Future work</b>	240
 <b>References</b>	244
 <b>Appendix</b>	282



## Publications

Osman NI, Mangera A, **Roman S**, Bullock AJ, MacNeil S, Chapple CR. Mesh social networking: a patient-driven process. BJUI Int. 2012 Jun;109(12): E45-6; author reply E46. doi: 10.1111/j.1464-410X.2012.11235\_3.x.

Osman NI, **Roman S**, Gigliobianco G, Mangera A, Bullock AJ, Chapple CR, MacNeil S. Tissue engineering as a potential alternative or adjunct to surgical reconstruction in treating pelvic organ prolapse: comment on Boennelycke et al. Int. Urogynecol J. 2013 May;24(5):881. doi: 10.1007/s00192-012-2023-5.

Mangera A, Bullock AJ, **Roman S**, Chapple CR, MacNeil S. Comparison of candidate scaffolds for tissue engineering for stress urinary incontinence and pelvic organ prolapse repair. BJU Int 2013 Sep;112(5):674-85. doi: 10.1111/bju.12186.

**Roman S**, Mangera A, Osman NI, Bullock AJ, Chapple CR, MacNeil S. Developing a tissue engineered repair material for treatment of stress urinary incontinence and pelvic organ prolapse-which cell source? Neurourol Urodyn. 2014 Jun;33(5):531-7. doi: 10.1002/nau.22443.

**Roman S**, Albersen M, Manodoro S, Zia S, Osman NI, Bullock AJ, Chapple CR, Deprest J, MacNeil S. Assessment in rats of the acute response to an engineered tissue designed for pelvic floor repair. Biomed Res Int. 2014 (in press).

Osman NI, **Roman S**, Bullock AJ, Chapple CR, MacNeil S. Developing a biomimetic pelvic floor repair material with enhanced mechanical properties. Proc Inst Mech Eng H. 2014 (in press).

Bye FJ, Bullock AJ, Singh R, Sefat F, **Roman S**, MacNeil S. Development of a basement membrane substitute incorporated into an electrospun scaffold for 3D skin tissue engineering. J. Biomater. Tissue Eng. 2014 (in press).

## **Published abstracts**

Abstracts of the 42nd Annual Meeting of the International Continence Society (ICS), 15 – 19 October 2012, Beijing, China. *Neurourol Urodyn.* 2012 Aug;31(6):709-1102. doi: 10.1002/nau.22287.

DEVELOPING AN AUTOLOGOUS ENGINEERED CONNECTIVE TISSUE USING A BIODEGRADABLE SCAFFOLD FOR THE TREATMENT OF STRESS URINARY INCONTINENCE AND PELVIC ORGAN PROLAPSE. Roman Regueros S, Mangera A, Osman NI, Bullock AJ, Chapple CR, MacNeil S.

28th Annual Congress of the European Association of Urology Abstracts. *European Urology Supplements.* 2013 Mar;12(1):e1-e1108, eV1-eV80.

IN VIVO ASSESSMENT OF THE ACUTE HOST RESPONSE AGAINST A NOVEL TISSUE ENGINEERED TO TREAT STRESS URINARY INCONTINENCE AND PELVIC ORGAN PROLAPSE. Roman Regueros S, Albersen M, Manodoro S, Zia S, Osman NI, Bullock AJ, Chapple CR, Deprest J, MacNeil S.

Abstracts of the 43rd Annual Meeting of the International Continence Society (ICS), 26 – 30 August 2013, Barcelona, Spain. *Neurourol Urodyn.* 2013 Aug;32(6):507-932. doi: 10.1002/nau.22472.

ACUTE HOST RESPONSE AGAINST A NOVEL TISSUE ENGINEERED REPAIR MATERIAL FOR THE SURGICAL MANAGMENT OF STRESS URINARY INCONTINENCE AND PELVIC ORGAN PROLAPSE. Roman Regueros S, Albersen M, Manodoro S, Zia S, Osman NI, Bullock AJ, Chapple CR, Deprest J, MacNeil S.

## **Presentations**

**Biomaterials & Tissue Engineering Group.** 13th Annual White Rose Work in Progress Meeting, Sheffield 20th December 2011 (oral presentation).

Developing an autologous engineered connective tissue using a biodegradable scaffold for the treatment of stress urinary incontinence and pelvic organ

prolapse. S. ROMÁN, A. MANGERA, A.J. BULLOCK, F. BYE, C.R. CHAPPLE and S. MACNEIL.

**UKCS** (UK Continence Society), Liverpool 18-20 April 2012 (poster presentation).

Developing an autologous engineered connective tissue using a biodegradable scaffold for the treatment of stress urinary incontinence and pelvic organ prolapse. S. ROMÁN, A. MANGERA, A.J. BULLOCK, N.I. OSMAN, C.R. CHAPPLE and S. MACNEIL.

**YUM** (1<sup>st</sup> Young Urology Meeting), Bristol 7-8 May 2012 (poster presentation).

Developing an autologous engineered connective tissue using a biodegradable scaffold for the treatment of stress urinary incontinence and pelvic organ prolapse. S. ROMÁN, A. MANGERA, A.J. BULLOCK, C.R. CHAPPLE and S. MACNEIL.

**TCES** (Tissue and Cell Engineering Society), Liverpool 4-6 July 2012 (poster presentation).

Developing an autologous engineered connective tissue using a biodegradable scaffold for the treatment of stress urinary incontinence and pelvic organ prolapse. S ROMAN, N OSMAN, A MANGERA, AJ BULLOCK, CR CHAPPLE, S MACNEIL.

**ICS** (International Continence Society), Beijing 15-19 October 2012 (podium poster presentation).

Developing an autologous engineered connective tissue using a biodegradable scaffold for the treatment of stress urinary incontinence and pelvic organ prolapse. ROMAN REGUEROS S, MANGERA A, OSMAN NI, BULLOCK AJ, CAPPLE CR, MACNEIL S.

**EAU** (European Association of Urologists), Milan 15-19 March 2013 (podium poster presentation).

*In vivo* assessment of the acute host response against a novel tissue engineered to treat stress urinary incontinence and pelvic organ prolapse. ROMAN

REGUEROS S, ALBERSEN M, MANODORO S, ZIA S, OSMAN NI, BULLOCK AJ, CHAPPLE CR, DEPREST J, MACNEIL S.

**YUM** (2<sup>nd</sup> Young Urology Meeting), Bristol 4-5 June 2013 (oral presentation).  
Developing an autologous engineered connective tissue using a biodegradable scaffold for the treatment of stress urinary incontinence and pelvic organ prolapse. S ROMAN, N OSMAN, A MANGERA, AJ BULLOCK, CR CHAPPLE, S MACNEIL.

**UK BOSE Users Meeting**, Loughborough 6<sup>th</sup> June 2013 (oral presentation).  
Looking for the rational biomechanical properties of a tissue engineering repair material for the treatment of stress urinary incontinence and pelvic organ prolapse. S ROMAN, N OSMAN, A MANGERA, J BISOLI. G GIGLIOBIANCO, AJ BULLOCK, CR CHAPPLE, S MACNEIL.

**TERMIS** (Tissue Engineering and regenerative medicine international society), Istanbul 17-20 June 2013 (podium poster presentation).  
Developing an Autologous Tissue Engineered Repair Material for the Treatment of Stress Urinary Incontinence and Pelvic Organ Prolapse. S ROMAN, NI OSMAN, A MANGERA, AJ BULLOCK, CR CHAPPLE, S MACNEIL.

**ICS** (International Continence Society), Barcelona 26-30 August 2013 (podium poster presentation). Acute host response against a novel tissue engineered repair material for the surgical management of stress urinary incontinence and pelvic organ prolapse. ROMAN REGUEROS S, ALBERSEN M, MANODORO S, ZIA S, OSMAN NI, BULLOCK AJ, CHAPPLE CR, DEPREST J, MACNEIL S.

## Abbreviations

%	percentage
$\alpha$	alpha
$\beta$	beta
$\lambda_{\text{ex}}$	excitation wavelength
$\lambda_{\text{em}}$	emission wavelength
$\mu\text{g}$	microgram
$\mu\text{l}$	microlitre
$\mu\text{M}$	micromolar
$\mu\text{m}$	micrometer
2D	two dimensional
3D	three dimensional
AB	avidin-biotinylated peroxidase
Ab	antibody
ADSCs	adipose-derived stem cells
ASC	adult stem cell
ATFP	arcus tendineous fascia pelvis
BMDSC	bone marrow-derived stem cell
BMI	body mass index
BSA	bovine serum albumin
CD	cluster of differentiation
cm	centimetre
$\text{cm}^2$	square centimetre
$\text{CO}_2$	carbon dioxide
Col	collagen
$^{\circ}\text{C}$	degree celsius
D	dextro
DAPI	4',6-diamidino-2-phenylindole
DCM	dichloromethane
DMEM	Dulbecco's Modified Eagle's Medium
DMSO	dimethyl sulphoxide
E2	17 $\beta$ -estradiol

ECM	extracellular matrix
EDTA	ethylenediaminetetraacetic acid
ER	estrogen receptor
FACS	fluorescent-activated cell sorting
FBS	fetal bovine serum
FDA	Food and Drug Administration
FITC	fluorescein isothiocyanate
FGF	fibroblast growth factor
FSH	follicle stimulation hormone
FSR	fluid shear rig
g	gram
GFP	green fluorescent protein
GMP	good manufacturing practice
h	hour
H <sub>2</sub> O <sub>2</sub>	hydrogen peroxide
H&E	haematoxylin and eosin
HM	hand minced
HOXA11	homeobox A11
HRP	horseradish peroxidase
HS	high speed
Hz	hertz
I	intermittent
ICS	International Continence Society
ICIQ	International Consultation on Incontinence Questionnaire
IMS	industrial methylated spirit
KCl	potassium chloride
kV	kilovolts
L	levo
LLP	leak point pressure
LOX	lysyl oxidase
LTBP-1	latent TGF- $\beta$ 1-binding protein-1
M	molar
MDSC	muscle-derived stem cell
mg	milligram

MHRA	Medicines and Healthcare products Regulatory Agency
min	minute
mL	millilitre
mM	millimolar
mm	millimetre
MMP	matrix metalloproteinases
MPa	megapascals
MRI	magnetic resonance imaging
MSC	mesenchymal stem cell
mtDNA	mitochondrial genetic material
n	number
NaOH	sodium hydroxide
nm	nanometre
nM	nanomolar
N	newton
N/mm	newton/millimetre
N/mm <sup>2</sup>	newton/square millimetre
OCT	optimal cutting temperature compound
OF	oral fibroblast
OH	alcohol
OM	osteogenic medium
P	passage
P4	progesterone
PBS	phosphate-buffered saline
PE	phycoerythrin
PECAM-1	platelet endothelial cell adhesion molecule-1
PGA	poly-glycolic acid
pH	potential of hydrogen
PLA	poly-(L)-lactic acid
PLGA	poly-(lactic-co-glycolic acid)
PNT	pudendal nerve transaction
POP	pelvic organ prolapse
POPQ	POP quantification system
PPL	polypropylene

PSNT	proximal sciatic nerve transaction
R	restrained
RCT	randomized clinical trial
ROSE	Research On Stress Incontinence Study
rpm	revolutions per minute
sec	second
SEM	scanning electron microscopy
SIS	small intestinal submucosa
SUI	stress urinary incontinence
SVF	stromal vascular fraction
TERM	tissue engineered repair material
TGF- $\beta$ 1	transforming growth factor beta-1
Th-PLA	thermoannealed-PLA
TIMP	tissue derived inhibitors of metalloproteinases
TNF $\alpha$	tumor necrosis factor $\alpha$
TOT	transobturator tape
TVT	tension free vaginal tape
U	unrestrained
UI	urinary incontinence
UUI	urge urinary incontinence
UTS	ultimate tensile strength
V	volts
VIT C	vitamin C
w/v	weight/volume
YM	Young's modulus



## List of figures

<b>Figure 1.1</b> A view of the hammock theory by Ulmsten.....	28
<b>Figure 1.2</b> Inferior view of the pelvic floor of an elderly female cadaver.....	29
<b>Figure 1.3</b> The role of the endopelvic fascia, arcus tendinius and levator ani in support of the urethra and bladder.....	30
<b>Figure 1.4</b> Anterior vaginal repair.....	35
<b>Figure 1.5</b> Colposuspension.....	36
<b>Figure 1.6</b> Needle suspension.....	36
<b>Figure 1.7</b> Different types of sling/tapes.....	37
<b>Figure 1.8</b> Illustrations of the prolapse of the different compartments.....	41
<b>Figure 1.9</b> DeLancey's levels of support.....	42
<b>Figure 1.10</b> Sacrocolpopexy.....	48
<b>Figure 1.11</b> Histological appearance of connective tissue.....	55
<b>Figure 2.1</b> Electrospinning technique.....	83
<b>Figure 2.2</b> BOSE Electroforce tensiometer.....	92
<b>Figure 2.3</b> Example of serial photographs for scaffold contraction.....	92
<b>Figure 2.4</b> Animal implantation.....	97
<b>Figure 2.5</b> Animal sacrifice.....	99
<b>Figure 3.2.1</b> SEM images of PLA scaffolds. Pores and fibre diameter.....	109
<b>Figure 3.2.2</b> SEM images of Th-PLA scaffolds. Pores and fibre diameter.....	109
<b>Figure 3.2.3</b> Mechanical properties of PLA and Th-PLA scaffolds.....	110
<b>Figure 3.3.1</b> Mechanical properties of Th-PLA scaffolds at day 0, day 14, day 30 and day 90 after being in DMEM medium.....	112
<b>Figure 4.2.1</b> Morphology of OFs and ADSCs on a tissue culture plastic flask.....	121
<b>Figure 4.2.2</b> Characterization of human ADSCs by flow cytometry.....	123
<b>Figure 4.2.3</b> Characterization of rat ADSCs by flow cytometry .....	124
<b>Figure 4.2.4</b> Representative images of immunostaining for anti-human fibroblasts surface protein.....	125
<b>Figure 4.2.5</b> Representative images of immunostaining for anti-human CD29, CD44 and CD73.....	126
<b>Figure 4.2.6</b> Osteogenic differentiation of human ADCSs.....	127
<b>Figure 4.2.7</b> Adipogenic differentiation of human ADCSs.....	127

<b>Figure 4.3.1</b> Colour change seen after incubation with AlamarBlue® staining.....	128
<b>Figure 4.3.2</b> AlamarBlue® staining for OFs, ADSCs and a mixture of both cells on Th-PLA scaffolds over 2 weeks in culture.....	129
<b>Figure 4.3.3</b> Representative images of DAPI staining for Th-PLA samples cultured with OFs, ADSCs and a mixture of both cell types for 2 weeks.....	130
<b>Figure 4.3.4</b> Representative images of frozen sections of ADSCs and OFs cultured for 2 weeks on Th-PLA scaffolds stained for H&E.....	130
<b>Figure 4.3.5</b> Examples of Sirius red staining after 14 days culture of OFs and ADSCs on Th-PLA scaffolds.....	131
<b>Figure 4.3.6</b> Sirius red staining after 14 days of OFs, ADSCs and a mixture of both cells cultured on Th-PLA.....	131
<b>Figure 4.3.7</b> Representative images of immunostaining for collagen I, collagen III and elastin of OFs, ADSCs and a mixture of both cell types cultured on Th-PLA scaffolds.....	132
<b>Figure 4.3.8</b> Assessment of the extent of immunostaining using a blind scoring for OFs, ADSCs and a mixture of both cells cultured on Th-PLA scaffolds.....	133
<b>Figure 4.3.9</b> Appearance by SEM of OFs and ADSCs cultured on Th-PLA scaffolds.....	134
<b>Figure 4.3.10</b> Percentage of contraction of Th-PLA scaffolds cultured with OFs, ADSCs and a mixture of both cells after 14 days.....	134
<b>Figure 4.3.11</b> Mechanical properties of Th-PLA scaffolds cultured with OFs, ADSCs and a mixture of both cells.....	135
<b>Figure 5.2.1</b> Improved version of Scaffoldex™ .....	144
<b>Figure 5.2.2</b> Metabolic activity using AlamarBlue® for OFs, ADSCs and a mixture of both cultured on Th-PLA scaffolds under unrestrained conditions and restrained conditions.....	145
<b>Figure 5.2.3</b> DAPI staining for Th-PLA scaffolds cultured with OFs, ADSCs and a mixture of both cultured under unrestrained conditions and restrained conditions.....	146
<b>Figure 5.2.4</b> Production of total collagen by OFs, ADSCs and a mixture of both cells cultured on Th-PLA scaffolds under unrestrained conditions and restrained conditions.....	147
<b>Figure 5.2.5</b> Mechanical properties of Th-PLA scaffolds cultured with OFs, ADSCs and a mixture of both under unrestrained conditions and restrained conditions.....	148

<b>Figure 5.2.6</b> Representative images for presence and distribution of collagen I, III and elastin (green color) with cell nuclei (blue color) using immunostaining and DAPI respectively, after 14 days culture on Th-PLA scaffolds of ADSCs under unrestrained conditions; OFs under restrained with intermittent stress conditions; and a mixture of OFs and ADSCs under restrained with intermittent stress conditions.....	149
<b>Figure 5.2.7</b> Extent of the immunostaining using a blind scoring for OFs, ADSCs and a mixture of both cells cultured on Th-PLA under unrestrained conditions and restrained conditions.....	150
<b>Figure 5.2.8</b> SEM of OFs cultured under unrestrained condition on Th-PLA scaffolds.....	151
<b>Figure 5.2.9</b> SEM of OFs cultured under intermittent stress conditions on Th-PLA scaffolds.....	152
<b>Figure 5.2.10</b> SEM of ADSCs cultured under unrestrained conditions on Th-PLA scaffolds.....	152
<b>Figure 5.2.11</b> SEM of ADSCs cultured under intermittent stress conditions on Th-PLA scaffolds.....	153
<b>Figure 5.2.12</b> SEM of a mixture of OFs and ADSCs cultured under intermittent stress conditions on Th-PLA scaffolds.....	153
<b>Figure 5.2.13</b> Platform rocker.....	154
<b>Figure 5.2.14</b> Metabolic activity using AlamarBlue® for OFs and ADSCs cultured on 6-well plates under static and dynamic conditions.....	155
<b>Figure 5.2.15</b> Total collagen production using Sirius red staining for OFs and ADSCs cultured on 6-well plates under static and dynamic conditions.....	155
<b>Figure 5.3.1</b> ADSCs on 6-well plates stained with Sirius red after 2 weeks in culture under static or dynamic conditions and with DMEM medium or DMEM medium supplemented with Vitamin C.....	156
<b>Figure 5.3.2</b> ADSCs on Th-PLA scaffolds stained with Sirius red after 2 weeks in culture under unrestrained conditions and with DMEM medium or DMEM medium supplemented with Vitamin C.....	157
<b>Figure 5.3.3</b> Total collagen production using Sirius red staining for ADSCs cultured on Th-PLA over 2 weeks under unrestrained conditions and with DMEM medium or DMEM medium supplemented with Vitamin C.....	158
<b>Figure 5.4.1</b> Metabolic activity of ADSCs seeded at density of $1 \times 10^5$ , $3 \times 10^5$ , $7 \times 10^5$ and $1 \times 10^6$ cultured on Th-PLA scaffolds.....	159

<b>Figure 5.4.2</b> Production of total collagen by ADSCs seeded at density of $1 \times 10^5$ , $3 \times 10^5$ , $7 \times 10^5$ and $1 \times 10^6$ cultured on Th-PLA scaffolds.....	160
<b>Figure 5.4.3</b> DAPI staining for Th-PLA scaffolds cultured with $1 \times 10^5$ , $3 \times 10^5$ , $7 \times 10^5$ and $1 \times 10^6$ .....	160
<b>Figure 5.4.4</b> Mechanical properties of Th-PLA scaffolds cultured without and with cells seeded at densities of $1 \times 10^5$ , $3 \times 10^5$ , $7 \times 10^5$ and $1 \times 10^6$ .....	161
<b>Figure 5.4.5</b> Metabolic activity of ADSCs seeded at density of $7 \times 10^5$ cells on Th-PLA scaffolds cultured over 1, 2 and 3 weeks.....	162
<b>Figure 5.4.6</b> Production of total collagen by ADSCs seeded at density of $7 \times 10^5$ cells on Th-PLA scaffolds cultured over 1, 2 and 3 weeks.....	163
<b>Figure 5.4.7</b> DAPI staining for Th-PLA scaffolds cultured with $7 \times 10^5$ ADSCs for 1, 2 and 3 weeks.....	163
<b>Figure 5.4.8</b> Mechanical properties of Th-PLA scaffolds cultured without and with $7 \times 10^5$ ADSCs for 1, 2 and 3 weeks.....	164
<b>Figure 5.4.9</b> SEM of $7 \times 10^5$ ADSCs seeded on Th-PLA scaffolds.....	165
<b>Figure 6.2.1</b> Confocal microscope images of fresh frozen sections of abdominal wall of rats after 7 days implantation of Th-PLA scaffolds on top, previously cultured with ADSCs labeled with green cell tracker.....	174
<b>Figure 6.2.2</b> H&E stained sections of normal abdominal wall.....	175
<b>Figure 6.2.3</b> H&E stained panoramic image of the abdominal wall, after 3 days implantation of Th-PLA scaffold on top, previously cultured with human ADSCs....	176
<b>Figure 6.2.4</b> H&E stained sections after 3 days implantation.....	177
<b>Figure 6.2.5</b> H&E stained sections after 7 days implantation.....	177
<b>Figure 6.3.1</b> Sections after 3 and 7 days implantation following immunohistochemistry for anti-CD68 antibody.....	178
<b>Figure 6.3.2</b> Sections after 3 and 7 days implantation following immunohistochemistry for anti-PECAM-1 antibody.....	179
<b>Figure 6.3.3</b> Semi-quantitative analyses of the host response against the implanted samples.....	179
<b>Figure 6.4.1</b> Sections after 3 days implantation following immunohistochemistry for anti-collagen I antibody.....	180
<b>Figure 6.4.2</b> Sections after 7 days implantation following immunohistochemistry for anti-collagen I antibody.....	181

<b>Figure 6.4.3</b> Sections after 3 days implantation following immunohistochemistry for anti-collagen III antibody.....	181
<b>Figure 6.4.4</b> Sections after 7 days implantation following immunohistochemistry for anti-collagen III antibody.....	182
<b>Figure 6.4.5</b> Sections after 3 days implantation following Sirius red staining.....	183
<b>Figure 6.4.6</b> Sections after 7 days implantation following Sirius red staining.....	183
<b>Figure 6.4.7</b> Sections of abdominal wall of female Sprague-Dawley rats after 7 days implantation followed by immunohistochemistry control procedure.....	184
<b>Figure 7.1.1</b> The ideal <i>in vivo</i> response to a material.....	194
<b>Figure 7.1.2</b> Anticipated <i>in vivo</i> response to a material.....	194
<b>Figure 7.2.1</b> Illustration of the electrospinning rig used to produce the mainly aligned PLA scaffolds.....	196
<b>Figure 7.2.2</b> Illustration of the electrospinning rig used to produce the hybrid PLA scaffold (150 $\mu\text{m}$ ).....	197
<b>Figure 7.2.3</b> Image of the electrospinning rig using the multichannel needle.....	198
<b>Figure 7.2.4</b> Illustration of the electrospinning rig used to produce the hybrid PLA scaffold (280 $\mu\text{m}$ ).....	199
<b>Figure 7.2.5</b> Thickness and bulk density of the 6 different PLA scaffolds.....	200
<b>Figure 7.2.6</b> Mechanical properties of 6 different PLA fibre configuration scaffolds.....	201
<b>Figure 7.2.7</b> SEM images of PLA scaffolds with different fibre configurations.....	202
<b>Figure 7.3.1</b> AlamarBlue <sup>®</sup> staining for ADSCs on Th-PLA random, hybrid PLA (280 $\mu\text{m}$ ) and PLA mainly aligned scaffolds.....	203
<b>Figure 7.3.2</b> Sirius red staining after 14 days of ADSCs cultured on Th-PLA random, hybrid PLA (280 $\mu\text{m}$ ) and PLA mainly aligned scaffolds.....	204
<b>Figure 7.3.3</b> Representative images of immunostaining for f-actin, collagen I and elastin of ADSCs cultured on PLA mainly aligned scaffolds.....	204
<b>Figure 7.3.4</b> Mechanical properties of Th-PLA random, hybrid PLA (280 $\mu\text{m}$ ) and PLA mainly aligned scaffolds cultured with ADSCs.....	205
<b>Figure 7.3.5</b> Examples of stress-strain plots of Th-PLA random, hybrid PLA (280 $\mu\text{m}$ ) and PLA mainly aligned scaffolds cultured with ADSCs.....	206
<b>Figure 7.4.1</b> Suture retention test of 5 different PLA fibre configuration scaffolds...	207
<b>Figure 7.4.2</b> AlamarBlue <sup>®</sup> and Sirius red staining for ADSCs cultured on hybrid PLA (280 $\mu\text{m}$ ) scaffolds treated and non-treated with 70% alcohol.....	208

<b>Figure 7.4.3</b> Examples of stress-strain plots of hybrid PLA (280 $\mu\text{m}$ ) scaffolds cultured with and without ADSCs and previously treated or non-treated with alcohol.....	209
<b>Figure 7.4.4</b> Mechanical properties of hybrid PLA (280 $\mu\text{m}$ ) scaffolds cultured with ADSCs and previously treated or non-treated with alcohol.....	210
<b>Figure 7.4.5</b> Mechanical properties of Th-PLA random and hybrid PLA (150 $\mu\text{m}$ ) scaffolds, previously treated or non-treated with alcohol, at day 0, 14, 30 and 90 cultured in DMEM medium.....	211
<b>Figure 8.2.1</b> ADSCs isolated from 3 donors cultured for 3 weeks with adipogenic or osteogenic medium.....	221
<b>Figure 8.2.2</b> AlamarBlue <sup>®</sup> staining for ADSCs isolated from 3 donors on PLA mainly aligned scaffolds.....	221
<b>Figure 8.2.3</b> Representative images of DAPI staining for PLA mainly aligned samples cultured with ADSCs from 3 different donors.....	222
<b>Figure 8.2.4</b> Sirius red staining after 14 days of ADSCs from 3 donors cultured on PLA mainly aligned scaffolds.....	223
<b>Figure 8.2.5</b> Representative images of immunostaining for collagen III and elastin of ADSCs at passage 3 cultured on PLA mainly aligned scaffolds.....	223
<b>Figure 8.3.1</b> Day of passage and number of cells counted in each passage passage since the isolation of ADSCs using high speed and hand minced methods.....	225
<b>Figure 8.3.2</b> ADSCs isolated using high speed and hand minced methods cultured for 3 weeks with adipogenic or osteogenic medium.....	226
<b>Figure 8.3.3</b> AlamarBlue <sup>®</sup> staining for ADSCs isolated using high speed and hand minced methods on hybrid PLA (280 $\mu\text{m}$ ) scaffolds.....	227
<b>Figure 8.3.4</b> Sirius red staining after 14 days of ADSCs isolated using high speed and hand minced methods cultured on hybrid PLA (280 $\mu\text{m}$ ) scaffolds.....	227
<b>Figure 8.3.5</b> AlamarBlue <sup>®</sup> staining of hybrid PLA (280 $\mu\text{m}$ ) scaffolds seeded with the SVF and ADSCs over 2 weeks in culture.....	228
<b>Figure 8.3.6</b> Sirius red staining after 14 days of hybrid PLA (280 $\mu\text{m}$ ) scaffolds cultured with the SVF and ADSCs.....	229

## Abstract

Stress urinary incontinence (SUI) and pelvic organ prolapse (POP) are diseases related to weakness of supportive tissues of the pelvic floor due to altered collagen production in middle-aged women and traumatic processes in younger women such as pregnancy and vaginal delivery.

Currently there is no recommended material for use in the surgical management of these disorders. Synthetic non-absorbable materials, such as polypropylene mesh produce a vigorous inflammatory response followed by dense fibrosis and have been associated with serious complications such as exposure. By contrast acellular biological materials have a tendency toward rapid absorption with questionable long-term mechanical integrity and concerns regarding early failure.

Our approach aims to develop a tissue engineered repair material (TERM) to provide the long-term durability of synthetic non-absorbable materials whilst avoiding complications such as exposures and pain. The TERM is composed of a scaffold designed to degrade slowly whilst the inclusion of autologous cells is anticipated to produce a new extracellular matrix (ECM) to remodel fascial tissue for long-term restoration of the mechanical properties.

Biodegradable poly-(L)-lactic acid (PLA) scaffolds were identified as the candidate material being more cell compatible *in vitro* than materials currently used to treat SUI and POP, and with mechanical properties close to the range of native tissues of the pelvic floor.

A comparison of oral fibroblasts and adipose-derived stem cells (ADSCs) showed similar results when these cells were cultured on PLA scaffolds to develop a TERM in terms of metabolic activity, ECM production and mechanical properties. Of the two, ADSCs were chosen for further experiments since these cells have been shown in the literature to have regenerative potential and also to be immunosuppressive and to stimulate angiogenesis. The number of cells seeded on the scaffolds, the period of culture and culture conditions were optimized for the production of the best TERM candidate. On the other hand, no significant effects were found when exploring chemical and mechanical stimulation with the aim of increasing ECM production.

The host response against the PLA scaffolds implanted cell-free and with ADSCs was studied in rats. The acute host response showed that after an inflammatory response, new collagen ingrowth and blood vessels were developed in all samples.

Work was then focussed on the modification of the electrospinning rig to develop a variety of PLA scaffolds with different mechanical properties due to different fibre configuration. Finally, the potential of ADSCs to develop the TERM was assessed using cells from different donors, as well as examining whether this potential was preserved when these cells were rapidly isolated from fat using an enclosed system.

In summary, we identified a suitable candidate material, cell candidate and culture conditions to develop a TERM designed for pelvic floor repair. Then, an initial animal study suggested a host response against our TERM leading to constructive remodelling for integration into the native tissues. Finally, a range of PLA scaffolds were produced with improved mechanical properties and preliminary data showed the potential to rapidly isolate ADSCs which were used to develop a TERM *in vitro*.



## **Chapter 1**

### **INTRODUCTION**

## **1.1 Stress urinary incontinence (SUI)**

### **1.1.1 Epidemiology**

Urinary incontinence (UI) is a problem affecting the quality of life of more than 200 million women in the world (1), exceeding that of other chronic pathologies such as arterial hypertension and angina pectoris or diabetes (2). This condition is described as urine leakage which occurs when the pressure in the bladder exceeds the pressure within the urethra. Micturition is normally regulated by neuromuscular mechanisms and an alteration in any of these anatomic and neurologic mechanisms can induce urinary incontinence (3).

Stress urinary incontinence (SUI) is the most common type of UI described as a leakage on effort or exertion by increased abdominal pressure (4). Intrinsic urethral sphincter muscle weakness and anatomical failure of the urethral support are the main problems associated with the development of SUI. Insufficient closure pressure in the urethra during physical effort may lead to leakage of urine. SUI is defined clinically, by the International Continence Society (ICS), as “the involuntary leakage of urine on effort or exertion, or sneezing or coughing” (5).

SUI is in contrast to urgency urinary incontinence (UUI), whereby a sudden compelling desire to void occurs which is difficult to defer. UUI is defined as an involuntary loss of urine accompanied by or immediately preceded by a sudden, strong desire to void. This is explained as result of involuntary bladder contraction, which in turn, has been proposed to be due to loss of the viscoelastic features of the bladder. This often shows detrusor overactivity during urodynamic testing.

SUI signs may be reproduced by the clinician on examination; however, if there is disparity in symptoms or surgical intervention is contemplated, urodynamics is considered beneficial. The urodynamic definition of incontinence proposed by the ICS is “the involuntary leakage of urine during increased abdominal pressure, in the absence of a detrusor contraction”.

In addition, while UUI predominates in old women, SUI is most common in young and middle age women (6). Occasionally both types of incontinence can occur simultaneously.

Since definitions for different UI disorders were not established by ICS until 2002, reports of the prevalence of SUI are variable. In a meta-analysis of 48 studies, the prevalence of UI was reported to be 16% for women younger than 30 years and 29% for women aged 30 to 60 years (7). The authors found SUI to be more common than UUI, with 78% of women having SUI versus 51% with urge urinary incontinence, and 27% of them having mixed urinary incontinence. Each year, an estimated 135,000 women undergo surgery for urinary incontinence in the United States alone (8). The estimated annual cost to the US economy is approximately \$19.5 billion (9). Moreover, it is believed that more than half of women suffering from SUI are embarrassed by the condition, are unable to mention this to their healthcare provider or may even accept some incontinence as a part of the ageing process (10).

SUI can be divided into 3 grades (11):

1. Leakage on severe stress i.e. Coughing laughing or sneezing.
2. Leakage on minimal stress e.g. walking, running.
3. Total incontinence.

Questionnaires like the Incontinence Impact Questionnaire (12) are used to characterize the impact caused by the incontinence symptoms on quality of life. As a measure of severity, the most widely used indexes are the Sandvik Severity Index (13) and the International Consultation on Incontinence Questionnaire-Short Form (ICIQ-SF) index (14); both have been validated (15).

### **1.1.2 Aetiology**

The continence apparatus has been described as the anterior vaginal wall, surrounded by muscles and fascial tissues. Levator ani muscles connect to anterior vaginal wall at pubovaginalis level, point where muscle contraction retracts anterior vaginal wall to support and make pressure on the urethra (16).

On the other hand, the sphincter unit, including multilayered urethra and alpha-adrenergically innervated vesical neck, also gives an important continence control. Where the urethra crosses the bladder, it is surrounded by the muscle of the trigonal ring. This sphincteric unit extends throughout the proximal two-thirds of the urethra and is composed of outer striated urogenital sphincter muscle (rhabdosphincter), with a

middle circular smooth muscle and an internal longitudinal layer. In 1980 was already showed the importance of each urethral layer for urethral closure pressure, and all layers were similarly relevant for the contraction of the urethral sphincter including submucosal plexus, which is highly vascularised (17). Submucosal vascular plexus is also very important for the neural mechanism of the entire complex which is not well understood (16).

In women integrity of the intrinsic urethral sphincteric mechanism is a major factor in maintenance of continence. Several researchers agree on “intrinsic sphincter deficiency” as a problem of the three different urethral elements which include pudendal innervation, striated sphincter mass and function, urethral smooth muscle, mucosa and submucosal cushions (18).

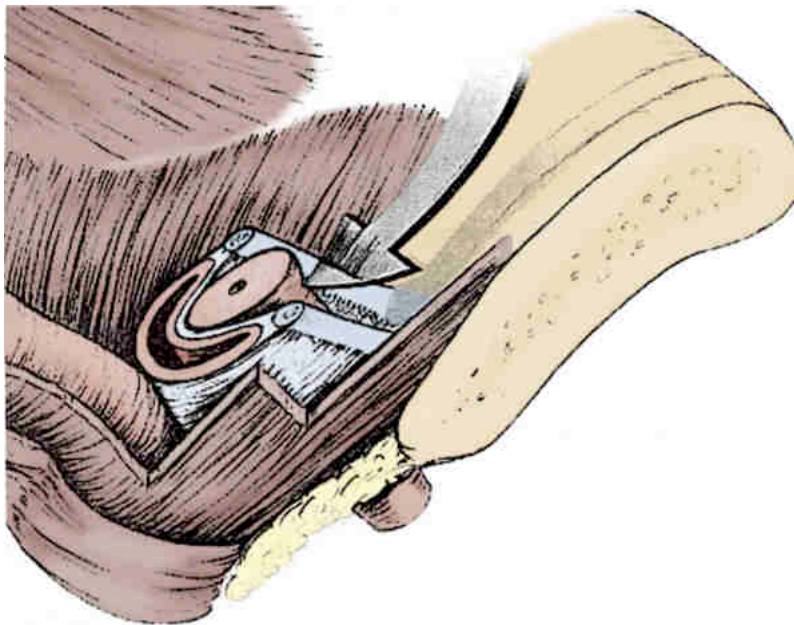


**Figure 1.1** A view of the hammock theory by Ulmsten, the supporting structures to the urethra provide a backboard upon which the urethral contraction may be stabilised (Image obtained from Wein: Campbell-Walsh Urology, 10th ed. Chapter 60. Elsevier).

However, the Integral theory of female urinary incontinence, put forward by Petros and Ulmsten, proposes that the cause of SUI is connective tissue laxity in the vagina itself, or in its anterior and/or posterior supporting ligaments (19). This produces urethra mobility, and contraction of pelvic floor muscles is unable to compensate the laxity of the connective tissues to give functional support and pressure to the urethra.

It is believed that both intrinsic sphincter weakness and para-vaginal connective tissue (also called para-urethral connective tissues or endopelvic fascia) weakness may co-exist in some degree in women with SUI (20).

For a better understanding of the anatomy of the urethral continence elements Delancey described the hammock model (21). The endopelvic fascia, which is found between the anterior vaginal wall and the urethra, is attached to both of these structures holding the urethra as a hammock (figure 1.1). In addition to this, the endopelvic fascia extends from the vaginal apex to perineum and laterally forms the arcus tendinius at both sides. Immediately anterior to the proximal urethra are condensations of endopelvic fascia. These are dense enough to be recognised and are termed the pubo-urethral ligaments (figure 1.2).

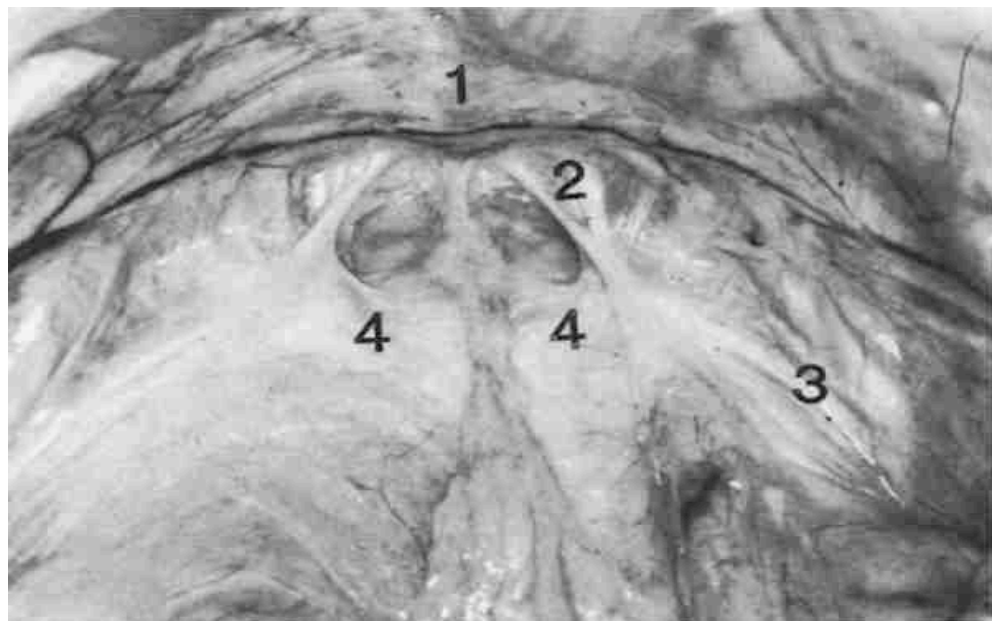


**Figure 1.2** *Inferior view of the pelvic floor of an elderly female cadaver showing the Pubic bone 1, right pubo-urethral ligament 2, lateral endopelvic fascia forming the arcus tendinius fascia 3, and central endopelvic fascia 4 (Image obtained from Mostwin JL: Current concepts of female pelvic anatomy and physiology. Urol Clin North Am 1991;18:175-195).*

The levator ani muscles run bilaterally from the superior ramus of the pubis to the spine of the ischium and coccyx. The middle fibres are attached to the rectal sphincter muscles and the anterior fibres descend upon the side of the vagina (figure 1.3). The fascial tissue covering the levator ani consists of two leaves: the endopelvic fascia (abdominal side) and pubo-cervical fascia (vaginal side). The two leaves fuse to insert into the arcus tendinius creating a hammock of support suburethrally (figure 1.1).

In summary the posterior urethra is intimately connected to the anterior vaginal wall by the endopelvic fascia, which is connected to levator ani muscle complex by the arcus tendinius fascia pelvis (ATFP). The levator ani muscles, in combination with the endopelvic fascia perform an important part of the continence mechanism in women (21). Contraction of the levator ani pulls the vagina against the posterior surface of the urethra thus closing it (22).

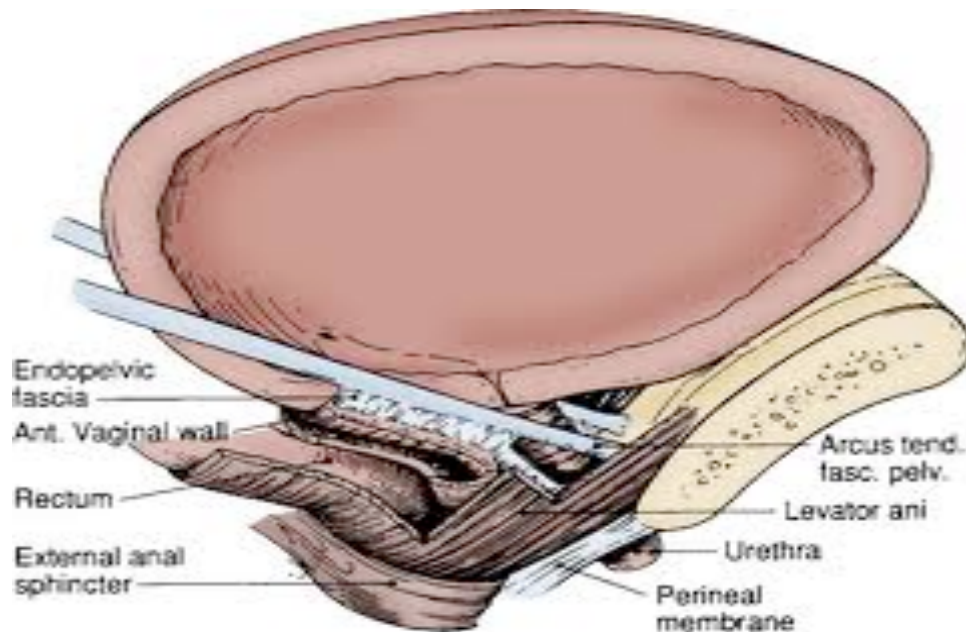


**Figure 1.3** *The role of the endopelvic fascia, arcus tendinius and levator ani in support of the urethra and bladder (Image obtained from Wein: Campbell-Walsh Urology, 10th ed. Chapter 60. Elsevier).*

In a series of magnetic resonance imaging (MRI) studies, it has been shown that the anterior and posterior walls of the bladder neck are pulled apart due to unequal movement of the opposing walls during stress (23, 24). The urethral sphincter is connected to the bladder neck by the suburethral complex suggesting that weakness at this point may be sufficient to permit distraction of the anterior and posterior urethral walls during rotational descent. Women with SUI have shown radiological features suggesting impairment of urethral support such as an increased urethrovesical angle, bladder neck and urethra hypermobility (25), reduced functional urethral length (26) or disruption of periurethral ligaments or defects in endopelvic fascia (27).

In summary, the essence of urethral support in women is multifaceted and both endopelvic fascia and pelvic floor muscle tone acting under neural control are

responsible for continence. On the other hand, as above, an intrinsic sphincteric deficiency can lead to incomplete sphincter closure thus predisposing to SUI (28, 29).

### **1.1.3 Risk factors**

Risk factors for development of SUI are classified as predisposing factors, obstetric and gynaecological factors, and promoting factors. Race (Caucasians are the most affected), genetics (other females in the same family with incontinence), congenital factors (i.e. ectopic urethra) and neurologic diseases are the main predisposing factors. Pregnancy, vaginal delivery (where the weight and number of babies are relevant), pelvic surgery and radiation (nerve and/or muscle damage), and pelvic organ prolapse (POP) are the most common obstetric factors affecting supportive tissues of the urethra or muscles of the urethral sphincter (30). Finally, there are age co-morbidities (i.e. diabetes, vascular disease), obesity, constipation (increase in intra-abdominal pressure), menopause, and medications which are all promoting factors (31-33).

Since the prevalence of SUI is increased in women over the age of 50 (4), ageing is associated with an increased risk of SUI (34). Elderly women may be affected by loss of muscle tone and long term effects of denervation injuries sustained during childbirth leading to urethral sphincter deficiency; on the other hand, changes in hormonal status leading to alterations in collagen of para-vaginal tissues may also disrupt the continence apparatus (35, 36).

However, it has been difficult to prove a link between the natural menopause and increasing risk of SUI (37, 38). Also there is no evidence for hormone replacement therapy reducing the risk of UI (39-41).

POP itself is considered as a risk factor of SUI (30). The prolapsed organs may give an extra tension producing laxity of the para-vaginal connective tissues or innervating the urethral sphincter.

Likewise body mass index (BMI) has been considered to be an important risk factor of SUI (42). It is proposed a laxity of support tissues after chronic strain and/or the existence of a greater abdominal pressure (34). Women in the highest quartile of BMI are 2-4 times more likely to have urinary incontinence than those in the lowest (39).

Furthermore, few studies agree with pregnancy and vaginal delivery as major obstetric risk factors for SUI. Childbirth leads to SUI due to denervation of sphincter muscles which progresses with age (43, 44). Child delivery may loosen para-vaginal connective tissues too, affecting the continence apparatus. Some studies demonstrated increased risk of SUI after childbirth via caesarean section compared with nulliparous women, but even greater comparing last group with women giving birth vaginally (34, 45). Finally, epidemiological studies have shown approximately half of all women develop transient UI during pregnancy and post partum the prevalence of UI is 9-31% (18).

Additionally medical co-morbidities such as the length of time with type II diabetes mellitus have been found to confer increased risk of SUI (31). Other co-morbidities presenting risk include neurological disorders and connective tissue disorders (32, 33).

#### **1.1.4 Treatments**

Since SUI has a multifactorial aetiology, there is no unified treatment for all patients and there is a necessity to adjust treatments to each case.

Conservative treatments of UI are weight loss, fluid management, and pelvic floor muscles exercises. However, in advanced grades of SUI, pharmacological and surgical treatments are required.

Alpha adreno-receptor agonists (ephedrine and norephedrine) and mixed pharmacological agents (duloxetine and imipramine) have been used for SUI with the aim to stimulate muscle contraction of the urethral sphincter. Also, injection of bulking agents into the suburethral tissues and placement of pessaries inside the vagina has been used to give urethral support/pressure.

Surgical treatments for SUI include urethral slings or tapes and retropubic suspensions (46) to support the structural continence mechanism of the pelvic floor.

##### **1.1.4.1 Non surgical treatments**

Changes in lifestyle such as weight loss together with supervised pelvic floor exercises are the first therapies for the treatment of SUI as stated by the National Institute of Clinical Excellence. SUI symptoms have been reported to be decreased after weight loss (47). Similarly, one study found subjective improvements in a range of 54-58% of SUI



patients after treatment with pelvic floor exercises, electrical stimulation or vaginal cones (48). Nevertheless, a placebo effect cannot be eliminated as urodynamic studies did not show differences between treated and untreated groups.

Due to the described defects of the supportive tissues of the urethra, it has been shown that there are lower resting urethral pressures in SUI patients compared to age matched continent women (49, 50). For this reason alpha adreno-receptors agonists have been used to maintain urethral muscles tone as a pharmacological treatment of SUI (51). Especially ephedrine and norephedrine (18) are used to increased contraction of the urethra by release of noradrenaline on alpha adreno-receptors.

Nevertheless, again, since SUI has a multifactorial aetiology, the urethral pressure increased by augmentation of the contraction of the urethral sphincter muscles may not be sufficient to improved SUI signs. Therefore, a patient, whose muscle tone is normal, but with an erratic continence apparatus due to para-vaginal fascial tissues defects may not notice a beneficial effect of alpha adreno-receptors agonists. Consequently, a systematic review in 2005 did not find evidence on the clinical benefit of these drugs, suggesting, as reported for pelvic floor exercises, a placebo effect improving just subjective parameters (52).

With a similar approach, beta adreno-receptor antagonists have been used to enhance alpha adrenoreceptor action by beta adrenoreceptor blockade; however, this has not shown any better effects than alpha adreno-receptors agonists (53).

Duloxetine, a serotonin and noradrenaline reuptake inhibitor was reported to be a very promising treatment of SUI as a stimulator of the contractions of the external urethral sphincter (rhabdosphincter) (54). Beneficial effects of this drug were observed leading to a higher mean urethral pressure profile, maximal urethral closure pressure but not functional urethral length (55). High doses significantly decreased the frequency of incontinence episodes in 64% of women; however, 15% of those discontinued the drug due to side effects such as nausea (56). More severe side effects such as psychiatric disorders have also limited their use (57-59).

Imipramine, a similar mixed pharmacological agent, has been developed with promising results (60); however at present there are no published randomized clinical trials (RCTs) with this treatment. Surgery is considered more cost effective than pharmacological treatments (61). Drugs may be beneficial in patients with urethral sphincter deficiency but may not help in SUI patients with defects of para-vaginal fascial tissues.

Estrogen replacement in women increases collagen I and collagen III production in the connective tissues of the pelvic floor (62-64). This has been postulated to have a positive effect on the maintenance of the urethral pressure since estrogen receptors are expressed in the vagina, levator ani muscle, ligaments and fascia (18). However, one study showed a decrease in collagen concentration and collagen cross linking in urogenital tissues (65), and a recent review described a worsening of SUI, after estrogen therapy (66).

Collagen has been injected, as a bulking agent, around the urethra to increase urethral pressure. A review reported a short term cure (67), but a multicentre RCT found 19% less success with collagen injections compared to surgery (68). It has been postulated that collagen injections may be beneficial after failure of surgery (69), and it has been suggested that it should be used just as a follow up treatment (70). Women with SUI represent a complex population and for cost effectiveness, treatments have to be well established.

Other urethral bulking agents have been used, ranging from autologous fat, carbon particles, calcium hydroxyapatite, ethylene vinyl alcohol copolymer, dextranomer and silicone based Macroplastique<sup>®</sup>. The last one consists of injected cross-linked polydimethylsiloxane which is encapsulated by fibrin leaving the fibrous capsule after reabsorption of the synthetic material (71). A recent study found better responses when using Macroplastique<sup>®</sup> compared to collagen injection in a blinded RTC with SUI women. On the other hand, a higher risk for urinary retention and urethral erosion were described in the Macroplastique<sup>®</sup> group (72). Moreover, its use as a first line treatment may complicate a consequent surgical intervention; therefore, again, this urethral bulking agent may be used just as a follow up treatment.

Pessaries are commonly used to treat POP. However, they have been also used to treat SUI since they are introduced intravaginally to give structural support which may give urethral support and pressure as well. On the other hand, they are not commonly used to treat SUI since some studies have not found improvements in SUI symptoms when using pessaries (73).

#### 1.1.4.2 Surgical treatments

The main propose of surgical treatments are to give urethral support, and depending on each case, there are 5 categories of surgery treatments which are the main choices for most patients suffering SUI, especially for severe cases:

1. Anterior vaginal repair or anterior colporrhaphy is used to treat POP (figure 1.4). If this prolapse is associated with incontinence then buttress sutures are placed on the bladder. After vaginal incision, the supportive tissue around the bladder, endopelvic fascia, is plicated to elevate the bladder neck and urethra giving them higher support. A meta-analysis has reported the success rate of this procedure to be in a range of 67.8-72% (74). On the other hand a significant decline in the continence rates has been reported after 5 years and, nowadays, the procedure is not popular anymore (75).

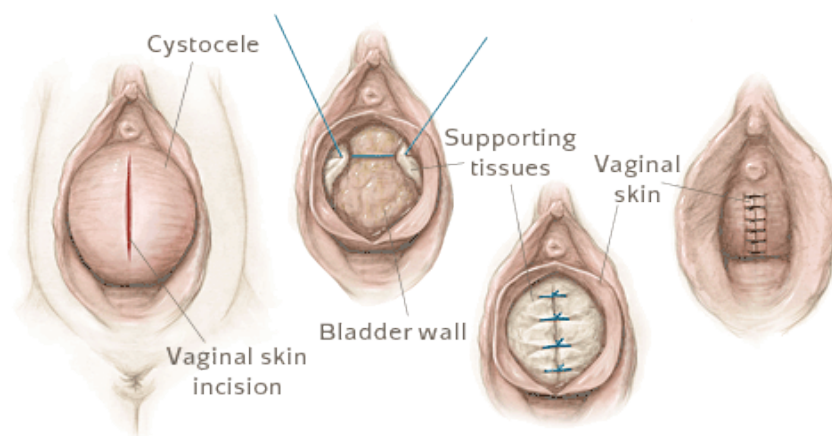
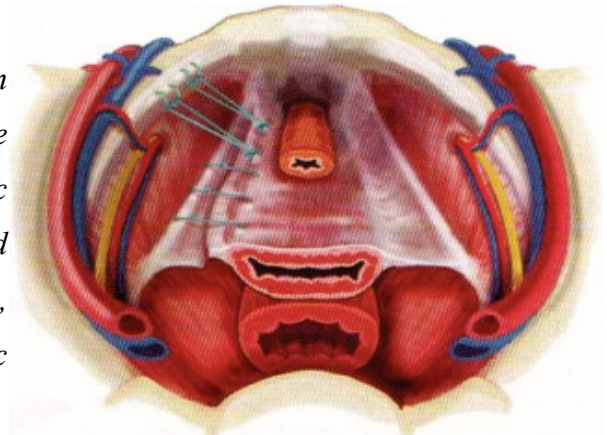


**Figure 1.4** Anterior vaginal repair illustrating sutures plicating endopelvic fascia (Image obtained from University of Virginia Health System).

2. Burch Colposuspension is used to fix the vagina into the space behind the pubic bone by lifting and suturing the para-vaginal fascial tissues (endopelvic fascia) from the anterior vaginal wall (figure 1.5). This surgical treatment is well established and continence rates of 83-87% have been reported after 1 year (76). Nevertheless, these rates were also reported to decline after 2 years to 51%, in a multicentre randomised trial (77). The same study also reported complications with a rate of 39.8% patients developing POP after this procedure and 3.4% of patients requiring a second operation due to recurrence of incontinence.

**Figure 1.5** Colposuspension illustrating sutures elevating the para-urethral fascia towards pubic bone ligaments (Image obtained from Dr. Cynthia Hall, Urogynecology and Pelvic Reconstructive Surgery).



3. A needle suspension procedure is used to fix the bladder neck with sutures to the bone anchors of the pubic bone (figure 1.6), and sometimes using patch materials as well. However, these procedures seems to have a very low success rates in most studies as reported in a 5 years follow up study with 12% of improvements, 5% of subjective success and 83% of failure (78).

**Figure 1.6** Needle suspension illustrating sutures form bladder neck to pubic bone (Image obtained from Healthbase Online Inc.).



4. Tension-free tape procedures use synthetic materials as a strip to be placed beneath the mid urethra. This procedure is cost-efficient, minimally invasive and it takes only a few minutes to be performed. Nowadays, it is the most popular technique, with high success in recent years. Long tapes are passed under the urethra to the other side and through the retropubic space or through the obturator internus muscle and out of the obturator foramen, to be fixed by sutures to the anterior abdominal wall (figure 1.7). The last one is termed transobturator tape (TOT). Short tapes are equally passed under the urethra and attached to the abdominal wall using suspending sutures at each end of the tape or to the pubic bones wall attaching same sutures to bone screws (figure 1.7).

Cystoscopy is usually conducted after the operation to assess that the surgical procedure has not perforated the bladder.

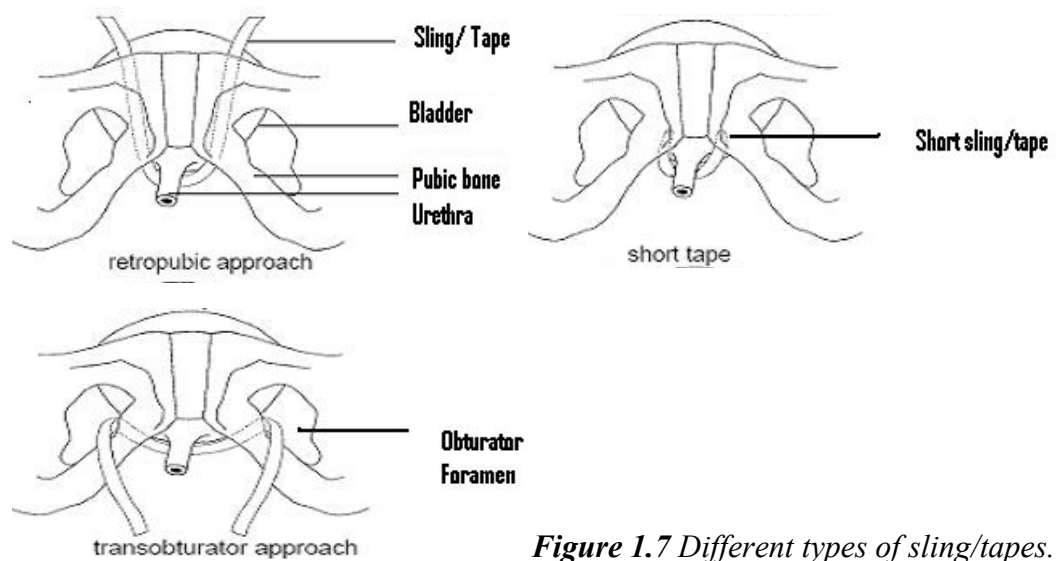


**Figure 1.7** Different types of sling/tapes.

5. Pubovaginal slings are biological materials which are implanted by procedures very similar to tension-free tapes (figure 1.7). These slings are placed beneath the bladder neck applying an adequate amount of tension to reinstate continence. A sling which is too tight may lead to urine retention and, conversely, a sling that is too loose may lead to recurrence of incontinence. Different materials have been used including autologous grafts, allografts and xenografts and different success rates are found with each. Cadaveric fascia has been reported to have success rates from 33 to 93% (79-81). For autologous rectus fascia, success rates are about 80% but depending on the level of patient selection and follow up (82, 83). After 36 months, porcine dermis showed success rates of 57% (84).

Currently, many companies have brought different tapes to the market. Different materials and kits are available resulting in different performance of the procedures. For instance, TOT are either placed from inside to out or from outside to in.

Tension free vaginal tape (TVT- Ethicon®) has being the most used with more than 1.4 million procedures around the world. In addition, TVT has been shown to have higher objective success rates than TOT; although, the subjective cure rates were similar with decreased risk of intraoperative complications for TOT (85). Satisfactory success rates have been reported after 2 years of TVT implantation being 63% and with an improvement noted in another 20% of patients (86). Comparing TVT to porcine dermis

pubovaginal slings, success rates are similar, in terms of quality of life, but slings have been found to have higher complication rates (87).

Surgical procedures aim for the well performance of the continence apparatus since these treatments give better support to the urethra. If SUI was just related to urethral sphincter deficiency all these procedures may not have the elevated improvements shown.

Nevertheless, all surgical treatments have the limitation of variations in success rates between clinicians since the procedures involve a subjective interpretation in each patient of how much the tissue is plicated or lifted to apply the adequate support of the urethra and restore the continence parameters.

Although its name suggests tapes are holding the urethra without tension, TVTs actually apply a small pressure to the urethra. Once the tape is placed and before the vaginal wall is closed, the urethra is pushed to loosen the tape and to avoid high pressure which could lead to urinary obstruction. But similar to pubovaginal slings, how much the clinician pushes the urethra or leaves the whole thing tight depends on a subjective interpretation of each clinician and for each patient.

Finally, just to mention that artificial urinary sphincters have been surgically implanted for over 30 years in about 100.000 men as a treatment for SUI after prostatectomy. This is a fluid-filled and solid silicone elastomer device which simulates normal sphincter function by opening and closing the urethra under patient control (88, 89). Although this device has shown to be an effective treatment for male, it is not useful for women being the main population suffering SUI.

#### 1.1.4.3 Surgical complications

While intraoperative complications are normally associated with the performance of the surgery, postoperative complications of SUI surgery are related to the response of the patient to the surgery and/or host reaction against the material implanted.

Intraoperative complications may involve injury of pelvic organs such as the urethra, bladder, ureter, bowel, but also, blood vessels and nerves.

The urethra can be damaged during transvaginal dissection or when passing trocars used to assist sling/tape procedures. This rarely occurs but it could lead to urethrovaginal fistula and infection and/or erosion of a tape.

Bladder injury is more likely to occur with colposuspension compared to sling procedures (90).

Uretric injury is also not common. Using mid-urethral tapes is very difficult to get this kind of complication; however, during colposuspension the ureter may be kinked.

Again, bowel injury is very uncommon. Only in case reports has this been reported (91), and there may be higher risks during retropubic dissection for colposuspension or during trocar passage for tape/sling placement.

Injury of blood vessels is more common since many vessels pass through the pelvis. Care is needed with the obturator fossa and pelvic side walls, and also with the iliac vessels and vascular pedicle of the bladder when passing needles and trocars.

Finally nerve injury may occur during harvest of rectus fascia to use as an autologous sling or during the passage of trocars (92, 93).

Postoperative complications include voiding dysfunction, vaginal or urinary tract damage and infection.

Although urgency incontinence may develop after surgical procedures, more cases have reported urinary retention. After 4 weeks post-surgery, difficulty in voiding has been reported in 4-8% of colposuspensions and 3-11% of sling procedures (94). A maximum of 5% women have reported needing an intervention for voiding dysfunction after mid-urethral tape procedures (91, 95).

Due to the implantation of a non-degradable material, tape procedures are the ones most associated with damage to surrounding tissues after an excessive inflammatory response. The presence of a tape in the vagina is called vaginal extrusion. Higher rates of this complication have been reported when using multifilament synthetic materials compared to monofilament synthetic materials (96, 97), being 5% for the latter (98). Erosion occurs when the tape is found in the urinary tract which only occurs in less than 1% of women treated with mid-urethral tapes (95, 98-100).

There is always a small risk of infection after a surgical treatment this has been mainly reported in case reports of tape/sling procedures to treat SUI. This may be due to the inflammatory response against the foreign materials and/or their physical properties which may not allow the passage of immune cells to combat bacteria (101-105).

#### 1.1.4.4 Surgical outcomes

Outcomes measures used for any kind of treatment must be reliable, valid, interpretable and responsive to change.

An ICIQ questionnaire is widely used and has been derived from other existing well validated questionnaires (18). The questionnaire scores symptom modules, quality of life modules and optional modules.

Objective assessments of outcomes after SUI surgical procedures include urodynamics, cough stress test, pad tests and bladder diaries.

Although urodynamics is the gold standard test used to objectively identify SUI, urodynamics did not show SUI in 15% of women with primary SUI (106). Moreover, this test is not reliable to determine the outcomes of surgical procedures, since 40% of women complaining about persistence of SUI after surgical treatment did not show leakage during urodynamics (107).

Since there is no standardized bladder volume and number and force of coughs to perform a cough stress test, this may be used to assess cure but not to assess improvement in SUI (108).

With different standardizations and durations of the test, pad tests have been used to define cure. Only 1 hour, 24 hours and 72 hours pad tests have been validated (109-111).

Also bladder diaries are not well standardized but this test seems to be a reliable assessment depending on its duration (112).

## 1.2 Pelvic organ prolapse (POP)

### 1.2.1 Epidemiology

POP occurs when the female pelvic organs fall from their normal position into or through the vagina.

Similar to SUI, POP is developed after weakness of the different supportive tissues of the pelvic floor affecting different vaginal segments including anterior and posterior



vaginal prolapse (cystocele and rectocele, respectively), apical or uterine prolapse, enterocele and perineal descent (113).

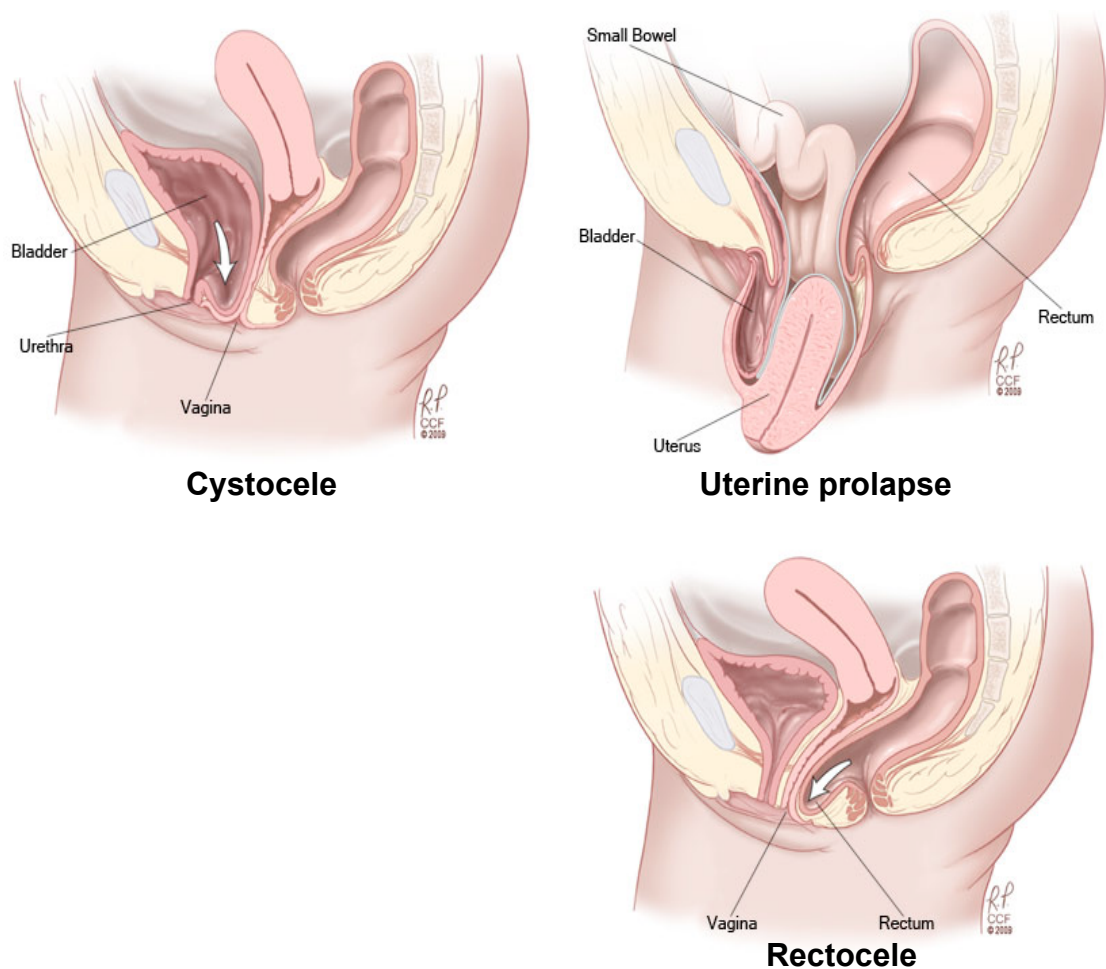


**Figure 1.8** Illustrations of the prolapse of the different compartments (Images obtained from Cleveland Clinic).

These are classified in 3 groups of prolapse depending on the compartment affected. Anterior prolapse entails the herniation of the bladder, the urethra or both into the vagina, resulting in a cystocele, urethrocele or cystourethrocele respectively (figure 1.8). Prolapse of the middle compartment refers to herniation of the uterus (figure 1.8). Finally, prolapse of the posterior compartment implies the descent of the rectum (figure 1.8). These were defined by ICS in 2002 (3) leading to the quantification of the degree of prolapse, which is called POP quantification system (POPQ):

Stage 0: no prolapse

Stage 1: more than 1 cm above the hymen

Stage 2: within 1 cm proximal or distal to the plane of the hymen

Stage 3: more than 1 cm below the plane of the hymen but protrudes no further than 2 cm less than the total length of the vagina

Stage 4: there is complete aversion of the vagina

It is difficult to determine the exact prevalence of POP since few studies have reported 35% of asymptomatic patients having POPQ stage 2 and between 0.2%-11% having vaginal segments at or below the plane of the hymen (114-118). Nevertheless, prevalence of symptomatic POP is estimated to be between 3.6%-11.4% (119, 120). Recently, in an Australian study, the lifetime risk for a woman of requiring POP surgery was reported at 19% (121), and each year, an estimated 225,964 women undergo surgery for POP in the United States (122).

### 1.2.2 Aetiology

Weakness in the supportive connective tissues of the vagina leads to herniation of the underlying tissues into the vagina, and consequently, the prolapse of female pelvic organs. These include para-vaginal tissues and, as above, their weakness may lead to SUI too.

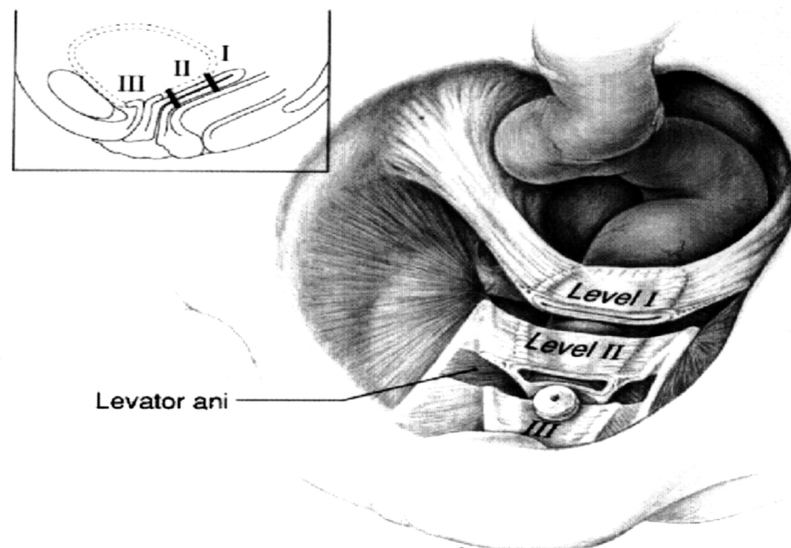


**Figure 1.9** DeLancey's levels of support (Image obtained from DeLancey: *The anatomy of the pelvic floor*. *Curr Opin Obstet Gynecol* 1994;6(4):313-6).

Conceptually, DeLancey described 3 vaginal supportive levels, which build up the support structure of the pelvic floor (123). Level I includes the cardinal-uterosacral

ligament complex. At level II, the middle part of the vagina (endopelvic fascia) is attached laterally to the ATRP pelvis which attaches to the superior fascia of the levator ani muscles. At the third level, the vaginal wall is connected to the perineal membrane and perineal body (figure 1.9).

After an increase in abdominal pressure, the levator ani muscle contracts closing the genital hiatus; however, if the supportive tissues are weak, this muscular contraction does not prevent pelvic floor organ descent (124).

To find out exactly which supportive structures are altered, several studies have been focused on describing alterations on the anatomy of the pelvic floor in women with POP. The complexity of this anatomy and different methods and techniques used it makes difficult to make a comparison between studies (125-127). These techniques include MRI, three-dimensional (3D) imaging and 3D ultrasound.

Series of fast magnetic resonance images are obtained while voluntary pelvic strain is increased. This allows the measurement of the distance between different anatomical structures of the pelvic floor to quantify pelvic descent for better understanding of the SUI and POP pathophysiology. Imaging studies are not routinely used for clinical diagnosis since they are very expensive; however, these should be used in failed operations and complex prolapse for better surgical results (23). These methods also contributed to introduce the POPQ in 2002. Alternatively, some studies included in this thesis using these methods do not contrast between different POP stages since they are previous to 2002 (128).

Electromyography is a technique which can be used during an urodynamic test to measure the electrical potential of skeletal muscle cells. This method has been also used to determine functional deficiencies of the pelvic floor muscles; however, these studies have not been included in this thesis since they are not within the scope.

The anatomy of the pelvic floor of 37 women with POP and 35 without POP was studied by MRI, matching both groups for age, BMI, childbirths, hysterectomy (uterus removal) and menopausal status. The study observed the descent of structures from level III, which includes the distal vagina, perineal body, apex and external anal sphincter, especially for the first two structures. The vagina apex was more ventrally displaced demonstrating its descent because of a shorter distance with distal vagina in subjects. Posterior vaginal wall showed longer length, such as larger urogenital hiatus

and levator ani muscle dimensions with a plate angle of the latest more caudally located in subjects. The length of the posterior vaginal wall suggests an alteration of the properties of the endopelvic fascia. All these differences were mainly observed in patients who belonged to an advanced stage POP (129). In addition, same anatomical alterations have been also found in other studies (23, 130).

Changes of the dimension of the levator ani muscle were also found by 3D imaging in women with POP. Muscle was thicker in asymptomatic women than in women with POP, which indicates muscle distention in affected women (131). This has been also proved in other studies by MRI and ultrasound imaging (132, 133).

DeLancey tried to summarize the association between supportive structures altered and the specific types of prolapse (134). While defects of supportive tissues from level III would be associated to rectocele (posterior compartment), weakness of endopelvic fascia and arcus tendinous, from supportive level II, would be related to cystocele and uterine prolapse from anterior compartments. Finally, defects on the uterosacral ligaments (supportive level I) would lead to descent of the uterus (middle compartment).

### **1.2.3 Risk factors**

Risk factors for development of POP are similar to SUI risk factors affecting similarly supportive tissues of the pelvic floor.

Any incident affecting innervation of the levator ani muscle or anal and urethral sphincters, and/or affecting structural properties of pelvic tissues may imply dysfunction of the pelvic floor.

Although the interaction between age and hormonal/menopausal status has not been associated in the development of POP, ageing has been described as a major risk factor when POP was studied in women from different ages (135, 136). As above, ageing may affect further deterioration of pelvic floor denervation and may decrease the production of collagen of fascial tissues of the vagina (35, 36).

Main injuries of pelvic floor tissues, such as tissue distension and/or denervation, are produced by obstetric factors, especially pregnancy and childbirth, which may lead to

the development of POP in the same way that affects SUI development. Many studies have reported the role of childbirth in the development of POP (137, 138).

One study classified 120 women according to vaginal delivery or caesarean delivery, and 100% and 87.5% of them, respectively, developed POP after 6 weeks postpartum. In addition, POP was more advanced in vaginal delivery subjects (139). Another study has also stated a partial protection to develop POP when child delivery is performed via caesarean (114). Analyzing a database of over 17,000 women, it was found a risk of surgery to treat POP of 8.4 in women with a history of 2 or more pregnancies compared to nulliparus women (114). In addition, birth weight has been shown to have an effect on risk for POP (138, 140).

Again similar to SUI, BMI has been related to the development of POP, as well as a family history of POP, heavy lifting at work (>10kg) and constipation (141).

It has been suggested that excessive weight gain causes severe injury of the pelvic floor tissues, in women with POP, since weight loss does not significantly restore the normal condition (142).

A few studies have found high rates of family incidence as an increasing risk for POP (143, 144), and genetic variants related to this have been reported (145).

Finally, neurological disorders and disorders related to alterations of connective tissues, such as Ehlers Danlos and Marfan's syndrome, have been shown to promote POP development (33, 146).

#### **1.2.4 Treatments**

Pharmacological treatments are not used for POP. Alternatively, again similar to SUI, the first treatment recommended in women with an early stage of POP is pelvic floor muscle training. If exercises do not improve the pathological condition the use of pessaries (mechanical devices such as rings or shelves) or surgical treatment are required, in women with more advanced POP stage.

##### **1.2.4.1 Non surgical treatments**

It has been described that once POP is detected in patients, exercise of the pelvic floor muscles may improve the condition only in a low percentage of these patients, since

most of them are not capable of adequate contracting the muscles at this stage (147). A systematic review has also summarized the limitations of pelvic floor muscle training (148).

However, these exercises are still being recommended for many patients since they have been shown to cause an improvement in objective and subjective symptoms in almost 50% of patients compared to a control group (149). On the other hand, pelvic floor muscle training needs supervision from a specialist, as well as a lifestyle advice to be given and this may vary between centres and patients.

Pessaries are placed intra-vaginally to provide structural support. Many different types have been developed but normally their shape is similar to the outer ring of a diaphragm. They can be placed temporarily or permanently and, although, they are more commonly used for prolapse of the uterus, they can be used to treat cystocele, rectocele and SUI.

Pessaries are widely used, and this has been elucidated from a survey in USA describing a preference for pessaries to surgical treatment (150). Estrogens can be prescribed, when pessaries are placed, to prevent the progression of POP (151).

Furthermore, a study with 203 women found a 30% of improvement of urinary symptoms after pessary treatment (73).

Nevertheless, success rates of non surgical treatments, such as pelvic floor exercises and pessaries, are not significantly relevant and surgical treatments are required in many patients with POP, particularly, in severe cases.

#### 1.2.4.2 Surgical treatments

Surgical treatments for POP are classified in 3 types depending on which vaginal tissues are repaired:

1. Colporrhaphy or anterior vaginal wall repair, which has been described previously for the surgical treatment of SUI (figure 1.4), is also used to treat prolapse of the anterior compartment such as cystocele, urethrocele and para-vaginal defect. Furthermore, when this procedure is performed to treat POP a mesh/graft material is used to reinforce the plication of the para-vaginal fascia.

When a mesh/graft is used in a colporrhaphy the recurrence of prolapse of the anterior compartment is half compared with same procedure when these meshes/grafts are not used, being 14% and 30% respectively. Looking at the type of mesh/graft used, a higher failure was found when using absorbable synthetic meshes (29%), followed by porcine dermis graft (18%) and to a lesser extent with non-absorbable meshes (9%). The same trend was observed after failure, by recurrence or development of other prolapse in 9% of cases using absorbable synthetic meshes, 3% for biological grafts and 1% for non-absorbable synthetic meshes (152).

Other people have shown a decreased risk of recurrence of POP 1 year after performance of colporrhaphy when using biological or absorbable synthetic materials (153), suggesting the relevance of the individual host response against these materials in the first months. In addition, similar to tape vs slings used to treat SUI, erosion rates were associated with the use of non-absorbable synthetic materials compared to the non-absorbable synthetic materials, being 14% and 2.9% respectively.

Mesh contraction is another problem which has been reported after colporrhaphy procedures which may lead to failure of the structural function of the mesh. About 50% of contraction has been observed by ultrasound measurements after implantation of non-absorbable polypropylene (PPL) meshes (154).

2. Upper vaginal repair is the term for the surgical repair of the uterine prolapse which is associated with defects of the uterosacral ligaments. This type of prolapse normally occurs in women above the age of 50, and the main choice of surgical treatment is the hysterectomy (uterus removal) with vaginal apex fixation, since these women may already be beyond the reproductive age. In the USA, hysterectomy is the main recommendation for women over 55 age suffering uterine or vaginal prolapse (155).

Vaginal sacrospinous colpopexy consists of the suture of the vagina in suspension from the sacrospinous ligament to the levator ani muscle, and it is used to treat vaginal vault prolapse which is the main complication associated with hysterectomy (156). Nevertheless, the incidence of vaginal vault prolapse is very low being between 0.2% and 4.3% of women who have had a hysterectomy (157). On the other hand, since vaginal sacrospinous colpopexy increases

abdominal pressure of the anterior compartment, this procedure has a risk of incidence of cystocele between 20% and 30% (158).

When uterine prolapse happens in younger women, a sacrohysteropexy is performed by suturing the uterus to the sacral bone in a tension free fashion. Although it has been reported that more complications are associated with sacrohysteropexy compared to hysterectomy (159), the first surgical treatment is performed in younger women to preserve their fertility.

Sacrocolpopexy is similar to vaginal sacrospinous colpopexy procedure, which is performed after hysterectomy, but consists in using a mesh/graft material to suture under suspension the vaginal vault to the ligament of the sacrum (figure 1.10). Sacrocolpopexy has shown better surgical outcomes, with less risk of developing SUI after surgical treatment, compared with vaginal sacrospinous colpopexy (160).

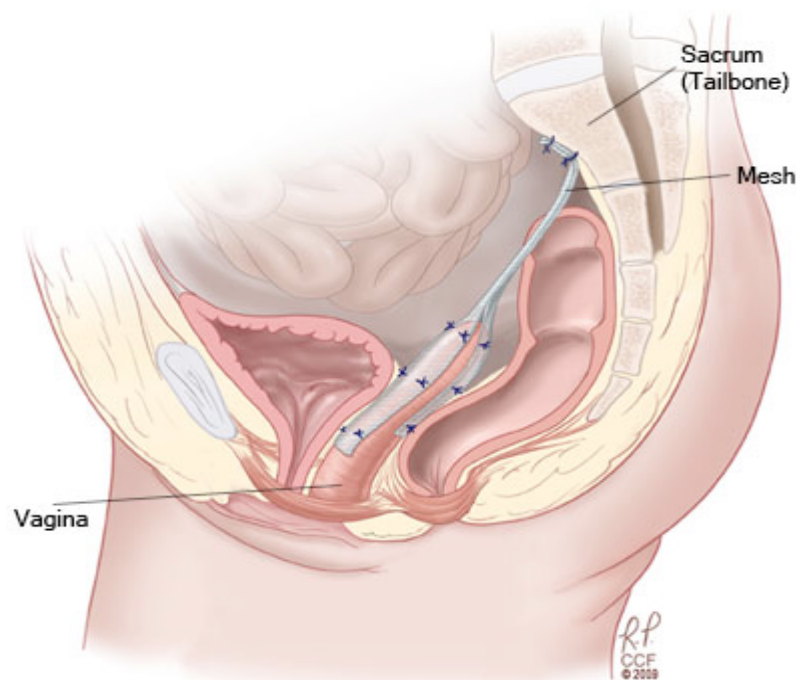


**Figure 1.10** Sacrocolpopexy illustrating the mesh/graft material sutured from the vaginal vault to the ligament of the sacrum (Images obtained from Cleveland Clinic).

Different mesh materials have been used in the sacrocolpopexy procedure such as cadaveric fascia lata and non-absorbable PPL mesh. Comparing both meshes, none of them have been reported to result in recurrence of vaginal vault



prolapse; however a higher incidence of prolapse in other sites has been associated with cadaveric fascia lata (161). On the other hand, when using non-absorbable materials, erosion has been observed with rates described to be between 2% and 11% (162). Cadaveric fascia lata does not pose a risk of erosion but failure and recurrence are more probable because this material can be reabsorbed very quickly and this is concluded as there have been no remains of this material found at reoperation (79, 163).

3. Posterior vaginal wall is repaired to treat prolapse of the posterior compartment of the pelvic floor which basically involves rectocele. Usually a colporrhaphy is performed by plication of the connective tissues of the posterior vaginal wall, consisting in fascial tissues which are connected to the rectum by the third supportive level described by DeLancey, the perineal membrane and perineal body.

Levatorplasty can also be used for same purpose involving plication of the levator ani muscles over the rectum.

Colporrhaphy for the posterior vaginal wall repair can be approached from the vagina or anus. Trans-vaginal repair has shown less failure rates and recurrence of prolapse, but only when looking at enterocele (prolapse of the intestine) development (160), having similar success rates for rectocele repair.

As for the repair of the anterior vaginal wall, a mesh/graft can be used for the treatment of rectocele when performing posterior colporrhaphy to reinforce the supportive tissues. Same rectocele recurrence has been reported when comparing colporrhaphy with or without an absorbable mesh (158). On the other hand, non-absorbable synthetic grafts have shown high rates of anatomical cure and functional outcomes (164, 165) when used for posterior vaginal wall repair; although, again, they are more associated to complications (166).

#### 1.2.4.3 Surgical complications

Surgical complications of POP are classified, as for SUI, as intraoperative and postoperative complications.

Intraoperative complications are the same as described for SUI which may involve direct injury of pelvic organs, blood vessels or nerves, depending on the approach and procedure.

The main postoperative complication is the recurrence of the specific prolapse surgically treated, or any other POP derived from the procedure.

Also SUI has been described to be a complication after surgical treatment of POP; although, it has been postulated that SUI may be developed at the same time as the prolapse condition, by an excessive distension or displacement of the vaginal wall which has an important role on the continence apparatus. Alternatively, a prolapsed organ itself may apply pressure on the urethra masking the SUI condition, which would only be expressed after the POP repair (167). Nevertheless, since similar surgical procedures are performed to treat both disorders, prolapse repair has always been considered to reduce the risk for SUI development (168, 169).

Abdominal sacrocolpopexy has also reported a small risk of ileus and small bowel obstruction (170).

Finally, although synthetic non-absorbable materials have shown better success rates than biological and absorbable synthetic materials, the last two types of materials are associated to low rates of complications. Non-absorbable materials may lead to erosion and extrusion, as well as contraction of these materials has been reported.

#### 1.2.4.4 Surgical outcomes

As for SUI, POP evaluation is divided into subjective measures, including validated questionnaires, and objective measures after clinical examinations which are the same used to determine the POP stages described above.

There are 3 main validated questionnaires which assess POP symptoms and quality of life (18).

Anatomical measurements are used to determine the persistence of POP; however, as above, this is difficult to interpret since a high percentage of women with some degree of prolapse are asymptomatic (171). Furthermore, patients after surgical treatment of POP are never going to present POP-stage 0, which is only found in healthy parous women (women having given birth to one or more children) (117).

### **1.3 Comparison of SUI and POP**

Including both conditions, pelvic floor disorders affect nearly one third of pre-menopausal women and nearly half of post-menopausal women (172).

Furthermore, it has been reported that the lifetime risk of undergoing a surgical procedure for SUI or POP by age 80 is 11.1%, with 30% of these requiring additional surgical procedures for recurrence of the same condition (173).

As above, POP can be a risk factor for the development of SUI. Same anatomical structures and tissues affected in the prolapse of the anterior vaginal wall may lead to SUI as well. On the other hand, a prolapsed organ itself from another compartment, may lead to laxity of the endopelvic fascia and consequent alteration of the continence mechanism. So, while the first event may lead to development of both conditions at the same time; in the second event, the prolapse occurs first which may cause later the incontinence condition.

Two types of prolapse of the anterior vaginal wall have been described (174). Distention of the anterior vaginal wall entails weakness of para-vaginal tissues supporting the urethra and bladder too. Alternatively, displacement of the anterior vaginal wall is attributed to the detachment or elongation of the ATFP.

As previously described, the continence apparatus is composed by levator ani muscle attached by arcus tendinius ligaments to the fascia of the anterior vaginal wall which, in turn, is connected to the urethra. Therefore, after levator ani contraction the vaginal wall gives urethral support/pressure.

Both types of prolapse of the anterior vaginal wall may have, as above, a parallel effect on SUI condition. And, while the distention of the anterior vaginal wall affects the continence mechanism at the supportive level of the urethra made by the para-vaginal connective tissues (endopelvic fascia); the displacement of the anterior vaginal wall affects the continence apparatus at the level of the arcus tendinius ligaments.

As mentioned previously, any type of POP can mask SUI symptoms by pressure from the prolapsed organ on the urethra. That is why SUI has been described after POP surgical treatment as a surgical complication.

In one study 151 women with POP were analyzed by MRI, and it was found that higher levator ani defects were associated with obstructive voiding and smaller SUI symptoms. Also, by ultrasound during coughing, same patients did not show SUI symptoms (175). Nevertheless, levator ani defects have also been associated with SUI when comparing anatomical measurements between primiparous women with or without SUI and nulliparous asymptomatic women. By ultrasonography during coughing, vesical neck movement, which is associated with a defect of the levator ani, was found only in the primiparous group with SUI. Moreover, no differences on urethral closure pressure were observed between groups (16). Other studies also found anatomical differences in levator ani muscle only in women with SUI who had delivered at least one child (176, 177), but not in middle age or elderly SUI nulliparous women (178).

On the other hand, urethral closure pressure seems to be the main problem associated with SUI. 103 incontinent women and 108 asymptomatic women were analyzed in the Research On Stress Incontinence Study (ROSE). After matching BMI and using a cough predictor, 61% of the incontinent women showed significant differences on urethral closure pressure, but not on levator defects (179). Furthermore, SUI in aging women has been associated with a decrease in the fibres of the circular smooth muscle of the external urethral sphincter (rhabdosphincter) when compared with young women (180). Another study found the same tendency of a reduction of the urethral function in elderly population due to a decrease in the striated muscles cells of their rhabdosphincter (181).

Consequently, while anatomical alterations are obviously observed in women with POP and these can be also found in women with SUI due to obstetric factors, a decrease of urethral closure pressure seems to be the main pathological alteration for development of SUI.

DeLancey postulated after looking at young and old nulliparous populations (16) an association between the development of SUI in young women and levator ani muscle anatomical defects, due to obstetric factors such as pregnancy and vaginal delivery whereas, in the elderly population SUI would be related to a decrease of the urethral closure pressure (16).

In summary, POP commonly associated to anatomical alterations, may be more likely to develop in young women by a traumatic process such as pregnancy and vaginal delivery. In addition, either anterior vaginal wall prolapse or overstretching of the para-vaginal tissues made by a prolapsed organ itself, which in turn are affected by anatomical alterations, may be responsible of SUI in primiparous women due to a traumatic process.

Alternatively, SUI is more likely to occur in elderly women with a higher prevalence, since the main problem with this condition is a decrease in urethral closure pressure which is most likely due to a decrease in the quality of the fascial para-vaginal tissues and/or urethral sphincter innervations, attributable to hormonal and aging factors.

Finally, although this section tries to allocate to each aging population different risk factors and pathological process for development of SUI and POP, both conditions have a multifactorial aetiology. Therefore, traumatic process in young women can also lead to a low level of urethral dysfunction, damage of para-vaginal tissues or anatomical alterations, which may be worsened by ageing leading to SUI and/or POP in elderly women.

## **1.4 Histology of the supportive tissues of the pelvic floor**

The histology of the fascial and muscular tissues of the supportive tissues of the pelvic floor has been widely investigated to explain differences between women with and without SUI and/or POP in terms of quality of these tissues. Similar to anatomical and functional differences described in previous sections, the histological differences may explain the development of SUI and POP compared to the asymptomatic group and differences between young and elderly populations.

When we specify the supportive tissues of the pelvic floor, usually, we are referring to the subepithelial connective tissue and a layer of smooth muscle, which together give a fibromuscular support, surrounded by loosely connective tissue, adventitia (182).

Moreover, the two main risk factors, including ageing and vaginal delivery, for development of SUI and POP have shown pathological defects of different connective and muscular tissues of the pelvic floor.

Light and electron microscopy have been the main techniques used to look at the pathological alterations of these tissues.

Using Gibson and Masson's trichrome staining and electron microscopy, alterations in the composition of all these tissues have been described when looking at biopsies from the cardinal ligaments of 10 aging women with POP and 10 asymptomatic aging women, matching for the same age, gravid number, parity times, number of pelvic surgeries and menopausal status. Loose connective tissue was described in POP patients as production of less dense extracellular matrix (ECM) with fibroblasts more dispersed, and fibres from muscle tissue were packed less regularly and densely and more widely spaced (183).

In rats, after vaginal delivery, the same findings were made in the connective and muscular urethral surrounding tissues by histological analyses (184).

#### **1.4.1 Connective/fascial tissue of the pelvic floor**

Connective tissue from the pelvic floor is composed mainly of fibroblasts, but also, it contains fat and mast cells and a few smooth muscle cells (figure 1.11). Fibroblasts synthesize the fibrillar components of the ECM which provide the mechanical properties of these tissues. Collagen and elastin are the main fibrillar components of the ECM of this tissue, which are embedded in a non-fibrillar ground substance (glycoproteins and proteoglycans) and are said to be in a process of constant dynamic remodelling (182).

The weakness of fascial supportive tissues of the pelvic floor is central to the development of SUI and POP. Histological studies have contributed to determining the importance of the quality of suburethral fascial tissues to the development of SUI, or the quality of connective tissues from other supportive levels of the pelvic floor for the development of the different types of POP.

In 1986 histological differences in connective tissues between 10 women with POP and 10 women without POP were described related to laxity of pelvic tissues of the first group (128). Not only the synthesis of those structural proteins but also the balance

between the activity of the major proteolytic enzymes that degrade them and the inhibitors of proteolysis are important components to consider in studies of the pathogenesis of the connective tissues of the pelvic floor.

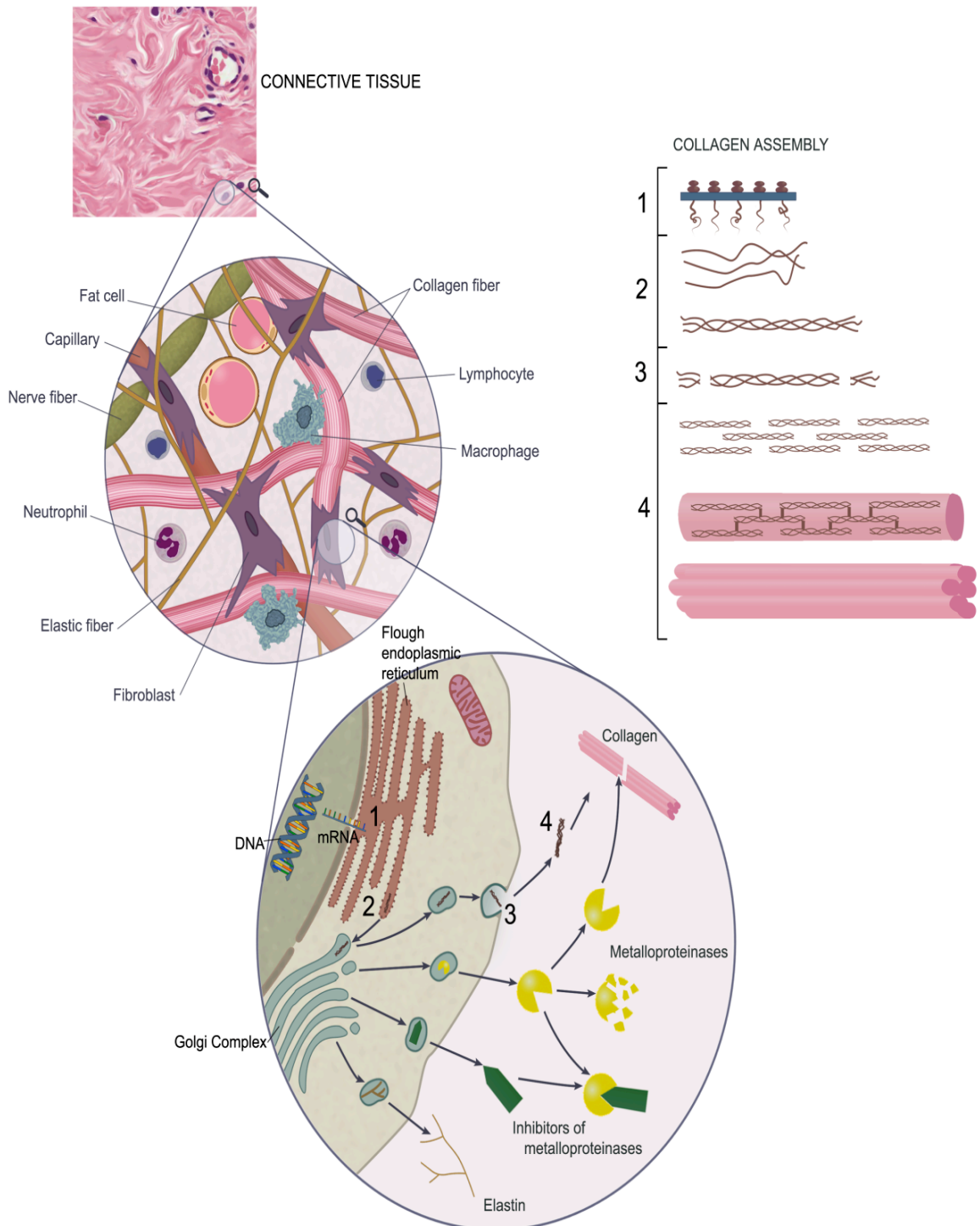


**Figure 1.11** Histological appearance of connective tissue, its cellular and extracellular matrix (ECM) components, and synthesis and assembly of the main fibrillar components of this ECM and its major proteolytic enzymes and inhibitors of proteolysis.

#### 1.4.1.1 Collagen

The synthesis and formation of collagen fibres were described many years ago by Ramachandran and Kartha (185). Fibroblasts synthesize a triple helical structure (procollagen) inside the endoplasmatic reticulum and then it is secreted into the extracellular space. This triple helical structure is the union of 3 collagen molecules inside of the fibroblasts which synthesise these. These twist together by numerous hydrogen bounds after post-translational modifications of proline and lysine residues. In the extracellular space, the triple helices become tropocollagen through covalent cross-linking by carboxyl- and amino-terminal peptidases action. The tropocollagen undergoes self-assembly into collagen fibrils which are finally packed into fibres (figure 1.11).

In soft tissues there are 3 main kinds of collagen. The relative quantity of them determines the strength of the tissue. Collagen I, found in most connective/fascial tissues, gives the greatest resistance to tension. Collagen III is predominantly found in tissues subjected to periodic stress, as articulations, producing increased flexibility and distension (186). Finally, there may be small fibres of collagen IV which have very low strength and are normally found around blood vessels. All three collagen types copolymerize to form fibrils. The mechanical characteristics of the tissue are influenced basically by the ratio of collagen I/III; if it increases there is greater strength; if it is decreased then tissue laxity is increased (186). Increases in collagen III and IV generate thinner collagen fibres in connective tissues (187).

Two mechanisms of collagen maturation have been described, as well as, how these processes are affected by aging. Both involve unions of fibres of collagen, but, while one is related to unions made by lysine aldehyde cross-links (188), the other, called the Maillard reaction or glycation reaction, binds collagen fibres by the addition of glucose leading to a stiffer tissue which is therefore more fragile (188, 189).

The degradation of collagen is produced by pro-enzymes synthesized in fibroblasts and which need to be transformed in active form in the extracellular space through an enzymatic action related to growth factors, growth factors binding-proteins, cell surface receptors and cell-cell-adhesion molecules (190). The enzymes which influence collagen breakdown are known as matrix metalloproteinases (MMP). MMP1, 8 and 13



are neutrophil collagenases with the function to degrade fibrillar collagen. The resulting denatured peptides are degraded by gelatinases, MMP2 and 9. All these MMPs are inhibited by tissue derived inhibitors of metalloproteinases (TIMPs), serum-borne inhibitors (191) and also they can suffer spontaneous inhibition by autocatalysis (192) (figure 1.11).

Collagen plays an important role in the mechanical properties of the connective tissue of the pelvic floor, which has been described in many studies. In elderly and menopausal women, the occurrence of POP is increased, at the same time, decreases of tensiometry resilience have been found at level I of supportive tissues of the pelvic floor (uterosacral ligament) (193). Lower mechanical properties of the endopelvic fascia of the vaginal wall from women with POP have also been reported, negatively correlated to age and menopausal status (194).

It is difficult to summarise simply the relationship between the dynamic process of collagen synthesis and breakdown and POP development as different studies look at patients with different POPQ, or do histological analyses of biopsies taken from different places. However, all of these studies include women matched for age, BMI, parity, and pre or postmenopausal status. The review of these studies to describe changes in connective tissue properties in pelvic diseases is within the scope of this thesis, however this has been done in great detail by Kerkhof recently (124).

Summarizing this and including some new studies, biopsies of fascia of the vaginal wall of women with POP and SUI have shown collagen I increase (195) and, in other study, collagen III decrease (196). At this anatomical point, a higher collagen concentration, probably of collagen I, could suggest more rigid connective tissue with impaired mechanical functions.

It has been shown that uterosacral ligament samples from women with POP demonstrated reduced resilience. Only one study found increase of collagen I at this level by histological analyses (195). On the other hand, other study found a reduction in collagen I (197), and an increase in collagen III was described in another study for the cardinal ligament of women with POP (198). Therefore, at level I of vaginal supports, the ratio of collagen I/III may be decreased by collagen III augmentation which would increase the laxity of these tissues and, at the same time, the strength of the tissue may be reduced due to a decrease in collagen I. The ratio of collagen I/III is similarly reduced at the ligaments of the level I (ATFP) of women with POP by decrease of

collagen I (199), which has been also observed in peri-urethral ligaments of women with POP and SUI (200-202).

Therefore, while in younger women the collagen I/III ratio is decreased in pelvic tissues as a result of damage to these tissues in obstetric trauma, in older women the para-vaginal fascia show an increase in collagen I production as a result of altered metabolism leading to dysfunction of the continence apparatus.

Contradictory results have been described for MMP activity. In the uterosacral ligament of women with POP the expression of MMP1, 9 (197, 203, 204) and MMP2 (205) is increased compared with the asymptomatic group, while other studies have not shown any differences for same enzymes or their inhibitors (205, 206) between the two groups. The same occurs for fascial vaginal wall tissues. An increase of MMP2 and 9 (207) activity in women with POP has been reported compared to the healthy population; however, it has been reported no differences for the expression of the same MMPs and its inhibitors (MMP2 and 3) in another study (208).

Alternatively, these studies do not look at the different ages of the patients which may explain the differences observed.

#### 1.4.1.2 Elastin

Elastin has an important role in the resilience of the connective tissue of the pelvic floor allowing the tissue to come back to its original position after elongation (209). While elastin biosynthesis is limited to a brief period of development in some tissues, in tissues of the reproductive tract its biosynthesis seems to be constant (210). This may be important for overstretching of these tissues during pregnancy and vaginal delivery. Lysyl oxidase (LOX) is the enzyme which catalyzes cross-link formation between tropo-elastin monomers in elastin assembly. The enzyme fibulin-5 is also responsible for assembling elastin fibres, and it has been shown that a decrease in fibulin-5 (211) or LOX (212) in women with POP may contribute to the development of this condition. Fibulin-5 is decreased in the connective tissue of women with POP obtained from uterosacral ligaments (213, 214), anterior vaginal wall (215) and para-urethral tissues (216). On the other hand, both enzymes have been demonstrated to be essential for recovery of POP. Fibulin-5 is increased in these same ligaments after injury and also in an advanced stage of POP (217).

Therefore it appears that a decrease in the production of fibulin-5 may contribute to developing POP in elderly women while damage of fascial pelvic floor tissues due to pregnancy or vaginal delivery leading to advanced POP in young women may lead to increased production of fibulin-5 for tissue recovery.

Several studies analyzed women with and without POP, matched for the same conditions, looking at elastin production in the connective tissue of the pelvic floor, including the major review by Kerkhof (124).

These studies seem to agree on the alteration in elastin metabolism in cardinal or uterosacral ligaments (198, 218, 219), and in anterior vaginal wall or peri-urethral fascial tissues (220-223) of women with POP. Some of these studies found a decreased expression of mRNA of elastin when culturing fibroblasts isolated from these tissues (218), or a decrease in total content of elastin of same tissues (219, 220). Similarly, other studies reported a reduction in endogenous inhibitors of elastases (222), or augmentation of elastolytic activity (223).

#### 1.4.1.3 Fibroblasts

Fibroblasts from connective tissue of the pelvic floor are responsible for collagen and elastin synthesis which will affect the mechanical properties of these tissues.

Endothelin-1 is expressed in fibroblasts with an important role in regulating their contractibility. Vaginal myofibroblasts from women with POP showed reduction in both their contractibility and the regulator of endothelin-1 expression compared to fibroblasts from asymptomatic women (224). Also, higher contraction of cells was observed in vaginal myofibroblasts from primiparous young women compared with vaginal myofibroblasts from multiparous young and old women with severe POP (225).

Fibroblast proliferation and biosynthesis of the ECM components is thought to be regulated by the strength of the tissue. Greater strength found in prolapsed pelvic tissues, as previously described for fascial tissues of the vaginal wall, may promote fibroblast proliferation, as a healing natural process, in a disorganized manner with an altered cytoskeleton architecture (226).

Expression of mRNA for p53 protein is decreased in fibroblasts from cardinal ligaments of women with POP, and this leads to an inability of cells to enter quiescence (G0 phase), and therefore, cells keep dividing and do not produce ECM components (218). Transforming growth factor- $\beta$ 1 (TGF- $\beta$ 1) is released from fibroblasts and stimulates collagen and elastin production. A reduction in TGF- $\beta$ 1 in fibroblasts from the vaginal wall has been reported in women with SUI (227). Previous *in vitro* studies showed similar collagen production from fibroblasts isolated from vaginal wall of women with and without POP (228) however, this may be explained by POP being related to another pelvic anatomical level.

#### 1.4.1.4 Estrogens

Estrogens have been used to treat SUI and POP by stimulating ECM biosynthesis (229-232). Since aging is a major risk factor for development of both conditions, how estrogens may affect the quality of connective tissues of the pelvic floor has been investigated in women after menopause (233).

The importance of the expression of estrogen receptors (ER) for ECM proteins production has been described (108 UI). However, while some investigators describe ER decreases in women with POP (233, 234), another study found ER increases in women with POP (235).

Estrogen replacement in women leads to an increment in the production of collagen I and III (62-64). Estrogen replacement in Macaques with POP also induced increases in collagen formation in para-vaginal connective tissue (62). With estrogen replacement, an increment in TIMP and a reduction in MMP was observed in para-urethral vaginal wall tissues of women with POP and without SUI, but not for patients with SUI associated with muscle dysfunction of the urethral sphincter (236).

This suggests a positive role of estrogens in collagen metabolism. However, it has been postulated that estrogen replacement stimulates collagen synthesis leading to immature cross-links which can be easily degraded by MMP, resulting finally, in a reduction of the collagen fibres of the ECM (207). This may explain the, previously described, low success rates of estrogen replacement in women with SUI (237). On the other hand, this low success rate may also be explained by its lack of success in the treatment of women with urethral sphincter denervation, who would have normal collagen production.

It was postulated that both estrogen and progesterone (P4) are required to reduce MMP synthesis in connective tissue of the pelvic floor (238). Administering 17 $\beta$ -estradiol (E2) and P4 in POP rat models and in the medium of fibroblasts isolated from the arcus tendinous of pre and postmenopausal women was shown to reduce MMP13 (239). Also a decrease of collagen I, and therefore a decrease of the ratio of collagen I/III, was found in ATRP of postmenopausal women compared to premenopausal women; however, after treatment with both estrogens and progesterone, collagen I and the ratio of collagen I/III were increased (199).

Latent TGF- $\beta$ 1-binding protein-1 (LTBP-1) regulates TGF- $\beta$ 1 activation and stimulation of ECM production by fibroblasts. TGF- $\beta$ 1, LTBP-1 and elastin microfibrils have been shown to be regulated by hormone therapy due to significantly decrease production of LTBP-1 in fibroblasts isolated from women with SUI (237). Later, it was found that similar results were obtained by relaxin treatment; a hormone secreted during pregnancy. In both, fibroblasts isolated from asymptomatic women and women with SUI showed decreased TGF- $\beta$ 1 production at high levels of relaxin (227). All this may suggest a regulation of the quality of the ECM of the fascial pelvic tissues during pregnancy to allow elongation by loosening these tissues.

Finally, the amount of E2 and follicle stimulation hormone (FSH) in serum was studied in 80 patients with SUI, matched for same characteristics and excluding POP. Premenopausal patients with SUI had more mobile proximal urethras and higher urethral pressures than postmenopausal patients with SUI. Only in postmenopausal patients, E2 did have a negative correlation with urethral mobility. In all subjects FSH was positively correlated with post void residual volume and flow times (240).

The role of the female reproductive hormones in connective tissue disorders of the pelvic floor is complex and highly regulated and more studies are required for a better understanding.

#### **1.4.2 Muscles of the pelvic floor**

Muscles of the pelvic floor, such as the anterior vaginal wall, are composed of epithelium, lamina propria, muscularis and surrounded by adventitia. The smooth muscle fibres of the muscularis allow the attachment to the levator ani muscle (241).

Biopsies of the apex of the anterior vaginal wall from 11 women with POP and 8 controls were analysed looking at smooth muscle alpha actin antibody staining and Masson's trichrome. Vaginal smooth muscles from controls were packed in bundles orientated in circular and longitudinal directions. Women with POP showed smaller smooth muscles bundles, fewer in number and poorly orientated. Collagen fibres were dispersed around the muscularis in women with POP while dense and compact collagen was found in women without POP (242). In addition, a decrease in the expression of smooth muscle proteins, such as alpha actin, in the anterior vaginal wall of women with POP was reported (243).

Culture of smooth muscle cells under hypoxia leading to cell apoptosis as consequence of denervation or trauma of the muscle showed an increase of cell migration and decrease of its contractibility capacity (244). Similar study demonstrated that myofibroblasts cultured under hypoxia may also modify the synthesis of collagen and hence the viscoelastic properties of the vaginal wall (245). On the other way around, it is possible that alterations of the collagen and blood vessels which surround muscle may have some effect on apoptosis of smooth muscle cells too (246).

Smooth muscle can adapt its contractibility in response to mechanical strength or trauma (247).

Caldesmon protein inhibits actin-activated myosin magnesium adenosine triphosphate activity, what is required to generate contractile force. Myosin phosphorylation (248) and calcium/calmodulin (249) are the main two mechanisms involved in smooth muscle contraction and are regulated by Caldesmon (250). This protein has been reported to be reduced in the vaginal wall of women with POP (251).

A study of the contractile response of the anterior wall muscularis of 6 women with POP, at least at stage III (3 of them with posterior wall prolapse too), and 6 controls showed an increased contraction in controls compared to women with POP after administration of KCl and phenylephrine (adrenergic agonist). These results were also consistent with a lower percentage of co-localized alpha-1A-adrenergic receptors and smooth muscle alpha actin in muscularis of women with POP (252). A reduction of sympathetic regulation may suggest nerve damage of the endopelvic fascia.

The smooth muscle of biopsies from uterosacral ligaments were studied in 9 women with POP and 9 women without POP, without significant differences in age, parity, menopausal status or hormone replacement therapy. Contradictory to above, the study

concluded there was an increase in mRNA expression of Caldesmon and an increase in the staining of Caldesmon associated with smooth muscle actin protein in women with POP (214).

Apoptosis of the cells of the uterosacral ligament has been reported in women with POP, what was thought to be due to a decrease in the neovasculature of the smooth muscle (246). Nevertheless, this apoptosis has been attributed to a reduction in the mitochondrial genetic material (mtDNA). A decrease in mtDNA and an increase in a deletion of the mtDNA (base number 4977) were positively correlated to an advanced stage of POP comparing the uterosacral ligaments of 45 women with POP and 38 controls (253).

Mitochondrial damage was also found in the levator ani muscle of women with POP. Biopsies of levator ani muscle of 3 women with III and 3 women with IV POP stage, diagnosed by POPQ, were subjected to histological analyses. Many myofibres from the cytoskeleton of smooth muscle cells did not stain for cytochrome c oxidase and succinyl dehydrogenase suggesting mitochondrial dysfunction. Also, Gomori and Masson's staining confirmed necrotic cells with loose myofilaments, again, a sign of abnormal mitochondrial accumulation (254).

Oxidative stress may play a role in mitochondrial damage since myogenic or neurogenic damage of the levator ani muscle has been also observed after vaginal delivery (255), in premenopausal women (256), as well as for women with POP. This suggests that apoptosis and mitochondrial damage of muscular cells may happen due to a traumatic process, such as vaginal delivery, leading to functional deficiencies of the pelvic floor muscles and being a cause of SUI or POP. Nevertheless, this has not been demonstrated and, on the other hand, it needs to be considered that the progression of POP may damage these tissues leading to this apoptosis and mitochondrial damage.

Finally, the Homebox A11 (HOXA11) gene for embryogenic development has been suggested to be involved in the maintenance of smooth muscle and collagen of the uterosacral ligaments, thus defects in this have been described as been a risk factor for the development of POP (257).

In summary, some of the anatomical and functional pathologies among young and elderly women with SUI and POP, which were summarized in the previous section, are

consistent with abnormal cellular features and changed quality of the ECM of the tissues of the pelvic floor.

As previously described, dysfunction of the continence mechanism or development of POP in young women due to a trauma may develop in parallel. This fact is supported by injury of the ligaments of the anterior vaginal wall shown by a decrease of collagen I leading to higher production of collagen III. Collagen III is the first collagen type to be produced after injury, before tissue remodelling happens and stable fibres of collagen I are formed. Therefore, this augmentation of collagen III fibres may be associated with laxity of the ligaments of supportive level II of the vagina (arcus tendinius) leading to displacement of the anterior vaginal wall. In addition, similar results have been observed for the supportive ligaments of level I of the vagina leading to uterine prolapse. All this suggests that injury of ligaments is more likely to be the responsible in young women for the development of SUI and POP, which in turn, is more likely to occur due to a trauma in childbirth (table 1).

On the other hand, dysfunction of the urethral sphincter and/or defective metabolism of ECM components of the supportive fascial tissues of the vagina and urethra are more common in elderly women. The connective tissue of the vaginal wall, endopelvic fascia, has been shown to become rigid due to poor remodelling of this tissue in ageing with higher amounts of collagen I (table 1).

	<b>Tissues affected</b>	<b>ECM alterations</b>	<b>Fibroblast behaviour</b>	<b>Explanation</b>
<b>Elderly women</b>	Endopelvic fascia	Increment of collagen I due to maturation process	Decrease of collagen production and contractibility	Poor metabolism and ECM remodelling affecting viscoelastic properties (tissue more rigid)
<b>Young women</b>	Uterosacral and pubo-urethral ligaments and ATPF	Decrease of the ratio collagen I/III	Normal behaviour	Tissue laxity due to collagen III production after traumatic process

**Table 1** Summary of connective/fascial tissues of the pelvic floor of women with SUI and POP.

Looking at the cellular level, it is again suggested that trauma is likely to lead to the development of SUI and POP in young women since fibroblasts isolated from connective tissues of this group have shown a normal behaviour in terms of



contractibility and collagen production. These same two parameters were reduced when were analyzed for same cells isolated from aging women (table 1).

Also when looking at the menopausal status, especially for women with SUI, premenopausal patients showed more mobile proximal urethras and higher urethral pressures than postmenopausal patients, suggesting again, higher functional and anatomical deficiencies for younger women due to obstetric factors, and pathological cellular activity for elder women.

Finally, studies of the muscles of the pelvic floor also agree with previous results when comparing women with POP and asymptomatic women (table 2). Muscularis of the vaginal wall shows fewer fibres with poorer orientation compared with controls, such as less smooth muscle alpha actin and less contractibility of the smooth muscle cells, associated with altered metabolism of these tissues in elderly women. Alternatively, ligaments of the supportive tissues of the vagina show normal contractility when looking at the caldesmon protein, and only apoptosis and mitochondrial damage was reported in these tissues, associated with oxidative stress which may be related to a traumatic process. Again, tissues/ligaments are more commonly damaged in young women by obstetric factors.

	<b>Tissues affected</b>	<b>Fibre behaviour</b>	<b>Explanation</b>
<b>Elderly women</b>	Vaginal wall muscularis	Low number of fibres, poor orientated and showing low contractibility	Poor cell metabolism
<b>Young women</b>	Uterosacral and pubo-urethral ligaments and ATPF	Normal fibre contractibility but cell apoptosis and mitochondrial damage	Oxidative stress after traumatic process

**Table 2** Summary of muscle tissues of the pelvic floor of women with SUI and POP.

We can conclude from last two sections that POP may be more commonly developed in young women due to pregnancy and vaginal delivery leading to damage of the ligaments of the supportive tissues of the pelvic floor, while SUI is more likely to develop in elderly women due to abnormal cellular behaviour and ECM production of poor quality. When SUI is developed in young women may be associated with POP due to an obstetric process, whereas POP in elderly women may be only related to distention of the anterior vaginal wall due to abnormal production of ECM of the para-vaginal

connective tissue (endopelvic fascia) with impaired mechanical function. Finally, any condition which develops in young women may also become worse with age.

### **1.5 Prostheses used for the surgical treatment of SUI and POP**

Although different supportive tissues of the pelvic floor may be affected on the development of SUI and POP, the same kind of anatomical, functional or molecular abnormalities are responsible for these conditions. Furthermore, these pathological alterations seen in different pelvic tissues have same aetiology and risk factors for young or elderly women and with SUI or POP. These may explain why similar treatments have been successfully used for both conditions.

Pharmacological, hormonal, and bulking agent treatments have not shown good results. These treatments are not used for POP where surgical treatments are required since big anatomical structures, such as the different pelvic organs, need to be relocated and held in place.

For SUI, pharmacological treatments to stimulate urethral sphincter contraction or hormonal and bulking agent treatments to reinforce the urethral support have been widely used. Both approaches have shown low success rates. Pharmacological treatments used for a woman with SUI due to dysfunction of the continence apparatus may not have beneficial effect; in addition there are reported side effects of the drugs used. Alternatively, hormonal treatment to simulate collagen production of the para-urethral connective tissues or a bulking agent to similarly give more support and pressure to the urethra may not help those women with SUI due to denervation of the urethral sphincter.

Pessaries have shown very low success rates to treat SUI, but have been widely used to treat POP. Surgical treatments for both disorders have demonstrated better results than any other type of treatment, particularly in severe cases.

All types of surgical procedures to treat SUI aim for higher pressure and better support of the urethra by plicating and/or suturing native supportive tissues to other pelvic structures. However, when using native tissues, SUI surgical treatments have shown

decreased success rates after a few years follow-up leading to recurrence of the condition and requiring a second surgical intervention with an even higher risk of failure and recurrence. These procedures may fail due to weakness of the native tissues and that may explain why better outcomes have been described when using slings or tapes for SUI surgical treatment. Different kits and materials are used to introduce and fix the sling/tape, but all of them are placed underneath the urethra to hold and give urethral pressure/support.

Similarly, better outcomes have been described when using synthetic materials in surgical treatments to relocate the prolapsed pelvic organs. Different materials and kits are used for POP which, are completely different to SUI sling/tapes in terms of shape/size.

The same materials are used to treat both conditions. Normally, synthetic non-absorbable materials have higher initial success rates; however, these materials have higher complications, such as erosion and extrusion, compared to degradable synthetic materials and biological materials.

Physical and mechanical properties are described in this section, as well as the host response to different materials and how this may explain the outcomes found for all these materials.

Biological materials are classified as autologous grafts, allografts and xenografts. Tissue engineered prosthesis, made from a scaffold and a cellular component, and which have not yet been tested in clinical trials, are included in this section based on preliminary experimental data in animal models.

### **1.5.1 Non-degradable synthetic prostheses**

The use of synthetic meshes was introduced based on efficacy and safety data for their use in abdominal wall hernia surgery. In 1995, these materials started to be used for the pelvic floor when the concept of TVT through the retropubic space was introduced (258). In 1996, transvaginal mesh (Marlex® mesh) was first reported for urogynecological POP procedures (259). Later, the first mesh “kit” for POP was introduced in 2002 (260).

The overall estimated percentage of patients with SUI treated with synthetic meshes in USA in 2010 was 79% (206,000 patients); while for POP treatment with mesh used in

transvaginal repairs from January 2006 to December 2010, estimated by Medicare, was 45% (96,487 patients) (261).

In a 2010 survey in UK, practitioners involved in POP surgery (20% urogynecologists, 52% gynecologists interested in urogynaecology and 21% general gynecologists) were asked about the current management of POP (262). With respect to mesh use, 5.5% of cases with primary anterior vaginal wall prolapse, 30% of recurrent anterior vaginal wall prolapse and 86% of POP with concurrent SUI, would have been treated with synthetic meshes in their surgeries. The use of synthetic meshes for primary posterior wall prolapse was 5% against 26% in recurrent posterior cases. A similar study in New Zealand (263) found an even higher number of synthetic meshes used in primary anterior repair (14%), recurrent anterior repair (63%) and recurrent posterior prolapse (40%).

On the other hand there are rising concerns amongst professional and regulatory bodies regarding the long term safety of using synthetic mesh in the pelvic floor (264). Mesh erosion, infection, dyspareunia and/or chronic pain, occurs in 4-5% and 14% of SUI and POP mesh procedures, respectively (265, 266).

Synthetic meshes can be classified according to the material they are made of, by their pore size, their fibre diameter, their knotting or weave configuration (knitted, woven, non-woven nor knitted), the nature of the fibres (monofilament or multifilament) and by their resistance to degradation (absorbable, non-absorbable or composite). However, the majority of the synthetic implants used to treat POP and SUI are made of non-degradable polymers such as PPL, polyethylene and polytetrafluoroethylene (261). They are generally classified according to their porosity as type I – totally macroporous (pore size > 75µm), type II – totally microporous (pore size < 15 - 20µm), type III – mixture of micro and macro pores and type IV – submicron pore size (267, 268).

PPL macroporous monofilament type I are the main subtype of these non-degradable synthetic meshes used for clinical practices. They can be tailored to have pores large enough for macrophages and lymphocytes to pass through, decreasing the risk of infection (269), they have low cost to produce and have good handling characteristics (270).

The *in vivo* host response against PPL meshes indicates little alteration in the morphological properties after implantation (table 3) with little changes in their

mechanical properties when compared to natural materials (271, 272). New generations of PPL meshes tend to be less stiff than precursors, with a view to causing less erosion (273). Few studies found that the PPL filament thickness might influence the mechanical performance of the prosthesis *in vivo*. TVT has been found to have the lowest stiffness and this might be the reason why it has a higher success rate with lower rates of erosion (274, 275).

A case study based on the use of a silicone-coated PPL mesh reported no tissue ingrowth or fibrosis with the removed prosthesis (276). Nevertheless, many animal studies agree that PPL meshes provoke a fairly pronounced inflammation, leading to a massive cell infiltration into the scaffold and ultimately to new collagen production (276-285).

Although PPL meshes is the gold standard material used for the treatment of SUI and POP, currently the regulatory bodies are considering these meshes for no longer clinical use. The serious complications already mentioned above which have been arisen after several years using these materials has led to complaints from many patients. Regulators in UK (Medicines and Healthcare products Regulatory Agency, MHRA) and USA (Food and Drug Administration, FDA) issued these alerts leading to withdrawal of meshes in the USA (286). Furthermore, in March 2014, the European Commission requested a scientific opinion from the European Scientific Committee on Emerging and Newly Identified Health Risks about 'The safety of surgical meshes used in urogynaecological surgery'; with deadline on January 2015.

### **1.5.2 Degradable synthetic prostheses**

Degradable synthetic prostheses are designed to be absorbed by the body and stimulate fibroblast activity leading to long lasting fibrosis. The synthetic material is absorbed by macrophages and the material is replaced by new collagen fibres forming a healthy scar tissue (287).

The most commonly used materials are Dexon (polyglycolic acid) and Vicryl (polyglactic acid). Vicryl and Dexon are completely absorbed, after 30 and 90 days respectively.

A recent meta-analysis reported absorbable synthetic material to have a lower objective recurrence rate at 12 months compared to no mesh procedures (153). In addition, as

above, the use of these materials has been reported to cause less erosion or infection when compared to the use of non-degradable synthetic materials (153). Nevertheless, clinically, absorbable meshes have performed less well for treating prolapse compared to non-absorbable meshes as there are higher recurrence rates of prolapse in using these (152), and therefore, they have not become popular for surgical treatment of POP (158, 288). For these reasons the use of degradable materials as sub-urethral tapes for SUI is minimal too (289).

### **1.5.3 Autologous prostheses**

Autologous grafts are obtained from the patients themselves. The main autologous tissues used for pelvic floor reconstruction are fascia lata, which is the deep fascia of the thigh, or rectus fascia, which covers the skeletal muscle of the abdominal wall. Autologous grafts are mainly composed of connective tissue, containing packed bundles of collagen fibres orientated in parallel, which are synthesized by fibroblasts located within the fascia. Fascia functions to surround and bind structures reducing friction between them. Once the origin of the fascia that is to be used is decided on, it is acquired to be transplanted during the same operation. Autologous grafts are obtained by a skin incision to reach the fascia underneath. A desired strip of fascia is harvested by pulling it from the underlying muscles. The advantage of using autologous fascia is that it is a non-immunogenic material; however, this procedure leads to perioperative donor site morbidity which can be further complicated by incisional hernia or unsatisfactory cosmetic results (290).

The mechanical properties of autologous grafts commonly used for pelvic floor reconstruction were assessed in only 3 studies (table 4), which also assessed the mechanical properties of allografts, xenografts and synthetic materials. All these studies agree that autologous grafts showed lower values for mechanical properties before implantation compared with the others (291-293). Two of these studied the mechanical properties of autologous rectus fascia and anterior rectus fascia, respectively, implanted in rabbit vagina. Both showed no significant decrease in mechanical properties but the grafts showed a 50% decrease in the surface area of implants after 12 weeks implantation suggesting a high rate of degradation (292, 293). Following histological evaluation, one of these studies observed collagen remodelling with moderate collagen

infiltration, but also small fragments which were encapsulated (293), what had been described previously (294). The same study also found a minimal inflammatory response and minimal neovascularization after implantation of autologous grafts in rabbits.

Autologous grafts implanted under the urethrovesical junction in a SUI rat model after laparotomy showed a lower inflammatory response and collagen production compared with synthetic materials and xenografts (281). This was supported by a later study reporting minimal inflammatory responses and fibrosis after autologous grafts were implanted in rabbits (295).

In women, histological studies of transvaginal revision of autologous rectus fascia implanted in five patients with SUI (296) showed collagen remodelling, with longitudinally-organized connective tissue, in grafts explanted after 4 years, and no evidence of inflammatory cell infiltrates or foreign body reaction. Grafts explanted after 5 and 8 weeks already showed moderate and uniform infiltration of host fibroblasts, as well as neovascularization. Similar results were reported by assessing autologous grafts implanted in five patients who underwent sling revision (283). Grafts showed a moderate and uniform infiltration of host fibroblasts, as well as little neovascularization. Collagen fibres were organized longitudinally and samples displayed no evidence of encapsulation or infection. Nevertheless, moderate degradation of the grafts was reported.

In summary, autologous grafts seem to be well accepted by native tissues due to the autologous source of the biological material. This material undergoes moderate remodelling, although it can be quickly degraded. On the other hand, the major problem associated with autologous grafts is the limited amount of material that can be harvested and the risk of donor site morbidity, particularly for treating POP where a bigger amount of material is needed.

#### **1.5.4 Allograft prostheses**

Allografts are obtained from a donor of the same species. Those used for pelvic floor repair are usually from cadaveric origin such as fascia lata, dermis or dura matter. The use of allografts avoids the morbidities of perioperative tissues caused by autologous grafts, but the disadvantages of these materials are the fact that they can only be sourced

via approved tissue banks which are properly regulated (297) and even with well run procedures the risk of viral transmission can never be completely eliminated (290). Usually, allografts may have all the epithelium and cellular components removed, leaving behind an acellular biological matrix. Different companies that manufacture allografts have patented processes for optimum cellular removal to render them non-antigenic. Moreover, other treatments are required to transport and store allografts, such as cleaning and drying, that may affect the properties of the graft.

As above, although allografts present higher baseline of mechanical properties than autologous grafts (before implantation), significant decreases in these properties have been reported for human dermis and fascia lata after implantation in the vagina of rabbits (table 5). At 12 weeks post-implantation, mechanical properties were similar to autologous grafts after explantation (293, 298). Human cadaveric dermis and fascia have been found to be well integrated onto the abdominal wall of different animal models by moderate fibroblast infiltration, new collagen production and neovascularization (299-303). However, the same materials have shown opposite results when implanted in the pelvic floor area of the same animals. Missing and fragmented prosthesis were found after 12 weeks implantation on the vaginal wall explaining the, already mentioned, drop in mechanical properties. The study describes a higher degradation rate for cadaveric fascia compared with autologous and synthetic materials (304).

Other people also found reasonable levels of cell infiltration and angiogenesis when human cadaveric dermis and fascia were anchored around the bladder neck of rats; however, all samples presented some degree of encapsulation (305).

Upon re-exploration of failure of allografts in humans, many authors describe allografts as being absent (296, 306), or highly degraded with remained portions being acellular and encapsulated (283).

In summary, allografts are well integrated by rapid host cell infiltration and remodelling of their ECM. However, allografts are quickly degraded and, as seen in animals, the pelvic environment may increase this degradation.



### 1.5.5 Xenograft prostheses

Xenografts for pelvic floor repair are obtained from other species, particularly from porcine origin, either porcine dermis, or small intestinal submucosa (SIS). These tissues are de-cellularised and gamma sterilized, as allografts. In addition, they are usually cross-linked to make them less likely to be digested by collagenases (307).

Mechanical properties of porcine dermis have been reported to be a bit lower than allografts, but much higher than autologous grafts (293).

Xenografts implanted in different animals have given different histological results when comparing the 2 main grafts used in pelvic floor repair: porcine dermis and SIS (table 6).

One study assessed 4 porcine dermis xenografts implanted on the abdominal wall and 4 on vaginal wall of rabbits (293). Two xenografts were absent after explantation from vaginal wall, and the other two together with those from the abdominal wall showed a decreased of 84.1% of their mechanical properties. Similarly, the mechanical properties of cross-linked porcine dermis were assessed in another study before and after 9 months implantation on the abdominal and vaginal wall of rabbits (285). They found 36% and 46% degradation of these materials implanted into abdominal and vaginal walls respectively. Fragments of xenografts implanted which were not degraded, presented similar mechanical properties post-explantation compared to baseline values, while values of degraded materials decreased by more than 50%. Both studies agreed that the degradation of biological materials is higher when the inflammatory response against them is more vigorous; furthermore, the vaginal environment may accelerate this process.

A chronic inflammatory response has also been described in porcine dermal xenografts due to encapsulation leading to minimal neovascularization and collagen ingrowth (293). Similar findings were reported in a histological study of porcine dermal biomaterial upon explantation from 4 women requiring revision of their sling surgery (283). They reported severe graft encapsulation, without fibroblast infiltration or neovascularization. In addition, these results are again supported by studies with rats (305, 308), rabbits (309), pigs (303) and primates (310).

In contrast to porcine dermis, several studies of implanted SIS found high collagen ingrowth with a moderate degree of collagen remodelling and orientation, and high neovascularization (281, 302, 305, 311-317). In addition, after an initial decrease, mechanical properties were shown to be increased to the same or even above baseline values (311-313, 315). Only 2 studies reported an absence of host fibroblast infiltration, collagen ingrowth and neovascularization for SIS implanted in rats (308) and rabbits (304).

On the other hand, many studies agree with a very rapid degradation of the SIS which is replaced by the host tissue (311, 312, 317-320).

In a recent randomized study, Feldner et al. found significantly higher anatomical cure rates (86% Vs 59%) by using a SIS graft compared to a traditional colporrhaphy for anterior prolapse, at a 12 months follow up (321). Nevertheless, few clinical cases correlate with the 2 main situations observed in animal studies; so while encapsulated and acellular SIS was removed due to obstruction (322); a patient with recurrent SUI had no longer recognizable SIS, as it had been replaced by host tissues (323, 324).

In summary, xenografts used for the reconstruction of the pelvic floor, porcine dermis and SIS, have shown elevated degradation rates, although, SIS seems to be better integrated into host tissues with new collagen formation and neovascularization. SIS has achieved reasonable success rates when used to treat POP; however, there are many cases still reporting recurrence of SUI or POP with both materials due to rapid degradation of these materials, or an undesirable chronic inflammatory response due to encapsulation.

#### **1.5.6 Tissue engineered prostheses**

Tissue engineering has arisen from the necessity to combat tissue damage and organ loss caused by degenerative diseases or neoplasia. Organ failure in some instances can be treated with donor organ transplantation but life-long immunosuppression is required that often results in complications. Therefore, tissue engineering tries to develop more compatible biomaterials and, at the same time, studies the mechanisms for regrowth of damaged tissues for function restoration.

Tissue engineering is defined as the use of a combination of cells and materials for the development of biological substitutes to restore, maintain or improve tissue functions or

a whole organ (325). The fabrication of engineered extracellular matrices (scaffolds) from different materials allows one in the laboratory, to grow cells on them producing biologically active molecules and obtaining a functional, but also, biomechanically stable tissue to be transplanted into a body. Depending on the part of the body injured, the success of this procedure will require different cell types, but also, different scaffold materials. Also it is important to create a biological environment to stimulate the normal development of the engineered tissue in the lab, such as the use of native growth factors or hormones, mechanical simulation or the use of bioreactors; besides the logical use of the same native temperature, oxygen concentration, humidity, nutrients and osmotic pressure maintenance.

The scaffolds can be produced from biological and synthetic materials. There is a huge range of natural polymers used for soft tissue engineering and techniques to construct scaffolds of different dimensions and shapes. The matrices also can be harvested from autologous, allogeneic or xenogeneic tissues. Then the cellular components are removed from matrices for eventual implantation as showed in current treatments of POP and SUI.

Anthony Atala performed the first clinical trial with neo-bladders. Bladders of 7 patients with myelomeningocele (aged 4-19 years) were reconstructed with degradable synthetic materials seeded and cultured previously with autologous urothelial and muscle cells from the bladder (table 7). 46 months post-operatively, the mean bladder leak point pressure (LLP) decreased, and the volume and compliance increased with recovery of bowel function (326).

In addition, several studies have used successfully mesenchymal stem cells (MSCs) for bladder wall regeneration combined with biological matrices (327-330). Adipose-derived stem cells (ADSCs) have been seeded on a degradable synthetic material and cultured with smooth muscle inductive medium to differentiate them into the desired cell type. Once the cells started to express smooth muscle specific markers, the engineered tissues were implanted into the bladder of rats which previously had been partially cystectomized. 12 weeks after, viable ADSCs increased the smooth muscle mass of the bladder with higher contractile function (327).

In 2003, urethra reconstruction was firstly approached by tissue engineering using decellularized SIS (331).

In our group, acellular sterilised donor de-epidermised dermis has been used as a matrix to seed buccal keratinocytes and fibroblasts. These cells were isolated from buccal mucosa biopsies of same patients who underwent for urethroplasty by implantation of a tissue engineered buccal mucosa. After 3 years follow-up, three patients had a patent urethra with the engineered tissue *in situ*, although all three required some form of instrumentation (332). Using exactly the same approach, since last few years a product called Mukocell® has been commercialized in Germany.

In 2012, Anthony Atala was the first to develop neo-urethras. He used acellular collagen matrices from descellularized porcine bladder tissues which were seeded with epithelial and smooth muscle cells from rabbit bladder biopsies. As an autologous approach, the tubularized matrices seeded with the cells were implanted in the same rabbits after a urethral defect was created. Post-implantation, biopsies of the implanted urethras were assessed with organ bath studies and these presented both physiological contractility and the presence of neurotransmitters (333).

Again Anthony Atala, in 2003, was the first to develop an engineered soft tissue for reconstruction of the pelvic floor (334). A vaginal tissue engineered was developed from epithelial and smooth muscle cells isolated from the vagina of rabbits and seeded in quick degradable synthetic scaffold.

Recently, muscle-derived stem cells (MDSCs) have been cultured in SIS for a vaginal repair in rats after hysterectomy and partial vaginectomy. MDSCs differentiated into smooth muscle cells stimulating vagina tissue repair, with formation of an epithelium and preventing fibrosis (335). Later, a tissue engineered fascia has been created from vaginal fibroblasts seeded in another biodegradable synthetic material coated with collagen for its use to repair connective/supportive injuries of the pelvic floor (336). This engineered tissue was assessed by subcutaneous implantation and was well integrated in host tissues of mice creating neo-fascia *in vivo*.

This year Anthony Atala has published a clinical study after 8 years follow-up of 4 patients who had an implantation of neo-vaginas. Vulvar biopsies were obtained from patients with congenital vaginal aplasia. Epithelial and muscle cells were cultured onto biodegradable scaffolds to develop organs which were constructed and allowed to mature in an incubator. Vaginal organs developed with autologous cells were surgically implanted in each patient. After 8 years, structural and functional vaginal organs were found with no post-operative complications. By vaginoscopy, serial tissue biopsies and

MRIs, a tri-layered structure was present consisting of an epithelial cell-lined lumen surrounded by matrix and muscle (337).

Finally, engineered tissues have been produced to be used as slings to treat SUI animal models. Cannon was the first in 2005 using SIS seeded with MDSC and implanting the engineered tissue suburethrally by suturing it to the pubic bone. LLP measured by urodynamics was improved in rats with urethral sphincter deficiency developed by bilateral proximal sciatic nerve transaction (PSNT). However, same LLP values were found compared to acellular SIS slings implanted as controls (338). Later, a similar study used bone marrow stem cells (BMDSCs) seeded in a silk sling implanted via trans-abdominal and sutured to abdominal wall in female rats with PSNT too (339). Again same successful rates were found after implantation of the tissue engineered sling or the acellular sling. However, in both studies, ligament-like tissue was formed when tissue engineered slings were implanted, which was postulated as having potential for better integration and long-term retention since higher collagen production and tensile strength was assessed for the cell seeded groups.

MSCs have been the main cell type used to develop engineered tissues for the pelvic floor, as it can be noticed from above. MSCs have high proliferative potential as well as potential for tissue regeneration (340). Particularly ADSCs have shown the capacity to release different factors which can stimulate neovascularization, stimulate fibroblast proliferation and suppress an inflammatory response (341). All these properties, which are further discussed in Chapter 4, make these cells interesting to be used for tissue regeneration.

Therefore, also described in Chapter 4, these cells have been injected into the urethral sphincter to treat SUI. In animals, although it has been shown the capacity to use these cells as a bulking agent treatment of intrinsic urethral sphincter deficiency (342), injected MSCs have also shown the capacity to functionally recover the urethral sphincter. However, high number of MSCs is needed since many cells are not retained within the injection area. Alternatively, while the urethral sphincter is a well localized area, supportive tissues involved in POP may be too large for this approach where supportive materials are needed. The introduction of the cells in these tissues could be difficult too.

Fewer cells are needed if materials previously cultured with cells are implanted and which has a similar approach than current surgical treatments but stimulating regeneration of native tissues and aiming for a better integration than current materials. In addition, this approach has potential to keep the cells in place giving them space to proliferate.

Finally, although MSCs have a regenerative potential, they lose some properties when they have been differentiated (340). Undifferentiated and differentiated MSCs have been used for urethral sphincter regeneration and in less extent in tissue engineering of the pelvic floor. Using already differentiated MSCs has the advantage of driving the cell phenotype against the desired tissue-specific cell type. Also, since these differentiated cells have lost some properties such as potential for migration they will stay in the implanted place. On the other hand, undifferentiated cells will have higher potential to proliferate and release growth factors which can, for instance, stimulate neovascularization for better regeneration and integration into native tissues. However, these cells have the potential to migrate and differentiate into different cell types (340). MSCs could produce undesired types of tissues in the implanted place or other places. Therefore, many investigations are nowadays going through these issues to assess the safety of using these cells and to achieve their approval for clinical use. These issues are not within the scope of this thesis but, while these are tackled by other people, we aim for the potential of undifferentiated ADSCs based in previous research and which is again further discussed in Chapter 4. These cells have fibroblastic behaviour in culture and they do not differentiate without the appropriate stimulus (343). ADSCs cultured on different materials have shown the potential to proliferate and produce ECM due to their fibroblastic behaviour (343). Furthermore, after being implanted into native tissues of the pelvic floor, the signals received from the microenvironment may drive these cells into the desired tissue-specific cell phenotype. In a recent study with a dog model, undifferentiated ADSCs, fibroblasts and ADSCs differentiated into fibroblast-like cells using connective growth factor were implanted. They found that the three cell groups had a wound healing effect with formation of the same tissue expressing same markers. In addition, undifferentiated and differentiated ADSCs had better regenerative effect (344).

In summary, degradable synthetic material is not commonly used since it degrades very quickly leading to elevated recurrence rates, which are higher than biological and non-

degradable materials. Fewer complications have been reported with absorbable materials, since they produce the lowest inflammatory response compared to the other materials (319); however, alternatively, this leads to the lowest production of collagen which is necessary for long lasting integration and repair.

A study proved this concept by higher amount of collagen fibres produced when an elevated inflammatory response is developed (319). Compared to biological materials, non-degradable synthetic materials cause higher inflammatory response. Only porcine materials produce an extensive inflammatory response too, and these 2 groups have demonstrated higher fibroblasts infiltration and better collagen formation and organization, especially for collagen III (281, 283, 313, 319). Furthermore, these two materials have shown the highest success rates when used to treat SUI and POP in humans.

All type of prostheses have been shown to present different mechanical properties, but it has been already reviewed that mechanical properties do not predict the success of a prosthesis (345). However, as shown in this section, the host response against each specific material may have an important role on the success of these prostheses. A limited inflammatory response seems to be needed for a rapid neovascularization, fibroblast infiltration and collagen ingrowth in the implant leading to better integration into host tissues, as shown for PPL and SIS. Alternatively, while SIS can be degraded very fast leading to recurrence of SUI and POP, such as the other biological materials; PPL can evoke a chronic inflammatory response due to the persistence of the non-degradable synthetic material leading in long-term to erosion, pain or infection. The complications reported for these materials are not acceptable and there is a need to look for alternative materials to treat pelvic floor disorders.

Tissue engineering may overcome these complications by developing a long-lasting repair material with regeneration of its ECM driven by an autologous cellular component, and leading to better integration into the native tissues of the pelvic floor. Nevertheless, more studies need to be performed to determine which scaffolds and cells may be the best candidates to develop a tissue engineered repair material (TERM) designed for the pelvic floor, such as to describe the host response against them.

## 1.6 Aims

The aim of this project is to develop a cell-impregnated bioabsorbable material designed for the treatment of SUI and POP.

We hypothesise that the inclusion of an autologous cellular component offers the potential to drive the formation of new ECM for better integration into native tissues by neovascularisation and constructive remodelling achieving long-term mechanical integrity, whilst the degradable nature of the scaffold will hopefully avoid a harmful chronic inflammatory response.

To achieve and study this, the project was divided in the following main experimental objectives:

1. To study the physical properties, *in vitro* degradation rate and mechanical properties of our biodegradable scaffold candidate.
2. To look for the cell candidate with the ability to attach, proliferate and produce ECM on the scaffold for developing a TERM.
3. To determine good culture conditions in terms of the number of cells seeded and the period of culture, as well as, to investigate the effects of chemical and mechanical stimulation on cells during culture of the TERMS.
4. To study the host response against the TERM to learn about inflammatory and immune responses and the integration into host tissues looking into neo-vascularisation and neo-tissue formation.
5. To investigate the possibility of modifying the mechanical properties of the scaffolds by altering the manufacturing procedure. This involved examining how cells behaved on scaffolds with different fibre configuration and examining their mechanical properties.



6. To study the performance of ADSCs isolated from different donors for developing the TERM and to assess the maintenance of this potential after rapid isolation of these cells using new technology.

## **Chapter 2**

### **MATERIALS AND METHODS**

## 2.1 Electrospinning of Poly-(L)-lactic acid (PLA) scaffolds

Sterile Poly-(L)-lactic acid (PLA) scaffold was produced in the laboratory clean rooms (Good Manufacturing Practice (GMP) accredited) via the electrospinning technique (figure 2.1).

A solution of 10% PLA (Sigma-Aldrich, Dorset, UK) with Dichloromethane (DCM) was made one day before electrospinning to dissolve the PLA crystals in DCM overnight with a rotating magnet inside. Polymer solutions were loaded into 5 mL syringes fitted with blunt tipped stainless steel needles with an internal diameter of 0.8 mm (I&J Fisnar Inc.). 4 needles with 5 mL solution each were used at the same time delivering the solutions at a constant flow rate of 2.4 mL/h using a programmable syringe pump (Aladdin 1000) and solutions were electrospun horizontally with an accelerating voltage of 17 kV supplied by a high voltage power supply (Brandenburg, Alpha series III). Fibrous mats were collected on aluminum foil sheets (18 cm by 16 cm) wrapped around an earthed aluminum rotating collector (rotating at 300 rpm) 17 cm from the tip of the needle. Jet formation/stability was assisted by means of an aluminum focusing ring at a voltage of 17 kV, 5 mm behind the tip of the needle.

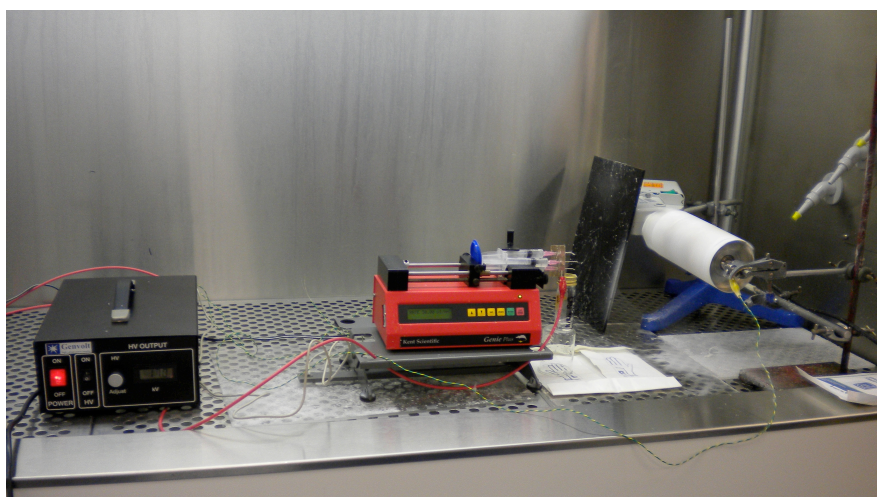


**Figure 2.1** *Electrospinning technique in a laboratory clean room.*

Everything was done under sterile conditions. All materials (foil, needles, tips) were autoclaved before their use and the electrospinning was performed in a GMP accredited clean room which maintains particulate-free air through the use filters employing laminar air flow.

After 2 h, a full sheet of PLA fibres (18 cm by 16 cm) was attached to the sterile foil. Then, using sterile gloves, forceps and scissors, the PLA sheet plus foil was collected and placed in a square Petri dish (20 cm<sup>2</sup>), which was closed with tape to maintain the PLA inside under sterile conditions.

Thereafter, the PLA sheet was heat annealed at 60<sup>0</sup>C for 3 h.

## **2.2 Isolation and culture of human oral fibroblasts (OFs) and rat and human adipose-derived stem cells (ADSCs)**

All procedures for human oral fibroblasts (OFs) and ADSCs were undertaken in a sterile laminar flow culture hood reserved specifically for human cell lines.

Rat ADSCs were isolated and cultured in Laboratory of Experimental Gynecology, Department of Obstetrics & Gynecology, University Hospital Leuven, Herestraat 49, B-3000 Leuven, Belgium, for animal experiments.

Human oral mucosa was selected as the source of fibroblasts. Tissue samples were obtained from normal volunteers with full and informed consent and ethical approval to produce small pieces of urethroplasty grafts which were surplus to requirements (346). All samples were handled on an anonymous basis under a research tissue bank license (number 08/H1308/39) under the Human Tissue Authority.

Specimens were cut into 0.5 cm<sup>2</sup> pieces and incubated overnight (12-16 h) at 4°C in (0.4%) Difco-trypsin plus 0.1% w/v D-glucose in phosphate buffer solution (PBS), pH 7.45 (Difco Labs, Michigan, USA). The epidermis was then manually parted from the dermis in a Petri dish. The epidermis was discarded and the dermis further minced with scalpel blades in a small volume of Dulbecco's Modified Eagle's Medium (DMEM) medium (Gibco Invitrogen, Paisley, UK) supplemented with 50 mL of fetal bovine serum (FBS) (Advanced protein products, Brierley Hill, UK), 5 mL penicillin (100 units/mL) and streptomycin (100 µg/mL), and 2.5 mL fungizone (630 ng/mL) (Gibco Invitrogen, Paisley, UK) (all experiments were in DMEM medium plus 10% FBS unless stated otherwise).

The minced dermis was transferred to a Petri dish containing 10 mL collagenase A (0.05% in DMEM medium) and incubated at 37°C in a 5% CO<sub>2</sub> atmosphere overnight.

The resulting suspension was centrifuged at 1300 rpm for 10 min and the pellet isolated and resuspended in DMEM medium. Thereafter a cell count was obtained to guide seeding into T25 flasks, which were seeded with a minimum of 5,000 cells per T25 flask incubated at 37°C in a 5% CO<sub>2</sub> atmosphere. Regular visual inspections were undertaken to observe cell morphology and exclude infection. Medium was changed 3 times a week and all cells were passaged prior to 80% confluence.

The passage procedure involved a wash in PBS followed by incubation for 5 min at 37°C 5%CO<sub>2</sub> atmosphere with 5 mL Trypsin/EDTA (Sigma-Aldrich, Dorset, UK) per T75 flask. Thereafter, the suspension was centrifuged at 1000 rpm for 5 min and the cells counted in a haemocytometer. Between 100,000 to 1,000,000 cells were added to each T75 flask, depending on the requirements.

As above, OFs were used from previous isolations. They had been frozen in 1 mL of 10% FBS with Dimethyl Sulfoxide (DMSO, Sigma-Aldrich, Dorset, UK), and in 1.5 mL cryogenic vials in liquid nitrogen at density of 1,000,000 cells per vial at passage 4. Each frozen vial was quickly defrosted adding 8 mL of DMEM medium. After that, the suspension was centrifuged at 1000 rpm for 5 min to obtain a pellet and eliminate DMSO which is toxic to cells at high concentrations. The isolated pellet was resuspended in DMEM medium to seed the cells at passage 5 in a T75 flask. Cells were utilized at passage 6 in the experiments.

Human subcutaneous fat was selected as the source of ADSCs. Biopsies were handled, from skin splits, on an anonymous basis under a research tissue bank license (number 08/H1308/39) under the Human Tissue Authority.

Samples were placed in Petri dishes, with 10 mL of PBS and 0.1 mL penicillin (100 units/mL) and streptomycin (100 µg/mL). Firstly, samples were mechanically minced with a scalpel and 10 mL of fat were collected in 50 mL tubes. The tissues were washed with 15-20 mL of 1% antibiotic (penicillin/streptomycin) in PBS by centrifugation at 1300 rpm for 5 min. The tissue was collected with a Pasteur pipette and collected in a new 50 mL tube. Twice of the volume of the samples was added for HANK solution. HANK solution is a saline solution to which it was added 0.1% collagenase type A (Roche Diagnostics GmbH, Mannheim, Germany), 0.1% albumin bovine fetal (BSA) (Sigma-Aldrich, Dorset, UK) and 1% antibiotic (penicillin/ streptomycin). 50 mL tubes were disposed in an incubator at 37°C for 40 min and they were periodically shaken for chemical disaggregation. Digested tissues were centrifuged at 1300 rpm for 8 min. The

floating fractions consisting of adipocytes were discarded and the pellets representing the stromal vascular fraction (SVF) were resuspended in DMEM medium. Cells were washed by centrifugation at 1300 rpm for 8 min with 20 mL of DMEM medium, and finally, pellets were resuspended and cells seeded with 5 mL of DMEM medium in one T25 flask. Cells were maintained at 37°C and 5% CO<sub>2</sub>.

After 24 h, non-adherent cells were discarded by washing with PBS. Regular visual inspections were undertaken to observe cell morphology and exclude infection. During all the period of culture, growth medium was changed 3 times a week. After one week, ADSCs reached 80%-90% confluence, and then, cells were detached by incubation for 5 min at 37°C and 5% CO<sub>2</sub> atmosphere with 2 mL Trypsin/EDTA (Sigma-Aldrich, Dorset, UK) per T25. Thereafter, the suspension was centrifuged at 1000 rpm for 5 min and the cells counted in a haemocytometer. 100,000 cells were added to a T75 flask. Cells between passages 3-6 were utilized in the experiments.

Rat ADSCs were also isolated from subcutaneous fat under ethical approval with license number LA 1210249 in the Laboratory of Experimental Gynecology, Department of Obstetrics & Gynecology, University Hospital Leuven.

After isoflurane anesthesia, a male Sprague-Dawley rat was sacrificed by neck dislocation and fat tissue was obtained after laparotomy; the rest of the protocol is exactly the same than for human ADCSs but pellets with SVF were seeded in a 6-well plate. Cells at passage 6 were utilized for the experiments.

## **2.3 ADSCs characterization**

### **2.3.1 Flow cytometry**

Human and rat ADSCs characterization by fluorescence-activated cell sorting (FACS) was performed in the Laboratory of Experimental Gynecology, Department of Obstetrics & Gynecology, University Hospital Leuven.

After 6 passages, the vascular cells from the subcutaneous human adipose tissue were analyzed by flow cytometry. The specific surface markers used were nine antibodies

(Ab) conjugated: mouse anti-human CD73-R-Phycoerythrin (PE) (1:100; BD, Pharmagien), mouse anti-human CD90-Fluorescein isothiocyanate (FITC) (1:100; BD, Pharmagien), mouse anti-human CD29-FITC (1:100; Acris), mouse anti-human CD105-PE (1:100; BD, Pharmagien), mouse anti-human CD44-PE (1:100; BD, Pharmagien), mouse anti-human HLA-a/b/c-FITC (1:100; BD, Pharmagien), mouse anti-human CD45-PE (1:100; BD, Pharmagien), mouse anti-human CD34-PE (1:100; BD, Pharmagien) and mouse anti-human HLA-DR-PE (1:100; BD, Pharmagien). As negative controls, cell aliquots were incubated only with isotype-matched mouse PE-IgG1  $\gamma$ 1 (BD, Pharmagien), mouse FITC-IgG1  $\gamma$ 1 (BD, Pharmagien), mouse FITC-IgG2 $\alpha$  (BD, Pharmagien) and mouse PE-IgG2b  $\kappa$  (BD, Pharmagien) under the same conditions.

To carry out this procedure, cells were washed with PBS and were detached by incubation with trypsin diluted 1:1 in PBS. After trypsin inactivation with DMEM medium and centrifugation at 1200 rpm for 5 min, pellets were resuspended with 5 mL of DMEM medium to count cells. 100,000 cells were transferred to cytometer tubes, for each Ab, and disposed in a float. Then, 1 mL of 1% Blocking Buffer, which contains 1% of BSA in PBS, was used to wash cells and to block nonspecific unions between Ab and other regions.

The samples were centrifuged at 1,200 rpm for 5 min and pellet was resuspended with 95  $\mu$ L of PBS and 5  $\mu$ L of each Ab, for each tube. Those were incubated at 37°C for 30 min in the dark at 4°C. The samples were washed with 5 mL of PBS, by centrifugation at 1200 rpm for 5 min, to eliminate excess of Ab. Pellets were resuspended in 500  $\mu$ L of 4% paraformaldehyde in PBS before analyze them using a FACScan flow cytometer with Cell Quest software. Data was analyzed using Flow Jo software.

Same analyses were performed for ADSCs isolated from rat at passage 4 but using seven conjugated Ab: mouse anti-rat I-E[ $\kappa$ ]-PE (1:100; BD, Pharmagien), mouse anti-rat CD90-FITC (1:100; BD, Pharmagien), mouse anti-rat CD29-FITC (1:100; Acris), mouse anti-rat CD31-PE (1:100; BD, Pharmagien), mouse anti-rat CD44-FITC (1:100; BD, Pharmagien), mouse anti-rat CD45-PE (1:100; BD, Pharmagien) and mouse anti-rat CD11b-PE (1:100; BD, Pharmagien). As negative controls, cell aliquots were incubated only with isotype-matched mouse PE-IgG2a  $\kappa$  (BD, Pharmagien), mouse FITC-IgG2a  $\kappa$  (BD, Pharmagien), mouse PE-IgG1  $\kappa$  (BD, Pharmagien) and American Hamster FITC-IgM  $\lambda$  (BD, Pharmagien) under the same conditions.

### 2.3.2 Adipogenic and osteogenic differentiation assays

At passage 6, 100,000 human ADSCs were seeded per well in a 6-well plate with DMEM medium.

After 24 h, culture medium was then replaced with specific differentiation inductive medium. However, one control for each cell type differentiation was cultured with DMEM medium changed every 3 days during 3 weeks.

For osteogenic potential cells were cultured with osteogenic induction medium containing 10 nM dexamethasone (Sigma-Aldrich, Dorset, UK), 50 µg/mL ascorbate-2-phosphate (Sigma-Aldrich, Dorset, UK), and 2 mM β-glycerophosphate (Sigma-Aldrich, Dorset, UK) in 4.5 mg/mL glucose-DMEM (GlutaMax™, Gibco Invitrogen, Paisley, UK) supplemented with 10% (v/v) FBS, 5 mL penicillin (100units/mL) and streptomycin (100 µg/mL), and 2.5 mL fungizone (630 ng/mL) (Gibco Invitrogen, Paisley, UK) for 3 weeks with medium changed every 3 days. Then, these cells and one control were fixed with 3,7% (v/v) paraformaldehyde for 20 min and washed with PBS. Fixed cells were stained with 1 mg/mL Alizarin Red™ solution (Sigma-Aldrich, Dorset, UK) for 30 min. After removing the staining excess with distilled water, several photos were taken with light microscope.

For adipogenic potential cells were cultured in adipogenic induction medium consisting of 4.5 mg/mL glucose-DMEM (GlutaMax™, Gibco Invitrogen, Paisley, UK) containing 10% (v/v) FBS, 5 mL penicillin (100units/mL) and streptomycin (100 µg/mL), 2.5 ml fungizone (630 ng/mL), 1 µM dexamethasone (Sigma-Aldrich, Dorset, UK), 0.5 mM methyl-isobutylxanthine (Sigma-Aldrich, Dorset, UK), 10 µg/mL insulin (Sigma-Aldrich, Dorset, UK), and 100 µM indomethacin (Sigma-Aldrich, Dorset, UK) for 3 weeks with medium changed every 3 days. Then, these cells and one control were fixed with 3.7% (v/v) paraformaldehyde for 20 min and washed with PBS followed by incubation with filtered 0.3% Oil Red O (Sigma-Aldrich, Dorset, UK) in 60% isopropanol (Fisher Scientific, UK Ltd.) (w/v) for 20 min. After excess stain was removed by washing with PBS, several photos were taken with light microscope.



### 2.3.3 Immunostaining for specific antigens

ADSCs and OFs were assessed in 2D culture immunostaining using Ab against fibroblasts and surface antigens of MSCs.

Primary Ab included mouse anti-human CD29, CD44 and CD73 PE conjugated (1:50; BD, Pharmagien); and mouse anti-human fibroblasts surface protein (1:50; Sigma-Aldrich, Dorset, UK) unconjugated. The secondary Ab, biotinylated anti mouse IgG (Vector labs, Peterborough, UK), was used against the primary Ab for anti human fibroblasts. A tertiary Ab, fluroescein-streptavidin (Vector labs, Peterborough, UK), was used, which binds the biotin molecule of the secondary Ab.

OFs at passage 6 and ADSCs from passage 3 and 6 were fixed in 3.7% formaldehyde, underwent for 10 min and were then washed in PBS thrice. Thereafter, samples were incubated in 0.5% Triton X for 20 min. After 3 washes with PBS, 10% goat serum was added as blocking buffer for 1 h. Samples were incubated with primaries Ab (diluted in 1% goats serum) and incubate for 1.5 h. After 3 more washes with PBS, samples incubated with anti fibroblasts Ab were incubated with biotinylated anti-mouse secondary Ab (1:1000 in PBS) for 1.5 h. Finally, these samples were incubated with tertiary Ab (1:100 in PBS) for 30 min, after 3 more washes with PBS.

All samples were again washed 3 times with PBS and 4',6-diamidino-2-phenylindole dihydrochloride (DAPI) (1:1000 in PBS) was added for 10 min.

After three washes in PBS, the fluroescein-streptavidin tertiary Ab used to detect the anti fibroblasts Ab was visualized using a green FITC filter through an Axon ImageXpress<sup>TM</sup> fluorescent microscope (Molecular Devices limited, Union city, CA). A Leica DM-IRB inverted research microscope (Leica, Bensheim, Germany) was used to visualize the 3 Ab PE conjugated using a red PE/Cy5 filter. Excitation and emission wavelengths:

- for DAPI were  $\lambda_{ex}$  385 nm/ $\lambda_{em}$  461 nm.
- for FITC were  $\lambda_{ex}$  495 nm/ $\lambda_{em}$  515 nm.
- for PE were  $\lambda_{ex}$  565 nm/ $\lambda_{em}$  670 nm.

For the 3 PE conjugated Ab, the same protocol was followed for fixed cells but avoiding incubation with any of these 3 Ab, which were used as negative control.

For the anti-human fibroblast protein surface, negative controls were performed for fixed cells following the same procedure avoiding incubation with primary and incubating only with secondary Ab and tertiary Ab.

## **2.4 Culture of OFs and/or ADSCs on PLA scaffolds**

### **2.4.1 PLA scaffold preparation**

Square samples of scaffolds cut at 2.5 x 2.5 cm (6.25 cm<sup>2</sup>) or 1.5 x 1.5 cm (2.25 cm<sup>2</sup>) were placed in a 6 well plates with a metal ring on top with a diameter of 2 cm or 1 cm respectively for cell seeding. All samples were wet with PBS for 30 min before seeding the cells.

### **2.4.2 Cell seeding**

Cells were detached by trypsinisation and counted before they were seeded onto the cut pieces with 2 mL or 0.5 mL of DMEM medium, depending on the size of the metal ring diameter (2 or 1 cm respectively) which maintains the cells on top of the scaffolds. After 2 h, to allow cell attachment, a further 5 mL of DMEM medium was added and the 6 well plates were incubated at 37°C in a 5% CO<sub>2</sub> atmosphere. We also included cell free scaffolds with or without DMEM medium as controls.

### **2.4.3 Metabolic activity assessed by AlamarBlue<sup>®</sup> staining**

AlamarBlue<sup>®</sup> (5 or 2.5 mL of 5 µg/mL of AlamarBlue<sup>®</sup> in PBS, AbD serotec, Kiddlington, UK) was added to each six well plate 2 h after seeding the cells. This was incubated for 60 min at 37°C in a 5% CO<sub>2</sub> atmosphere and then read at 570 nm (manufacturer's recommendations) in a colorimetric plate reader (Bio-TEK, NorthStar Scientific LTD, Leeds, UK) to obtain baseline values of colorimetric absorbance. On days 0, 7 and 14 of culture, each sample was washed with PBS and incubated with AlamarBlue<sup>®</sup> to assess metabolic activity at these time points.

#### **2.4.4 4',6-Diamidino-2-phenylindole (DAPI) staining**

DAPI was utilized to identify the presence and location of nuclei via fluorescence imaging. After culture for varying periods, small portions from samples were cut and fixed in 3.7% formalin solution (3.7% formaldehyde in PBS) for 10 min. After 3 washes with PBS, 0.8 mL of 1 ng/mL of DAPI (Gibco Invitrogen, Paisley, UK) diluted in PBS was added to each well (24 well plate) and incubated at 37°C in a 5% CO<sub>2</sub> atmosphere for 40 min. After 3 washes in PBS, the samples were observed through an Axon ImageXpress<sup>TM</sup> fluorescent microscope (Molecular Devices limited, Union city, CA) at  $\lambda_{\text{ex}}$  385 nm/ $\lambda_{\text{em}}$  461 nm. Samples were imaged through their depth in all quadrants.

#### **2.4.5 Total collagen production assessed by Sirius red staining**

Total collagen produced by the cells on the scaffolds was assessed using Sirius red staining. After the culture period constructs were washed 3 times in PBS and fixed in 3.7% formalin. Following further 3 washes with PBS samples were stained with 0.8 mL of Sirius red stain (0.1% Direct Red 80 in saturated picric acid, Sigma-Aldrich, Dorset, UK). After 16 h, excess stain was washed off with distilled water. The specimens were then patted dry and weighed. For a quantitative analysis, the stain from the samples was eluted with 2 mL 0.2 M NaOH-methanol 1:1 added to each well of the 12 well plates. After 10 min 50  $\mu$ L from each well was transferred into a 96 well plate to read the absorbance at 490 nm in a plate reader spectrophotometer (Bio-TEK, NorthStar Scientific LTD, Leeds, UK).

Data analysis involved calculating absorbance of stain per gram of dry construct. In addition, the difference in collagen stain absorbance per gram of construct between samples with cells and controls without cells was calculated to give an indication of “new collagen production” by cells on the scaffolds.

#### **2.4.6 Mechanical testing using BOSE electroforce tensiometer**

Uniaxial tensile testing was performed after periods of culture and all samples remained in medium until the time of testing. Samples were cut, partially dried, measured and then the moist samples were clamped in the tensiometer (BOSE Electroforce test

instruments, Minnesota, USA) (figure 2.2a). A small load cell was selected ( $< 22\text{ N}$ ) as this was found to be the most accurate during tuning.

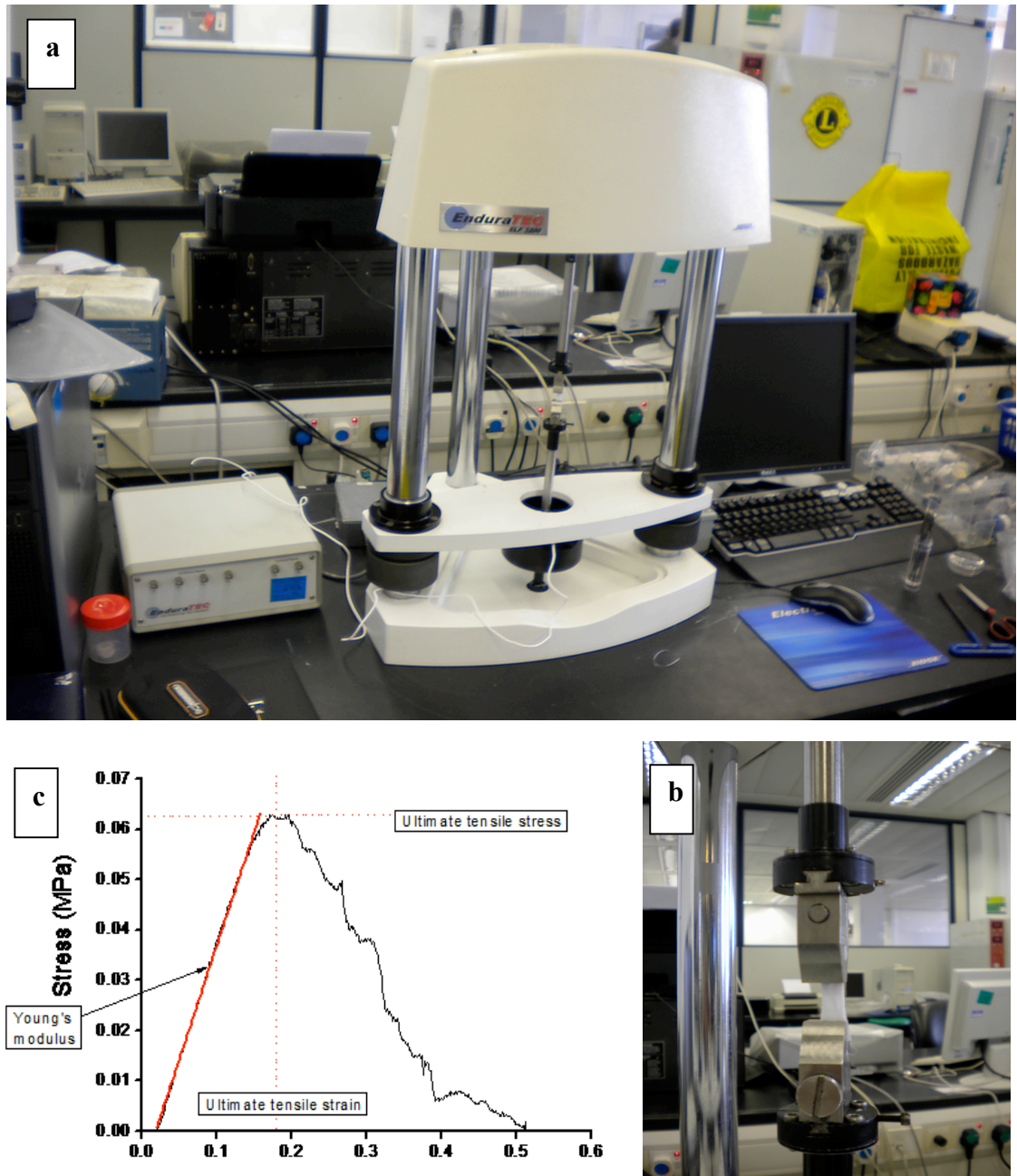


**Figure 2.2** (a) BOSE Electroforce test instruments. (b) Clamps stretching PLA sample. (c) Typical stress vs. strain plot resulting from testing of prosthesis on the BOSE electroforce instrument.

PLA material was tuned prior to commencing the experiments. A ramp test was applied at a rate of  $0.1\text{ mm/sec}$  with a maximum displacement of  $7\text{ mm}$ . The two grids stretch

each sample (figure 2.2b) and the load cell records the strength produced by the sample. Then, the first failure point or plateau was recorded as the load at failure (or ultimate tensile strength, UTS), and the displacement at this point was also recorded (strain at ultimate tensile strength). These values are represented in figure 2.2c, and the slope of this plot was later calculated for the Young's modulus (or elastic modulus).

#### 2.4.7 Contraction

Scaffold contraction on days 7 and 14 was calculated relative to day 0 using digital photographs (figure 2.2) and ImageJ software (NIH, USA). Cell mediated contraction was calculated by subtracting the difference between scaffolds with and without cells (controls).

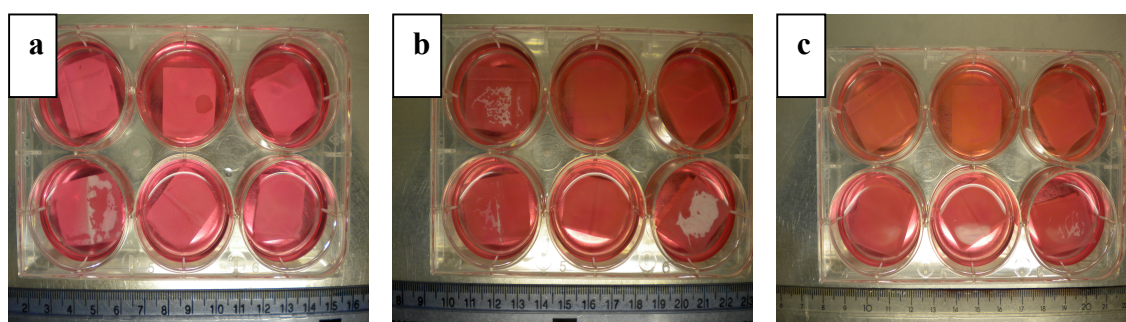


**Figure 2.3** Example of serial photographs for scaffold contraction at day 0 (a), day 7 (b) and day 14 (c).

#### 2.4.8 Immunostaining of extracellular matrix components

The presence and distribution of collagen I, III and elastin were assessed using FITC Ab. Primary antibodies included goat anti-human collagen I and collagen III, and rabbit anti-human alpha elastin antibody (sensitive to both alpha and beta elastin). The respective secondary antibodies included FITC labeled anti-goat IgG and anti-rabbit IgG. All antibodies were polyclonal (AbD serotec, Oxford, UK).

The same samples were fixed and stained by DAPI as explained above, and were then washed 3 times in PBS. Thereafter, 2 mL of 1% BSA was added to each construct in 24 well plates to reduce non-specific binding. This was washed away with PBS 3 times after 30 min. Then 200  $\mu$ L of primary antibody (Diluted 1:50 in PBS) was added to each

sample and these were incubated at 37°C in a 5% CO<sub>2</sub> atmosphere for 30 min followed by 3 washes with PBS. Finally 200 µL of secondary antibody (Diluted 1:200 in PBS) was added and samples were incubated at 37°C in a 5% CO<sub>2</sub> atmosphere for 30 min and washed thrice with PBS. The constructs were imaged with an Axon ImageXpress<sup>TM</sup> fluorescent microscope (Molecular Devices limited, Union City, CA).

The relative positions of nuclei (DAPI stained) and collagen I, III, IV and elastin were ascertained by switching between DAPI and FITC filters. Excitation and emission wavelengths for FITC were  $\lambda_{\text{ex}}$  495 nm/ $\lambda_{\text{em}}$  515 nm, and for DAPI were  $\lambda_{\text{ex}}$  385 nm/ $\lambda_{\text{em}}$  461 nm.

#### **2.4.9 Histology and Haematoxylin and Eosin staining (H&E)**

Samples were placed in a plastic cassette and embedded with Optimal Cutting Temperature (OCT) compound (Tissue-Tek® 4583) to freeze them down immersing samples in liquid nitrogen for few seconds. After formation of blocks, samples were labeled and kept at -80°C.

Samples were sectioned with a cryostat (Leica CM300), refrigeration sectioning device, to get 10 µm sections in the School of Dentistry, University of Sheffield, Sheffield and mounted on frosted slides (Fisher Scientific, UK Ltd.).

Slides were kept at cold temperature with ice and they were brought back to the Kroto Research Institute for direct staining with haematoxylin and eosin staining (H&E). The OCT melts and the slides were soaked in water for 2 min before they were stained with Harris haematoxylin (Sigma-Aldrich, Dorset, UK) for 8 min. After 2 washes in tap water by dunking samples, the slides were stained with eosin (Sigma-Aldrich, Dorset, UK) for 3 min. Then, samples were dehydrated through 70% alcohol (IMS; Industrial Methylated Spirit, Fisher Scientific, UK Ltd.) for 1 min, 95% alcohol for 1 min and 100% alcohol for 5 min, respectively. Finally, they were cleaned in 2 changes of xylene (Fisher Scientific, UK Ltd.), 1 min each and mounted with a coverslip using a DPX mounting medium (Fisher Scientific, UK Ltd.).

Several images were taken of each slide using a light microscope.

#### **2.4.10 Scanning electron microscope (SEM)**

All samples were fixed in 3.7% formaldehyde. After three washes in PBS, the samples were incubated for 5 min with the addition of 2 mL 0.1 M cacodylate buffer. After removal of the cacodylate, 2 mL 2.5% glutaraldehyde in distilled water was added and incubated as above for 30 min. The glutaraldehyde was aspirated and again 2 mL of cacodylate buffer added to rinse any remaining glutaraldehyde. Thereafter 500  $\mu$ L of osmium tetroxide was added and incubated for 2 h. The osmium tetroxide was aspirated and 2 mL cacodylate buffer added and left for 15 min. Subsequently the samples were incubated for 15 min with 75, 95 and 100% ethanol and finally freeze dried for 16 h.

Samples were bisected and mounted on 12.5 mm stubs. The samples were sputter coated with approximately 25 nm of gold (Gold coater; Edwards sputter coater S150B, Crawley, England), and then examined using a scanning electron microscope (SEM) (Philips/FEI XL-20 SEM; Cambridge, UK) at an accelerating voltage of between 10-15 kV and a SPOT size between 2 and 3.A

### **2.5. Rapid extraction of ADSCs**

#### **2.5.1 GentleMACS<sup>®</sup> Dissociator**

9 mL of subcutaneous human adipose tissue was transferred into the gentleMACS C Tube (Miltenyi Biotec Ltd, Surrey, UK) containing 1 mL of PBS with 1% of antibiotics; penicillin (100 units/mL) and streptomycin (100  $\mu$ g/mL). The C Tube was tightly closed and attached upside down onto the sleeve of the gentleMACS Dissociator (Miltenyi Biotec Ltd, Surrey, UK). A defined gentleMACS Program by the manufacturer was run (we tried 2 programs both of 30 sec but at different speeds). After termination of the program 10 mL of HANK solution with 0.1% collagenase type A (Roche Diagnostics GmbH, Mannheim, Germany), 0.1% BSA and 1% antibiotic (penicillin/ streptomycin) were added to the tissue, and incubated for 45 min at 37 °C, 5% CO<sub>2</sub> under continuous rotation using the MACSmix Tube Rotator (Miltenyi Biotec Ltd, Surrey, UK).

Digested tissues were centrifuged at 1300 rpm for 8 min. The floating fractions consisting of adipocytes were discarded and the pellets representing the SVF were resuspended in DMEM medium. Cells were washed by centrifugation at 1300 rpm for 8 min, and finally, pellets were resuspended and cells seeded with the same medium in one T25 flask. Cells were maintained at 37°C and 5% CO<sub>2</sub>.

### **2.5.2 MACS<sup>®</sup> Separation**

After isolation of the SVF, the cell number was determined. Cell suspension in DMEM medium was centrifuged at 1300 rpm for 10 min and afterwards the supernatant was completely aspirated. The cell pellet was resuspended in 60 µL of buffer per 10<sup>7</sup> total cells. Buffer composed by PBS, pH 7.2, 0.5% BSA and 2 mM EDTA.

20 µL of FcR Blocking Reagent (Miltenyi Biotec Ltd, Surrey, UK) and 20 µL of CD271 MicroBeads (Miltenyi Biotec Ltd, Surrey, UK) were added, well mixed and incubated for 15 min in the refrigerator (2–8 °C). Then, cells were washed by adding 1–2 mL of buffer and centrifuged at 1300 rpm for 10 min. The supernatant was completely aspirated and cells were resuspended in 500 µL of buffer.

A LS column (Miltenyi Biotec Ltd, Surrey, UK) was placed in the magnetic field of a suitable MACS Separator (Miltenyi Biotec Ltd, Surrey, UK). The column was firstly prepared by rinsing 3 mL of buffer. The cell suspension was applied onto the column and the flow-through containing unlabeled cells was discarded. The column was washed 3 times with 3 mL of buffer discarding all the unlabelled cells. Finally, the column was removed from the separator and placed it on a suitable collection tube. 5 mL of buffer was pipetted onto the column. Labelled cells were centrifuged at 1300 rpm for 5 min and pellets were resuspended and seeded with DMEM medium into one T25 flask. Cells were maintained at 37°C and 5% CO<sub>2</sub>.

## **2.6 Animal studies**

Scaffold production and human ADSCs isolation was performed in the Kroto Research Institute, University of Sheffield, as described above. Cells and PLA scaffolds were sent to the Laboratory of Experimental Gynaecology, University Hospital Leuven, for



sample preparation. Rat ADCSs isolation and characterization of rat and human ADSCs were also carried out in this laboratory. Animal surgery was conducted in the Centre for Surgical Technologies, Katholieke Universiteit Leuven. After sacrifice, samples were paraffin fixed in the Laboratory of Experimental Gynecology and histological analyses were conducted at the Kroto Research Institute.

### 2.6.1 Implantation

All procedures were conducted under Ethical Approval with license number LA 1210249 from the Ethical committee of the Katholieke Universiteit Leuven.

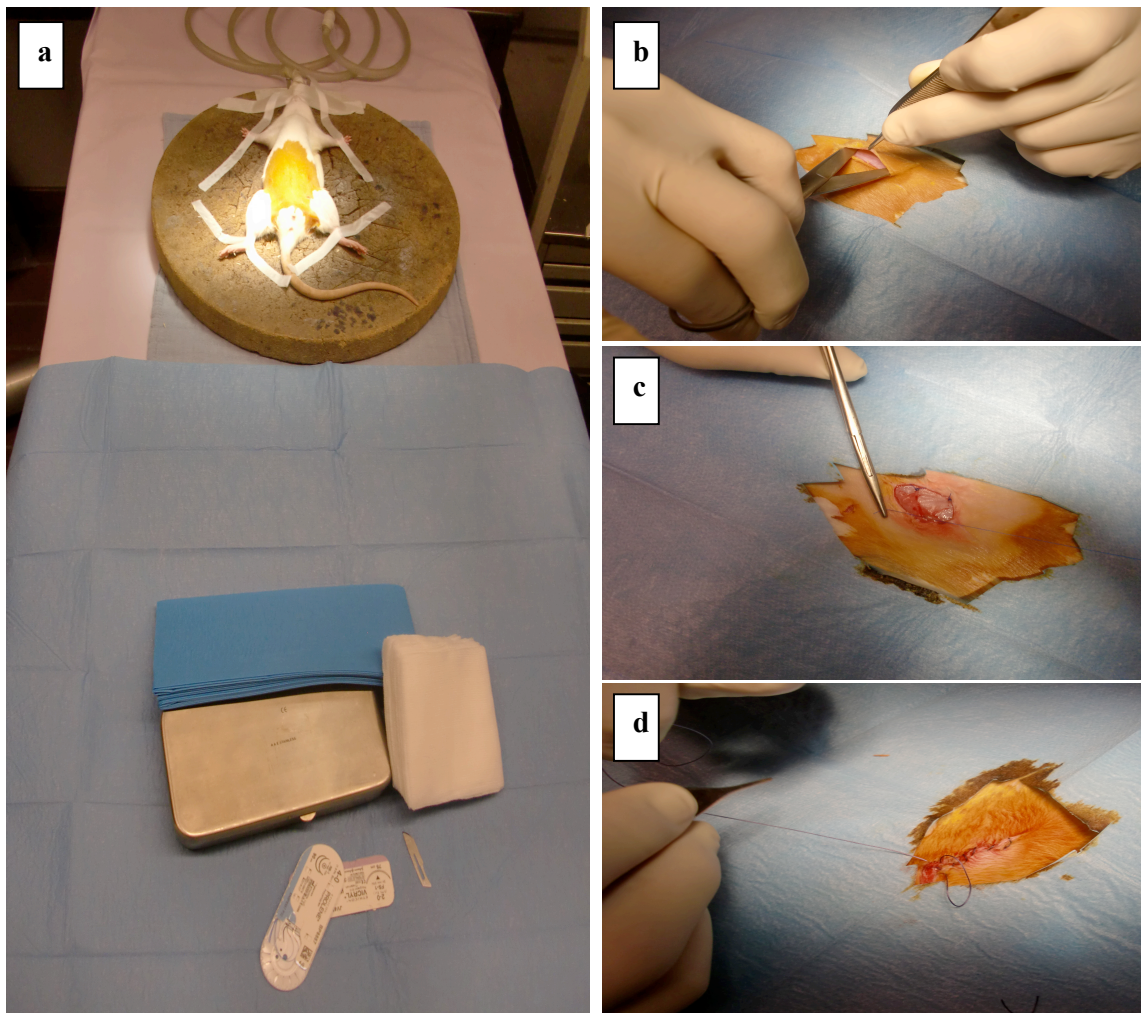


**Figure 2.4** Animal implantation of Th-PLA scaffolds cultured with and without human or rat ADSCs. (a) Preparation for surgical procedure. (b) Skin incision and flaps of the subcutaneous layer were raised. (c) Suture of sample at four corners. (d) Subcutaneous and skin layers closure.

6 different groups of samples were implanted subcutaneously on the abdominal wall of female Sprague-Dawley rats:

1. 6 Th-PLA scaffolds without cells cultured for 2 weeks in DMEM medium were implanted in 6 rats respectively to sacrifice them at day 3.
2. 6 Th-PLA scaffolds without cells cultured for 2 weeks in DMEM medium were implanted in 6 rats respectively to sacrifice them at day 7.
3. 6 Th-PLA scaffolds cultured with rat ADSCs for 2 weeks in DMEM medium were implanted in 6 rats respectively to sacrifice them at day 3.
4. 6 Th-PLA scaffolds cultured with rat ADSCs for 2 weeks in DMEM medium were implanted in 6 rats respectively to sacrifice them at day 7.
5. 6 Th-PLA scaffolds cultured with human ADSCs for 2 weeks in DMEM medium were implanted in 6 rats respectively to sacrifice them at day 3.
6. 6 Th-PLA scaffolds cultured with human ADSCs for 2 weeks in DMEM medium were implanted in 6 rats respectively to sacrifice them at day 7.

All samples were incubated with CellTracker™ Green BODIPY ® dye (Gibco Invitrogen, Paisley, UK) before seeding on Th-PLA scaffolds to track the rat or human ADSCs after implantation and sacrifice.

When the cells reached the desired confluence, the medium was removed from the dish and prewarmed CellTracker™ dye working solution was added. Cells were incubated for 30 min under growth conditions. Then, the dye working solution was replaced with fresh prewarmed medium and cells were incubated for another 30 min at 37°C. During this time, the chloromethyl group (and for some probes, the acetate group) of the dye undergoes modification or are secreted from the cell. At this point we centrifuged cells, counted them and 700,000 cells were seeded on 1 cm<sup>2</sup> PLA scaffolds using a metal ring of 1 cm diameter.

All samples were cultured for 2 weeks with DMEM medium changing medium every 3 days.

For surgical procedures, animals were placed in a 100% isoflurane (Isoba®) induction chamber. After adequate induction of anesthesia (initiated at 3% and further determined by lack of response to stimulation and toe pinch) the animal was moved to a warming pad. The animal was kept under anesthesia by isoflurane via a nose cone (figure 2.4a).

After the belly of the animals were shaved and disinfected with Braunol® 7.5% (B/BRAUN), they received a skin incision and flaps of the subcutaneous layer were raised (figure 2.4b). Then, samples were sutured on the abdominal wall with reabsorbable sutures Ethicon®/Prolene\* (4-0/RB-1 17 mm 1/2c) on four corners of each sample (figure 2.4c). Closure of subcutaneous and skin layers was performed with reabsorbable sutures Ethicon®/Vicryl\* (2-0/FS-1 24 mm 3/8c) (figure 2.4d).

After recovery from anesthesia 6 animals from each group were housed in labeled cages and observed for recovery.

### 2.6.2 Sacrifice and sample fixation

After 3 or 7 days post-implantation, as specified above, animals were sacrificed by intra heart injection of T-61 (Embutramide 200 mg, mebenzoniumiodide 50 mg, tetracaine hydrochloride 5 mg, per mL) (Intervet, International B.V.) after isoflurine anesthesia.

Skin and subcutaneous sutures were removed and abdominal walls with scaffold on top were exposed (figure 2.5). Square pieces of abdominal wall with samples on top were cut, as well as, spleen, liver and lymphoid nodes were removed.

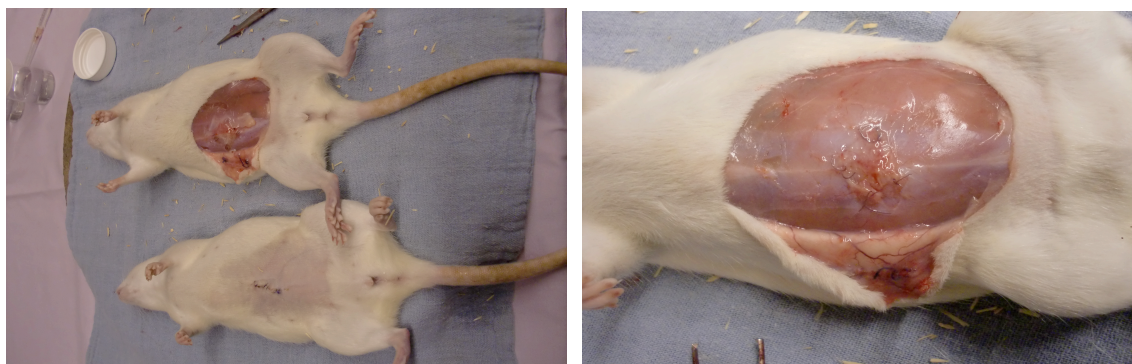


**Figure 2.5** *Animals sacrificed and the appearance of sample on top of abdominal wall.*

Each sample from sacrifice at day 3 of implantation was placed in labeled tubs containing 10% formalin (Sigma-Aldrich). Samples from groups sacrificed at day 7 were cut in half, and half was kept in 10% formalin as well, and the other half was placed in a plastic cassette and embedded with OCT compound (Tissue-Tek® 4583). To freeze them down samples were immersed in smashed dry ice with 2-methylbutane

solution (Sigma-Aldrich). After block formation, OCT labeled samples were kept at -80°C.

### **2.6.3 Histology**

After 24 h in 10% formalin, samples were placed in labeled plastic tissue cassettes and were moved to new labeled pots containing 96% ethanol (Farogon).

At this point samples can be kept for a long period, but all of them were placed in a tissue processor after 1-3 days being in 96% ethanol. At this stage, samples were dehydrated by transfer from 96% ethanol to more concentrated ethanol (100%). Then, samples were transferred through baths with toluidine (Labnord) from lower to higher concentrations to remove alcohol with a hydrophobic clearing agent. Samples were finally placed in molten paraffin wax, as infiltration agent which replaces the toluidine. To make the final paraffin blocks samples were processed in an embedding machine (Chandon CITADEL 1000, HVL) using molten paraffin and molds which were quickly cooled down to form the blocks.

#### **2.6.3.1 Fresh frozen section**

Frozen tissues from animals sacrificed 7 days after implantation were processed with a cryostat (Leica CM300), refrigeration sectioning device, to get 10 µm sections in the School of Dentistry, University of Sheffield and mounted on frosted slides.

The OCT melts and the slides are soaked in water for 2 min before they were mounted with a coverslip using DPX mounting medium. Finally, slides were imaged using Zeiss Laser Confocal Microscope LSM 510 META (Carl Zeiss Inc., Germany).

#### **2.6.3.2 H&E**

Paraffin formalin fixed samples were processed with a microtome (Leica TP 1020 Automatic Tissue Processor) for sectioning to produce 6 µm sections placed on frosted slides. After letting them dry for one day, samples from each group were processed for conventional H&E staining.

Sections were deparaffinized by 2 changes of xylene, 3 min each, and then re-hydrated in 3 changes in IMS from 100% absolute alcohol (5 min) to 95% alcohol (1 min) and finally 70% alcohol (1 min). After this, samples were washed briefly in distilled water, and were stained in Harris haematoxylin for 8 min. After another wash in running tap water for 5 min samples were stained in eosin for 3 min. Then, samples were dehydrated through 70% alcohol (IMS) for 1 min, 95% alcohol for 1 min and 100% alcohol for 5 min, respectively. Finally, they were cleaned in 2 changes of xylene, 3 min each and mount with a coverslip using a DPX mounting medium. Several images were taken of each slide with a light microscope.

#### 2.6.3.3 Immunohistochemistry and Sirius red staining

Paraffin formalin fixed samples were processed with a microtome (Leica TP 1020 Automatic Tissue Processor) for sectioning to produce 6 µm sections placed on Superfrost® plus slides (Menzel-Gläser, Denmark).

After letting the samples dry for one day, samples from each group were processed for immunohistochemistry.

Primary Ab included mouse anti-human CD29, CD44 and CD73 R-Phycoerythrin (PE) conjugated (1:50; BD, Pharmagien); and 6 Ab non-conjugated: mouse anti human beta-2 microglobulin (1:50; Abcam, UK), mouse anti-rat CD68 (1:200; Abcam, UK), goat anti-rat Platelet Endothelial Cell Adhesion Molecule-1 (PECAM-1) (1:50; Santa Cruz Biotechnology, Inc.), goat anti-human collagen I (1:50; AbD serotec, Oxford, UK) and goat anti-human collagen III (1:50; AbD serotec, Oxford, UK).

As secondary antibodies, biotinylated goat anti-mouse Ig (1:200; BD, Pharmagien) (for CD68), biotinylated goat anti-mouse IgG (1:1000; Vector labs, Peterborough, UK) (for beta-2 microglobulin) and biotinylated anti-goat Ig (1:200; ImmunoCruz<sup>TM</sup> goat ABC Staining System, Santa Cruz Biotechnology, Inc.) (for PECAM-1, collagen I and collagen III) were used.

Samples were deparaffinized by 2 changes of xylene, 1 min each, and then, re-hydrated with 2 changes in 100% absolute alcohol (IMS), 3 min each, and 10 min in 95% alcohol. After this, samples were washed briefly in distilled water, and 2 washes more

with Tween 20-PBS (PBS 1% Tween 20, Sigma-Aldrich, Dorset, UK) were given of 2 min each.

An antigen retrieval step was performed to break the protein cross-links, therefore unmasking the antigens and epitopes in formalin-fixed and paraffin embedded tissue sections, thus enhancing staining intensity of antibodies, with 0,05% trypsin (v/w) (Porcine trypsin, Sigma-Aldrich, Dorset, UK) and 0.1% Calcium Chloride (v/w) (Sigma-Aldrich, Dorset, UK) in distilled water, by 20 min incubation at 37°C.

After 10 min at room temperature to cool down samples, sections were washed by two changes in Tween 20-PBS, 2 min each, and incubated with 1,5% blocking serum (ImmunoCruz<sup>TM</sup> goat ABC Staining System, Santa Cruz Biotechnology, Inc.) in PBS for 30 min to avoid non-specific staining.

After this, 2 washes were given with Tween 20-PBS, 2 min each, and samples were incubated overnight at 4°C with primary antibodies diluted in 1.5% blocking serum.

The day after, sections were washed 3 times in Tween 20-PBS, 2 min each, and incubated for 10 min with 3% H<sub>2</sub>O<sub>2</sub> (hydrogen peroxide) in distilled water to quench endogenous peroxidase activity.

Again slides are washed once in Tween 20-PBS for 2 min and then incubated with secondary antibodies diluted in 1.5% blocking serum.

After 3 more washes with Tween 20-PBS and samples were incubated with AB reagent (2% avidin and 2% biotinylated HRP in PBS, ImmunoCruz<sup>TM</sup> goat ABC Staining System, Santa Cruz Biotechnology, Inc.) binding secondary antibodies.

Samples were washed 3 more times with Tween 20-PBS, 2 min each, and HRP (horseradish peroxidase) activity developed brown staining by a final incubation for a few min with chromogen/peroxidase substrate (10X substrate buffer, 50X DAB chromogen and 50X peroxidase substrate in distilled water, ImmunoCruz<sup>TM</sup> goat ABC Staining System, Santa Cruz Biotechnology, Inc.). When the desired staining was developed, by checking samples under light microscope, these were washed briefly with distilled water to stop the reaction followed by 2 more washes with Tween 20-PBS, 2 min each.

Samples were counterstained with Harris haematoxylin for 3 seconds and excess staining was eliminated by several washes in distilled water.

Finally, samples were dehydrated again for 10 min in 95% alcohol, followed by 2 changes in 100% alcohol of 3 min each. Samples were cleaned by 2 changes of xylene, 3 min each, and were mounted with a coverslip using DPX mounting medium.

Several images were taken of each slide with a light microscope.

For the 3 conjugated Ab (CD29, CD44 and CD73) and for beta-2 microglobulin Ab, the slides were processed as previously described in section 2.3.3. For the latter a secondary Ab biotinylated anti-mouse Ig (1:1000; Vector labs, Peterborough, UK) against the primary Ab was used and a tertiary Ab, fluorescein-streptavidin (1:100; Vector labs, Peterborough, UK) was used to image the slides using a Leica DM-IRB inverted research microscope (Leica, Bensheim, Germany), as described in section 2.3.3.

Groups of controls were added for this fluorescent staining as described in section 2.3.3. For the slides detected by peroxidase detection, 3 more groups of controls were performed for each sample following the same immunohistochemistry procedure but avoiding incubations with primary and secondary antibodies, or incubating only with secondary antibodies (no primary antibodies), therefore, only with biotinylated goat anti mouse Ig (1:200; BD, Pharmagien) (for CD68), or only with biotinylated anti-goat Ig (1:200; ImmunoCruz<sup>TM</sup> goat ABC Staining System, Santa Cruz Biotechnology, Inc.) (for PECAM-1, collagen I and collagen III).

In another experiment, new sections were stained for Sirius red (0.1% Direct Red 80 in saturated picric acid) following a similar protocol.

Paraffin formalin fixed samples were processed with a microtome (Leica TP 1020 Automatic Tissue Processor) for sectioning to produce 6 µm sections placed on Superfrost® plus slides.

After letting them dry for one day, samples were deparaffinized with 2 changes of xylene, 3 min each, and then, re-hydrated with 2 changes in 100% absolute alcohol (IMS), 3 min each, and 10 min in 95% alcohol. After this, samples were washed briefly in distilled water and incubated with Sirius red for 1 h. Then, samples were rinsed briefly in distilled water and washed in acetic acid solution (VWR International Ltd.) for 1 min. Again, sections were rinsed briefly in distilled water and dehydrated by 10 min in 95% alcohol, followed by 2 changes in 100% alcohol, 3 min each. Slides were cleaned by 2 changes of xylene, 3 min each, and were mounted with a coverslip using DPX mounting medium.

Several images of each slide were taken with a light microscope.

## 2.7 Statistical analysis

All the *in vitro* experiments were carried out at least 3 times. At least 9 images from each group were used for the blind scoring of immunostaining and histology images. The data was reported as mean $\pm$  SEM. To determine the significance of differences between groups two-sample Student's t-test analysis was performed for all analyses in this thesis.



## **Chapter 3**

### **PRODUCTION OF CANDIDATE SCAFFOLDS**

### 3.1 Introduction

PLA is an FDA approved synthetic biodegradable and biocompatible polymer of lactic acid produced by ring opening polymerisation of lactic acid. PLA is hydrophobic, semi-crystalline and amorphous polymer, and has a glass transition temperature between 60-65° and a melting temperature of around 170°. The monomer has chirality, and has two conformations dextro (D) and levo (L), P(L)LA, P(D)LA or P(D,L)LA. Pure P(L)LA was first used as a suture material in 1960 (347). Currently, both conformations have been used as a biomaterial for a variety of different clinical applications.

Degradation of PLA occurs via acid catalysed hydrolysis into lactic acid, which is metabolised *in vivo* via the Krebs cycle (348, 349). PLA has a high degree of crystallinity and degradation starts in the amorphous regions with random hydrolysis. After sufficient degradation has occurred the edges of the crystalline regions become degraded. P(D)LA has a significantly reduced crystalline structure, and therefore degrades more rapidly than P(L)LA.

Several methods have been used to fabricate highly porous biodegradable polymer scaffolds; including particulate-leaching, fibre extrusion and bonding, phase separation, gas foaming, emulsion freeze drying, 3-D printing techniques and electrospinning (350-355).

The choices of polymer such as its fabrication method and scaffold morphology are critical determinants for production of an engineered tissue before adding the cellular component (356, 357). A good example for this is PPL mesh which is the gold standard material used to treat SUI and POP. Type 1 PPL mesh that is macroporous (>75µm) is said to be most favourable for tissue integration into native tissues as microporous (<15-20µm) mesh may allow infiltration by bacteria but not by the larger host inflammatory cells (172).

Electrospinning is a technique where a polymer in a solution is exposed to a high voltage and simultaneously drawn into a fibre shape via electrostatic forces as it attempts to bridge the gap to earth. The most commonly used setup for an electrospinning rig is that of a horizontal rotating collector earthed or negatively charged, and of a syringe containing the polymer connected to a voltage generator. The

syringe with the polymer solution is placed in front of the collector and when the electrostatic force goes above a critical value it overcomes the surface tension of the polymer solution and a thin jet travels through the syringe and onto the collector. The fibres are stretched and elongated and quickly solidify due to evaporation of solvent.

Over the years there have been several different setups developed for the production of scaffolds made of electrospun fibres. Techniques have been modified to allow the spinning of more than one polymer mixed in one collector, to improve the thickness of the fibres and/or to produce aligned fibres (358). All these parameters can affect the mechanical properties of electrospun scaffolds. Also, post-production treatment can impact on mechanical characteristics; we have previously shown that thermo-annealing of poly lactic-co-glycolic (PLGA) scaffolds in a dry oven at 60° for 3 hours improved the mechanical and handling properties (359). This effect is thought to occur due to heating above the glass transition temperature which increases the crystallinity of the polymer and leads to changes in fibre morphology from purely fibrillar to a mix of fibrillar and nanogranular with greater inter-fibrillar bonding (360).

Electrospinning, in general, has gained increasing popularity in tissue engineering as it can be used with a wide range of synthetic and natural polymers. Constructs from the nano to micrometer range can be produced for 3D tissue engineering and closely mimic the environment of native tissue ECM. In 1999, the electrospinning technique was first used for tissue engineering, where spun silk-like polymer was used to produce a biocompatible film which was implanted into the central nervous system (361).

PLA electrospun scaffolds have now been used for a variety of purposes ranging from bone (362), skin (363), bladder (364), nerve guide conduits (365), adipose tissue (366) and cartilage (367).

Neural stem cells have been seeded and cultured on electrospun PLA made of aligned fibres for nerve tissue guides (368). A lot of work is currently done on this with potential for peripheral nerve repair (369, 370). Electrospun PLGA scaffolds have been used to create tubes simulating small blood vessels (371). Furthermore, during the last few years, electrospun PLA has been combined with osteoblasts as a bone substitute (372).

*In vivo*, electrospun PLA has been shown to undergo slow degradation since the scaffold retained an acceptable strength 8 months after implantation (373). Compared to PPL, PLA scaffolds showed a significantly lower inflammatory response when both

materials were implanted into the abdominal wall of rats. In addition, the collagen produced was better organized in PLA scaffolds (374). They also found decreased mechanical properties when the scaffolds were gamma sterilised before implantation. On the other hand, mechanical properties of PLA scaffolds post explantation were always higher than PPL at all time points up to 90 days implantation *in vivo*. The same authors also reported PLA to have less infection risk compared to other meshes in a rat infected abdominal model (375).

The scaffold candidate to develop a TERM for pelvic floor repair was chosen from previous work undertaken in our group.

The potential of 7 different scaffolds materials to develop a TERM were assessed. These included synthetic and biological materials currently used as acellular materials to treat SUI and POP, including PPL. By seeding and culturing OFs on these materials, it was determined that thermo-annealed PLA (Th-PLA) and SIS represented the best candidate scaffolds in terms of cell attachment and proliferation and formation of ECM proteins (346). From this initial work Th-PLA was chosen as the scaffold to be investigated further to avoid the use of animal material, such as SIS, with risk of infectious disease transmission and the potential concerns of surgeons and patients with using such material. In addition, already reviewed in the introduction of this thesis, acellular SIS is often quickly degraded leading to failure and recurrence when used in patients with SUI and POP.

### **3.2 Comparison between PLA and thermo-annealed PLA (Th-PLA) scaffolds**

Morphological, physical and mechanical properties of PLA scaffolds before and after being thermo-annealed were assessed. For this, the pores and fibre diameter (figure 3.2.1 and 3.2.2) were determined by using ImageJ software from SEM images (n>100 fibres and from at least 2 images), the bulk density was calculated from the size and weight of the different samples and mechanical properties (figure 3.2.3) of these scaffolds were assessed by using a BOSE tensiometer.

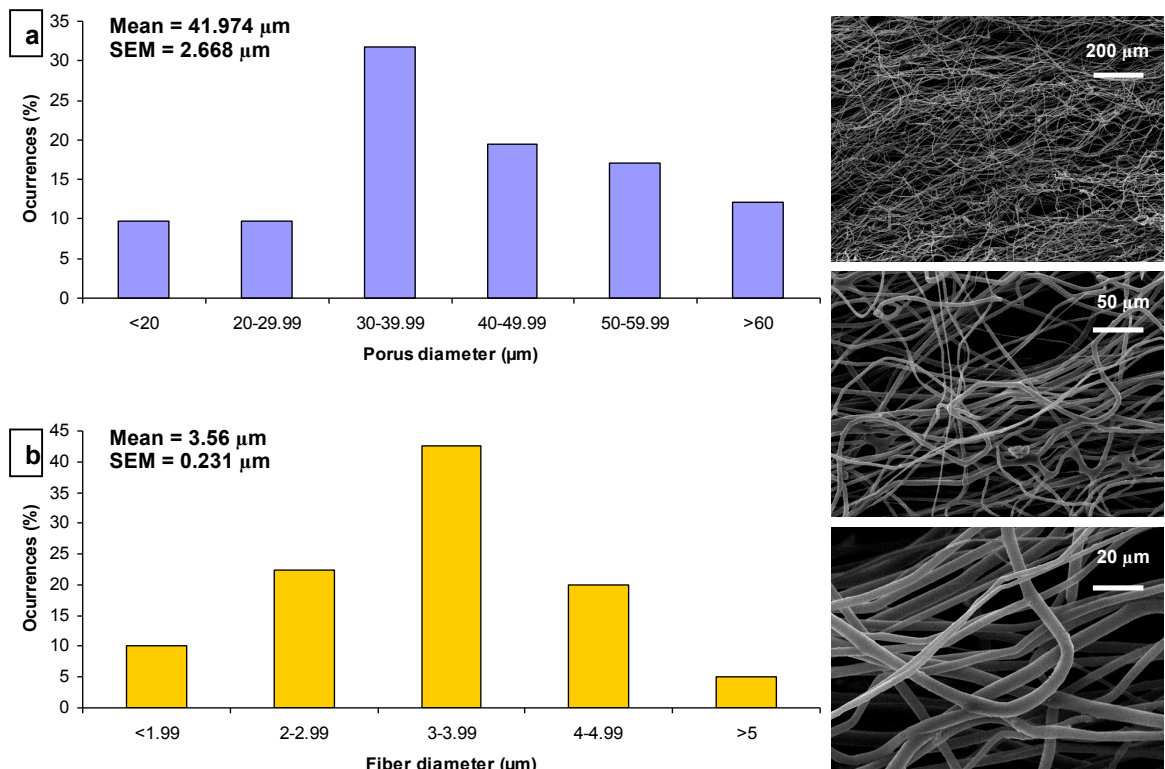


**Figure 3.2.1** SEM images of PLA scaffolds (right). Pores diameter (a) and fibre diameter distribution (b) calculated from 100 fibres ( $n = 3$ ).

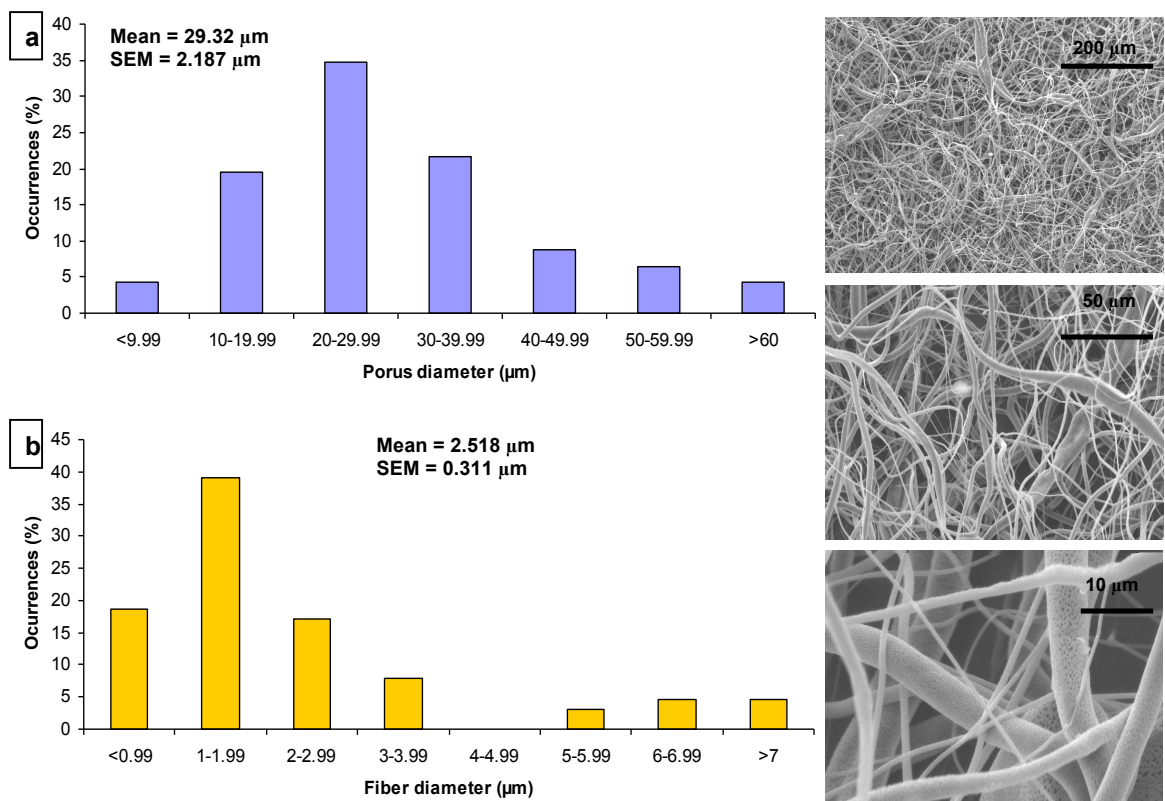


**Figure 3.2.2** SEM images of Th-PLA scaffolds (right). Pores diameter (a) and fibre diameter distribution (b) calculated from 100 fibres ( $n = 3$ ).

As shown in SEM images, PLA scaffolds consisted of random microfibrils which form a microporous scaffold simulating the ECM of native tissues. From our results, fibres of PLA scaffolds had a mean diameter of 3.5  $\mu\text{m}$  forming pores of 40  $\mu\text{m}$  of diameter; however, after being thermo-annealed the mean for fibre diameter was reduced at 2.5  $\mu\text{m}$ , as well as the pores diameter being reduced to around 30  $\mu\text{m}$ .

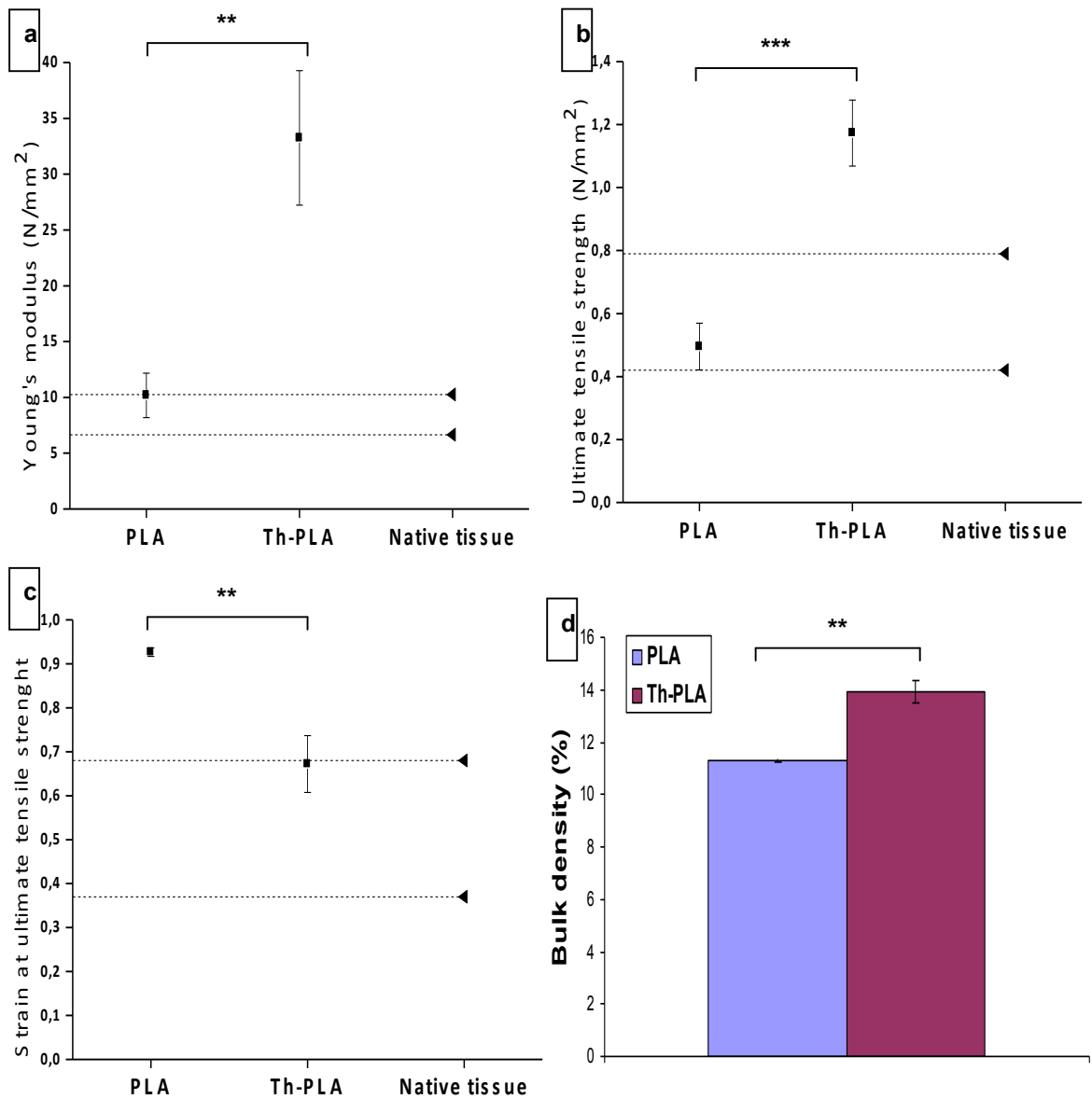


**Figure 3.2.3** Mechanical properties of PLA and Th-PLA scaffolds, mean $\pm$ SEM ( $n = 3$ ). Last sample shown is the range for native tissue represented by 2 dashed lines (the range for native healthy paravaginal tissue). (a) YM, \*\* $p < 0.005$ . (b) UTS, \*\*\* $p < 0.0005$ . (c) Strain at UTS, \*\* $p < 0.005$ . (d) Bulk density of PLA and Th-PLA scaffolds (\*\* $p < 0.001$ ) and its thickness ( $n = 3$ ).

As previously explained, when measuring the tensile properties of a material, Young's modulus is the first linear slope when a material is stretched, observed from a typical stress-strain plot (figure 2.2). The higher the slope, the stiffer is the material; however, this parameter is called elastic modulus too, because, the elongation of the material during this linear slope is elastic deformation allowing recoil to its original size. Once the linear portion finishes all the elongation observed is plastic deformation. Then, the other 2 parameters, normally found in literature, to describe the tensile properties of a material are the UTS and the strain at UTS. UTS is the maximum strength of a material, and the strain at UTS shows the maximum elongation of the material before it starts to snap.

All samples assessed in this thesis for a uniaxial tensile test were measured for size. Stress-strain data from each sample was normalized before the 3 mechanical properties were plotted, dividing the stress by the area of the scaffold (width x thickness) and dividing the strain by the length between the 2 grids (length of the scaffolds tested) to obtain a percentage of elongation from its original length.

Th-PLA scaffolds showed significantly higher Young's modulus and UTS when compared to non thermo-annealed PLA scaffolds. Alternatively, the strain at UTS was significantly higher for non thermo-annealed PLA scaffolds (figure 3.2.3).

These parameters were compared to the range for the native healthy paravaginal tissues (endopelvic fascia) obtained from the literature (194). Non thermo-annealed PLA scaffolds were between this range for Young's modulus and UTS, while Th-PLA scaffolds showed a strain at UTS between this range (figure 3.2.3).

Finally, the bulk density and thickness of these scaffolds were measured. The bulk density was calculated by measuring the volume of small pieces of these scaffolds (length x width x thickness) and their weight. Then, since we know the density of PLA we can work out the expected weight for this volume, if it was a compact sheet; and finally, the data shown is the percentage of material found in this volume, the rest of this is "air" and this is a way to describe the porosity of these materials. The thickness was measured with a micrometer.

Th-PLA scaffolds were significantly more compact leading to lower porosity (figure 3.2.3).

### 3.3 *In vitro* degradation of Th-PLA scaffolds

From previous results we had already chosen our scaffold candidate; therefore, the *in vitro* degradation was only studied for Th-PLA scaffolds by looking at the mechanical properties of these scaffolds at 0, 14, 30 and 90 days. These were kept in DMEM medium under sterile conditions inside the incubator (37°C in a 5% CO<sub>2</sub> atmosphere).

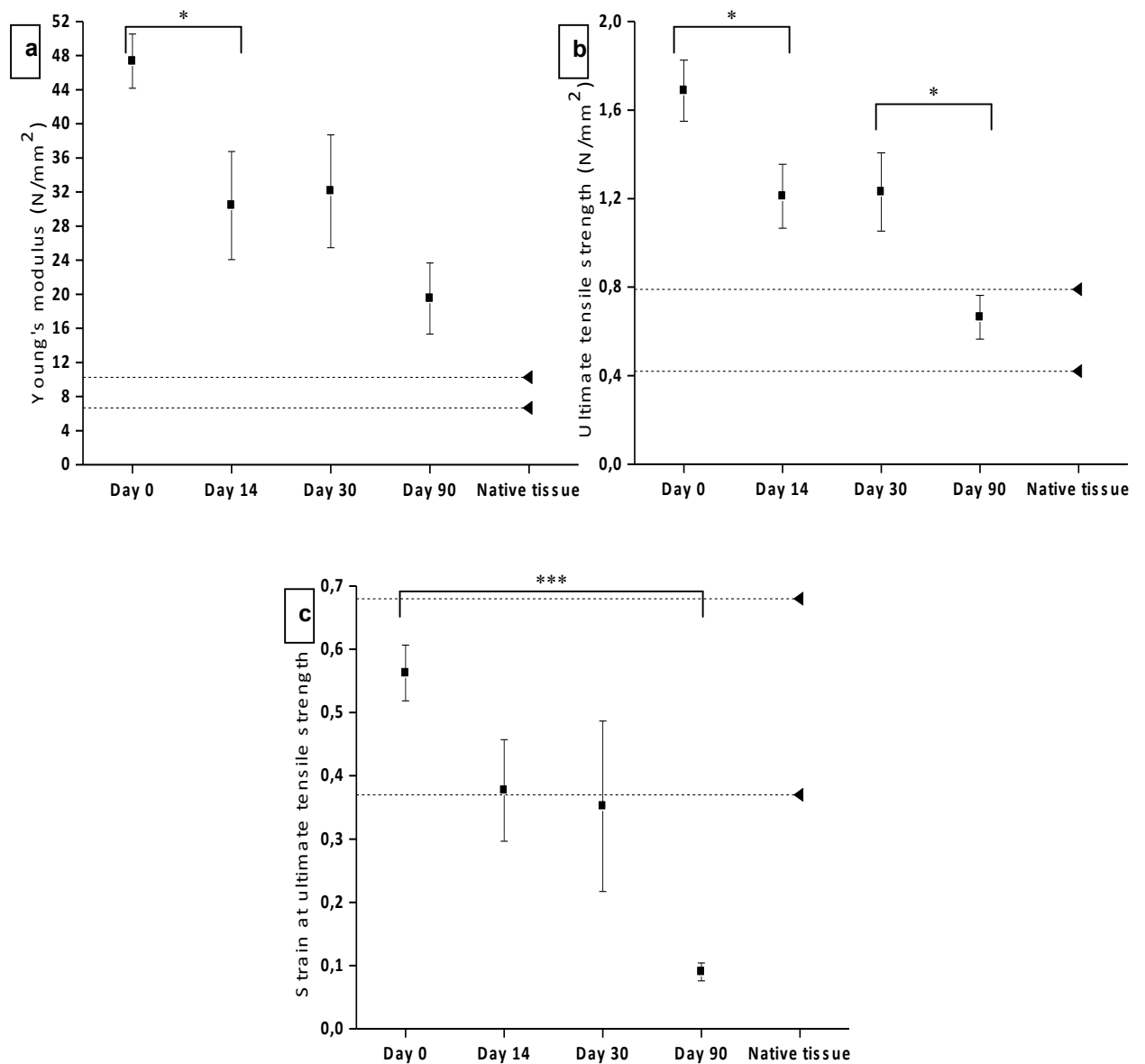


**Figure 3.3.1** Mechanical properties of Th-PLA scaffolds at day 0, day 14, day 30 and day 90 after being in DMEM, mean±SEM (n = 3). Last sample shown is the range for native tissue represented by 2 dashed lines (the range for native healthy paravaginal tissue). (a) YM, \**p*<0.05. (b) UTS, \**p*<0.05. (c) Strain at UTS, \*\*\**p*<0.0001.



Th-PLA scaffolds reduced their tensile properties over time. Young's modulus and UTS were significantly reduced from day 0 to day 14. At day 30, both values were unchanged, but after 90 days in DMEM medium these were reduced again. At 90 days, Young's modulus remained slightly greater than the range for native tissues though. On the other hand, strain at UTS was maintained between the values for native tissues without significant differences up to 30 days. Only at day 90, this was reduced very significantly and now fell within the range for native tissues (figure 3.3.1).

### **3.4 Discussion**

With electrospinning we were able to produce scaffolds made of biodegradable and biocompatible PLA. With this technique we can produce a sheet of 18 cm by 16 cm in about 2 h. Furthermore, PLA is an extremely cheap product which, as an FDA approved material, has been already used for different clinical applications.

PLA scaffolds are composed of microfibrils which in turn form microporous scaffolds. As described in the first Chapter of this thesis, macroporous materials present pores bigger than 75  $\mu\text{m}$ . PPL mesh, that is macroporous, is said to be most favourable, as microporous (<15-20  $\mu\text{m}$ ) mesh may allow infiltration by bacteria but not by the larger host inflammatory cells (376). PLA scaffolds present pores of 40  $\mu\text{m}$ , and are reduced to 30  $\mu\text{m}$  after thermo-annealing. Both scaffolds also have a low percentage of macropores.

Most of the fibres of PLA scaffolds seem to reduce their diameter after being thermo-annealed; nevertheless, a small percentage of fibres are wider, compared with non thermo-annealed scaffolds, thus scaffolds are made of 2 different groups of fibres. Fibre morphology is changed after thermo-annealing from purely fibrillar to a mix of fibrillar and nanogranular fibres. Some parameters such as temperature and humidity have an enormous effect on the electrospinning of PLA scaffolds, and this can affect the fibre diameter and pore size (377), making the electrospinning process poorly reproducible unless these are tightly controlled.

On the other hand, thermo-annealing of PLA scaffolds increases the inter-fibrillar unions what may be the main reason for the effect on mechanical properties. Th-PLA scaffolds were stiffer (higher Young's modulus) and stronger (higher UTS) compared to non thermo-annealed PLA scaffolds. Similarly, these 2 parameters may be also increased by a higher crystallinity of the PLA fibres after being thermo-annealed. At the same time, this higher crystallinity may lead to more brittle fibres which correlates with lower elongation of Th-PLA scaffolds at the point they start to snap.

Also, the thickness of Th-PLA scaffolds was found to be reduced compared to non thermo-annealed PLA scaffolds, which is explained by higher bulk density leading to more compact scaffolds (with less porosity), explaining the small reduction in pore diameter.

These changes had an impact on the handling of the Th-PLA scaffolds, making this material less fluffy and the fibres less sticky, making it easier to peel the scaffold from the foil after the electrospinning.

For these reasons, Th-PLA scaffolds were chosen for further experiments. In addition, the fact that they have stronger mechanical properties than native tissues (194) was desirable because of the expected degradation of the PLA fibres over the time. We believe if after implantation the mechanical properties drop to under the values for native tissues this may lead to the failure of the material and the recurrence of SUI/POP, which is further discussed in Chapter 7 of this thesis.

It was observed that there was a reduction of all 3 mechanical properties of Th-PLA scaffolds over 90 days when cultured in DMEM medium *in vitro*.

Although Young's modulus and UTS were reduced since the second week in culture, this was not very significant and both properties remained always over the values for native tissues or within these, respectively. Alternatively, strain at UTS was only dropped after 90 days but being very significantly and becoming a brittle material which snaps at lower elongation than native tissues.

Other studies have shown long term retention, for up to 8 months, of mechanical properties of PLA scaffolds after implantation (373) as they have a slow degradation rate. Furthermore, neo-tissue formation by collagen remodelling, that normally happen in most materials before 90 days since they are implanted (311, 313), may increase or maintain the mechanical properties of the scaffolds for long-term repair. Nevertheless,

animal studies are needed for better understanding of this since, for instance, PLA scaffolds may be degraded faster in the vaginal environment as has been seen for other materials (293).

It is difficult to answer which are the desired mechanical properties of a material for pelvic floor repair, and this will be further discussed in another Chapter of this thesis. Our group have published a systematic review trying to answer this question and it was impossible to predict the clinical outcomes of a material based on its mechanical properties alone (378).

In conclusion, we found that Th-PLA scaffolds increased in stiffness and strength, compared to non thermo-annealed PLA scaffolds. We emphasize the relevance of this in preparing material for the repair of the pelvic floor, to obtain a material which is easy to handle surgically, with the necessary mechanical properties to fulfill its purpose at the point of insertion and to maintain the long-term integrity of the repair (378).

## **Chapter 4**

### **EXPLORING CELL CANDIDATES FOR A TISSUE ENGINEERED REPAIR MATERIAL (TERM)**

## **4.1 Introduction**

Cells can be isolated from several sources. The ethical use, safety isolation, timing, proliferation, viability, production of the ECM components, and their capacity to promote neovascularization or to induce an inflammatory response after their transplantation are all relevant. All these characteristics should be considered when exploring which cell type is the most appropriate for production of a TERM such as their potential for further new tissue formation after their implantation.

### **4.1.1 Fibroblasts**

At first glance vaginal fibroblasts seem to be the most appropriate cell candidate since they come from the native tissue. Fibroblasts from vaginal wall have been easily excised during vaginal hysterectomies as a minimally invasive method, in patients with POP.

However, studies of cultured vaginal fibroblasts from patients with POP found a correlation between slow proliferation and a low ratio of collagen I/III. Patients with a higher ratio of collagen I/III had fibroblasts with faster proliferation; nevertheless, this fibroblastic behaviour cannot be predicted since it did not correlate with age or POP stage (336). Neo-fascia was formed when seeding these cells isolated from the vaginal wall of patients with POP on collagen coated PLGA. Alternatively, the ECM was not very well organized for slow proliferative fibroblasts. A few more studies have also investigated the capacity of vaginal fibroblasts to coat different meshes (379) and to synthesize collagen (380) for POP repair.

How collagen metabolism is affected in vaginal fibroblasts from patients with SUI and POP is not completely understood. Nevertheless, there is a high risk of finding cells with altered synthesis of structural components and of their metabolic enzymes if autologous fibroblasts are isolated from the vaginal wall of these patients. Since we aim for an autologous approach where cells used are isolated from same patient during the same operation, and which is further discussed in the last Chapter of this thesis, we did not consider vaginal fibroblast for this research. In addition, the excision of these tissues can lead to donor site comorbidities and further complications.

Buccal mucosa tissue is composed of a thick epithelium and highly vascularized lamina propria (381). Buccal mucosa grafts have been used in urethroplasty for fifty years (382). OFs are considered the most versatile cell candidate to develop an engineered urethral substitute (383). Fibroblasts from buccal mucosa can also adapt easily to new environments, the grafts underwent limited contraction, have useful strength and are resistant to infection (384). In addition, they present minimal donor and recipient site complications, and it is an easy to access tissue (384). These cells have shown good proliferation and ECM formation when used in a biodegradable scaffold to form an engineered tissue for urethroplasty (385).

There are only a few studies looking at the potential of vaginal fibroblasts or OFs to develop engineered tissues for pelvic floor reconstruction. *In vivo*, only de Filippo et al. assessed a vaginal engineered tissue produced from vaginal epithelial cells and smooth muscle cells from female rabbits (334).

#### **4.1.2 Adult stem cells**

Stem cells can be isolated from different sources, and all of them share several characteristics such as long-term replicative potential and self-renewal, maintenance of undifferentiated properties and multi-lineage differentiation ability (340).

Multipotent stem cells are also known as foetal/adult stem cells (ASCs) or tissue-derived stem cells. An ASC is an undifferentiated cell found in a differentiated tissue with the primary function to maintain the steady state functioning of a tissue (called homeostasis) and, with limitations, to replace cells that die because of injury or disease. When these cells divide into two cells, one cell will keep undifferentiated to maintain their population and the other cell is called a somatic stem cell or progenitor cell, which are limited in their potential, and will differentiate into mature functioning cells responsible for normal tissue renewal. These progenitor cells can be specialized to yield all of the cell types of the tissue from which it originated. MSCs are ASCs present in tissues derived from the mesodermal embryogenic layer and usually divide to generate progenitor or precursor cells, which then, differentiate or develop into "mature" cell types that have characteristic shapes and specialized functions (386).

Their multi-lineage differentiation capacity has been extensively characterized (387). They remain able to proliferate and differentiate into tissues of mesenchymal origin, as

well as into tissues of both endodermal and ectodermal origin thus allowing speculation about their pluripotency (388, 389).

Furthermore, these cells also are characterised as being nonimmunogenic (390) and it is believed they release paracrine factors to stimulate the regeneration of surrounding tissues (391).

All these properties make these cells an interesting source for tissue regeneration. In pelvic floor tissues, MSCs have been used to regenerate the middle urethra in SUI animal models. Most of these cell therapy studies are based on MSCs derived from bone marrow, muscle and adipose tissue. They have been injected into the extrinsic sphincter of the urethra, which comprises striated rhabdosphincter voluntary musculature or into the intrinsic sphincter of the urethra, which includes mucosa, submucosa, estrogen-dependent vascular plexus, and smooth muscle layers (one longitudinal and the other circumferential) (27).

BMDSCs were the first MSCs to be studied and not only for urethral sphincter regeneration. BMDSCs have been implanted into the bladder musculature with 5-azacitidine as a myogenic differentiation stimulator, and they verified the expression of striated and smooth muscles antigens in these cells (392). BMDSCs were also transplanted into the urethral sphincter of Sprague-Dawley rats after urethrolisis. After 13 weeks, the skeletal muscle of the urethral sphincter was regenerated by integrated BMDSCs labelled with green fluorescence protein (GFP) although, the abdominal leak point pressures were not improved (393). A later study found similar tissue regeneration when BMDSCs were implanted into the urethral sphincter of rats after pudendal nerve transaction (PNT). In addition, they also found significantly improved Valsava LLP 4 weeks after injection (394).

On the other hand, biopsies from bone marrow are painful, frequently requiring general or spinal anaesthesia and often a low number of BMDSCs are isolated (395).

MDSCs are obtained under local anaesthesia. They can be isolated from different sources; however, those from striated muscle have shown huge improvements for other disease models, such as a myocardial infarct model (396). In addition, these cells can be differentiated into all mesenchymal cells layers and into neuronal and endothelial lineages as well (397, 398). MDSCs are naturally fused into postmitotic multinucleated

myotubes with a great potential for ligament/supportive structures formation (399). This cell type is the one most proposed to regenerate the urethral sphincter and several studies found good tissue regeneration, improved LLP and recovered contractile urethral sphincter function when injecting these cells into the urethral sphincter of different SUI animal models (table 8).

On the other hand, to obtain a reasonable content of MDSCs, a large biopsy of skeletal muscle (5-30g) is needed with the disadvantage of scar formation. They differentiate quickly without any stimulation before you can expand them to get a large number. They differentiate into multinucleated fibres which do not have the regenerative properties of the MSCs, such as multipotential and releasing paracrine factors (both for nerve and blood vessels regeneration). Furthermore, their slow proliferative potential increases the cost of the procedure (400).

Finally, in 2000 ADSCs were the last MSCs to be discovered and they have huge potential in mesodermal tissue differentiation (401, 402), such as in regeneration and revascularization (403, 404). Only 40-60% of the adipose tissue is composed of mature adipocytes. ADSCs are easily and quickly isolated from the SVF of the adipose tissue which is composed of fibroblasts, macrophages, endothelial cells, hematopoietic cells and ADSCs (400). They proliferate very quickly and do not differentiate without stimulating differentiation medium. Furthermore, they secrete organized endogenous ECM in culture conditions which is interesting for connective tissue formation (343).

ADSCs have been proven to differentiate into striated muscle, showing specific markers (desmin, myod1, myogenin, myosin heavy chain) (405) and to regenerate damage skeletal muscle in rabbits restoring volume and muscular contraction (406). Also, ADSCs have been used for urethral sphincter reconstruction to improve continence outcomes in SUI animal models (table 9), due to their capacity to differentiate into smooth muscle cells (401) and to contract and relax under pharmacological stimulation (405). In addition, inside the ADSCs population some cells express endothelial surface antigen (CD34) and myogenic surface antigen (CD59). The injection of these subpopulations of ADSCs in postnatal mice increased neovascularization through an increment in blood flux and capillary density compared with controls (403). Finally, their multipotential has been proven by their differentiation into neural cells (407).

ADSCs have shown good potential to regenerate the urethral sphincter (table 9); however, all the studies agree that more studies should be done to explain how MSCs



improve urethral function and to investigate whether the cells could release trophic factors that modify both cellular and extracellular elements of the urethra. Also, further studies are necessary to determine, at long-term, possible migrations and/or undesirable differentiations of these cells.

## 4.2 Isolation, culture and characterization of OFs and ADSCs

From the background given in this section, OFs and ADSCs were chosen to develop a TERM.

Frozen OFs were used for these experiments which had been previously isolated by other researchers for another project (346).

ADSCs were isolated, and then, characterized for specific surface antigen expression, and for differentiation assays to prove their potential to differentiate into other cell types.

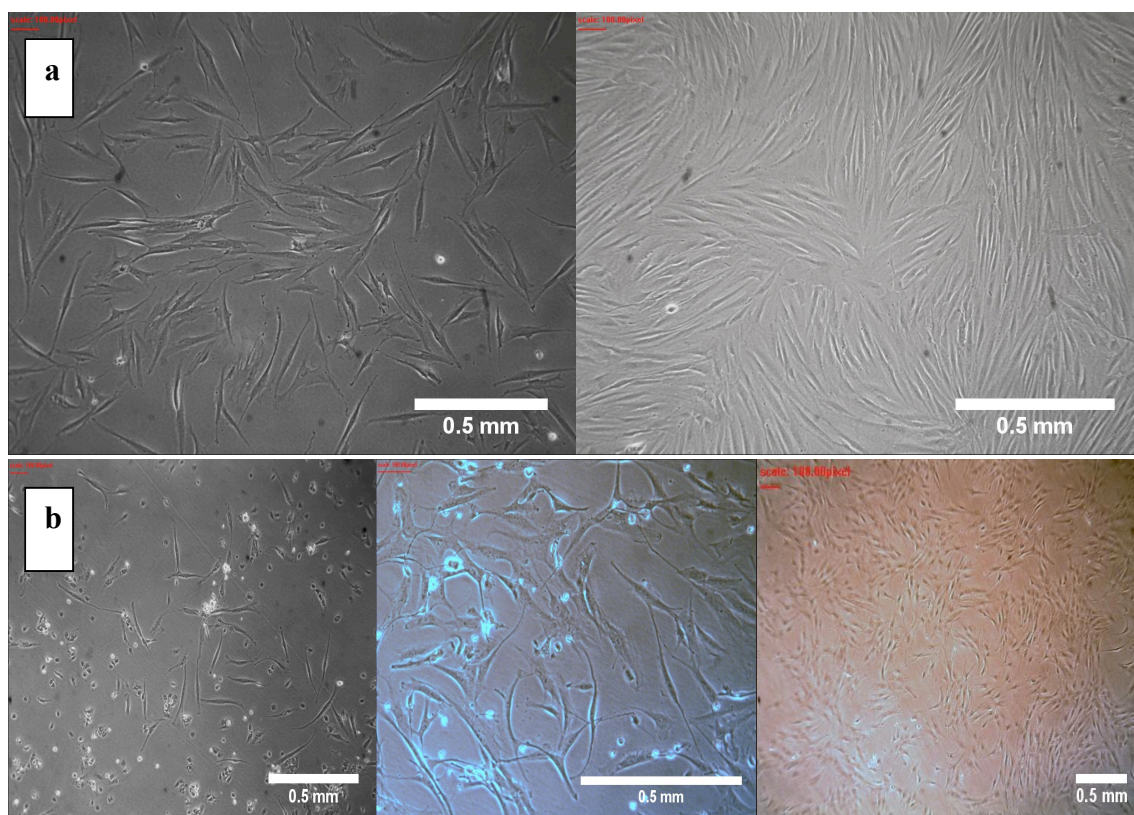


**Figure 4.2.1** Morphology of OFs (a) and ADSCs (b) on a tissue culture plastic flask under light microscope.

After isolation, cell cultures of OFs and ADSCs were regularly visualized to inspect cell morphology and exclude infection.

As above, OFs had been isolated previously by other researchers, and were resurrected from a cryogenic frozen vial and cultured OFs in a T75 (figure 4.2.1a).

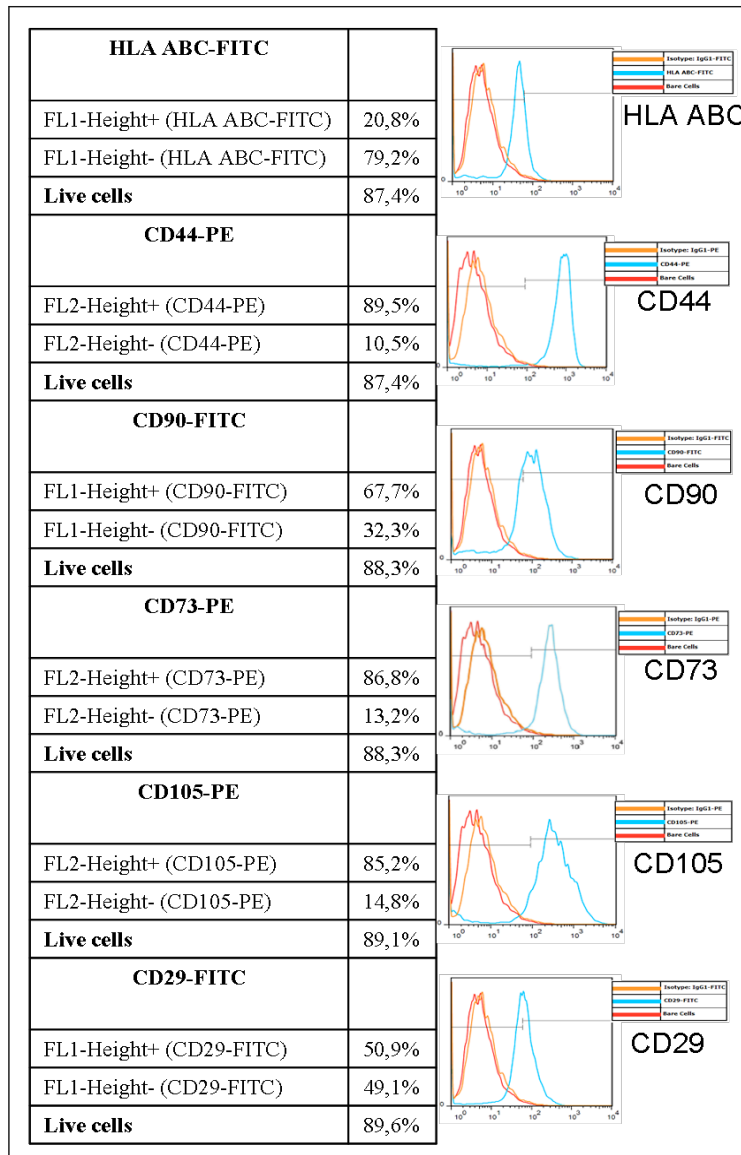
ADSCs were isolated from the SVF of human subcutaneous fat which is composed of other vascular cells. Nevertheless, ADSCs have a higher potential to attach to the plastic culture flask and higher proliferation potential than the other cells. Subsequently, after first washes, non-adherent cells were discarded and after two passages, due to higher proliferation potential, ADSCs displaced the other cell types obtaining a homogeneous confluent population of ADSCs as morphologically observed (figure 4.2.1b).

OFs showed typical fibroblastic morphology reaching a confluent culture of these cells without any infection (figure 4.2.1a). ADSCs showed, as well, typical fibroblastic morphology but with longer prolongations which is characteristic of mesenchymal/adult stem cells. In addition, we could not see any sign of infection (figure 4.2.1b).

Adherent cells isolated from subcutaneous human adipose tissue were characterized by flow cytometry at passage 6 cultured in DMEM medium. Human cells showed high expression for MSCs markers, such as membrane receptor CD-29 (integrin beta-1, which is involved in cell adhesion for processes including embryogenesis, tissue repair, immune response and metastatic diffusion of tumour cells), major histocompatibility class I receptor HLA-a/b/c, anchored conserved cell surface CD-90 (or Thy-1, glycoposphatidylinositol protein involved in cell-cell and cell-matrix interactions), adhesion molecule CD-105 (endoglin, involved in the cytoskeletal organization affecting cell morphology and migration), surface glycoprotein CD-44 (receptor molecule involved in cell-cell interactions, cell adhesion and migration) and enzyme CD-73 (5' ecto-nucleotidase) (figure 4.2.2).

On the other hand, human cells showed low expression of major histocompatibility class II receptor HLA-DR (T-cell receptor for immune recognition and antigen presentation), surface glycoprotein CD-34 (cell-cell adhesion factor, may mediate attachment of bone marrow-derived stem cells to one marrow extracellular matrix or directly to stromal cells) and hematopoietic marker CD-45 (member of the protein tyrosine phosphatase family, signalling molecules that regulate a variety of cellular processes including cell growth, differentiation, mitotic cycle, and oncogenic transformation) (figure 4.2.2).

## POSITIVE CELL SURFACE MARKERS



## CONTROLS

BARE CELLS	
Live cells	89,2%
ISOTYPE 1 (IgG1)	
FL1-Height+ (IgG1-FITC)	1,78%
FL1-Height- (IgG1-FITC)	98,2%
FL2-Height+ (IgG1-PE)	1,58%
FL2-Height- (IgG1-PE)	98,4%
Live cells	89,6%
ISOTYPE 2 (IgG2)	
FL2-Height+ (IgG2α-PE)	1,80%
FL2-Height- (IgG2α-PE)	98,2%
Live cells	91,0%

## SCATTER PLOT

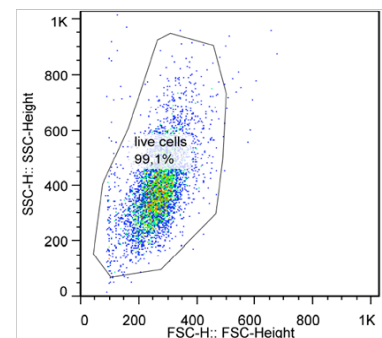
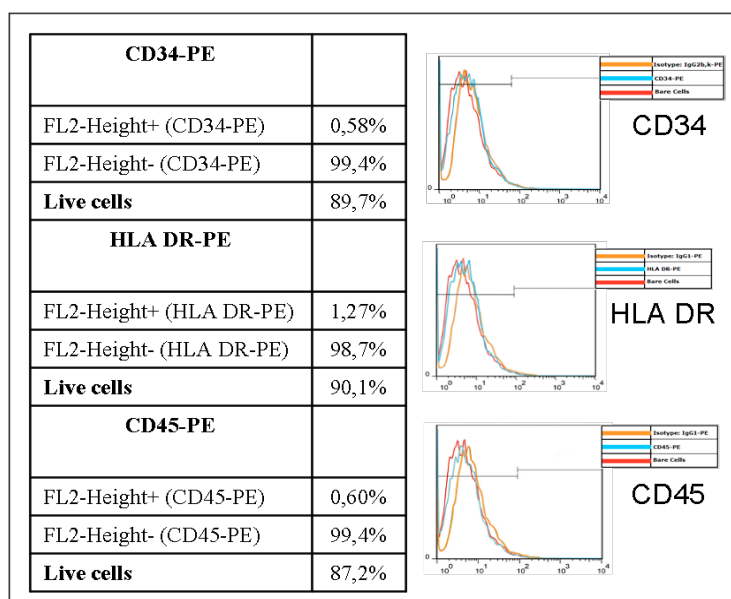


**Figure 4.2.2**

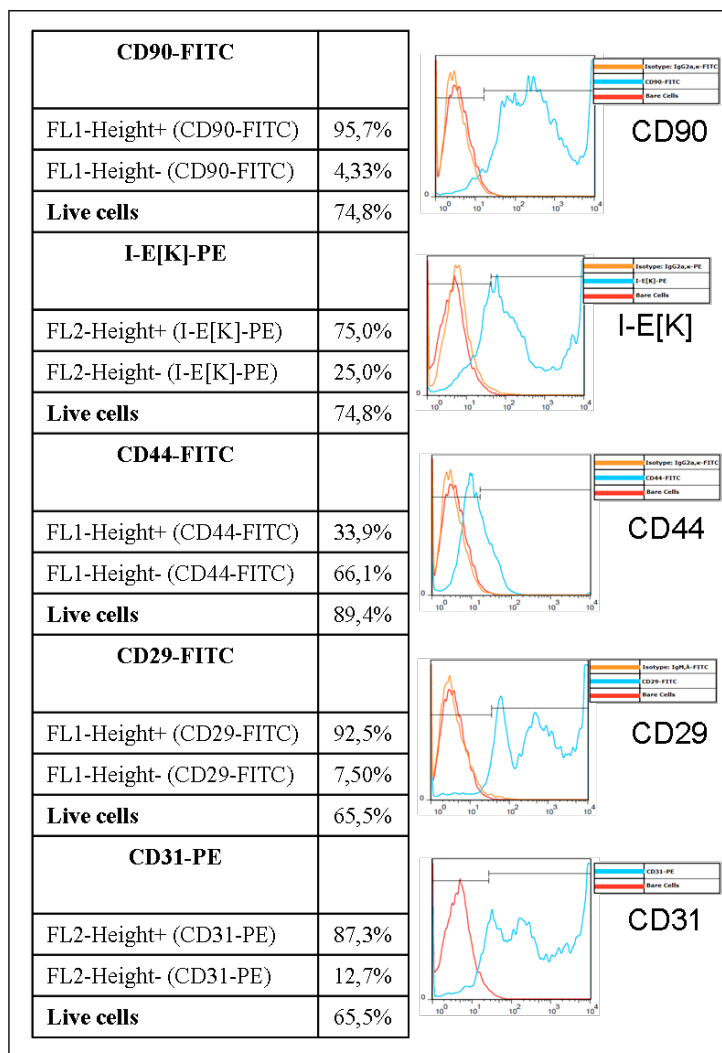
Characterization of rat ADSCs by flow cytometry.

Fluorescent intensity for unlabelled cells is shown in red, for isotype controls in orange and for each specific antigen marker in blue along with the percentage of expression. The number of live cells, volume and morphological complexity of cells is shown in the scatter plot.

## NEGATIVE CELL SURFACE MARKERS



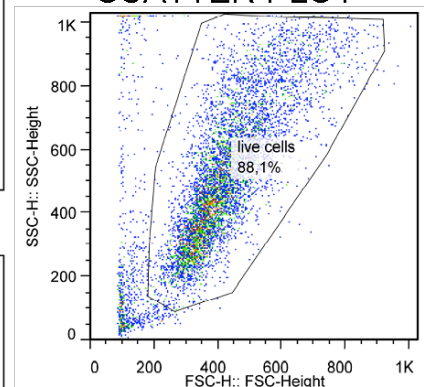
## POSITIVE CELL SURFACE MARKERS



## CONTROLS

BARE CELLS	
FL2-Height+ (Bare cells-PE)	1,76%
FL2-Height- (Bare cells-PE)	98,2%
<b>Live cells</b>	88,1%
ISOTYPE (IgG2a,κ)	
FL2-Height+ (IgG2a,κ-PE)	2,10%
FL2-Height- (IgG2a,κ-PE)	97,9%
<b>Live cells</b>	87,9%
ISOTYPE (IgM,λ)	
FL1-Height+ (IgM,λ-FITC)	1,64%
FL1-Height- (IgM,λ-FITC)	98,4%
<b>Live cells</b>	87,9%
ISOTYPE (IgG2a,κ)	
FL1-Height+ (IgG2a,κ-FITC)	1,61%
FL1-Height- (IgG2a,κ-FITC)	98,4%
<b>Live cells</b>	84,2%

## SCATTER PLOT



## NEGATIVE CELL SURFACE MARKERS

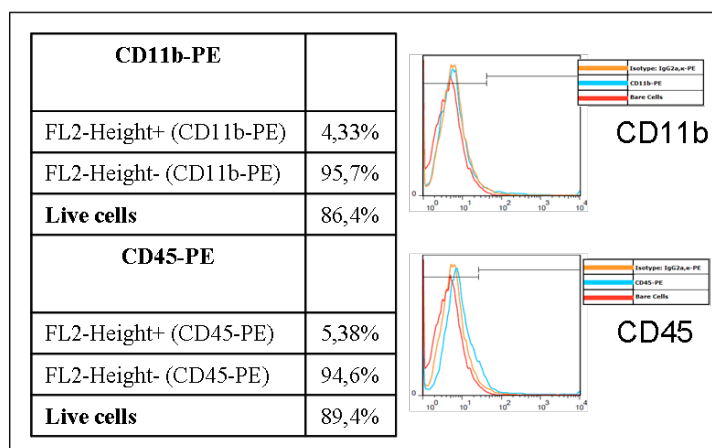


**Figure 4.2.3** Characterization of rat ADSCs by flow cytometry. Fluorescent intensity for unlabelled cells is shown in red, for isotype controls in orange and for each specific antigen marker in blue along with the percentage of expression. The number of live cells, volume and morphological complexity of cells is shown in the scatter plot.

Similar results were found for cells isolated from rat subcutaneous adipose tissue when characterized by flow cytometry. At passage 4, cells showed high expression for anchored conserved cell surface CD-90, surface glycoprotein CD-44, membrane receptor CD-29, major histocompatibility class II receptor alloantigen I-E[K] (antigen-specific T cells) and platelet endothelial cell adhesion (PECAM-1 involved in leukocyte migration, angiogenesis, and integrin activation) (figure 4.2.3).

On the other hand, these cells showed low expression for adhesion molecule CD11b (integrin alpha M expressed on surface of many leukocytes mediating inflammation by regulating leukocyte adhesion and migration, phagocytosis, cell-mediated cytotoxicity, chemotaxis and cellular activation) and the hematopoietic marker CD-45 (figure 4.2.3).

Specifically for the characterization of rat ADSCs, the scatter plot (figure 4.2.3) shows a non-homogenous population, as well as some of the plots for specific antigens expressions have different profiles suggesting different cell complexity and morphology.

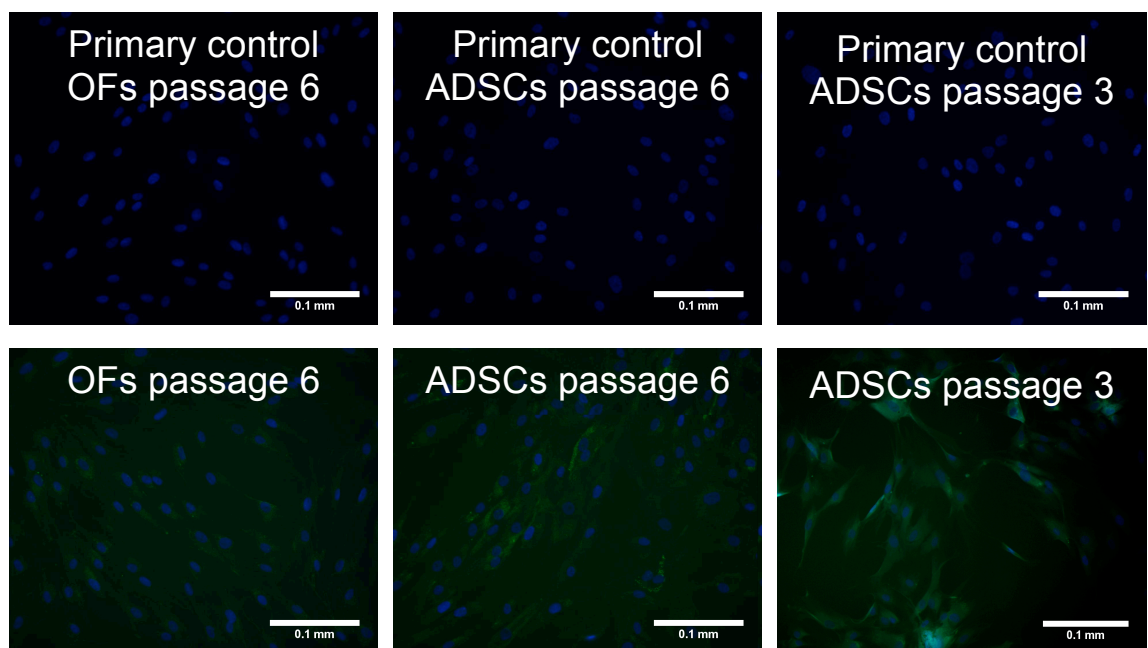


**Figure 4.2.4** Representative images of immunostaining for anti-human fibroblasts surface protein of OFs at passage 3 and ADSCs at passage 3 and 6 cultured in 2D. Scale bar = 0.1 mm.

The positive percentages of the positive surface antigens, CD-44 for rat cells, and CD29 and HLA-a/b/c for human cells are low (figure 4.2.3). These results are obtained



because profiles for bare cells (not labelled) and for these specific antigens overlap to some extent; however, we can distinguish two different profiles which prove the expression of these antigens for rat and human cells.

Human ADSCs at passage 3 and passage 6 and human OFs at passage 6 were cultured in 2D and stained for anti-human CD29, CD44, CD73 and fibroblast surface protein.

OFs at passage 3 and ADSCs at passage 3 and passage 6 were positively stained for the anti-human fibroblast surface protein (figure 4.2.4). On the other hand, only ADSCs at passage 3 were clearly positive for the 3 CD markers. While OFs were not stained for any of these Ab, ADSCs at passage 6 were slightly positive for CD44 (figure 4.2.5).

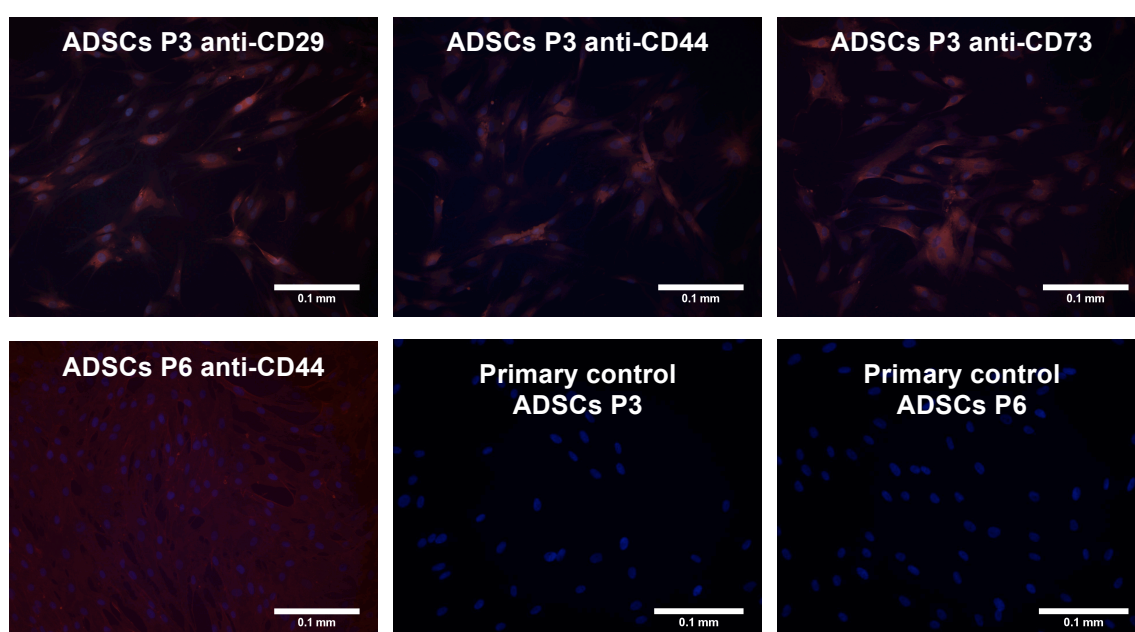


**Figure 4.2.5** Representative images of immunostaining for anti-human CD29, CD44 and CD73 of ADSCs at passage 3 and anti human CD44 of ADSCs at passage 6 cultured in 2D. Scale bar = 0.1 mm.

Multipotency of human ADSCs was evaluated by showing the adipogenic and osteogenic differentiation potential of these cells isolated from SVF of human subcutaneous adipose tissue.

Cells were cultured for three weeks in adipogenic and osteogenic mediums; however, after 7 days in culture, cells already exhibited some morphological modifications. Indeed, cell appearance changed from an elongated fibroblastic to a more cuboidal shape (408), when ADSCs were cultured in osteogenic medium, showing higher cell

density and orientation. Adipogenic differentiation was also observed by lipidic vesicle formation and morphological changes from elongated fibroblastic cells to rounded, adipocyte cell-like (409).

After 3 weeks, human ADSCs cultured with osteogenic differentiation medium were stained positively with 5% Alizarin Red (in red color), which stains calcium deposition, a late osteogenic marker. Alternatively, these same cells cultured with DMEM medium were completely negative for Alizarin Red staining, with no calcium deposition (figure 4.2.6).

Human ADSCs cultured for 3 weeks in adipogenic differentiation medium stained positively with 0,3% Oil Red O in 60% Isopropanol, which stains specifically lipid vesicles. Oil Red O did not stain same cells when cultured with DMEM medium for 3 weeks (figure 4.2.7).

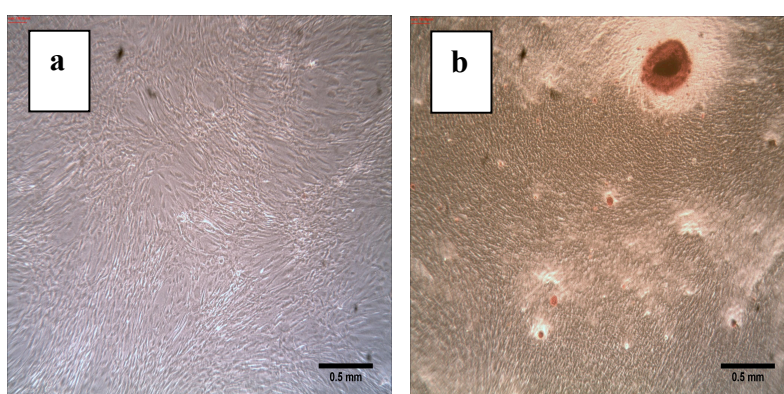


**Figure 4.2.6** (a) Human ADSCs cultured for 3 weeks with DMEM medium and stained with 5% Alizarin red, after fixation with paraformaldehyde. (b)

Human ADSCs cultured for 3 weeks with osteogenic medium and stained with 5 % Alizarin red, after fixation with paraformaldehyde. Scale bar = 0.5 mm.

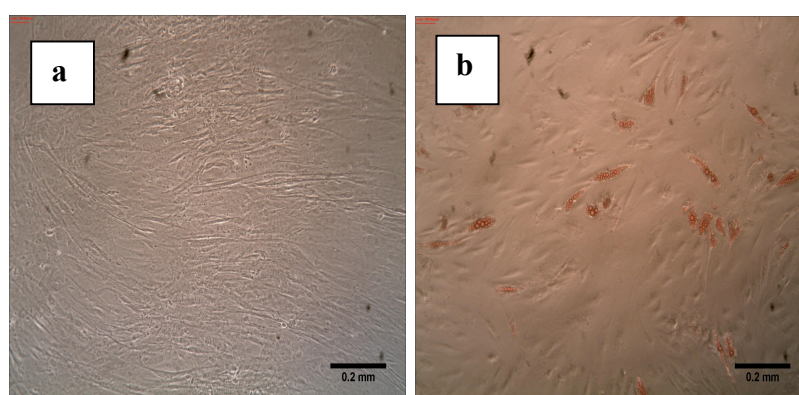


**Figure 4.2.7** (a) Human ADSCs cultured for 3 weeks with DMEM medium and stained with 0,3% Oil Red O, after fixation with paraformaldehyde.

(b) Human ADSCs cultured for 3 weeks with adipogenic medium and stained with 0,3% Oil Red O, after fixation with paraformaldehyde. Scale bar = 0.2 mm.

### 4.3 Comparison of OFs and ADSCs cultured on Th-PLA scaffolds

$1 \times 10^6$  OFs, ADSCs or a mixture of both, all at passage 6, were seeded on  $6.25 \text{ cm}^2$  Th-PLA scaffolds using metal rings with an external diameter of 2 cm (about  $3.2 \times 10^5$  cells seeded per  $\text{cm}^2$ ).

Each sample was cultured for 2 weeks and the potential of each cell type to attach and proliferate on Th-PLA scaffolds was assessed, such as, their capacity to produce ECM and the impact of this neo-tissue formation on mechanical properties of the material.

Our material candidate was biodegradable and microporous Th-PLA scaffold made of random microfibres as described in previous Chapter of this thesis.

#### 4.3.1 Cell attachment and proliferation

Cell attachment and proliferation was assessed by metabolic activity of the cells at day 0, 7 and 14 using AlamarBlue<sup>®</sup> staining. Then, samples were stained with DAPI after 2 weeks culture to look at the cell density and distribution into the scaffolds. Similarly, cell infiltration was assessed from frozen sections of these samples analyzed by H&E staining.

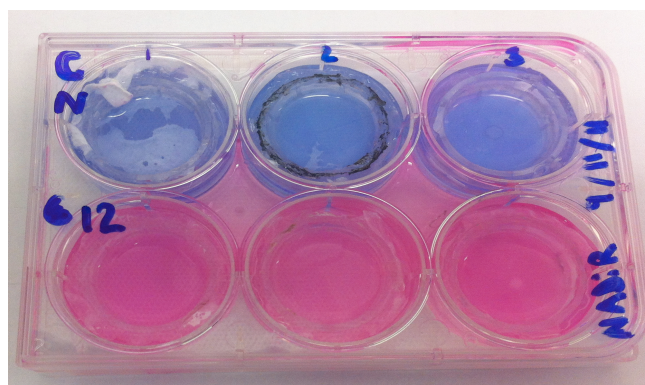


**Figure 4.3.1** Example of colour change seen after incubation with AlamarBlue<sup>®</sup> staining. Top row (Blue) no cells seeded. Bottom row (pink) cells seeded.

AlamarBlue<sup>®</sup> staining has been used as a surrogate marker of proliferation (410). It uses an oxidation-reduction indicator, resazurin (blue) which is reduced to resorufin (pink), and can be assessed by fluorescence and colorimetric methods (figure 4.3.1). The stain is non toxic and can simply be washed away and thus used repeatedly on the same



sample without damaging cellular viability (411). The resorufin continually develops and therefore a precise time point is required for assessment.

The absorbance of AlamarBlue<sup>®</sup> is plotted below for each sample (figure 4.3.2) minus the absorbance of controls (Th-PLA scaffolds cultured without cells).

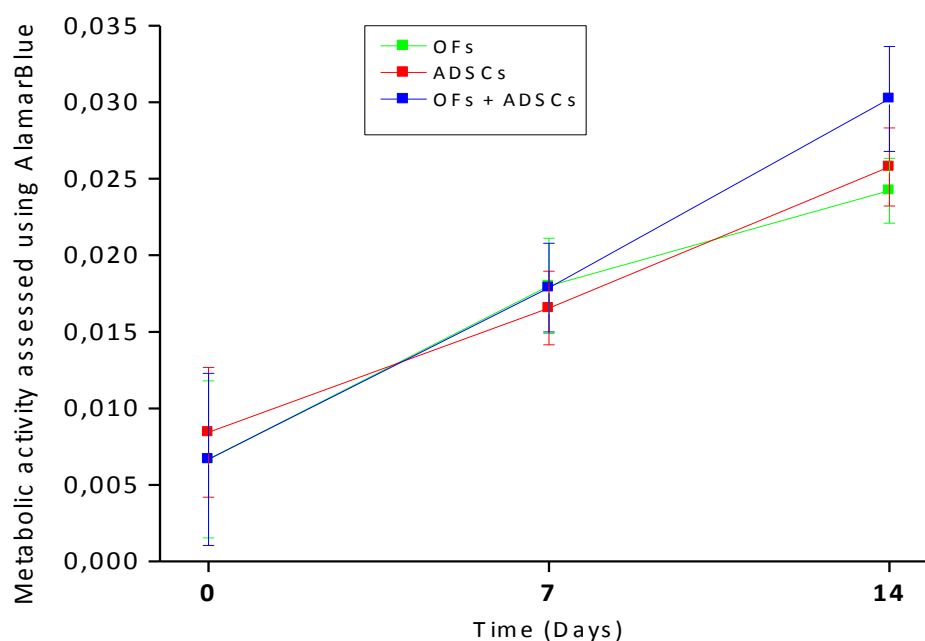


**Figure 4.3.2** AlamarBlue<sup>®</sup> staining for OFs, ADSCs and a mixture of both cells on Th-PLA scaffolds over 2 weeks in culture ( $n=3\pm SEM$ ).

Cells attached on Th-PLA scaffolds since metabolic activity from cells was measured for all samples a few hours after seeding them. Since some cells can pass underneath the metal ring or through big pores of the scaffolds being attached on the tissue culture plastic of the well, before performing AlamarBlue protocol<sup>®</sup>, samples were placed in a new 6-well plate and non-adhered cells were washed out with PBS, in terms to just read metabolic activity of cells attached to the scaffolds.

There were no significant differences between samples at any time point and all showed evidence of cell proliferation as seen by an increase in metabolic activity from day 0 to day 14.

DAPI stains DNA within cells. Images of each sample were undertaken to determinate the distribution of cells within scaffolds after 14 days in culture (figure 4.3.3).

Under a qualitative method, significant differences were not observed between samples, achieving a reasonable cell density in all of them.

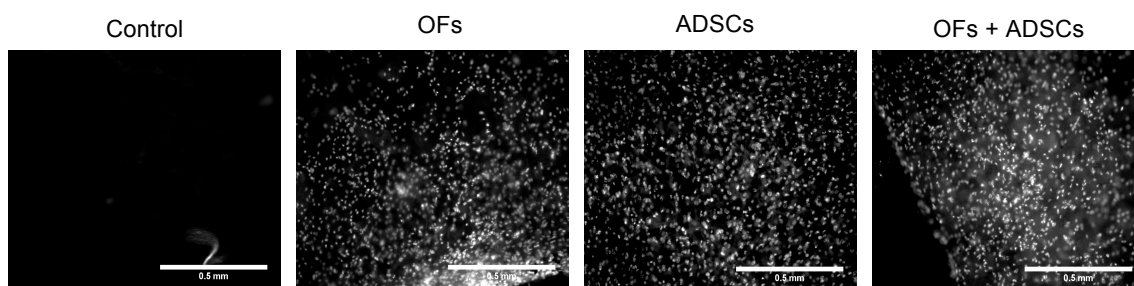


**Figure 4.3.3** Representative images of DAPI staining for Th-PLA samples cultured with OFs, ADSCs and a mixture of both cell types for 2 weeks. Plain Th-PLA scaffold cultured without cells is shown as a negative control. Scale bar = 0.5 mm.

Frozen sections of these samples stained with H&E showed, similarly, a confluent cell population homogeneously distributed, for both cell types, throughout the thickness of the Th-PLA scaffolds (figure 4.3.4).

Samples cultured with ADSCs were thicker due to a few layers of cells accumulated on one side of the scaffolds (cell seeded side). Also a thin layer of ECM was seen on both sides of the scaffolds for both cells types.

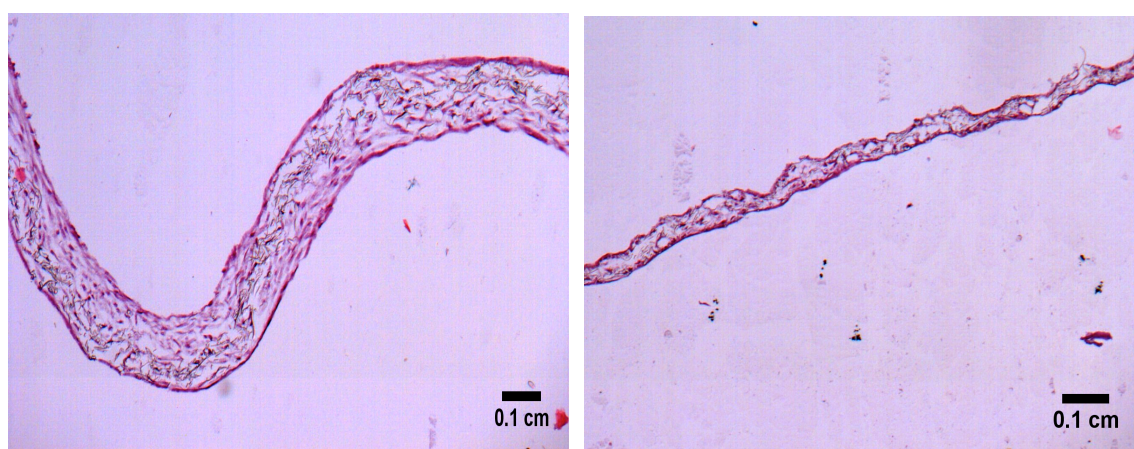


**Figure 4.3.4** Representative images of frozen sections of ADSCs (left) and OFs (right) cultured for 2 weeks on Th-PLA scaffolds stained for H&E.

### 4.3.2 Extracellular matrix (ECM) production

ECM formation was observed by SEM after 2 weeks of culture of Th-PLA scaffolds with OFs, ADSCs or a mixture of both cells. The nature of this ECM was analysed by looking for the specific production of collagen I, collagen III and elastin fibres using immunostaining. Quantitatively, total collagen formation was assessed by Sirius red staining.

Sirius red stains collagen a red colour (figure 4.3.5) and can be detected by polarized light and the birefringence of the dye has been described as being specific for collagen (412).

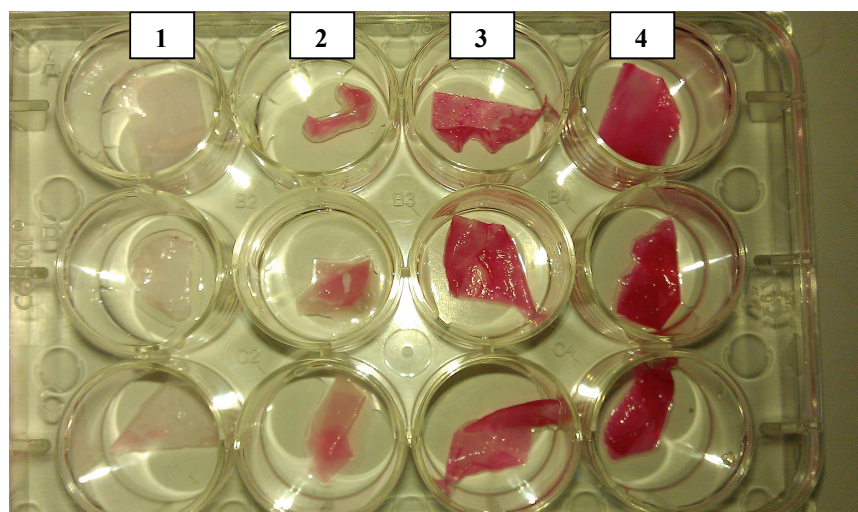


**Figure 4.3.5** Examples of Sirius red staining after 14 days culture of OFs and ADSCs on Th-PLA scaffolds. 1: Control (no cells, no medium); 2: Control (no cells but with medium); 3: OFs; 4: ADSCs.

The absorbance of Sirius red is plotted below (figure 4.3.6) minus the absorbance of controls without cells (but with medium) per gram of dry constructs.

ADSCs produced the highest amount of total collagen per gram of dry sample, significantly higher than scaffolds cultured with OFs.

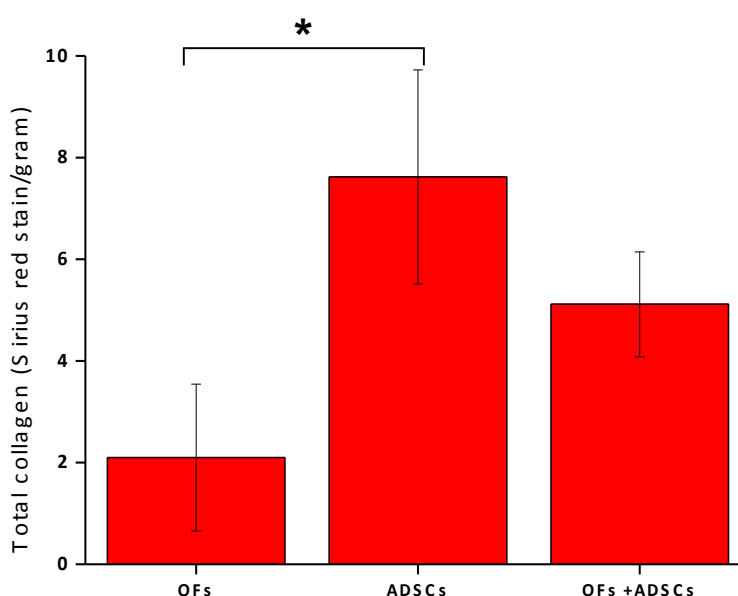


**Figure 4.3.6** Sirius red staining after 14 days of OFs, ADSCs and a mixture of both cells cultured on Th-PLA. ( $n=3 \pm \text{SEM}$ ).  $*p < 0.05$ .

All samples stained with DAPI were later assessed by immunostaining to determine the presence and distribution of fibres of collagen I, collagen III and elastin (figure 4.3.7), using specific antibodies. Also, samples of Th-PLA scaffolds cultured in DMEM medium without cells were assessed as negative controls for each ECM component.

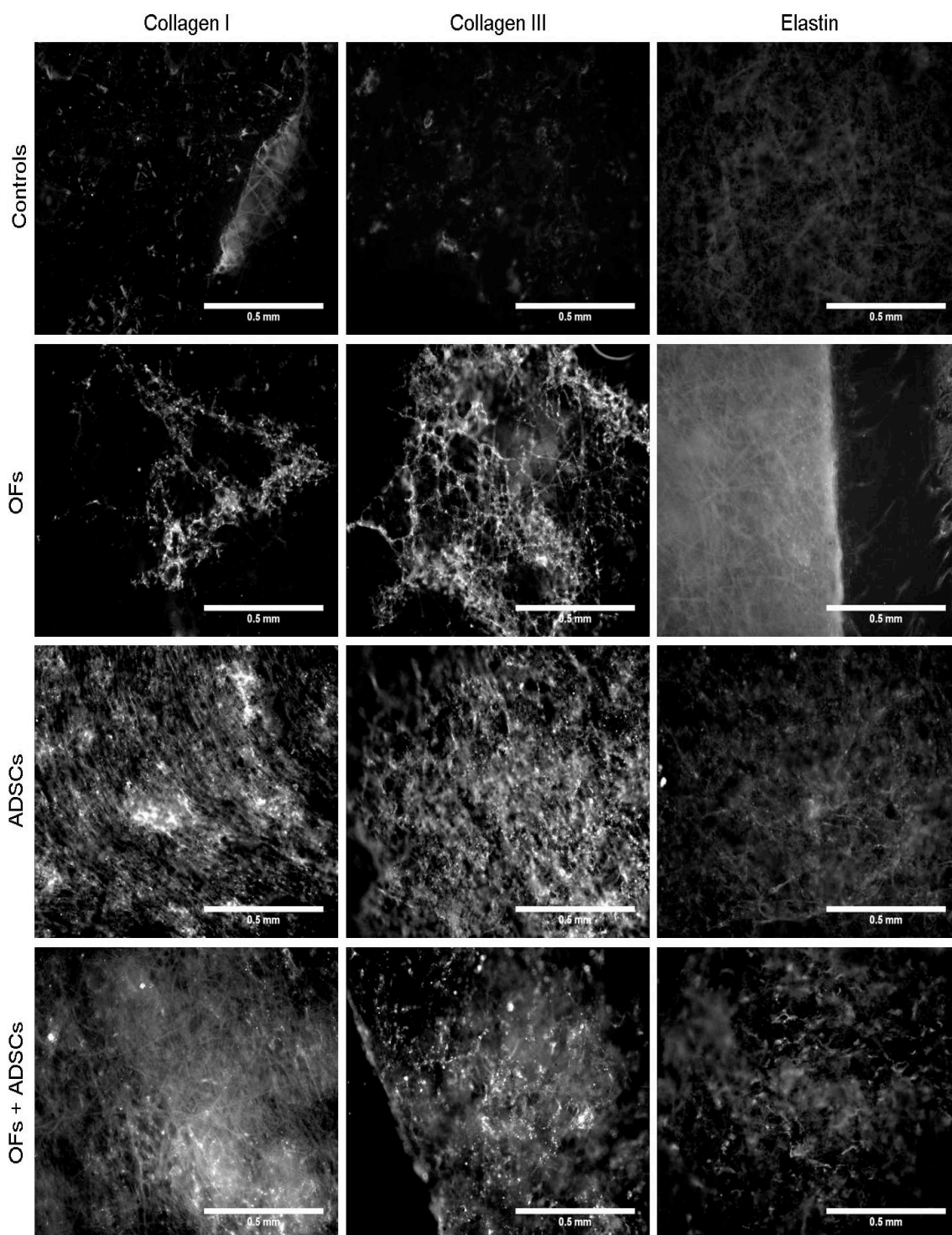


**Figure 4.3.7** Representative images of immunostaining for collagen I, collagen III and elastin of OFs, ADSCs and a mixture of both cell types cultured on Th-PLA scaffolds for

2 weeks. Controls of Th-PLA scaffolds cultured in DMEM medium without cells are shown as well. Scale bar = 0.5 mm.

Qualitatively, ADSCs produced higher amounts of collagen I and collagen III fibres. Elastin production was similarly low for all groups.

Semi-quantitative assessment of the extent of immunostaining was done on a blinded observer basis and the median value was used.

As seen in figure 4.3.7, ADSCs produced more collagen compared with the other 2 groups being significant for collagen I fibres (figure 4.3.8). The production of elastin was low in general, although, this was higher when both cells were cultured together.

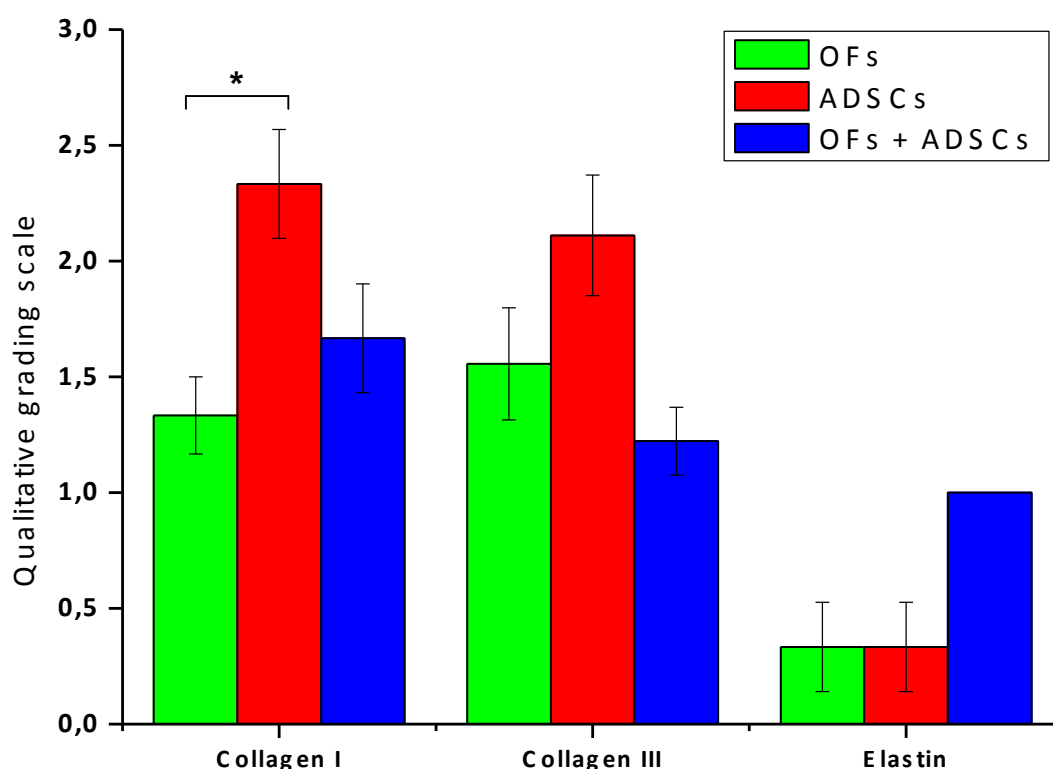


**Figure 4.3.8** Assessment of the extent of immunostaining using a blind scoring for OFs, ADSCs and a mixture of both cells cultured on Th-PLA scaffolds for 2 weeks. Results shown as mean $\pm$ SEM, ( $n = 3$ ) for collagen I, \*\* $p < 0.005$ ; collagen III; and elastin. Scale: 0 = absent, 1 = small amount, 2 = moderate amount, 3 = extensive amount.

With SEM, a denser layer of ECM was observed on Th-PLA scaffolds cultured with ADSCs, in comparison with the samples cultured with OFs (figure 4.3.9), by covering most fibres and pores of the scaffolds.



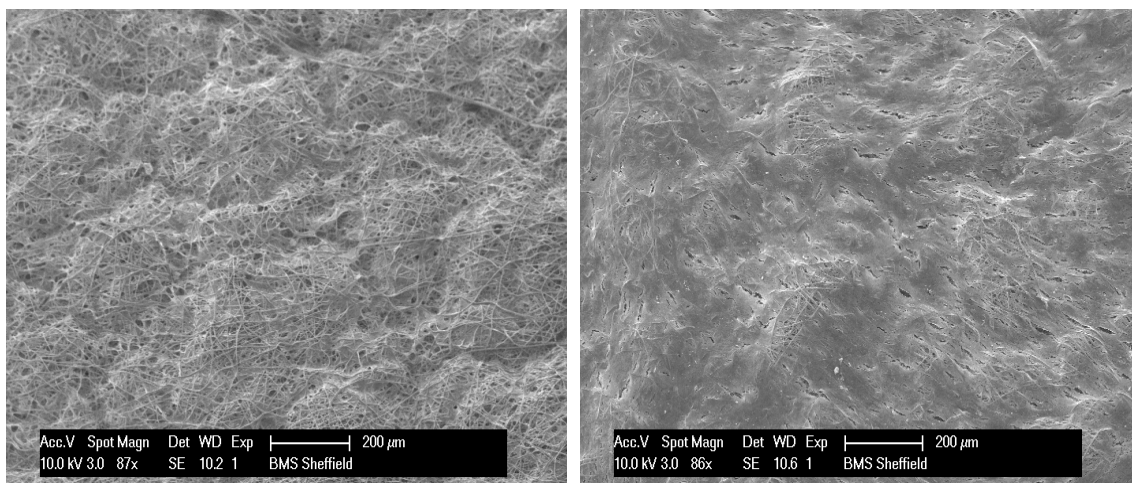


**Figure 4.3.9** Appearance by SEM of OFs and ADSCs cultured on Th-PLA scaffolds for 2 weeks in DMEM medium. Scale bar = 200  $\mu$ m.

### 4.3.3 Contraction

Cell mediated contraction was calculated using digital serial photographs of the size of the scaffolds relative to their area on day 0 (figure 4.3.10). The data is shown with and without subtracting the contraction of the controls (Th-PLA scaffolds cultured for 2 weeks in DMEM medium without cells) at day 14.

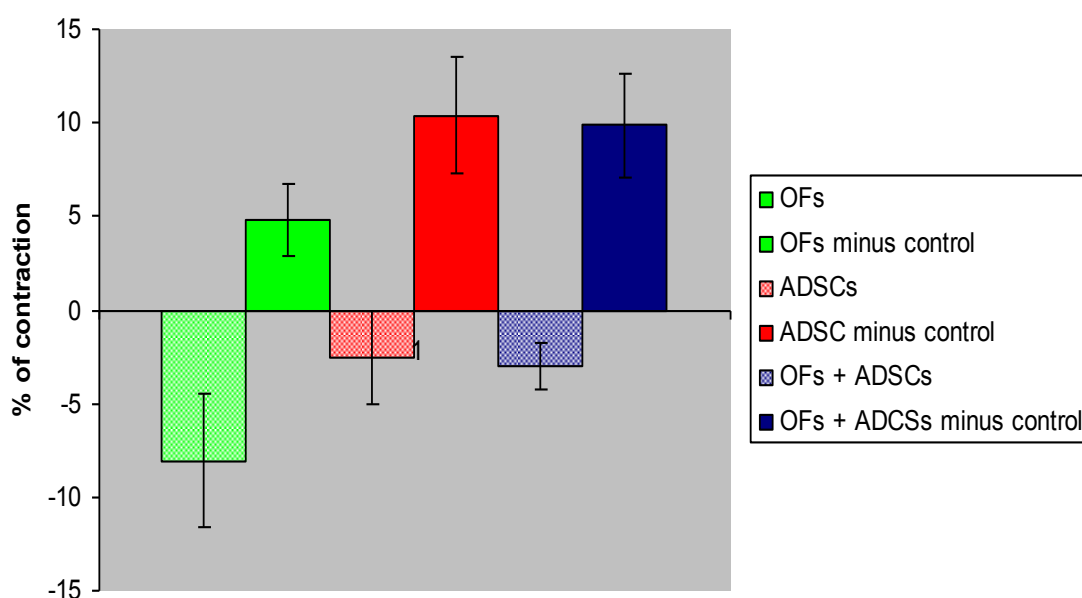


**Figure 4.3.10** Scaffold contraction represented as percentage reduced of the original scaffold area of Th-PLA scaffolds cultured with OFs, ADSCs and a mixture of both cells after 14 days ( $n=3 \pm \text{SEM}$ ). Data is also shown subtracting to the scaffolds with cells the percentage reduced for the controls.

All samples showed a slight expansion with no significant differences measured between groups (negative contraction).

Controls were more expanded than scaffolds cultured with cells and that is why the samples have a positive contraction when contraction from controls is subtracted.

#### 4.3.4 Mechanical properties

Mechanical properties of scaffolds cultured with cells were tested at day 14 for Young's modulus, UTS and strain at UTS using a BOSE electroforce tensiometer. Each property is plotted below (figure 4.3.11) and compared to the range for native healthy paravaginal tissue (194).

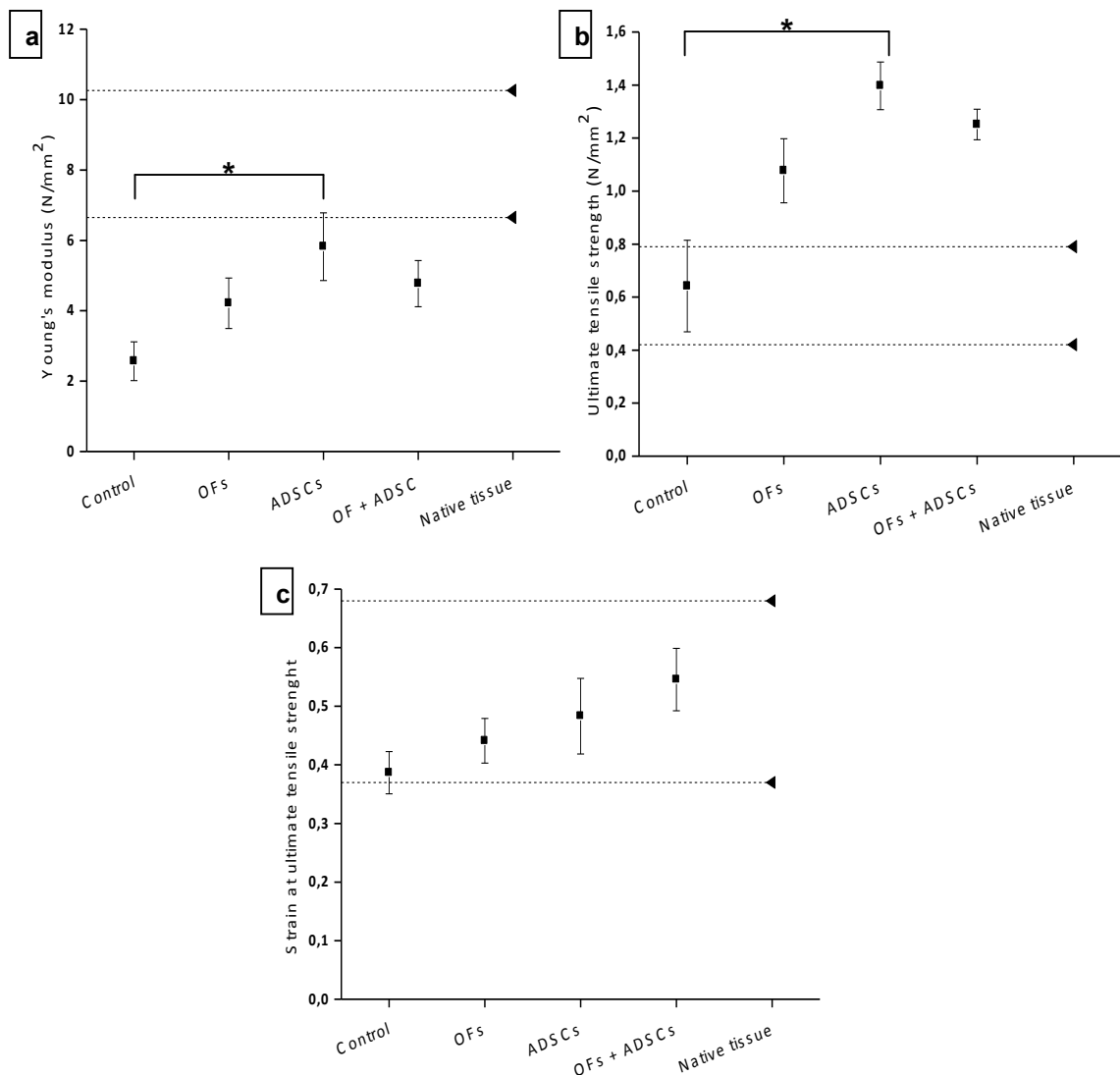


**Figure 4.3.11** Mechanical properties of Th-PLA scaffolds cultured with OFs, ADSCs and a mixture of both cells for 2 weeks. Results shown are mean $\pm$ SEM, ( $n = 3$ ). The last

*sample shown is the range for native tissue represented by 2 dashed lines (the range for native healthy paravaginal tissue). (a) YM, \* $p < 0.01$ . (b) UTS, \*\*\* $p < 0.0001$ . (c) Strain at UTS.*

All 3 mechanical properties were increased with the inclusion of cells. ADSCs gave the most significant differences with respect to the controls (scaffolds without cells), especially for UTS and were also slightly significant for Young's modulus.

## 4.4 Discussion

Cells from different sources have different biological properties. Vaginal fibroblasts isolated from patients with POP have shown a low proliferation rate and can migrate from the injection site (413). As an autologous cell candidate, OFs seem to be more appropriate to develop a TERM for pelvic floor repair since oral mucosa can be easily accessed and these cells have desirable properties, as seen in many studies when using grafts of this tissue for urethroplasty (384).

Alternatively, MSCs have been widely used as a cell therapy for the treatment of SUI, specifically by repair/regeneration of the urethral sphincter unit. MSCs have been injected at the submucosal level of the urethra wall, repairing connective tissue, and therefore, urethral support as well (413). MSCs are characterized as being nonimmunogenic (390). ADSCs, specifically, inhibit inflammatory responses by secretion of inhibitor of tumor necrosis factor  $\alpha$  (TNF $\alpha$ ), which is desirable for an anticipated better integration into host tissues (341). ADSCs have been shown to release fibroblastic growth factor (FGF) for regeneration of surrounding native tissues by stimulation of fibroblast proliferation and fibroblast ECM production (341). This, along with the proposed integration of the ADSCs into the whole urethral wall (414), their capacity to restore connective tissue (343), their angiogenic potential (403) and their easy isolation (400), makes ADSCs an attractive cell candidate to be investigated for the production of an autologous engineered tissue to repair fascial defects of the pelvic floor.



We looked at human OFs, human ADSCs and a mixture of both cells since FGF released from ADSCs may stimulate OFs proliferation and/or their ECM production.

To compare OFs and ADSCs, both cell types were isolated, characterized and cultured on Th-PLA scaffolds, and their ability to make ECM examined (415) to develop a TERM.

Human OFs, which had been previously isolated, were used from only one patient.

Human ADSCs were isolated from different patients and were used for the *in vitro* and *in vivo* experiments of this thesis while, rat ADSCs were isolated only from one rat since these cells were only used for the *in vivo* experiments.

Only one batch of human ADSCs were characterized by FACS (the batch of cells used for the *in vitro* experiments of this Chapter, Chapter 5, and the *in vivo* experiments), such as the batch of rat ADSCs.

Adult MSCs have been shown to have slightly different behaviours between different donors. In addition, the passage number may affect the mesenchymal potential of the cells with higher potential for lower passages (390). To test this, differentiation assays were performed for different batches of human ADSCs and at different passages to compare their mesenchymal potential, to compare their performance when seeded and cultured on PLA scaffolds. These results are shown and discussed in Chapter 8 of this thesis.

Human ADSCs cultured in 2D at passage 3 expressed 3 CD markers specific for mesenchymal stem cells. Human ADSCs at passage 6 may lose expression of some of these CD markers, as seen when cultured in 2D; in addition, same cells at the same passage also showed low expression for some of these markers. However, these cells were well characterized by FACS, expressing surface markers specific of MSCs and being negative for hematopoietic markers. Furthermore, by differentiation assays, it was shown that these cells retained the potential at passage 6 to differentiate into osteogenic (by calcium deposition) and adipogenic (by lipidic vesicle formation) cell lineages.

On the other hand, anti-human fibroblast Ab showed expression of the specific protein on the surface of OFs and it was bound to ADSCs at passage 6 as well. This could suggest the possible differentiation of the ADSCs at high passage into fibroblast; however, since the Ab was also bound to these human ADSCs at passage 3 too, this suggests low specificity of this Ab or that this surface protein is also expressed in MSCs.

In general, no significant differences were identified when comparing ADSCs and OFs cultured for 2 weeks on Th-PLA scaffolds, and there was no advantage to having a co-culture of both.

No differences were observed between groups at any day for metabolic activity. This is supported by DAPI images and frozen sections since a confluent cell population homogeneously distributed into the scaffolds was found for all groups after 2 weeks culture. This also proved the ability of the cells to pass through the pores of the scaffolds which have been described in the previous Chapter of this thesis as being microporous. Macroporous scaffolds ( $>75\ \mu\text{m}$ ) have been postulated to be better for host cell infiltration, however, this infiltration may be explained by the presence of some macropores in our Th-PLA scaffolds or due to the mobility of individual fibres which are not fixed at their intersections allowing cell infiltration.

Alternatively, big errors were obtained for metabolic activity at day 0 which means high differences between samples seeded with the same type and number of cells. The cell seeding may need to be improved in the future for more reproducible experiments. However, as explained in the previous Chapter of this thesis, electrospinning is not a very reproducible technique and small differences between thickness of fibres and pore sizes were found between different sheets of PLA (377). We analyzed 3 samples for 3 repetitions using different sheets of electrospun PLA; therefore, PLA samples with wider pores, for instance, may contribute to a poor cell seeding as cells may rapidly move through these scaffolds and go to the bottom of the well.

Alternatively, these differences at day 0 may not be very relevant since they are reduced at day 14 with all samples achieving a confluent cell population with similar metabolic activity.

All the analyses for ECM production agree with significantly higher collagen production from the ADSCs. Both cells formed an ECM sheet on both sides of the scaffold, as seen by frozen sections stained for H&E, and which was denser for ADSCs as seen by SEM. This may be explained as a consequence of the few layers of ADSCs accumulated on the cell seeded side of the scaffold as seen in H&E images. Furthermore, all groups of cells were able to specifically produce fibres of collagen I, collagen III and elastin.

After cell culture, all cell-seeded groups increased the mechanical properties of the scaffolds compared to the controls, all being close to the range of values for native paravaginal tissues of women. Nevertheless, only ADCSs cultured on Th-PLA scaffolds achieved a significant increase for Young's modulus and UTS compared to controls without cells, being very significant for the latter, which fits with the ADSCs higher production of collagen.

The variability between Th-PLA scaffolds made by the electrospinning technique had an effect on mechanical properties, particularly for Young's modulus. Th-PLA scaffolds from previous Chapter are much stiffer compared with the scaffolds from this Chapter. Similarly to metabolic activity, differences between scaffolds did not interfere in the purpose of these experiments. However, especially for mechanical properties, these differences may have a relevant effect on the final product for developing a material which needs to give enough support to the pelvic floor. The importance of the mechanical properties is further discussed in Chapter 7 of this thesis. In addition, as discussed in the last Chapter of this thesis, the chosen material will need to go through Good Manufacturing Practice conditions for reproducibility when developing the final clinical product.

No significant differences were observed in terms of scaffold contraction. All samples expanded in size at day 14 relative to day 0. This is very desirable since contraction has been observed in implanted skin grafts leading to clinical complications (416). In addition, this expansion seems to be lower for the scaffolds cultured with ADSCs which may be explained again by higher production of collagen. ECM components would bind PLA fibres restricting their expansion in culture.

In summary, on the basis of the current *in vitro* results we would conclude that both cell types are suitable candidates to develop a TERM for fascial repair of the pelvic floor as both gave promising results with very small differences between the cell types.

## **Chapter 5**

### **OPTIMISING CULTURE CONDITIONS FOR THE TERM<sub>s</sub>**

## 5.1 Introduction

After identifying the best scaffold and cell candidates to develop a TERM designed for pelvic floor repair, in this Chapter we tried to identify the best culture conditions for the TERM. For this, we studied the effect of mechanical forces and chemical stimulation on cells cultured on Th-PLA scaffolds and we optimized the number of cells seeded and period of culture for developing a TERM.

### 5.1.1 Mechanical stimulation

Mechanical forces have been shown to have a direct impact upon the function of cells both *in vivo* and *in vitro* (417). Many physical activities of our body are essential for life such as the pumping of the heart and the respiratory movement. In addition, mechanical forces also regulate cellular processes including migration, adhesion and morphogenesis, among others (418, 419). The conversion of a mechanical force into cell activity is termed mechanotransduction and can be produced by extracellular and intracellular forces (420). Diseases such as arthritis and osteoporosis have been shown to be related to the impairment of the cells ability to respond to mechanical signals (421).

Mechanical conditioning has been used to stimulate the production of ECM proteins and improve the mechanical properties of tissue engineered constructs of scaffolds seeded with cells (422). Most of these studies are found in the field of musculoskeletal tissue engineering where the effect of forces affecting bone and cartilage tissues seems to be more established (423).

Bioreactors have been designed to study the effect of different mechanical forces on engineered tissues (424, 425). A variety of forces have been utilized including fluid shear (426), uni-axial (427), biaxial (428) and multi-axial strain (429), compression (430) and hydrostatic forces (431). Some of the outcomes of mechanical loading include alignment of cells and organization of ECM (432), cell differentiation (433) and proliferation and formation of greater ECM (434).

There are no studies to the best of our knowledge looking at the mechanical conditioning of scaffolds seeded with cells for their use in the treatment of SUI or POP.

The tissues of the pelvic floor are subjected to forces which are not well characterized. These forces will include cyclical increases in intra abdominal pressure due to breathing, intermittent increases in pressure associated with movement or more marked pressure rises due to heavy lifting and coughing or straining, for instance. The weight of the pelvic organs along with their contents will also exert a constant force applied to the supportive tissues of the pelvic floor. Furthermore, these forces are unlikely to be equally distributed across the whole pelvic floor.

Traditionally, pressure in urology has been measured in cm/H<sub>2</sub>O during urodynamic studies. In an upright position, a pressure of about 40 cm/H<sub>2</sub>O has been measured in the bladder during the storage phase of micturition (i.e. relaxed). It has been proposed that since the bladder is situated just above the pelvic floor, there would be a similar pressure found in the pelvic floor when standing (435). Cadaveric studies from the same group, have provided the dimensions of the female pelvis with an average pelvic floor area of 94 cm<sup>2</sup> (435). Using both values the estimated physiological loads acting on the pelvic floor were described to be around 37 N standing, 19 N supine, 129 N coughing and 92 N straining (436).

Nevertheless, the forces that the materials that are implanted to treat SUI and POP undergo may be different. There are no reports of these measurements and there are no computational models to obtain these values as yet.

In this Chapter, we first of all studied how different mechanical forces can affect the activity of different cells seeded onto a scaffold, as well as, the effect on the mechanical properties of the TERM. Although the forces applied to the TERM *in vivo* may be different, affecting the cell behavior in a different way, these studies had the aim of showing the potential to increase ECM production and mechanical properties of the engineered tissue before implantation by applying mechanical forces.

### **5.1.2 Chemical stimulation**

The addition of chemical factors to the *in vitro* cell culture environment has been widely used in tissue engineering to promote cell proliferation and ECM production, similar to mechanical stimulation.

Collagen is the main ECM component of the supportive tissues of the pelvic floor and it determines the strength of these. Intrinsic and extrinsic growth factors have been used in tissue engineering since these have an essential role in the development and remodeling of tissues (437). *In vitro*, TGF-beta-1 has been shown to significantly increase production of collagen for development of tissue engineered ligaments (438), as well as, having an effect on the maximal tensile load of these engineered tissues (439). Similarly, human aortic cells seeded on to poly-glycolic acid patches showed an increase in collagen production with more densely organized ECM by TGF-beta-1 stimulation (440).

Growth factors can be manufactured using recombinant technology and these are a lower risk for clinical use than natural growth factors. Both synthetic and naturally derived chemicals can be used to stimulate collagen formation.

Vitamin C is an essential factor for various steps in collagen biosynthesis (441, 442). For the post-production of collagen, these molecules undergo post-translational modifications which include the hydroxylation of proline and lysyl residues. This process is important for cross link formation leading to a strong and stable collagen (443). Hydroxylation occurs through prolyl hydroxylase and lysyl hydroxylase, and Vitamin C is a cofactor for both of these enzymes (444). A deficiency in Vitamin C produces a disruption in collagen formation leading to diseases such as scurvy.

Vitamin C supplementation has been shown to promote collagen production of cells *in vitro* (445, 446), and also, it has been used as an additive to the nutrient medium in tissue engineering to promote collagen biosynthesis *in vitro*.

The effect of 3 different concentrations of Vitamin C was assessed on temporo-mandibular joint cells cultured on non-woven poly-glycolic acid scaffolds. A concentration of 25 µg/mL was found to significantly increase total collagen production compared to control cells (447). Similarly, dermal fibroblasts seeded on fibronectin pre-treated SIS scaffold increased collagen I production when cultured with Vitamin C (448). Another study found an increase in collagen production by ascorbic acid supplementation on fibroblast seeded on to freeze-dried poly hydrogels (449).

## 5.2 Mechanical stimulation of TERMS

For free or unrestrained conditions,  $1 \times 10^6$  OFs, ADSCs or a mixture of both were seeded on  $6.25 \text{ cm}^2$  Th-PLA scaffolds using metal rings with hall diameter of 2 cm, as previously described in Chapter 2 and 4 (figure 5.2.1).

### 5.2.1 Restrained and intermittent stress conditions

For restrained and intermittent stress conditions an improved version of Scaffdex™ (Scaffdex Oy, Tampere, Finland) cell culture ring was used. This ring is composed by two tightly fitting plastic rings.  $4 \text{ cm}^2$  scaffolds were clamped between the two rings being restrained between one plastic ring and the other, the ring lock (figure 5.2.1). The final size of the Th-PLA scaffold for culture is a circle of 2.5 cm of diameter. However, for the improved version of Scaffdex™, the bottom ring was cut to reduce the height of the Scaffdex™. The cut non clamped end was used as a base and the ring clamp side was used as intended by the manufacturer (figure 5.2.1).

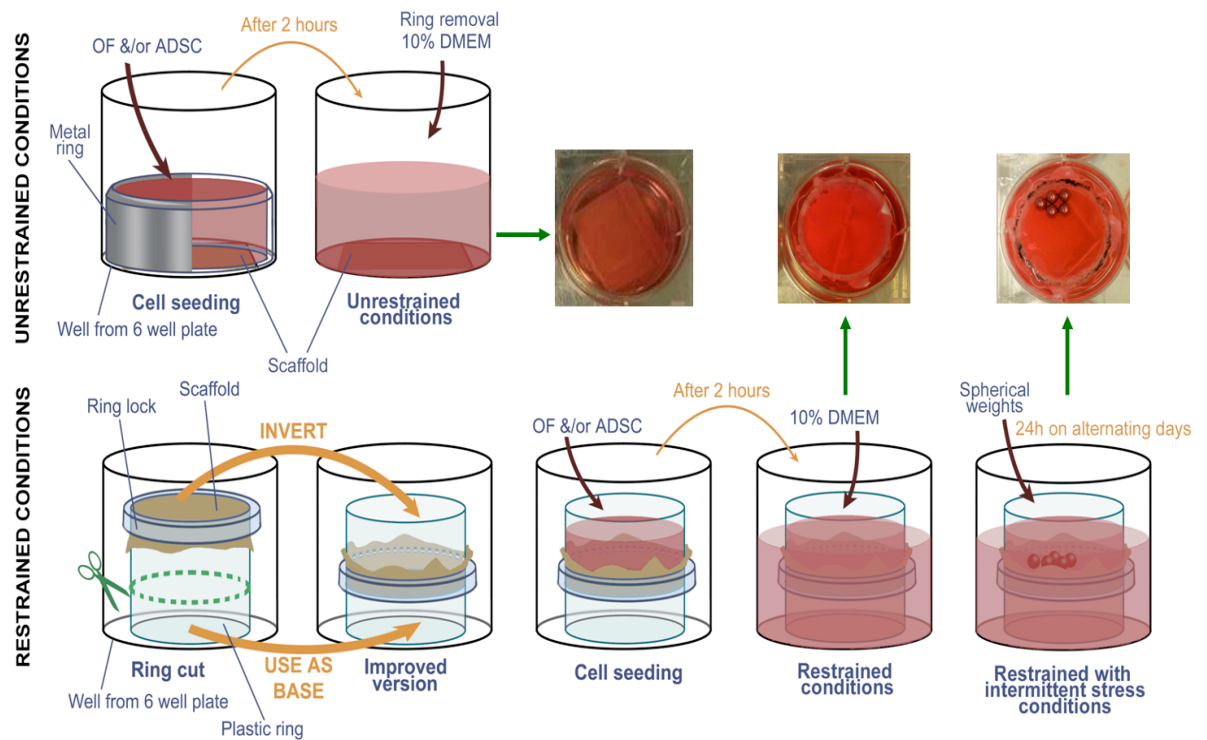


**Figure 5.2.1** Improved version of Scaffdex™ for static and intermittent stress conditions.



The improved version of Scaffoldex<sup>TM</sup> allowed better cell seeding on Th-PLA scaffolds since cells are contained on the top of the scaffold by the plastic ring (figure 5.2.1). This version was used for restrained and intermittent stress conditions, and after cell seeding, spherical steel weights, 0.261 g each, were placed in the centre of each scaffold for 24 h on alternating days, only for samples under intermittent stress conditions (figure 5.2.1). The improved version of the Scaffoldex<sup>TM</sup> was also useful for this last condition because the ball bearings were contained on top of the scaffold and pressed on this to compress it against the well since the scaffold does not touch the bottom of the 6 well plate.

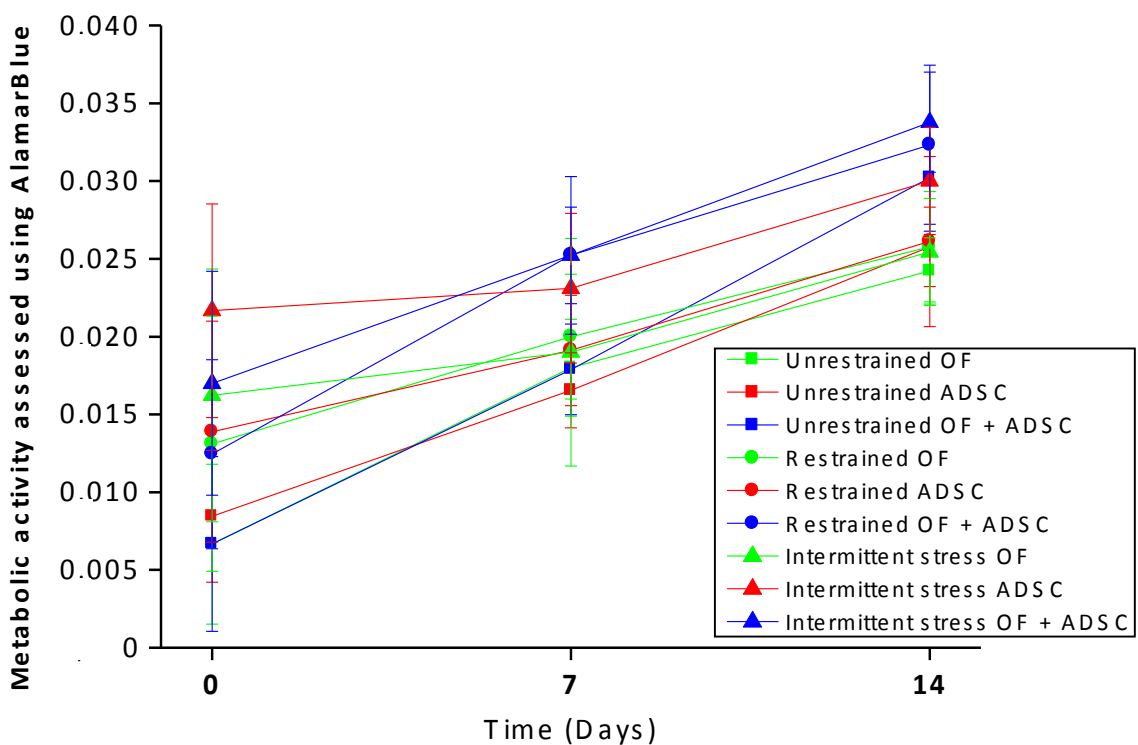


**Figure 5.2.2** Metabolic activity using AlamarBlue<sup>®</sup> for OFs, ADSCs and a mixture of both cultured on Th-PLA scaffolds under unrestrained conditions and restrained (with and without intermittent stress) conditions over 2 weeks. Results shown are mean $\pm$ SEM, ( $n = 3$ ).

As with unrestrained conditions, scaffolds under restrained (with and without intermittent stress) conditions were seeded with  $1 \times 10^6$  OFs, ADSCs or a mixture of both, and cultured for 2 weeks with DMEM medium.

Then, all samples were analyzed for cell attachment and proliferation using AlamarBlue<sup>®</sup> staining and DAPI staining, total collagen production using Sirius red

staining, mechanical properties using a BOSE tensiometer, collagen I, III and elastin production using specific antibodies, and appearance of the ECM using SEM, as described in Chapter 2.

AlamarBlue<sup>®</sup> absorbance was recorded on days 0, 7 and 14, and is plotted above minus the absorbance of controls without cells (figure 5.2.2).

Results showed at day 14 showed no significant differences between samples. On the other hand, the errors are quite big particularly at day 0 (figure 5.2.2).

Using a qualitative assessment, DAPI staining did not any clear differences between samples, achieving a confluent amount of cells in all of them (figure 5.2.3).

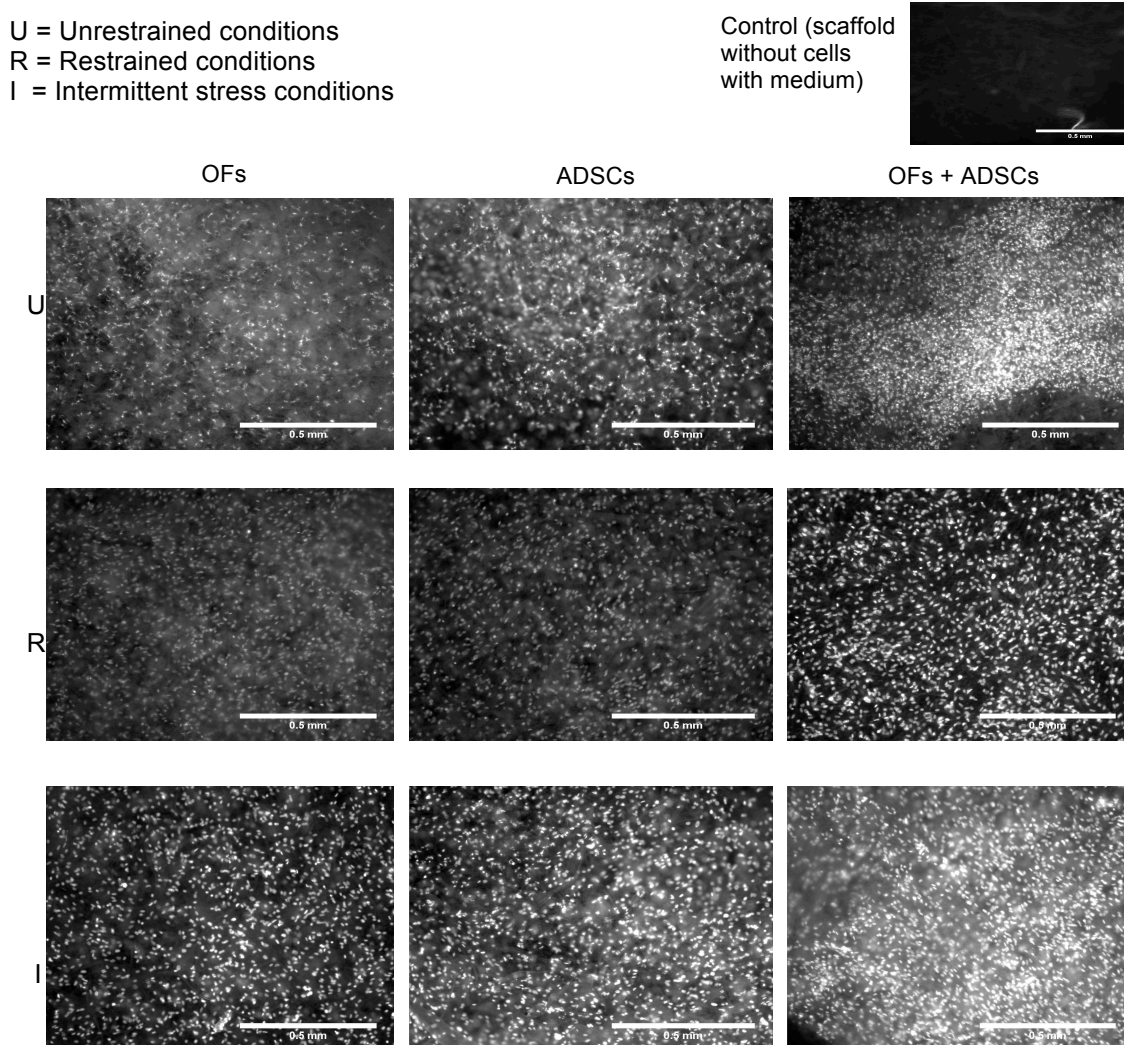


**Figure 5.2.3** DAPI staining for Th-PLA scaffolds cultured with OFs, ADSCs and a mixture of both cultured under unrestrained conditions and restrained (with and without intermittent stress) conditions over 2 weeks. Control of Th-PLA scaffold cultured in DMEM medium without cells is shown as well. Scale bar = 0.5 mm.

Sirius red was read from all samples at day 14 to calculate total collagen production. The absorbance of Sirius red is plotted below (figure 5.2.4) minus the absorbance of controls without cells expressed per gram of dry constructs.

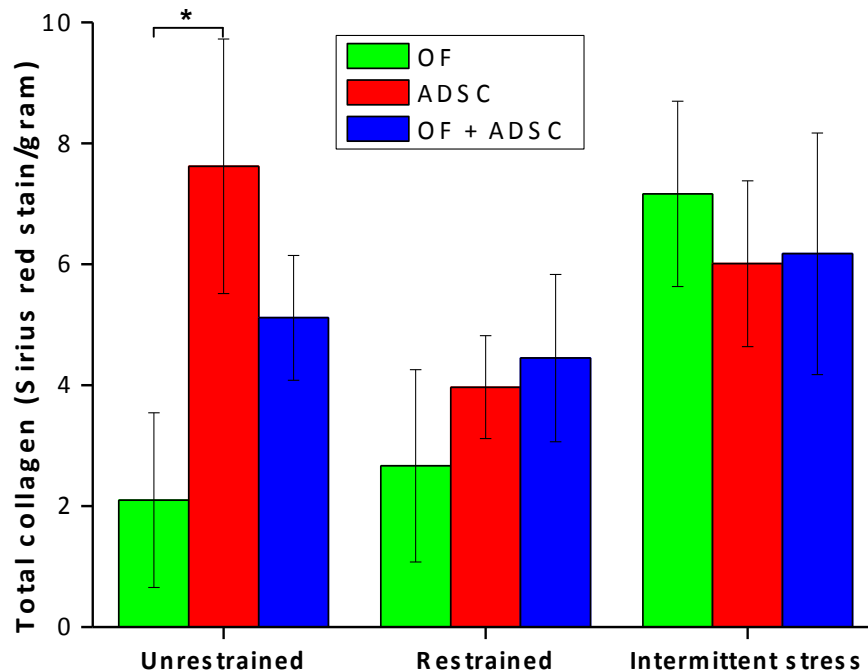


**Figure 5.2.4** Production of total collagen by OFs, ADSCs and a mixture of both cells cultured on Th-PLA scaffolds under unrestrained conditions and restrained (with and without intermittent stress) conditions. Results from Sirius red staining after 14 days shown as means  $\pm$ SEM, ( $n = 3$ ),  $*p < 0.05$ .

In unrestrained conditions, ADSCs produced significantly ( $p < 0.05$ ) more total collagen per gram of sample, than OFs (figure 5.2.4). Restrained (with and without intermittent stress) conditions did not lead to a significant increase in collagen production for any cell group. Similarly, a combination of both cell types did not significantly enhance collagen production under any culture conditions.

All 3 mechanical properties increased with the inclusion of cells compared to acellular scaffolds (controls) under any culture conditions.

Th-PLA scaffolds cultured with ADSCs gave the greatest improvement of these properties under unrestrained conditions compared with acellular controls (figure 5.2.5), and were statistically significant for Young's modulus ( $p < 0.01$ ) and UTS ( $p < 0.0001$ ).

Comparing OFs with ADSCs and a mixture of both, the results were similar with no benefit in culturing cells under restrained conditions.

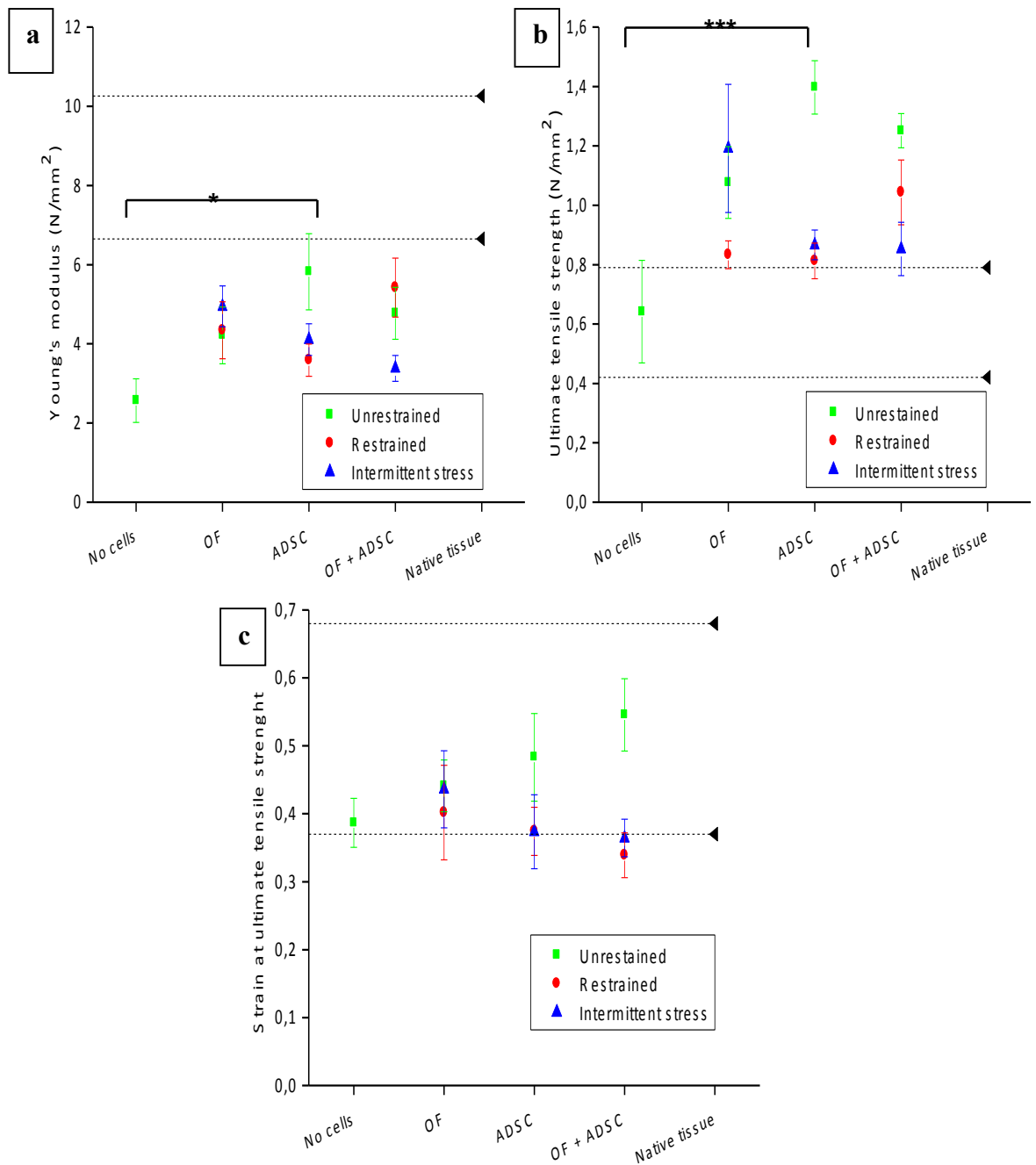


**Figure 5.2.5** Mechanical properties of Th-PLA scaffolds cultured with OFs, ADSCs and a mixture of both under unrestrained conditions and restrained (with and without intermittent stress) conditions for 2 weeks. Results shown are means  $\pm$ SEM, ( $n = 3$ ). The last sample shown is the range for native tissue represented by 2 dashed lines (the range for native healthy paravaginal tissue). (a) YM,  $*p < 0.01$ . (b) UTS,  $***p < 0.0001$ .

All samples stained with DAPI were later assessed to determine the presence and distribution of collagen types I, collagen III and elastin, using immunostaining. Also, samples of Th-PLA cultured in DMEM medium without cells were added to the immunostaining protocol; as controls for the 3 ECM components.



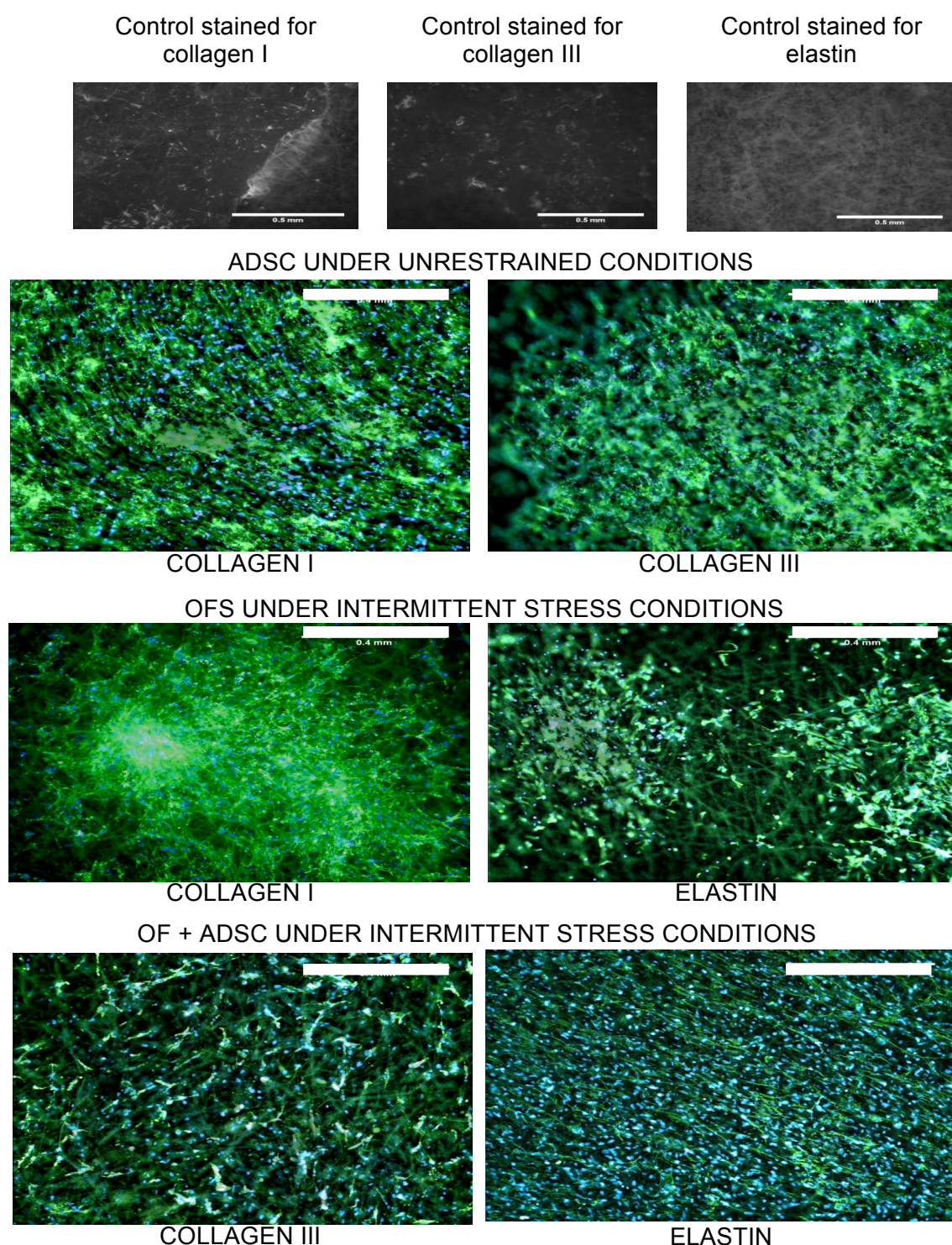


**Figure 5.2.6** Representative images for presence and distribution of collagen I, III and elastin (green colour) with cell nuclei (blue colour) using immunostaining and DAPI respectively, after 14 days culture on Th-PLA scaffolds of ADSCs under unrestrained conditions; OFs under restrained with intermittent stress conditions; and a mixture of OFs and ADSCs under restrained with intermittent stress conditions. Controls of Th-PLA scaffolds without cells are shown for immunostaining of collagen I, III and elastin. Scale bar = 0.5 mm.

Representative images for the presence and distribution of specific ECM components are shown above in colour (figure 5.2.6), for samples from the 3 group of cells under the mechanical culture conditions which gave the best results, respectively. For each sample, 2 images were taken at the same point; one for DAPI, which is colored in blue, and one for collagen I/ III/ elastin which are colored in green. In the same image cell nuclei and collagen or elastin fibres are shown.

Semi-quantitative assessment of the extent of immunostaining was done on a blinded observer basis using a qualitative grading scale; absent = 0, small amount = 1, moderate amount = 2, extensive amount = 3. Example photographs depicting 0, 1, 2 and 3 were provided for reference and the median value from these scores was used (figure 5.2.7).

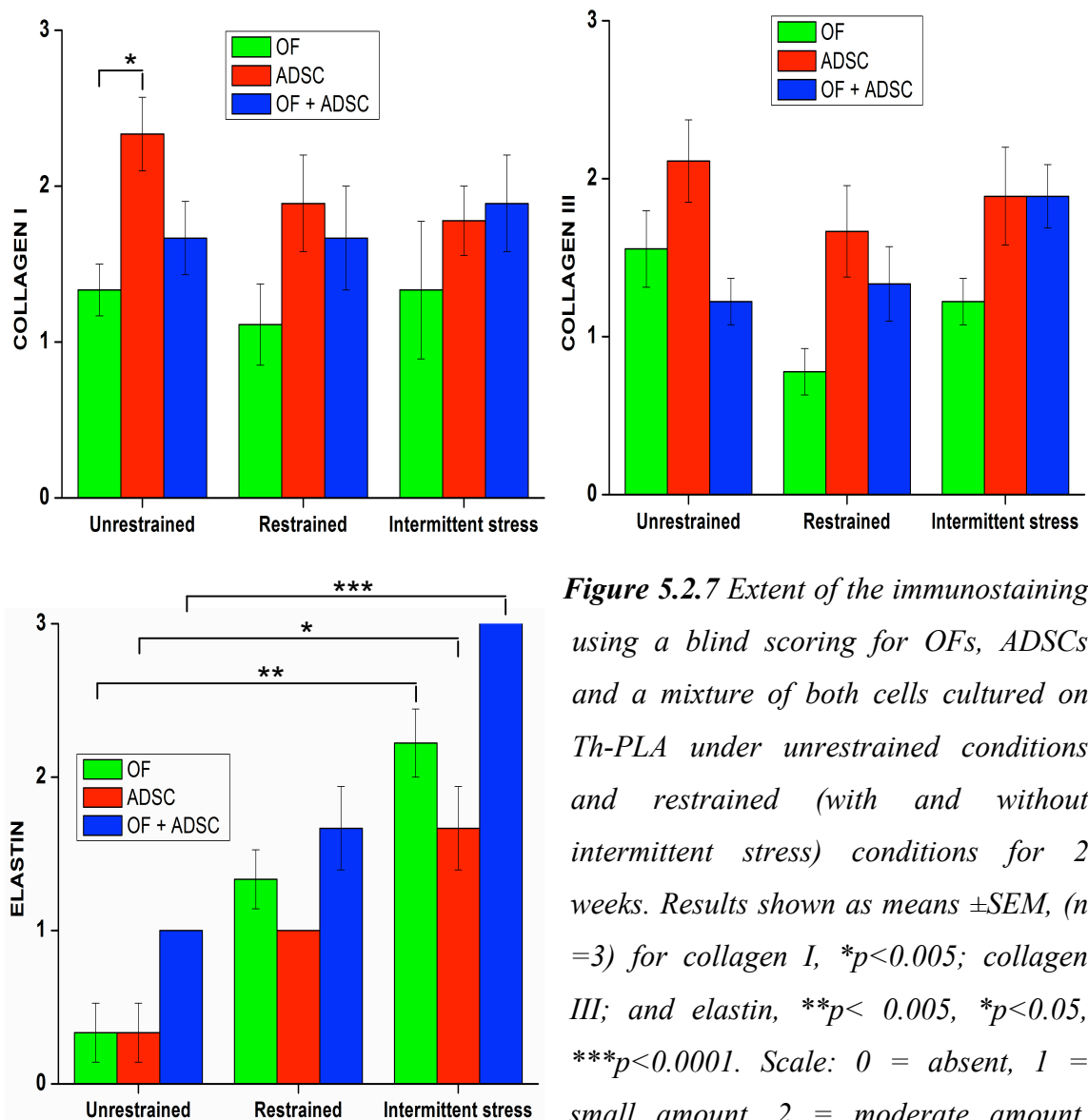


**Figure 5.2.7** Extent of the immunostaining using a blind scoring for OFs, ADSCs and a mixture of both cells cultured on Th-PLA under unrestrained conditions and restrained (with and without intermittent stress) conditions for 2 weeks. Results shown as means  $\pm$  SEM, ( $n=3$ ) for collagen I, \* $p<0.005$ ; collagen III; and elastin, \*\* $p<0.005$ , \* $p<0.05$ , \*\*\* $p<0.0001$ . Scale: 0 = absent, 1 = small amount, 2 = moderate amount, 3 = extensive amount.

All the cell-seeded scaffolds produced collagen I, III and some elastin fibres (figure 5.2.6). Semi-quantitatively, ADSCs showed the highest amount of collagen I and III cultured under unrestrained conditions (figure 5.2.7). For collagen I, this was significantly greater than for OFs under the same conditions ( $p<0.005$ ). Furthermore, there was a suggestion of orientation of collagen I fibres for ADSCs cultured under these conditions (figure 5.2.6). There was a trend of increasing elastin when cell types were cultured under restrained conditions (figure 5.2.7). Each cell group showed significantly higher amounts of elastin under intermittent stress conditions compared, individually, to unrestrained conditions ( $p<0.005$  for OFs,  $p<0.05$  for ADSCs and  $p<0.0001$  for a mixture of both cells) (figure 5.2.7). This was more obvious and significant when using OFs, and with a mixture of both cells again with a suggestion of fibre orientation (figure 5.2.6).

The quality of the ECM was studied by SEM looking at the amount and distribution of the ECM for each sample.

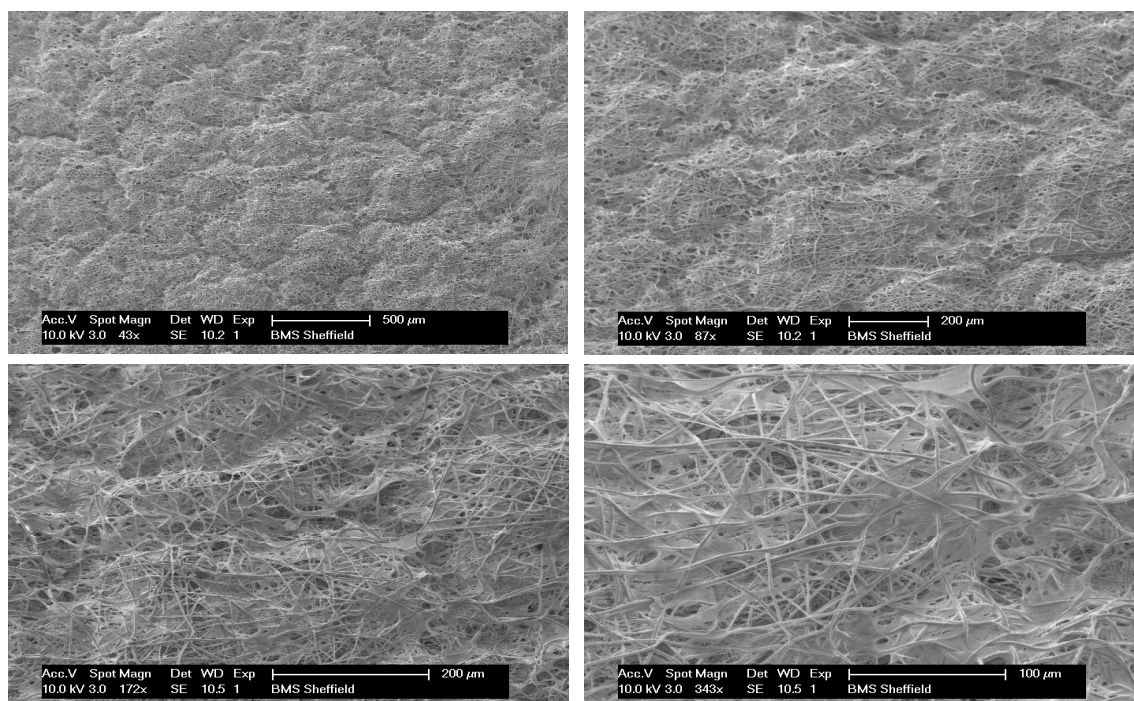


**Figure 5.2.8** Appearance by SEM of OFs cultured under unrestrained condition on Th-PLA scaffolds for 2 weeks in DMEM medium.

Qualitatively, OFs cultured under unrestrained conditions produced the least ECM as shown by SEM (figure 5.2.8). Consistent with the immunostaining results, ADSCs



cultured under unrestrained conditions produced a denser layer of ECM on top of the scaffolds (figure 5.2.10).

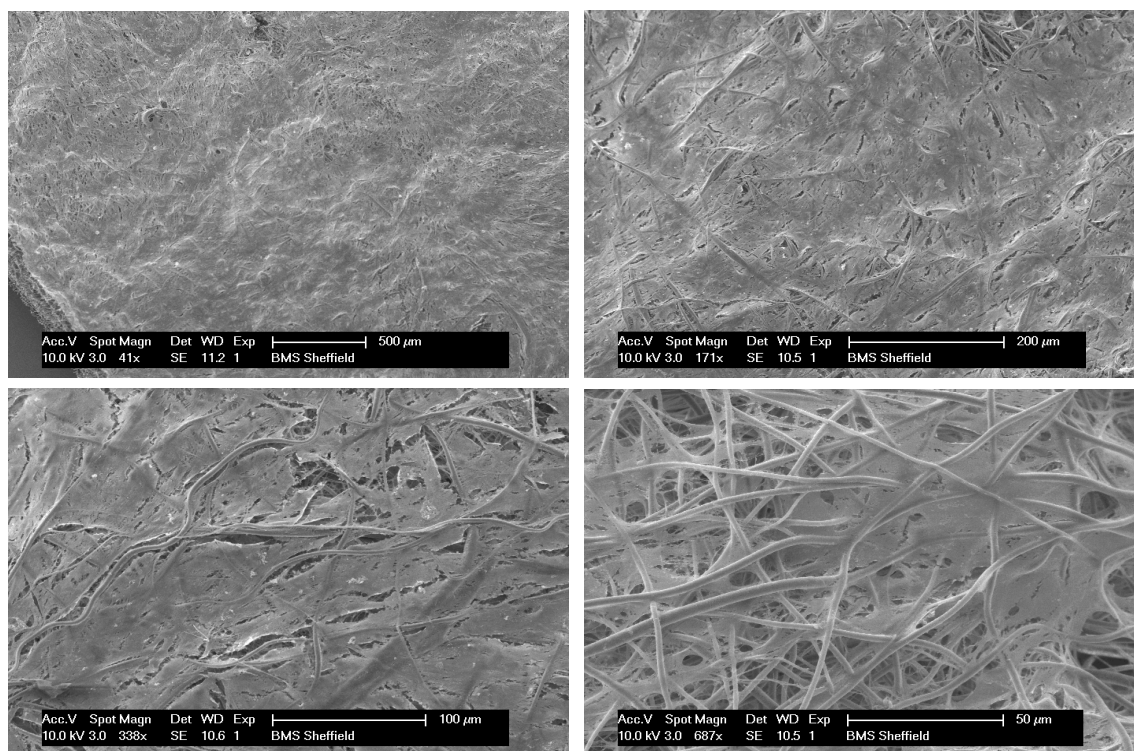


**Figure 5.2.9** Appearance by SEM of OFs cultured under intermittent stress conditions on Th-PLA scaffolds for 2 weeks in DMEM medium.

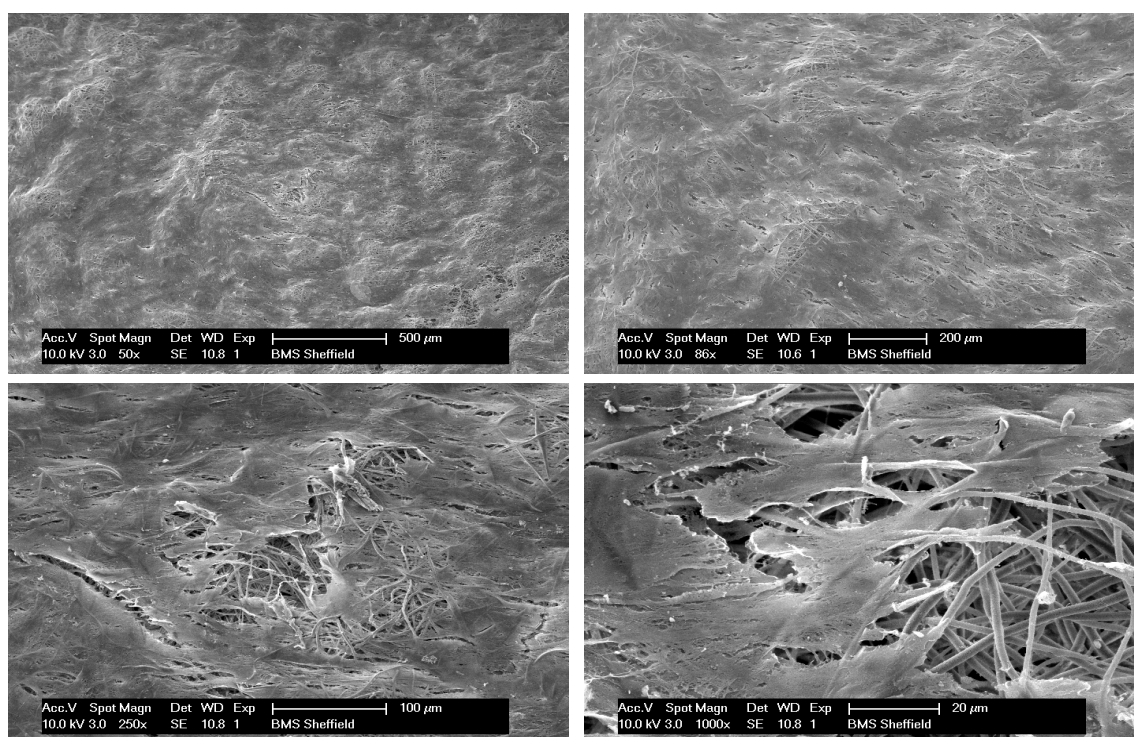


**Figure 5.2.10** Appearance by SEM of ADSCs cultured under unrestrained conditions on Th-PLA scaffolds for 2 weeks in DMEM medium.



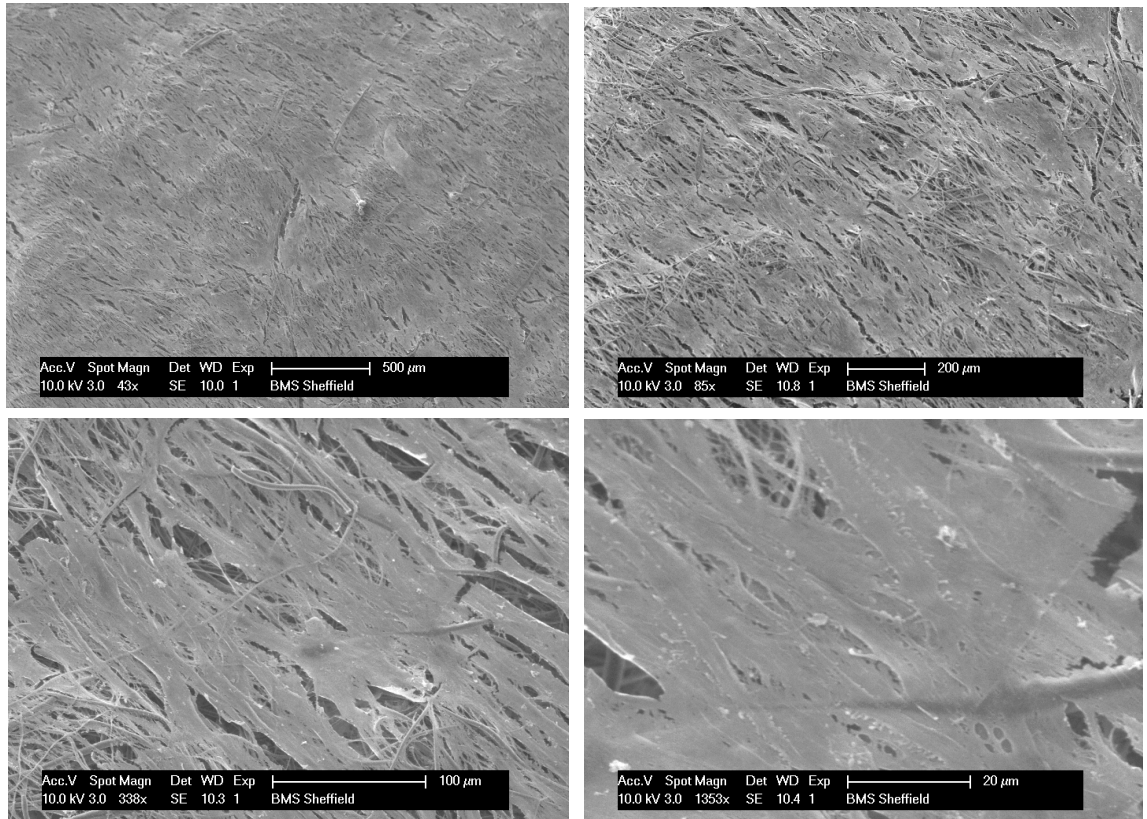


**Figure 5.2.11** Appearance by SEM of ADSCs cultured under intermittent stress conditions on Th-PLA scaffolds for 2 weeks in DMEM medium.

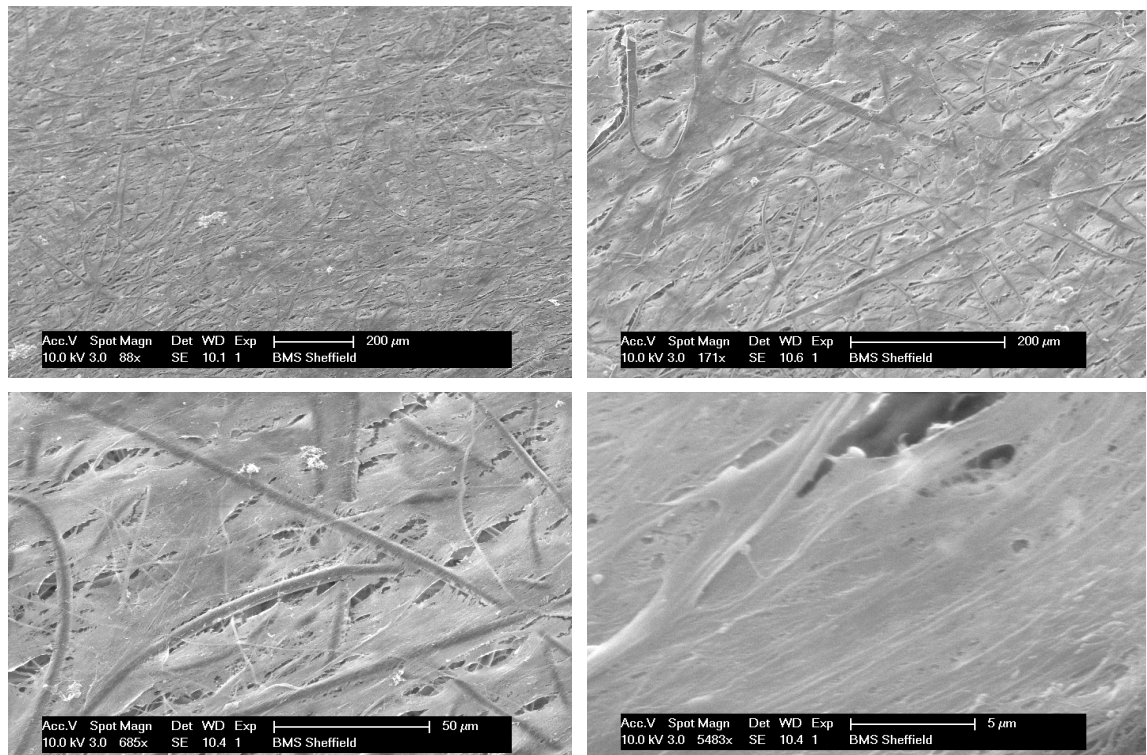


**Figure 5.2.12** Appearance by SEM of a mixture of OFs and ADSCs cultured under intermittent stress conditions on Th-PLA scaffolds for 2 weeks in DMEM medium.

Again, similar to immunostaining results, ADSCs under unrestrained and intermittent stress conditions (figure 5.2.10 and 5.2.6), and a mixture of OFs and ADSCs cultured under intermittent stress conditions (figure 5.2.12) showed some orientation of the ECM components, as indicated by the small fissures.

For all cells under restrained conditions there appeared to be more uncoated fibres and small fissures in an otherwise continuous sheet of ECM (figure 5.2.9, 5.2.11 and 5.2.12).

The highest magnification of ADSCs under unrestrained conditions shows, from a small fissure, how cells are completely confluent on top of the scaffold producing a dense layer of ECM, but do not appear to have penetrated into the entire thickness of the scaffold.

### 5.2.2 Dynamic conditions

Since previous studies did not show a big effect of direct mechanical force on cell activity, we next looked at the effect of dynamic conditions on cells in 2D cell culture.

Fluid shear forces were applied to the cells with the aim to increase production of ECM. For this,  $1 \times 10^5$  OFs or ADSCs were seeded in 6-well plates with DMEM medium. After, 48 hours incubation, the 6-well plates were placed on a rocking platform outside of the incubator and rocked at a tilt angle of  $6^\circ$  flat 40 rpm for 2 hours (figure 5.2.13). Fluid shear forces were applied every 2 days. The volume of medium and tilt angle ensured the cells were immersed throughout the rocking cycle. Static controls were added to these experiments, using the same number of cells seeded in 6-well plates, which were left outside the incubator during the duration of rocking.



**Figure 5.2.13** Platform rocker.

All samples were analyzed for cell attachment and proliferation using AlamarBlue<sup>®</sup> staining and total collagen production using Sirius red staining.

AlamarBlue<sup>®</sup> absorbance was recorded on days 0, 7 and 14, and is plotted below (figure 5.2.14) minus the absorbance of controls without cells (AlamarBlue<sup>®</sup> read after 1 h in a 6-well plate without cells).

The results showed no significant differences between these samples at any time point.

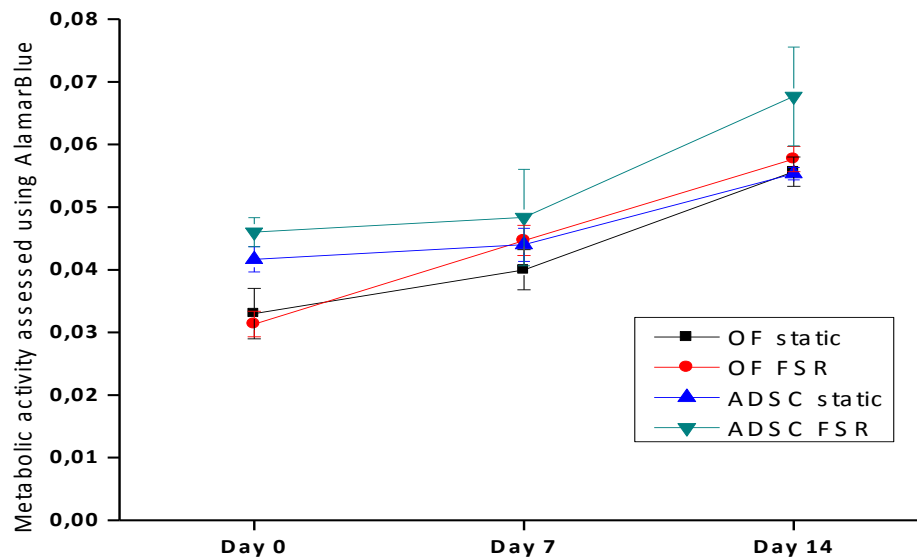


**Figure 5.2.14** Metabolic activity using AlamarBlue<sup>®</sup> for OFs and ADSCs cultured on 6-well plates under static and dynamic conditions over 2 weeks. Results shown are means  $\pm$  SEM, ( $n = 3$ ). FSR = Fluid shear rig.

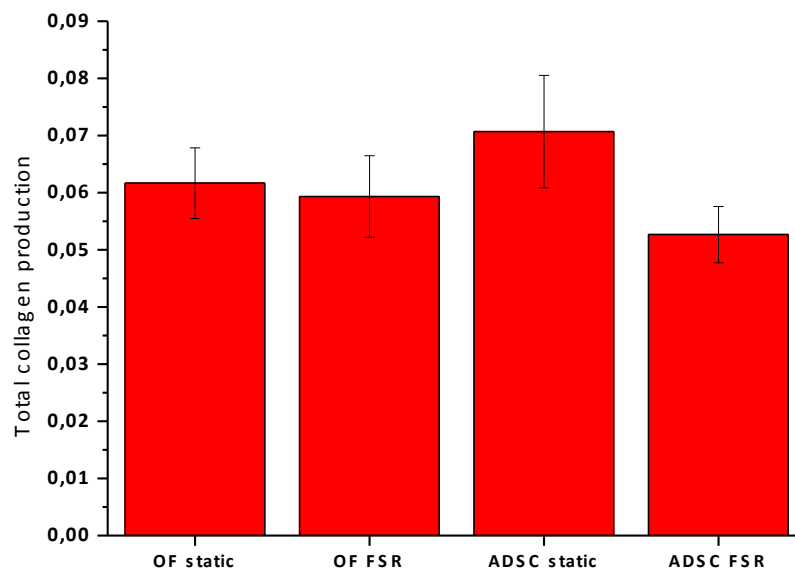


**Figure 5.2.15** Total collagen production using Sirius red staining for OFs and ADSCs cultured on 6-well plates under static and dynamic conditions over 2 weeks. Results shown are means  $\pm$  SEM, ( $n = 3$ ). FSR = Fluid shear rig.

Sirius red was read from all samples at day 14 to calculate total collagen production. Since all the stain read is from collagen made from cells, no controls need to be included. Scaffolds can absorb some staining, therefore, the absorbance of controls was subtracted from the absorbance of the samples. Also, in this experiment the values do not need to be normalized per gram of dry constructs. The total absorbance of Sirius red from the plate reader is plotted above (figure 5.2.15).

Again, similar to metabolic activity, no significant differences were found between groups.

Since dynamic conditions did not affect cell activity, we did not do any further experiments for this condition.

### 5.3 Chemical stimulation of TERMS

The effect of Vitamin C on the cell activity of ADSCs was firstly assessed in 2D culture. For this,  $1 \times 10^5$  cells were seeded in 6-well plates and these were cultured with DMEM medium or DMEM medium supplemented with Vitamin C at 0.3 mM. Then, the respective medium was changed every 2 days being samples cultured for 14 days.

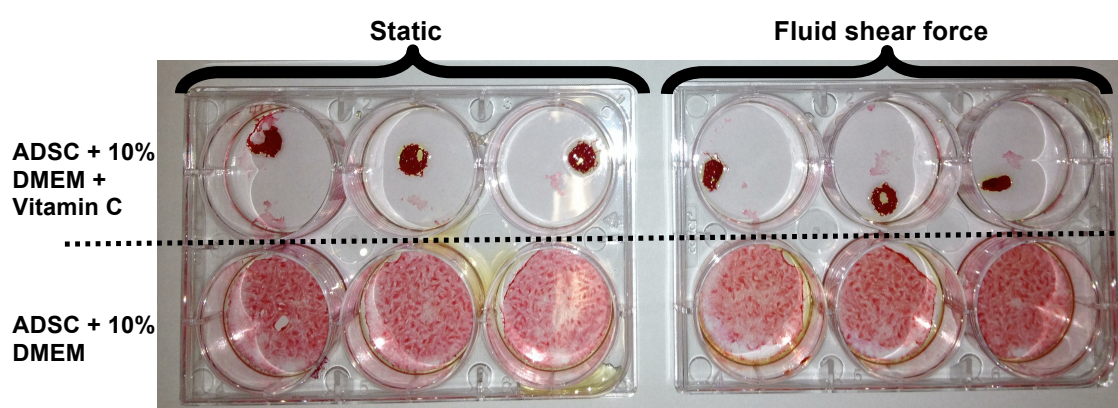


**Figure 5.3.1** ADSCs on 6-well plates stained with Sirius red after 2 weeks in culture under static or dynamic conditions and with DMEM medium or DMEM medium supplemented with Vitamin C.

In parallel, the chemical stimulation was combined with fluid shear forces, as described in section 5.2.2, and as shown in figure 5.3.1.

Again, fluid shear forces did not have an effect on cell proliferation or ECM production. By visual inspection under the microscope, cells cultured with DMEM medium supplemented with Vitamin C proliferated faster than control cells; however, by 2 weeks of culture, all samples detached from the well plates forming the compact clumps of cells observed in figure 5.3.1.

It did not prove possible to assess the total collagen made by these collapsed cells as it was impossible to elute all of the stain from these clumps after incubation with 0.2 M NaOH-methanol 1:1.

The effect of vitamin C was then assessed on cells cultured on scaffolds.  $1 \times 10^6$  ADSCs were seeded on Th-PLA scaffolds and cultured over 2 weeks under unrestrained conditions, as previously described, with DMEM medium or DMEM medium supplemented with Vitamin C at 0.3 mM.

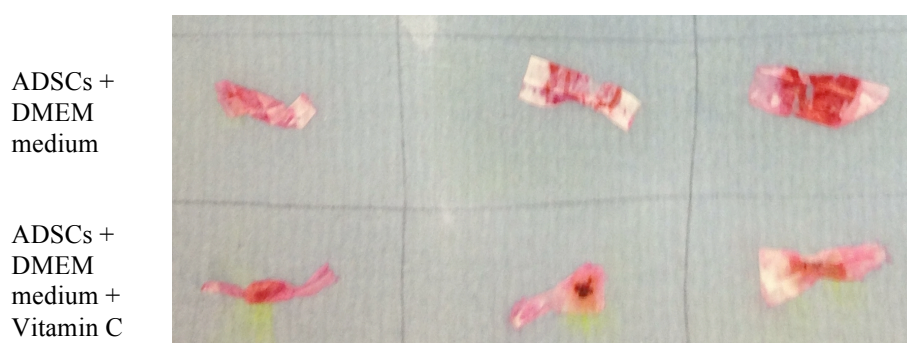


**Figure 5.3.2** ADSCs on Th-PLA scaffolds stained with Sirius red after 2 weeks in culture under unrestrained conditions and with DMEM medium or DMEM medium supplemented with Vitamin C.

All samples were analyzed for cell attachment and proliferation using AlamarBlue<sup>®</sup> staining, total collagen production using Sirius red staining and mechanical properties using a BOSE tensiometer.

Similar results to 2D culture were found. Clumps of cells in the middle of the seeding region were formed leading to an observed contraction of the samples (figure 5.3.2).

No differences were found between the 2 groups for metabolic activity at any time point (day 0, 7 and 14) (data not shown). In addition, mechanical properties of samples cultured with DMEM medium supplemented with Vitamin C showed lower mechanical properties compared to controls without cells and samples cultured with DMEM medium (data not shown).



Sirius red was eluted from all samples at day 14 to calculate total collagen production. The absorbance of Sirius red is plotted below (figure 5.3.3) minus the absorbance of controls without cells and expressed per gram of dry constructs.

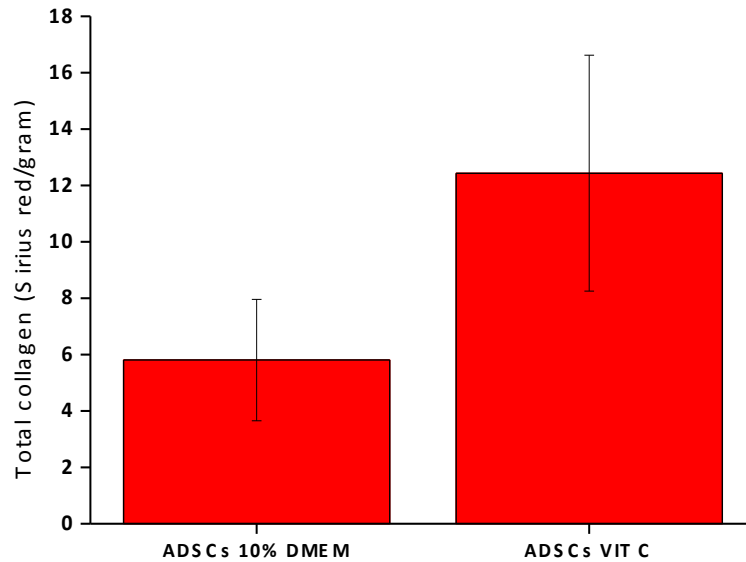


**Figure 5.3.3** Total collagen production using Sirius red staining for ADSCs cultured on Th-PLA over 2 weeks under unrestrained conditions and with DMEM medium or DMEM medium supplemented with Vitamin C (VIT C). Results shown are means±SEM, ( $n = 3$ ).

Although no significant differences were found between the 2 groups (figure 5.3.3); similarly to the 2D culture of these cells, again it was not possible to elute all of the Sirius red staining from the clumps formed by the ADSCs cultured with DMEM medium supplemented with Vitamin C on the Th-PLA scaffolds using 0.2 M NaOH-methanol 1:1.

## 5.4 Optimal number of cells and period of culture

Since ADSCs were chosen as our cell candidate for future experiments, only these cells were then used in future studies in which different numbers of cells were seeded and different periods of culture were assessed on Th-PLA scaffolds. For this, ADSCs were seeded on 6.25 cm<sup>2</sup> Th-PLA scaffolds using metal rings of 2 cm of diameter at densities of  $1 \times 10^5$ ,  $3 \times 10^5$ ,  $7 \times 10^5$  and  $1 \times 10^6$  and cultured for 2 weeks with DMEM medium under unrestrained conditions (optimal mechanical culture condition).

Then, the optimal number of cells ( $7 \times 10^5$ ) were seeded on Th-PLA scaffolds and cultured under unrestrained culture conditions with DMEM medium for 1, 2 and 3 weeks.

In both experiments, all samples were analyzed for cell attachment and proliferation using AlamarBlue<sup>®</sup> staining and DAPI staining, total collagen production using Sirius red staining and mechanical properties using a BOSE tensiometer, as described in Chapter 2.

Finally, the appearance of the ECM of the best samples for the optimal number of cells and period of time were analyzed by SEM, as described in Chapter 2.

#### 5.4.1 ADSCs seeded on Th-PLA scaffolds at different cell concentrations

AlamarBlue<sup>®</sup> absorbance was recorded on days 0, 7 and 14, and is plotted below minus the absorbance of controls without cells (figure 5.4.1).

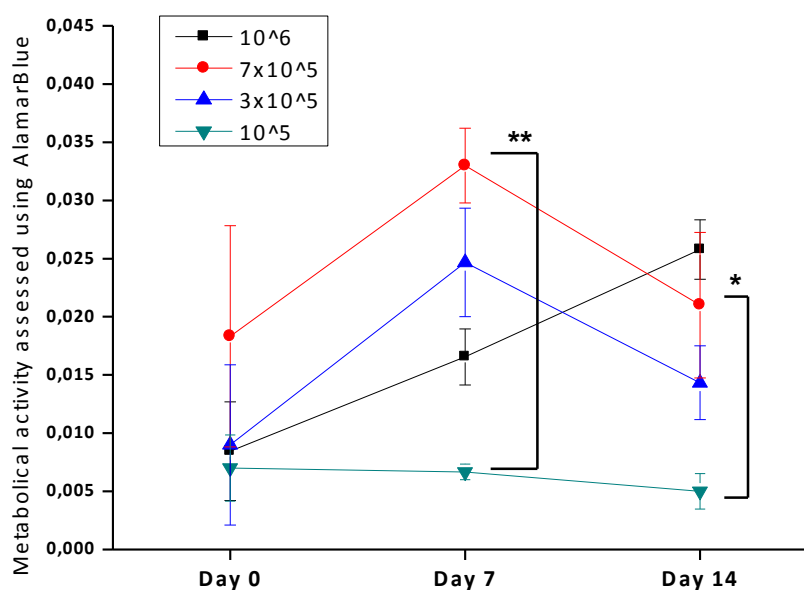


**Figure 5.4.1** Metabolic activity of ADSCs seeded at density of  $1 \times 10^5$ ,  $3 \times 10^5$ ,  $7 \times 10^5$  and  $1 \times 10^6$  cultured on Th-PLA scaffolds under unrestrained conditions over 2 weeks, stained with AlamarBlue<sup>®</sup> ( $n=3 \pm \text{SEM}$ ). \* $p < 0.05$ ; \*\* $p < 0.005$ .

After 7 days in culture, samples seeded with  $7 \times 10^5$  cells achieved the highest metabolic activity being significantly higher when compared with samples seeded with the lowest number of cells ( $1 \times 10^5$ ) ( $p < 0.005$ ). At day 14, the difference in metabolic activity between these 2 groups was reduced, but was still significant ( $p < 0.05$ ). After 14 days

culture, the metabolic activity of the 3 groups with the highest cell density was similar (figure 5.4.1).

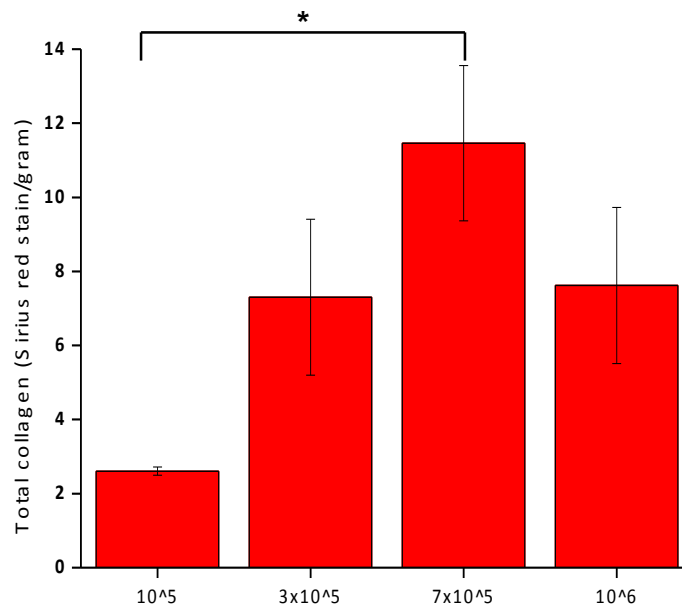


**Figure 5.4.2** Production of total collagen by ADSCs seeded at density of  $1 \times 10^5$ ,  $3 \times 10^5$ ,  $7 \times 10^5$  and  $1 \times 10^6$  cultured on Th-PLA scaffolds under unrestrained conditions. Sirius red staining after 14 days ( $n=3 \pm \text{SEM}$ ). \* $p < 0.01$ .

The absorbance of Sirius red is plotted above (figure 5.4.2) minus the absorbance of controls without cells and expressed per gram of dry constructs.

Similarly to metabolic activity, samples seeded with  $7 \times 10^5$  cells had the highest values for total collagen production at day 14, which was significantly higher compared to samples seeded with  $1 \times 10^5$  cells ( $p < 0.01$ ), but similar to the other 2 groups (figure 5.4.2).

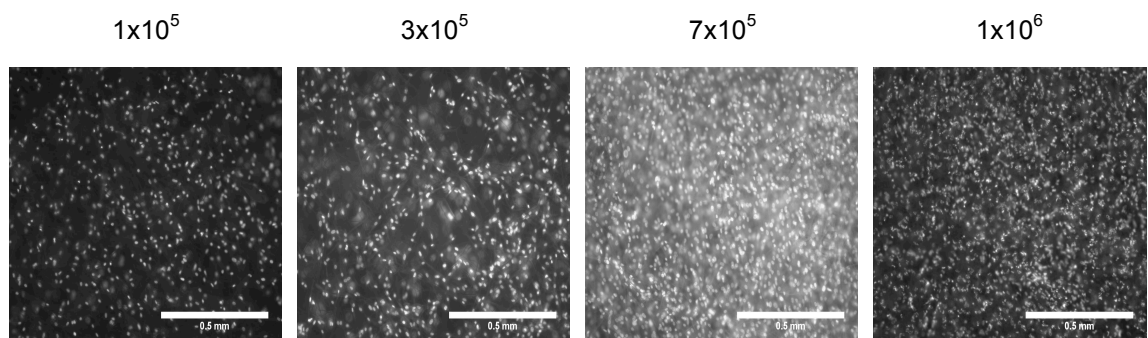


**Figure 5.4.3** DAPI staining for Th-PLA scaffolds cultured with  $1 \times 10^5$ ,  $3 \times 10^5$ ,  $7 \times 10^5$  and  $1 \times 10^6$  over 2 weeks under unrestrained conditions. Scale bar = 0.5 mm.



Images from each sample were taken to determine the distribution of cells stained with DAPI within scaffolds after 14 days in culture (figure 5.4.3). By qualitative assessment, ADSCs showed a similar confluent cell population for samples seeded with  $1 \times 10^6$  and  $7 \times 10^5$  cells, which were more confluent than samples seeded with  $3 \times 10^5$  cells, which in turn, were more confluent than samples seeded with  $1 \times 10^5$  cells.

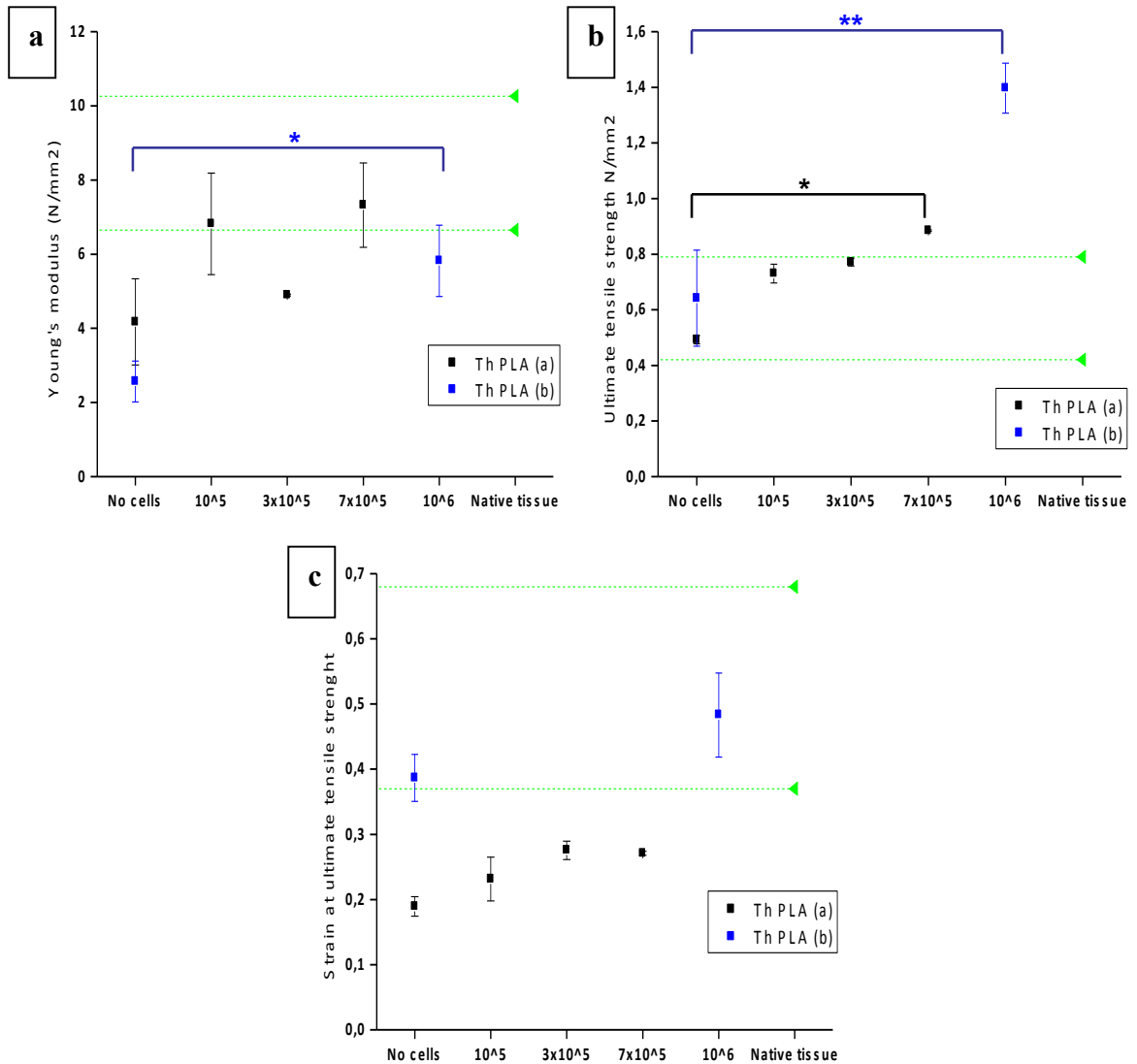


**Figure 5.4.4** Mechanical properties of Th-PLA scaffolds cultured under unrestrained conditions over 2 weeks without and with cells seeded at densities of  $1 \times 10^5$ ,  $3 \times 10^5$ ,  $7 \times 10^5$  and  $1 \times 10^6$  ( $n=3 \pm \text{SEM}$ ). The last sample shown is native tissue represented by 2 dashed lines (the range for native healthy paravaginal tissue). Blue color for samples seeded with  $1 \times 10^6$  ADSCs and Th-PLA controls (from same electrospun sheet of PLA). Black color for samples seeded with  $1 \times 10^5$ ,  $3 \times 10^5$ ,  $7 \times 10^5$  ADSCs and Th-PLA controls (from same electrospun sheet of PLA, different from previous one in blue color). (a) Young's modulus.  $*p < 0.01$ . (b) UTS.  $**p < 0.0001$ ;  $*p < 0.02$ .

Mechanical properties are plotted above (figure 5.4.4) and compared to the range for native healthy paravaginal tissue (194).

Experiments for samples seeded with  $1 \times 10^6$  ADSCs (blue color) were conducted at different time and with a different sheet of PLA than the rest of the samples (black color). The 2 controls, Th-PLA cultured for 2 weeks without cells, from the two different sheets of PLA showed mechanical properties with small differences. However, for all groups, when scaffolds were cultured with cells, mechanical properties were increased respect to the controls, being significantly higher for UTS when  $7 \times 10^5$  and  $1 \times 10^6$  cells were seeded compared to their own controls (figure 5.4.4).

### 5.4.2 Culture of ADSCs on Th-PLA scaffolds for different periods

Since  $7 \times 10^5$  ADSCs was the optimum number of cells to develop a TERM when seeded on  $3.14 \text{ cm}^2$  of Th-PLA scaffolds, this number of cells was assessed then for different periods of culture (1, 2 and 3 weeks) with DMEM medium under unrestrained conditions.

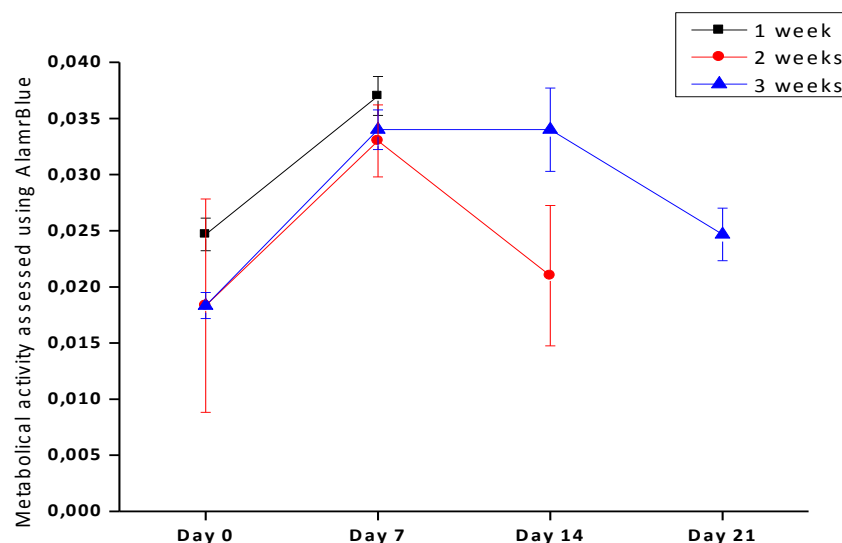


**Figure 5.4.5** Metabolic activity of ADSCs seeded at density of  $7 \times 10^5$  cells on Th-PLA scaffolds cultured under unrestrained conditions over 1, 2 and 3 weeks, stained with AlamarBlue<sup>®</sup> ( $n=3 \pm \text{SEM}$ ).

AlamarBlue<sup>®</sup> absorbance was recorded on days 0, 7 and 14 and 21. The total absorbance of AlamarBlue<sup>®</sup> is plotted above minus the absorbance of controls without cells (figure 5.4.5).

At day 7, very similar metabolic activity was seen between the 3 different groups. Thereafter, AlamarBlue® staining showed a small decrease of the metabolic activity for the groups cultured for 2 and 3 weeks.

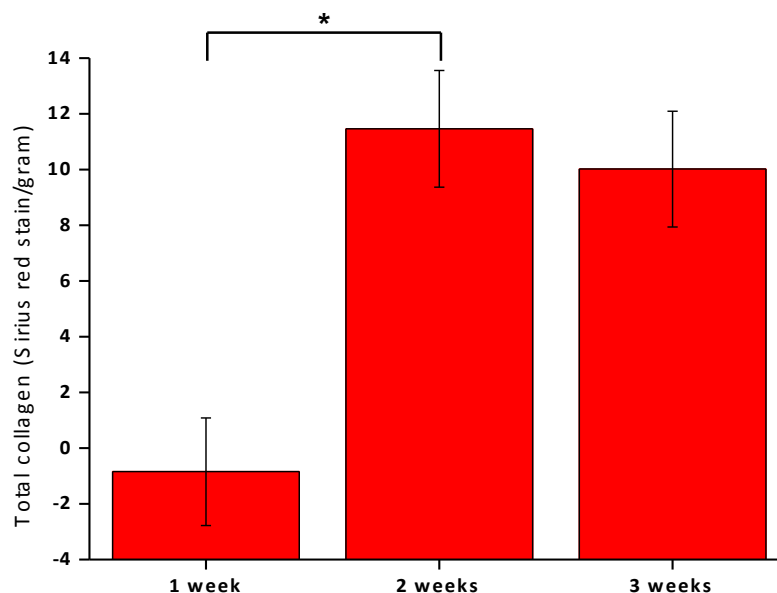


**Figure 5.4.6** Production of total collagen by ADSCs seeded at density of  $7 \times 10^5$  cells on Th-PLA scaffolds cultured under unrestrained conditions. Sirius red staining after 1, 2 and 3 weeks ( $n=3 \pm \text{SEM}$ ).  $*p < 0.05$ .

The absorbance of Sirius red is plotted above (figure 5.4.6) minus the absorbance of controls without cells per gram of dry constructs.

Samples cultured for 2 weeks had the highest values for total collagen production. They were significantly higher than samples cultured for 1 week, but similar to samples cultured for 3 weeks.

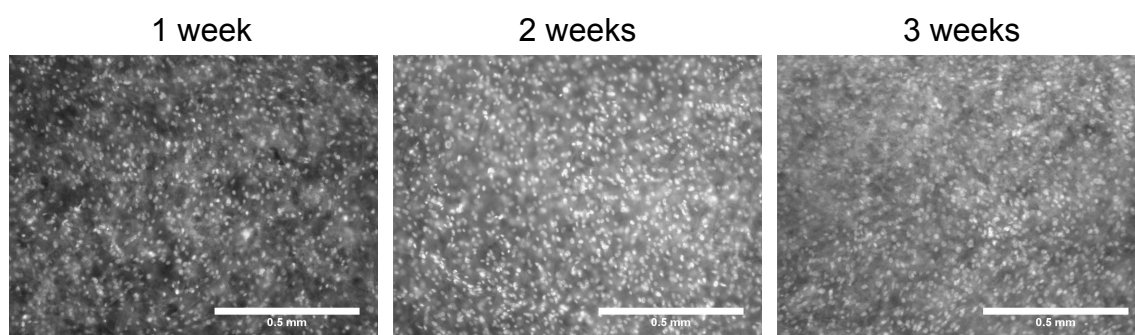


**Figure 5.4.7** DAPI staining for Th-PLA scaffolds cultured with  $7 \times 10^5$  ADSCs under unrestrained conditions for 1, 2 and 3 weeks in DMEM medium. Scale bar = 0.5 mm.

Images were undertaken from all samples and were stained with DAPI to determine the distribution of cells (figure 5.4.7). With qualitative assessment, samples cultured for 2 and 3 weeks showed a similar high confluence of cells, being slightly greater than for samples cultured for 1 week.

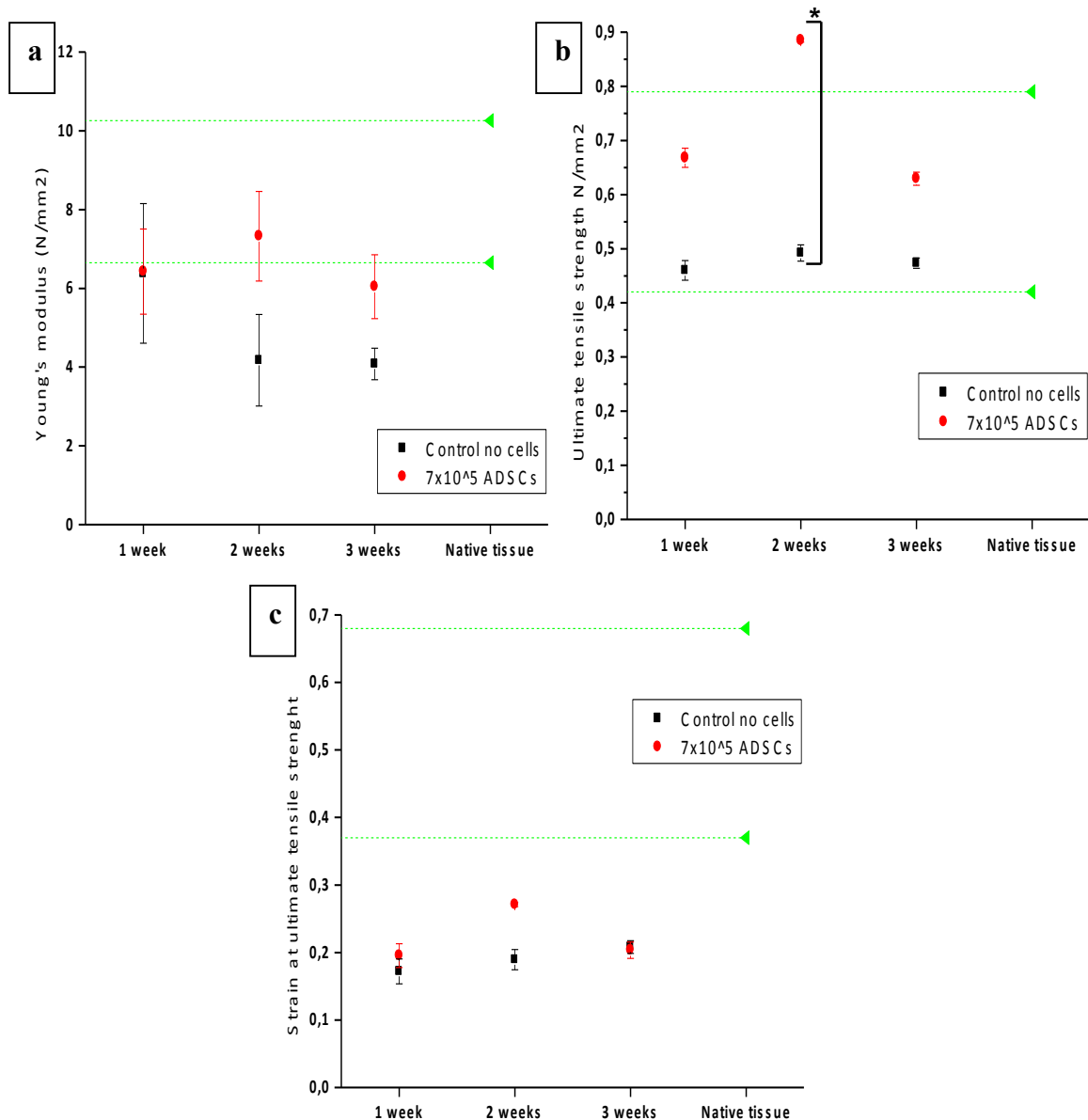


**Figure 5.4.8** Mechanical properties of Th-PLA scaffolds cultured without and with  $7 \times 10^5$  ADSCs under unrestrained conditions for 1, 2 and 3 weeks ( $n=3 \pm \text{SEM}$ ). The last sample shown is native tissue represented by 2 dashed lines (the range for native healthy paravaginal tissue). (b) UTS.  $*p < 0.02$ .

The mechanical properties are plotted above (figure 5.4.8) and compared to the range for native healthy paravaginal tissue (194).

Compared to the other 2 groups, samples cultured for 2 weeks showed the highest differences between samples cultured with and without cells.

All samples cultured with cells showed an increase in UTS compared to samples cultured without cells. This was significantly higher only for samples cultured for 2 weeks.

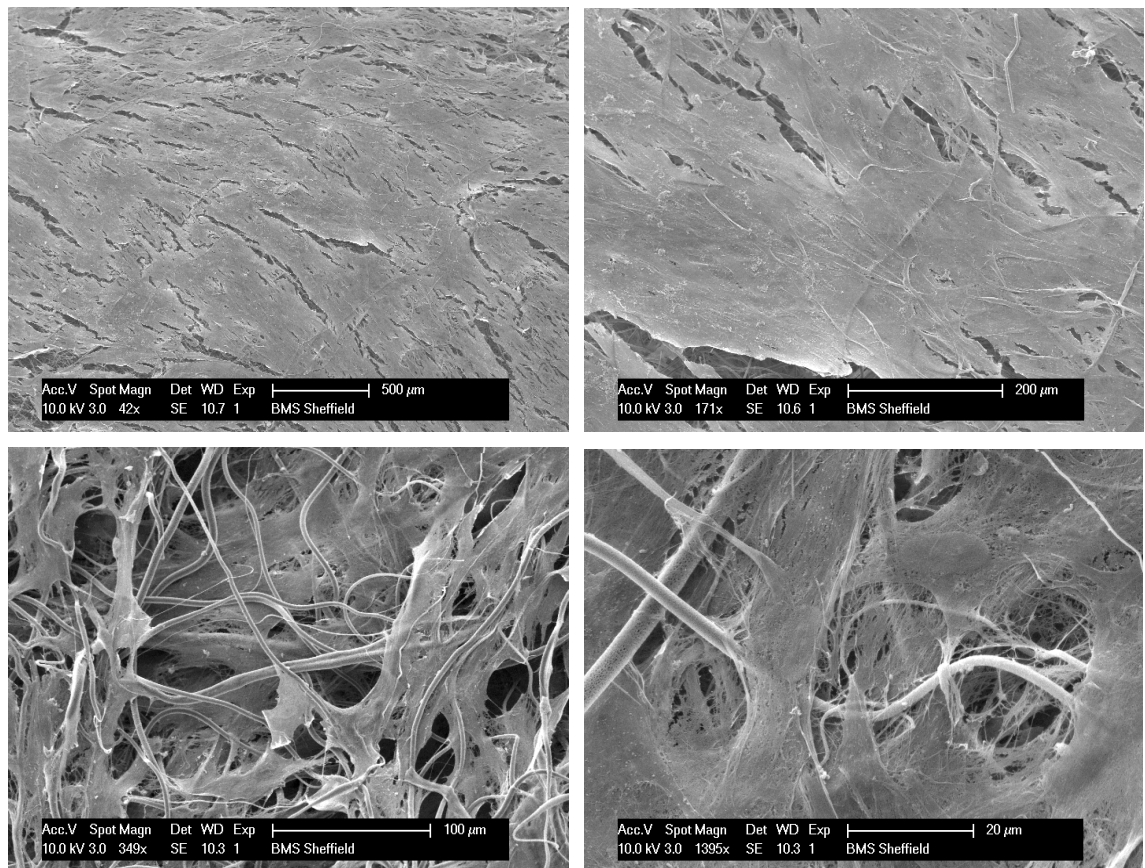


**Figure 5.4.9** Appearance by SEM of  $7 \times 10^5$  ADSCs seeded on Th-PLA scaffolds and cultured under unrestrained conditions for 2 weeks in DMEM medium.

The appearance of the ECM produced was studied by SEM for the best cell candidate seeded with the optimum number of cells and cultured for the optimum period of time on Th-PLA scaffolds (figure 5.4.9).

As shown for  $1 \times 10^6$  ADSCs,  $7 \times 10^5$  ADSCs seeded and cultured on Th-PLA scaffolds over 2 weeks presented a dense sheet of ECM on top of the scaffold. Again, small fissures between components of the ECM indicated an orientation of these.

The highest magnification shows the ability of these cells to penetrate inside the Th-PLA scaffolds and form ECM within the scaffolds.

## 5.5 Discussion

The aim of this Chapter was to investigate which culture conditions may give the best outcomes for developing a TERM.

For this, we attempted to study cells on the scaffolds cultured under mechanical stress conditions by simulating the anticipated strain the cells would experience *in vivo*. However, the stress model we used does not mimic the degree of strain that cells will experience *in vivo*. As discussed earlier, the true strains the female pelvic floor undergoes are, to the best of our knowledge, only now beginning to be assessed.

The rationale for this was to assess the ability of cells on scaffolds to survive and proliferate when under stress and in these experiments cells were not adversely affected. Mechanical stimulation can be a useful method of enhancing the functional characteristics and mechanical properties of engineered tissues prior to implantation (450).

The comparison of OFs and ADSCs showed little difference between them under the different mechanical conditions and there was no advantage of having a co-culture of both cells, as seen in Chapter 4.

No differences were observed between groups at any day for metabolic activity. Alternatively, as seen in Chapter 4, big errors were found for metabolic activity at day 0 for all groups when same number of cells was seeded. This may be, as explained in previous Chapters, due to differences between Th-PLA samples in pore size, fibre diameter and thickness, due to the initial low reproducibility of the electrospinning technique which may have lead to poor reproducibility in cell seeding.

Irrespective of this, these errors were reduced by day 14 with cells achieving a confluent cell population with similar metabolic activity for all samples.

All groups were able to produce fibres of collagen I and collagen III and a little elastin. Using semi-quantitative assessment, collagen production was not increased under any mechanical stimulation for any cell type. Although little elastin production occurred, all cells increased this production when they were subjected to restraint conditions.

Between cell groups, ADSCs under unrestrained conditions produced more collagen than OFs under the same conditions, as seen in Chapter 4. In addition, only ADSCs under unrestrained conditions had significantly higher Young's modulus and UTS compared to the controls (Th-PLA scaffolds cultured without cells).

Again, the qualitative appearance of the ECM assessed by SEM indicates that ADSCs cultured under unrestrained conditions had denser and more uniform ECM compared to the other groups. As seen in Chapter 4 by H&E staining, this ECM seems to be produced particularly on the surface of the Th-PLA scaffolds (figure 5.2.10) although cells are able to penetrate the scaffold and produce ECM inside them in some areas (figure 5.4.9).

Since culturing cells on scaffolds under restrained conditions did not show any improvement when developing a TERM, dynamic mechanical stimulation was firstly assessed in 2D culture to not waste time and research consumables. Then, since this condition did not affect any cell type in 2D culture, we did not do any further experiments on cells on scaffolds.

At this point in this project we decided to do further experiments only with ADSCs as the preferred cell candidate for developing a TERM due to the slightly better *in vitro* results shown with them compared to OFs but also because of their reported regenerative potential as described in a previous Chapter.

Vitamin C stimulated ADSCs to increase collagen production on the scaffolds. However, this had a negative effect on the ADSCs leading to contraction of the new matrix produced. This effect may have clinical implications as could be seen in skin grafts implanted in patients (416), and also Vitamin C may have a negative effect on mechanical properties since the contraction pulls the PLA fibres leading to scaffold distension.

In conclusion, we could not identify any adverse effect of mechanical stimulation on OFs or ADSCs cultured on Th-PLA. On the other hand, this mechanical stimulation together or not with chemical stimulation do not have a positive effect for the development of a TERM as a method to enhance their functional characteristics.

Only elastin was increased by mechanical stimulation but this did not have a positive effect on the mechanical properties of the scaffolds.

Therefore, all further experiments in this thesis involved ADSCs cultured under unrestrained conditions.

We found that  $7 \times 10^5$  and  $1 \times 10^6$  ADSCs seeded on  $3.14 \text{ cm}^2$  of Th-PLA scaffolds gave similar results in the development of a TERM. Therefore, we concluded that 223.000 ADSCs per  $\text{cm}^2$  are sufficient to develop a TERM.

We observed, that the variations previously commented on between different sheets of Th-PLA scaffolds was also evident by comparing mechanical properties of these 2 groups (figure 5.4.4).

These experiments showed that the quality of a Th-PLA scaffold itself is the main factor in obtaining the desired mechanical properties. The addition of cells did however significantly increase the UTS which may be explained by the new ECM produced.

Finally, 2 weeks was determined to be the best period of culture for developing a TERM before implantation. Cell proliferated during the first week populating the whole thickness of the scaffold, as seen by the increase of metabolic activity (figure 5.4.5) achieving a confluent cell population after 1 week (figure 5.4.7). However, cells then produced most of the ECM during the second week, since the total collagen production was significantly higher after 2 weeks of culture compared with 1 week of culture, but similar to that seen after 3 weeks of culture (figure 5.4.6).

As above, although only UTS was significantly increased, the best results for mechanical properties were observed for samples after 2 weeks of culture. While after 1 week of culture cells did not appear to have produced enough ECM to increase these properties, after 3 weeks of culture no more ECM produced by the cells made any further increment of these properties compared to 2 weeks culture. In addition, longer periods of culture could negatively affect the mechanical properties of the scaffolds as seen by a decrease of Young's modulus when looking at the controls from the different periods of culture (figure 5.4.8), a fact that is further discussed in Chapter 7 of this thesis.



## **Chapter 6**

### ***IN VIVO* ASSESSMENT OF TERMS**

## 6.1 Introduction

No appropriate animal models for SUI or POP exist since most animals do not develop pelvic floor disorders as humans do.

The vaginal support in humans, made up of the levator ani muscle, ligaments and fascial tissues of the pelvic floor, is critical to avoid development of SUI or POP which occurs in women due to human bipedal posture. (451). The human anatomy of the pelvic floor has been adapted by recruiting the striated muscle of the levator ani to assist in upright walking (452, 453).

Nevertheless, animal models have been used to study the importance of different risk factors and progression of different events, which may affect different structures of the pelvic floor.

The choice of an animal model has to be based on a specific research question which in different cases may need a different animal model. The main points to consider are the anatomy, the appearance of these tissues, their cellular and extracellular components and their biomechanical properties.

Currently, non-human primates, sheep, rabbits and rodents are all used in studies for the pelvic floor. Each model serves a different function.

Rodents are inexpensive and easy to work with because of their behavior and size. While levator ani muscle is mainly associated to tail movement in these animals, anatomy of the connective tissues is similar to humans and these make the main vaginal support (451).

Mice and rats require less space and resources than other animals to maintain, and offer an accelerated injury recovery time. On the other hand, their small size can increase the technical skill required for surgery in some studies.

At present, rodents are the most common animal model used for prolapse and incontinence research, especially for studying the connective tissues. In addition, only mice are accessible for developing transgenic knockouts to study the development of SUI or POP (454, 455).

The larger size of rabbits gives the advantage of allowing easier access to the caudal section of the vagina, the creation of several defects in the same animal, the harvesting of larger tissue specimens and longer follow-up studies. On the other hand, the rabbit vagina anatomy differs from humans more than that of rodents. The rabbit vagina is not supported by connective tissues, thus, the histological appearance is not similar to the human vagina. Rabbits do not show weakness of vaginal tissues after birth and do not develop POP. Furthermore, collagen metabolism is different to humans, which may have an impact on wound healing (456).

Nevertheless, meshes clinically used to treat POP have been successfully studied in rabbits for abdominal wall reconstruction (457-460), and have been also implanted on the external posterior vagina wall of these animals (461, 462).

Sheep have been used to develop a POP animal model to study the outcomes of implanted different meshes. Sheep spontaneously develop POP related to pregnancy and vaginal delivery (463-466). Similar to humans, the same risk factors, such as increased intra-abdominal pressure, age and multi-fetal gestation, lead to a similar prevalence of uterovaginal prolapse as in humans (8-12%) (465). The anatomy of the connective tissues of the pelvic floor is also very similar to humans with 3 supportive levels.

Non-human primates represent the POP animal model closest to humans (453, 467, 468). On the other hand, they are less accessible, more expensive than any other animal model and they require more space and resources. For ethical reasons, primates are only used when absolutely necessary.

Primates have similar reproductive physiology to humans including reproductive cycles, levels of estrogens and progesterone which affects metabolism of the components of the supportive tissues, and, spontaneously, develop POP related to vaginal delivery.

Vaginal connective tissues attach similarly to the lateral and apex of the vagina, and para-vaginally, to the levator ani muscle (through ATRF ligaments, as in women). At this point, remodeling of ATRF has been associated with anterior and posterior vaginal wall prolapse. As in humans (123, 199, 469), changes in the rate of collagen I and III have been shown to be altered after vaginal delivery associated with POP (467).

Urodynamic measurements used in women for SUI diagnosis require intention since women are requested to cough and exercise to increase their abdominal pressure. In

addition, anesthesia is usually required in animals which may affect urodynamic measurements. Therefore, SUI in animal models is assessed by measuring the resistance of the urethra based on a modification of clinical methods of diagnosing SUI.

As above, rodents are the main animal used to study SUI. Methods to determine this condition in rats include sneeze testing (470), manual, vertical tilt table (471) and electrical stimulation for LPP testing (472).

Three main strategies have been used to develop SUI models in rats: simulation of childbirth injury, simulation of anatomic support damage and intrinsic urethra deficit.

Balloons inflated into the vagina of rats produce vaginal distension and simulate childbirth injury leading to SUI (473-477). Anatomical support damage has been caused in rats by urethrolisis for a SUI animal model leading to urethra hypermobility. However, these methods are difficult to reproduce without injury to other structures. For this, proximal urethra detachment by incision of the fascia has been used (478, 479), as well as, injury of the pubo-urethral ligament of rats (480). Finally, direct sphincter injury also develops a more durable SUI model which includes peri-urethral cauterization (481), urethral sphincterectomy (482), reagent peri-urethral injection (by botulinum-A toxin injection) (483) and pudendal nerve transaction (PNT) (484-486), the last one used for extrinsic urethra sphincter denervation.

#### **6.1.1 Animal models to assess materials used to treat SUI and POP**

An animal model also allows us to improve the management strategy to treat SUI and POP. These involve the implantation in animals of materials currently used, or with potential to be used, for the surgical management of these disorders.

These animal models also have the purpose of answering questions about the safety and the efficacy of using these materials in women.

As described in the first Chapter of this thesis, many studies have implanted in animals different synthetic and biological materials clinically used to treat SUI and POP to assess the host response to them.

Although many factors may influence the clinical outcome of mesh surgery including the physical properties of the material and surgical and constitutional factors (487), the host response to the implanted materials is particularly important.

Polypropylene implants cannot be remodelled and induce release of a pro-inflammatory cytokine and some patients respond to them with chronic inflammation leading to excessive fibrosis and encapsulation (488). Alternatively, a range of acellular biological grafts have also been trailed in small studies, but the main problem encountered was a host response leading to rapid degradation, and consequently, to high failure rates (376). Although the “ideal” biomaterial is often described as inert, in practice any material can cause a degree of inflammation; and indeed, an acute host response is considered to be necessary leading to rapid neovascularization and collagen deposition for constructive remodelling of the implant to be long-term integrated into the host tissues (489).

It is well established in most studies that the host response is analyzed after 7, 14, 30, 60 and 90 days post-implantation. While inflammatory and acute immune responses are studied in the first stage, long-term implantation allows us to evaluate integration, chronic immune response and mechanical properties post-implantation. The last one is particularly important for POP reconstruction since most of these materials implanted in humans have been shown to be degraded leading to failure (283).

Materials used to treat SUI and POP have been implanted subcutaneously on the abdominal wall of mice (305) and rats (490) to assess inflammation, immune response, angiogenesis and ECM production.

Mechanical properties have been also assessed from long-term implantation of bigger samples of these materials to repair an abdominal wall defect in rats (491), pigs (492) and rabbits (458, 493-495).

Only in rabbits (458, 459, 494) and sheep (496) have these materials been implanted on the vaginal wall for fascial repair. These models would be more reliable since the material is under dynamic distension and the vaginal environment has been demonstrated to increase the degradation of the implant (494).

As the immediate host response elicited by any biomaterial is critical to its long-term success, in this Chapter, we assessed the acute host response against our best TERM candidate chosen from experiments described in previous Chapters.

For this, we subcutaneously implanted in Sprague-Dawley rats Th-PLA scaffolds previously seeded and cultured with human ADSCs. Th-PLA scaffolds were implanted

as a control, and scaffolds previously cultured with rat ADSCs were also included in this study as an allogeneic implantation control.

The simplest animal model, which has been already used to assess the host response against an implanted material, was chosen before moving to more complex models.

## 6.2 Integration into host tissues

All animals survived both the operation and period of implantation without any observed alteration in their physiological functions.

Furthermore, after sacrifice, by visual inspection, there was no infection or rejection of any implant.

Human and rat ADSCs cultured with Th-PLA scaffolds were labeled with green cell tracker before being implanted into the animals with the idea of being able to identify them after animal sacrifice to check whether or not our cells would survive in the scaffolds after implantation, and/or if they could migrate to some other parts of the tissue or to other organs.

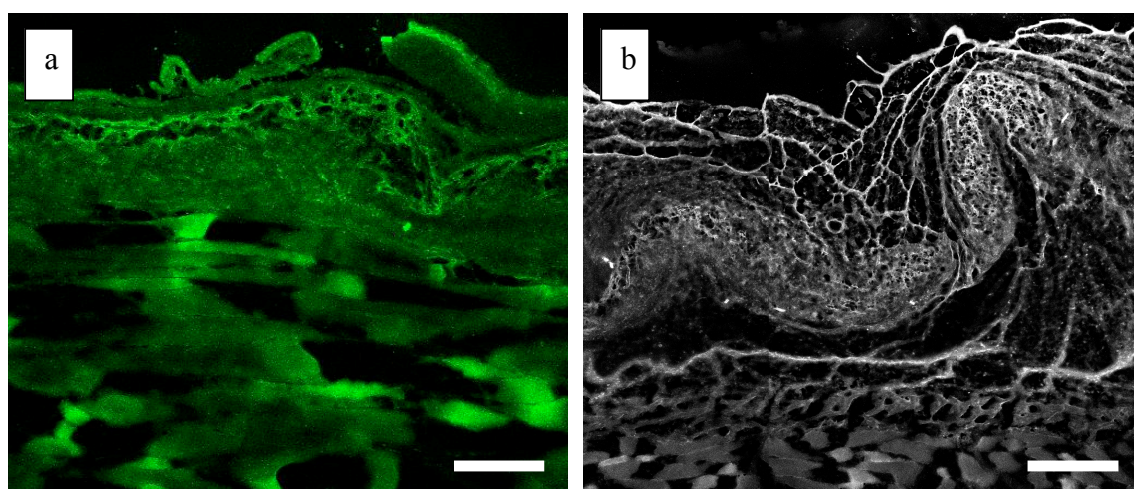


**Figure 6.2.1** Confocal microscope images using a green filter of fresh frozen sections of abdominal wall of Sprague-Dawley rats after 7 days implantation of Th-PLA scaffolds on top, previously cultured with rat (**a**) or human (**b**) ADSCs labeled with green cell tracker in DMEM medium for 2 weeks. Images are shown as colored in green or in black and white respectively. Scale bars of 0.2 mm.

Frozen sections were analyzed with a confocal microscope to identify in the host tissues the ADSCs by fluorescence due to the green cell tracker. However, we could not recognize the ADSCs from the implanted TERMS (figure 6.2.1). Cell tracker is diluted after cell proliferation, and furthermore, collagen has a strong green autofluorescence which could mask low fluorescence intensity from the cells.

Figure 6.2.2 shows a panoramic image of a normal rat abdominal wall without scaffold implantation, which is composed of multiple bundles of skeletal muscle fibres held together by connective tissue called fascia. This fascia is composed by a thick layer of collagen fibres and a submesothelium and mesothelium on top. The fascia covers the skeletal muscle of the abdominal wall and is where blood vessels and nerves are found. On top of the mesothelium, not shown in this figure, we would find the cutaneous and subcutaneous layers which compose the skin.

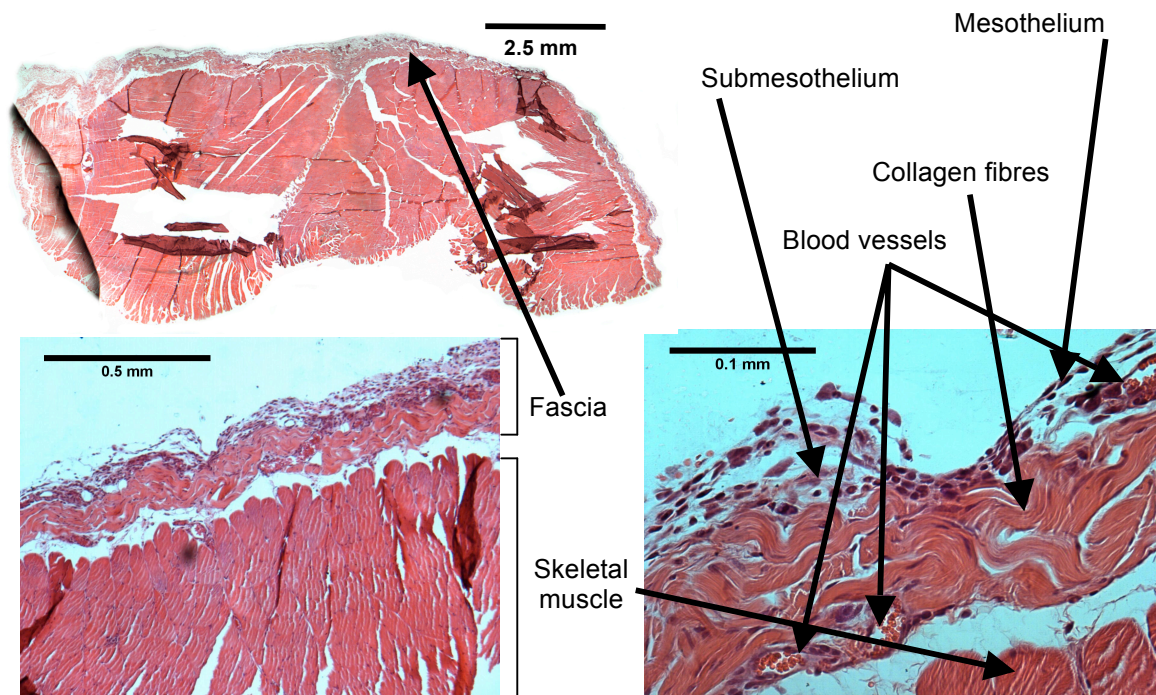


**Figure 6.2.2** Representative light microscopy H&E stained sections of normal abdominal wall of female Sprague-Dawley rats (no implantation).

1 cm<sup>2</sup> Th-PLA scaffolds cultured with and without rat or human ADSCs were implanted subcutaneously on top of this mesothelium by suturing the 4 corners. All scaffolds previously cultured with and without cells were well integrated into the fascia, as shown



by H&E staining, with the mesothelium on top which covered all the scaffolds (figure 6.2.3).

Figure 6.2.3 is a representative panoramic image of the full section of abdominal wall showing where the scaffold was integrated.

After 3 days implantation all samples were already integrated into the fascia and host cells infiltrated samples, as seen in the control group of Th-PLA scaffolds implanted without cells (figure 6.2.4).

After 7 days the cell infiltration was increased in all samples, as well as the thickness of the fascia and new small blood vessels were visible inside all samples (figure 6.2.5).

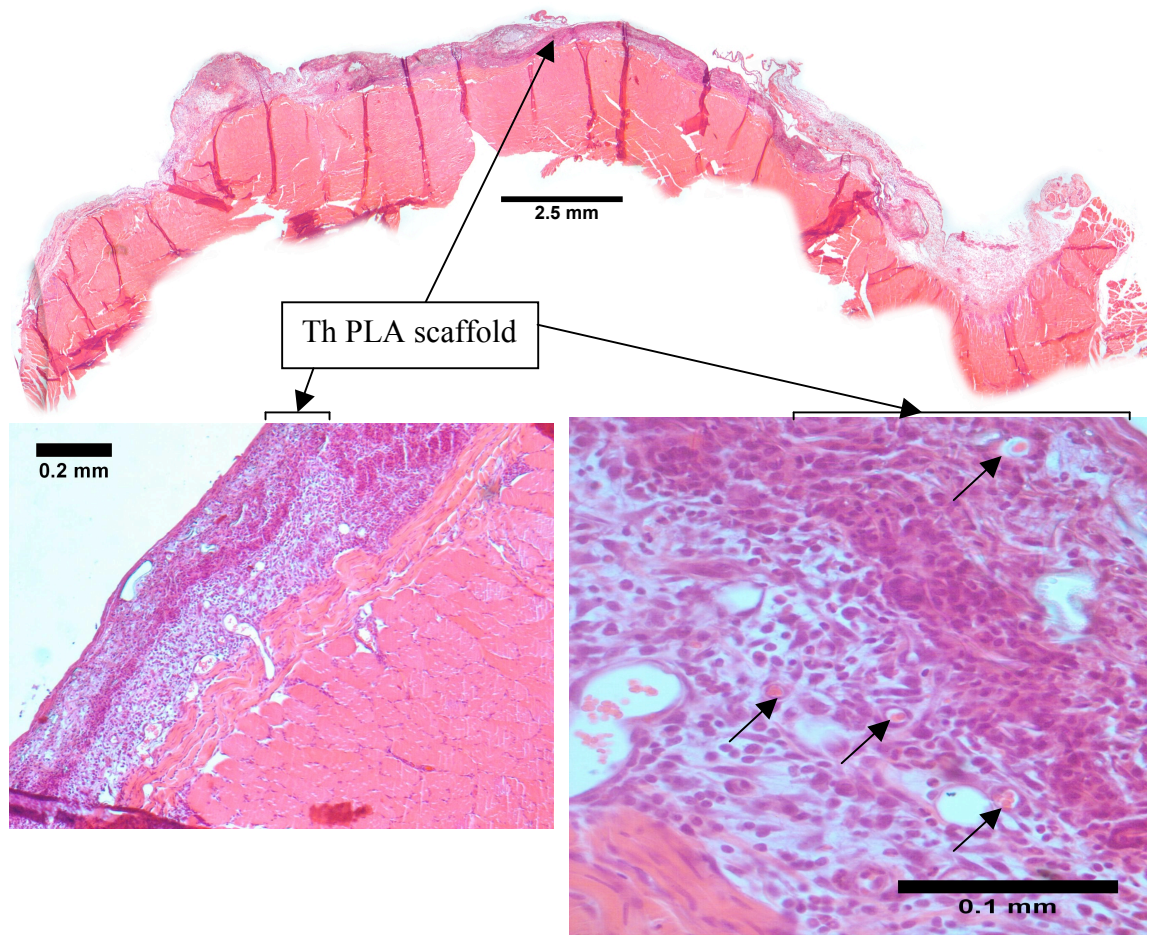


**Figure 6.2.3** Representative light microscopy H&E stained panoramic image of the abdominal wall of female Sprague-Dawley rats, after 3 days implantation of Th-PLA scaffold on top, previously cultured with human ADSCs in DMEM medium for 2 weeks. Small blood vessels are identified by (↑).



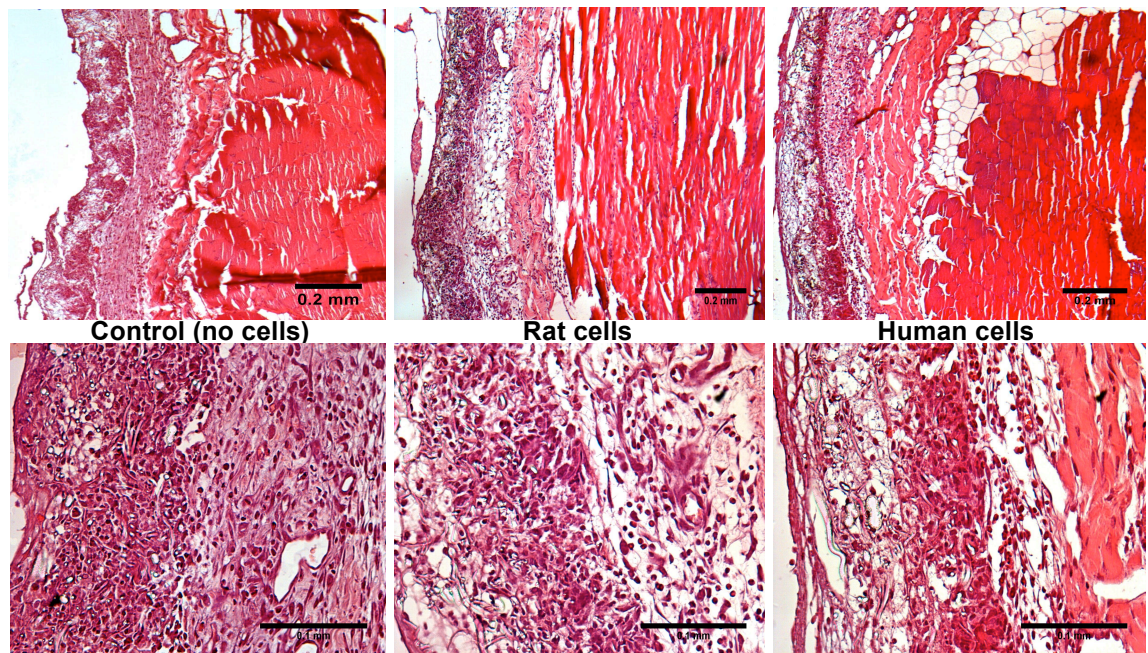


**Figure 6.2.4** Representative light microscopy H&E stained sections of abdominal wall of female Sprague-Dawley rats after 3 days implantation of Th-PLA scaffolds on top, previously cultured with and without (control) rat or human ADSCs in DMEM medium for 2 weeks. Top images: scale bars of 0.2 mm (10X magnification). Bottom images: scale bars of 0.1 mm (40X magnification).

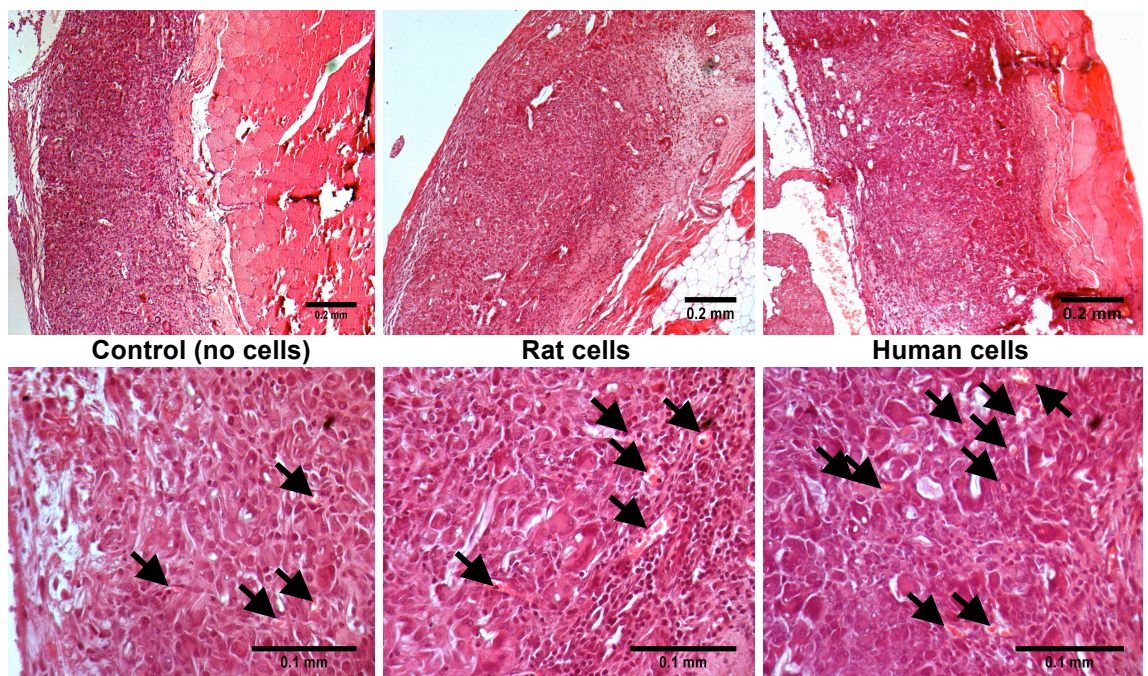


**Figure 6.2.5** Representative light microscopy H&E stained sections of abdominal wall of female Sprague-Dawley rats after 7 days implantation of Th-PLA scaffolds on top, previously cultured with and without (control) rat or human ADSCs in DMEM medium



for 2 weeks. Small blood vessels are identified by (↑). Top images: scale bars of 0.2 mm (10X magnification). Bottom images: scale bars of 0.1 mm (40X magnification).

### 6.3 Acute inflammatory response

At day 3, an acute macrophage response was observed with CD68 positive cells seen throughout all samples, localized inside the scaffolds and not found in the surrounding tissues (figure 6.3.1).

Semi-quantitative assessment of the immunohistochemistry demonstrated the macrophage response to be moderate, becoming more intense after 7 days implantation (figure 6.3.5) and again limited to the samples (figure 6.3.1).

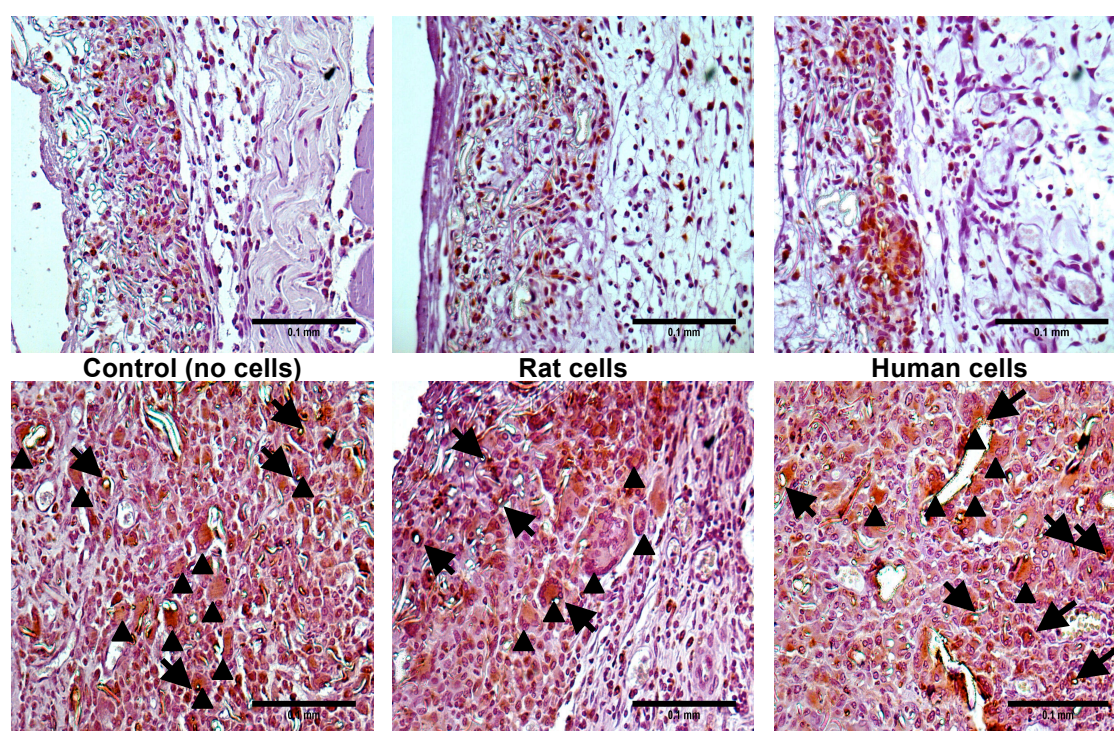


**Figure 6.3.1** Representative light microscopy image of sections of abdominal wall of female Sprague-Dawley rats after 3 (top images) and 7 days (bottom images) implantation of PLA scaffolds on top, previously cultured with and without (control) rat or human ADSCs in DMEM medium for 2 weeks; following immunohistochemistry for anti-CD68 antibody. Macrophages stained for CD68 surrounding individual Th-PLA fibres are identify by (↑); and foreign giant cells containing several macrophages are identified by up pointing triangle (▲). Scale bars of 0.1 mm (40X magnification).



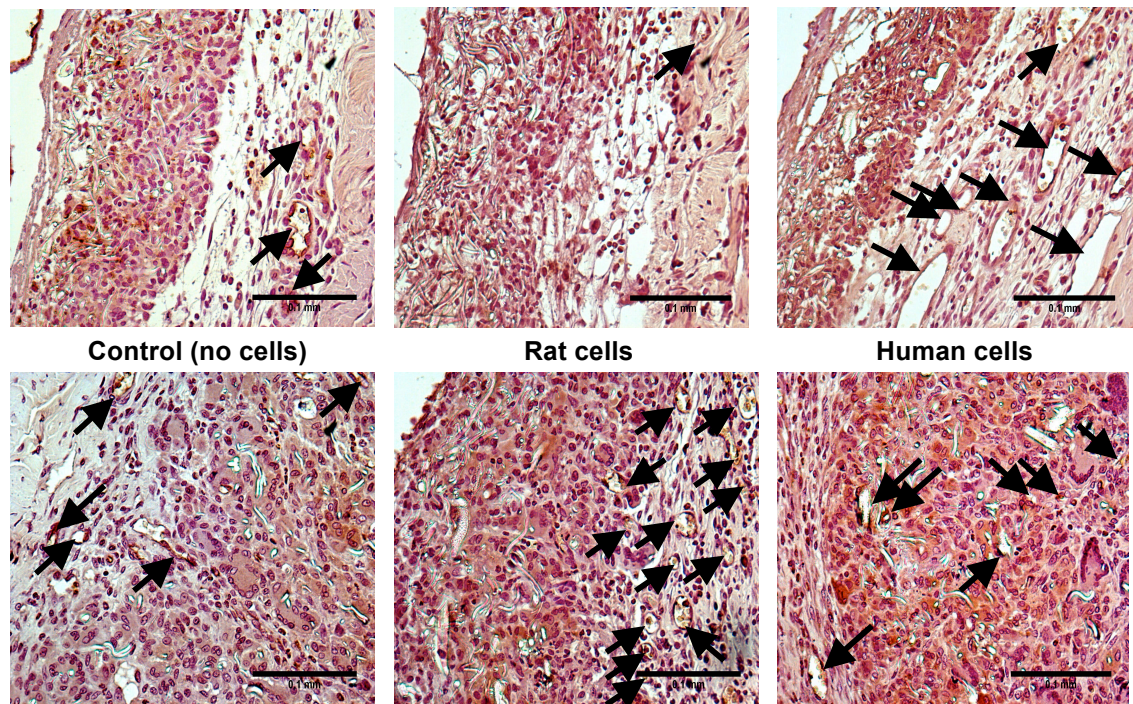


**Figure 6.3.2** Representative light microscopy image of sections of abdominal wall of female Sprague-Dawley rats after 3 (top images) and 7 days (bottom images) implantation of Th-PLA scaffold on top, previously cultured with and without (control) rat or human ADSCs in DMEM medium for 2 weeks; following immunohistochemistry for anti-PECAM-1 antibody. Endothelial cells stained for PECAM-1 around blood vessels are identified by (↑). Scale bars of 0.1 mm (40X magnification).

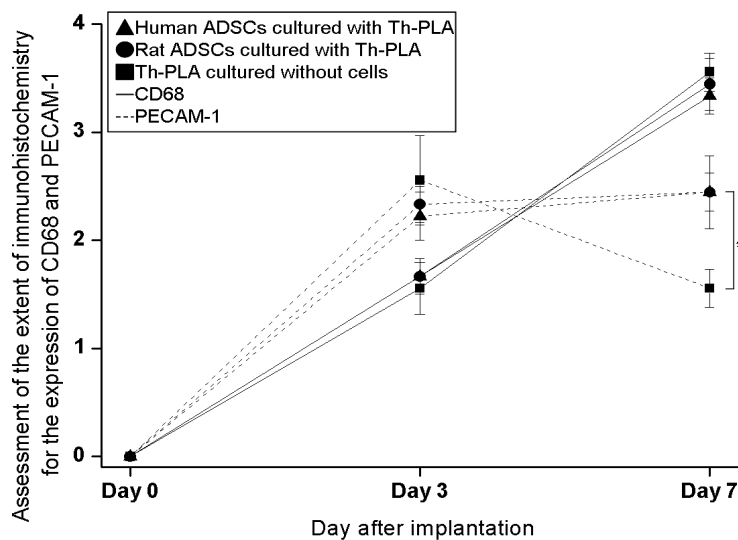


**Figure 6.3.3** Semi-quantitative analyses of the host response against the implanted samples. Assessment of the extent of immunohistochemistry using a blind scoring for the expression of CD68 and PECAM-1 from sections of abdominal wall of female Sprague-Dawley rats after 3 and 7 days implantation of Th-PLA scaffold on top, previously cultured with and without (control) rat or human ADSCs in DMEM medium for 2 weeks. Results shown as mean  $\pm$  SEM (n=3). Scale: 0=absent, 1=mild presence, 2=large presence, 3=abundance, 4=great abundance.

Although PECAM-1 stained many cells only inside the samples, similarly to CD68, at both days of sacrifice (figure 6.3.2); this staining was also found around large blood vessels in the fascia at day 3, while, after 7 days implantation, new small blood vessels inside the scaffolds for all samples were stained (figure 6.3.2).

A moderate staining was identified after 3 days with no differences between groups (figure 6.3.3). By 7 days, there was a similar expression between samples with rat or human ADSCs but lower staining for cell-free Th-PLA scaffolds (figure 6.3.3).

## 6.4 ECM remodelling

Connective tissue of the fascia was stained for collagen I from all sections at any day. On the other hand, after 3 days implantation, only a small amount of collagen I was observed inside the scaffolds for all samples (figure 6.4.1), which was slightly increased after 7 days implantation without visible differences between them (figure 6.4.2).

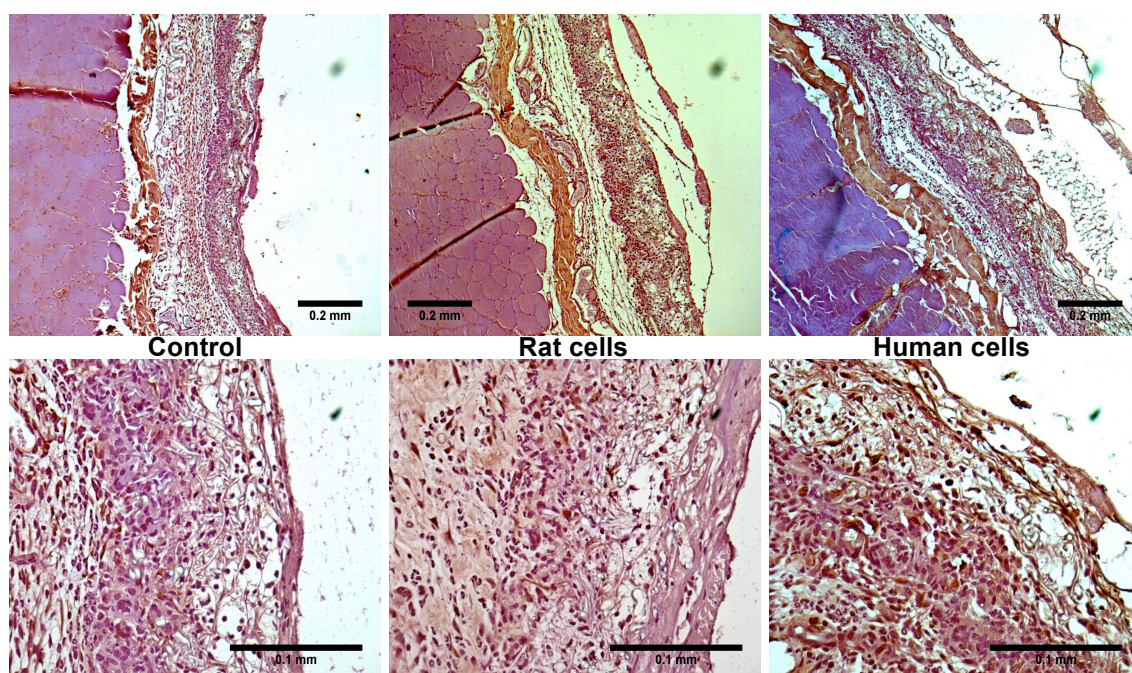


**Figure 6.4.1** Representative light microscopy of sections of abdominal wall of female Sprague-Dawley rats after 3 days implantation of Th-PLA scaffold on top, previously cultured with and without (control) rat or human ADSCs in DMEM for 2 weeks; following immunohistochemistry for anti-collagen I antibody. Top images: scale bars of 0.2 mm (10X magnification). Bottom images: scale bars of 0.1 mm (40X magnification).



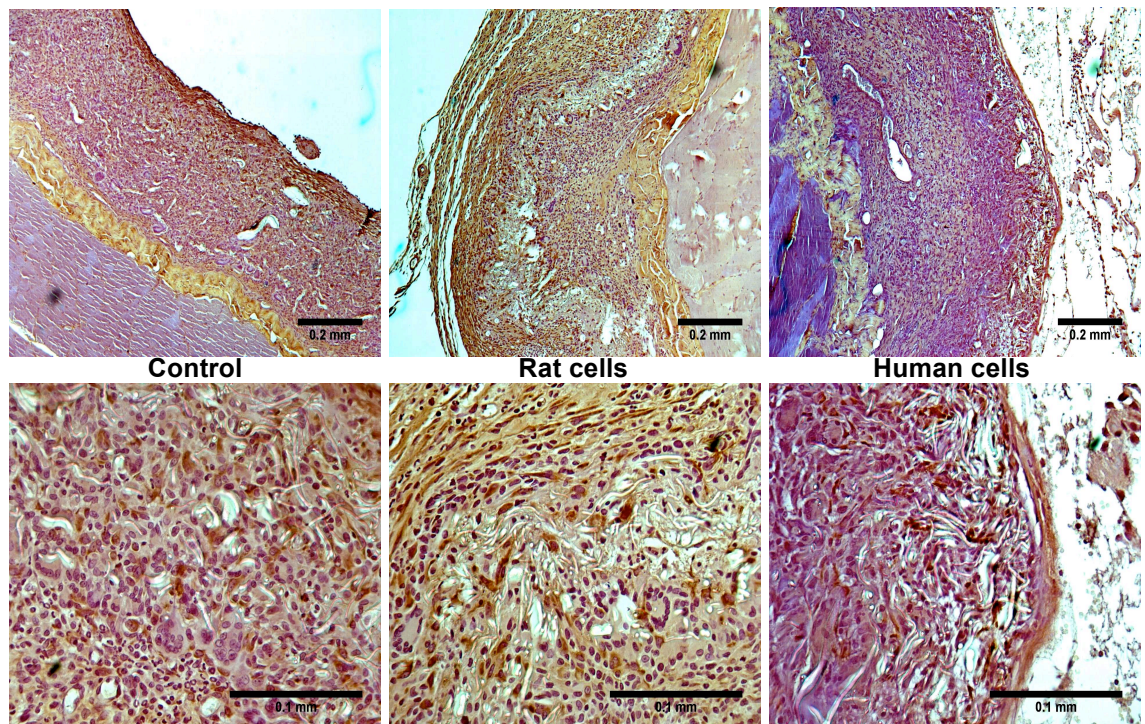


**Figure 6.4.2** Representative light microscopy of sections of abdominal wall of female Sprague-Dawley rats after 7 days implantation of Th-PLA scaffold on top, previously cultured with and without (control) rat or human ADSCs in DMEM for 2 weeks; following immunohistochemistry for anti-collagen I antibody. Top images: scale bars of 0.2 mm (10X magnification). Bottom images: scale bars of 0.1 mm (40X magnification).

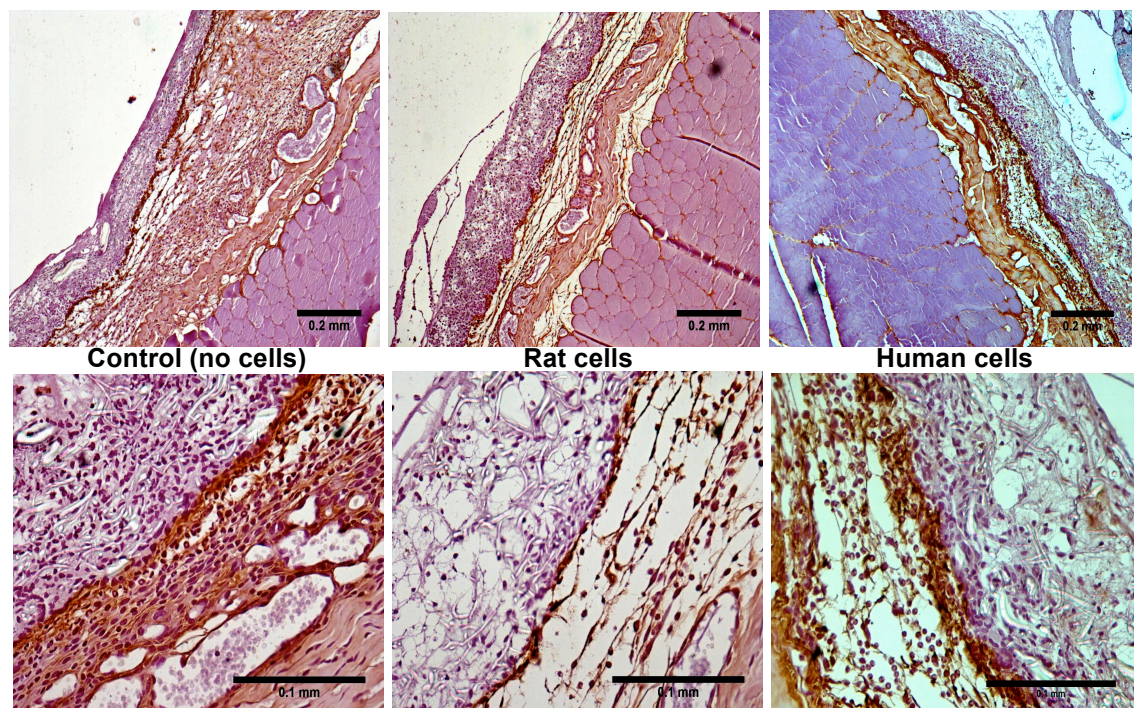


**Figure 6.4.3** Representative light microscopy of sections of abdominal wall of female Sprague-Dawley rats after 3 days implantation of Th-PLA scaffold on top, previously



cultured with and without (control) rat or human ADSCs in DMEM medium for 2 weeks; following immunohistochemistry for anti-collagen III antibody. Top images: scale bars of 0.2 mm (10X magnification). Bottom images: scale bars of 0.1 mm (40X magnification).

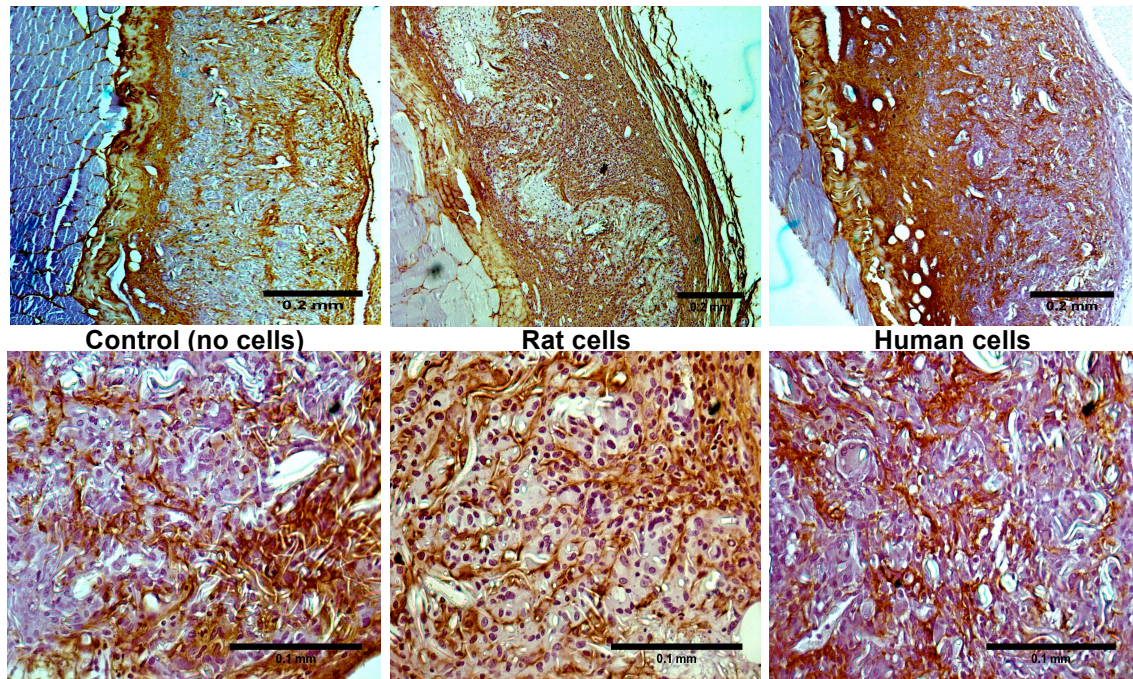


**Figure 6.4.4** Representative light microscopy of sections of abdominal wall of female Sprague-Dawley rats after 7 days implantation of Th-PLA scaffold on top, previously cultured with and without (control) rat or human ADSCs in DMEM medium for 2 weeks; following immunohistochemistry for anti-collagen III antibody. Top images: scale bars of 0.2 mm (10X magnification). Bottom images: scale bars of 0.1 mm (40X magnification).

After 3 days implantation, immunohistochemistry for collagen III revealed a thin layer of collagen production on the lower surface of the scaffolds from all the samples (figure 6.4.3). Nevertheless, by day 7, thin new fibres of collagen III were visible throughout the scaffolds of all samples, as shown in figure 6.4.4.

Total collagen from all samples was stained with Sirius red staining. Similar to collagen I staining the connective tissue of the fascia was highly stained for all sections at any day. Alternatively, similar to collagen III staining, while a thin layer of collagen was found on the lower surface of the scaffolds from all the samples (figure 6.4.5), new thin fibres of collagen were stained throughout the scaffolds of all samples (figure 6.4.6).



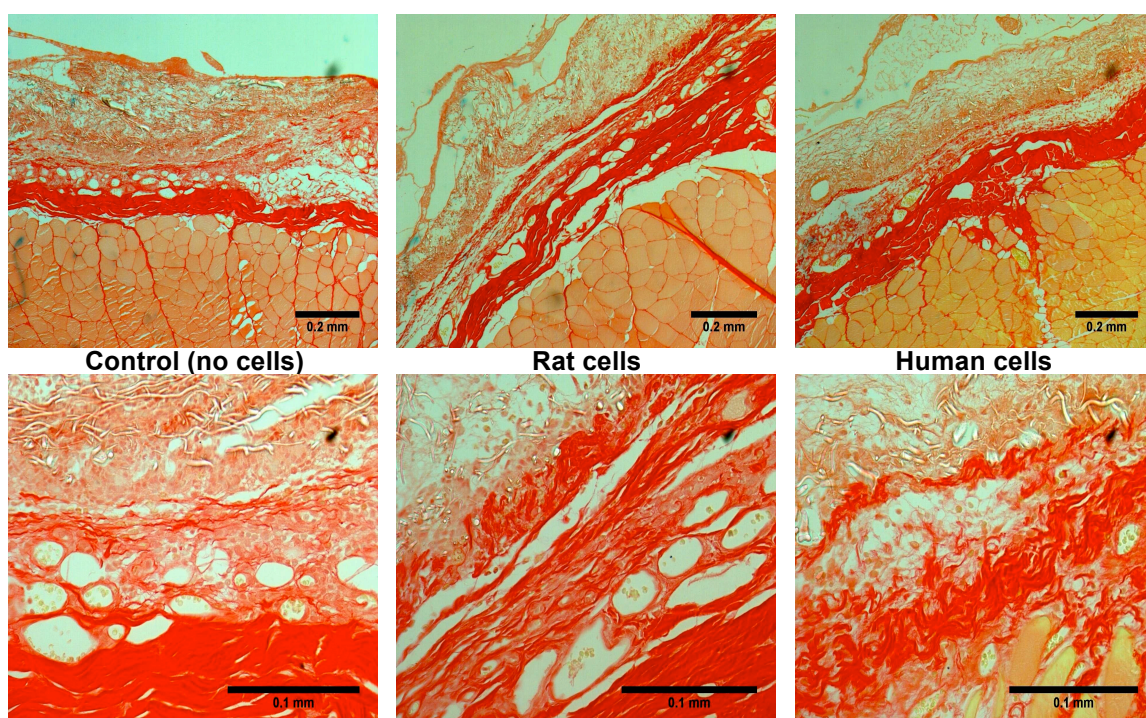


**Figure 6.4.5** Representative light microscopy of sections of abdominal wall of female Sprague-Dawley rats after 3 days implantation of Th-PLA scaffold on top, previously cultured with and without (control) rat or human ADSCs in DMEM medium for 2 weeks; following Sirius red staining. Top images: scale bars of 0.2 mm (10X magnification). Bottom images: scale bars of 0.1 mm (40X magnification).

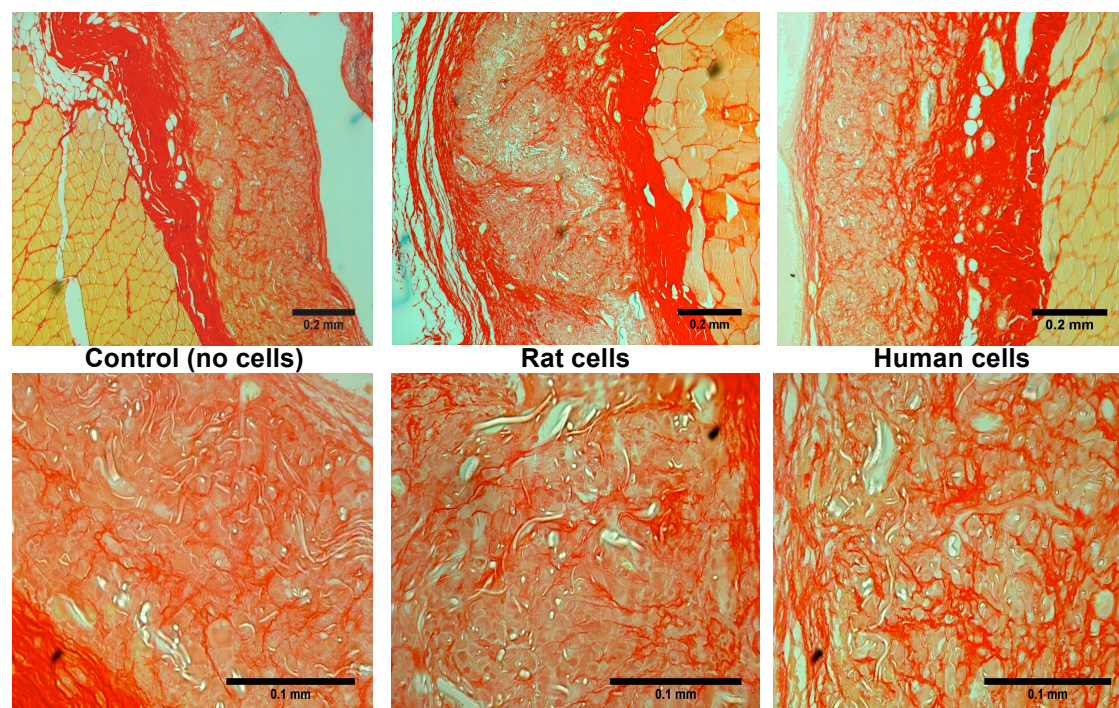


**Figure 6.4.6** Representative light microscopy of sections of abdominal wall of female Sprague-Dawley rats after 7 days implantation of Th-PLA scaffold on top, previously



*cultured with and without (control) rat or human ADSCs in DMEM medium for 2 weeks; following Sirius red staining. Top images: scale bars of 0.2 mm (10X magnification). Bottom images: scale bars of 0.1 mm (40X magnification).*

Finally, the controls for all 3 groups did not show any staining when sections were incubated without primary and secondary antibodies, or incubated only with secondary antibodies, but following the rest of the immunohistochemistry protocol (figure 6.4.7).

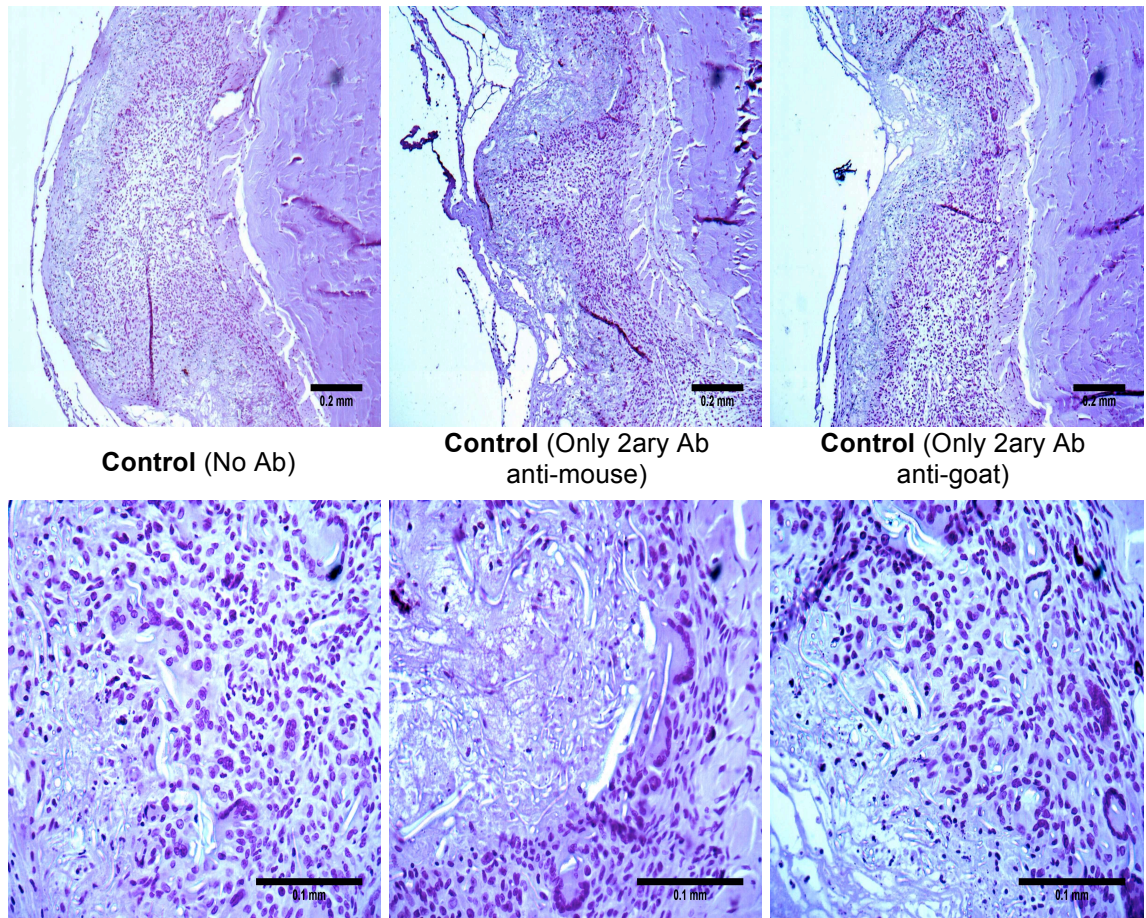


**Figure 6.4.7** *Representative light microscopy of sections of abdominal wall of female Sprague-Dawley rats after 7 days implantation of Th-PLA scaffold on top, previously cultured with and without (control) rat or human ADSCs in DMEM medium for 2 weeks. Each sample was followed by immunohistochemistry control procedure; the same process only avoiding incubations with primary and secondary antibodies, or incubating only with secondary antibodies. Top images: scale bars of 0.2 mm (10X magnification). Bottom images: scale bars of 0.1 mm (40X magnification).*



## 6.5 Discussion

Ideally, a biomaterial to be implanted into the pelvic floor of humans has been described as being sterile, inert, non-carcinogenic, non-inflammatory, non-immunogenic, mechanically durable, not degradable, inexpensive, readily accessible, and easy to use (497).

Clearly, currently there is no material that meets the above criteria. Alternatively, a material that produces an initial vigorous inflammatory response is more likely trigger the cascade of events leading to tissue integration and reduce risk of encapsulation (498). However, the persistence of the inflammatory response into a chronic phase (M1 macrophage response) (499) is undesirable and is associated with pain, erosion or infection, as seen with non-degradable materials.

A degradable material may be preferable since, ideally, it can undergo controlled degradation whilst at the same time inducing the production of new ECM and remodeling of the tissue (M2 macrophage response) with ingrowth of fibroblast and rapid angiogenesis (489).

As above, several studies have investigated in animals the acute host response against different cell-free synthetic and biological materials as being a critical indicator to predict their long-term outcomes.

Nevertheless, only a few studies have previously assessed in animals a TERM designed for pelvic floor repair. These were developed from biodegradable poly-glycolic acid (PGA) (334) or PLGA (336, 500) scaffolds. *In vivo*, PGA scaffolds have been shown to be completely degraded in a few weeks and PLGA scaffolds in 3 months whilst PLA scaffolds are present after 12 months (501). The degradation rate has relevance for maintenance of mechanical properties of the implants and needs to be studied for pelvic floor repair.

Cells used to develop the TERMS in these previous studies were obtained from rabbits (334) or humans (336, 500) and were subcutaneously implanted in nude mice. All demonstrated integration of the samples into the host tissues with neo-fascia formation, particularly for the cell-seeded scaffolds. Alternatively, the immune response against the implants was not characterized in any study.

Only 2 studies have used rat models for SUI, both by direct sphincter injury using PNT, to implant and assess a TERM. MDSCs and BMDSCs isolated from same rats, respectively, were used to develop engineered tissues from biological (338) and synthetic degradable scaffolds (339). Both studies showed neo-tissue formation for the cell-seeded scaffolds which was hypothesized as having potential for long-term integration; however, continence outcomes were similar for the acellular and cell-seeded groups and again the host response to the implants was not assessed.

Although in our study we implanted human cells in immunocompetent Sprague-Dawley rats, rat cells were also included as a control. All samples were implanted in different rats since interpretation of responses to different materials in the same animal is not recommended with a body wide immune response.

There were little differences, in terms of the host inflammatory response elicited, between cell-free scaffolds and those seeded with human or rat ADSCs. ADSCs were well characterized prior to implantation but there was no identification of them post implantation so it is not possible to comment on any direct regenerative effect of these cells, however, there were no major differences with non cell-seeded implants and in these acute experiments the major objective was to assess the acute inflammatory response to implants.

Although PECAM-1 is an adhesion molecule expressed on platelets and subsets of leukocytes, it mainly stains endothelial cells with cell adhesion, trans-endothelial migration of myeloid-derived cells and angiogenesis functions; and therefore, it has been widely use to assess neovascularization (502). PECAM-1 stained blood vessels inside samples and the semi-quantitative assessment of this staining was higher after 7 days implantation for cell-seeded scaffolds compared to acellular samples. However, we cannot explain this as an effect of the ADSCs since these cells were not identified post implantation.

There is no data showed about the immunohistochemistry of these slides for anti-human CD29, CD44, CD73 and beta-2 microglobulin. Since the cell tracker staining failed, the idea was to identify the human cells implanted into rat tissues by using these Abs; however, while the PE conjugated Abs (CD29, CD44 and CD73) did not work beta-2 microglobulin Ab stained all the cells from the fascia of the rats. The secondary Ab control did not shown any staining; however, sections from the control group (scaffolds

implanted without cells) showed staining for this Ab suggesting unspecificity against human specie and probably it reacted against rat cells too.

All PLA scaffolds, both without and with cells, were integrated into the fascia of the abdominal wall with rapid host cell infiltration and ingrowth of small blood vessels after 7 days implantation as seen for H&E and PECAM-1 staining.

The macrophage response against the cell-seeded Th-PLA scaffolds is clearly evident, especially 7 days after implantation. This response seems to be specific to the synthetic foreign material since macrophages were not found in tissues surrounding the samples and macrophages enclosed individual PLA fibres.

Macroporous polypropylene mesh is said to be more favourable to permit host cells infiltration (376). The current study shows that a microporous electrospun Th-PLA scaffold permitted the infiltration of host inflammatory cells throughout its entire thickness which is highly encouraging for its potential to resist infection by any bacteria during implantation in a clean contaminated environment.

Additionally, the host response led to host fibroblast infiltration and ECM formation, as seen for collagen I, collagen III and Sirius red staining, for all samples.

Small amounts of collagen I was produced inside all scaffolds, particularly after 7 days; while loads of new collagen III fibres were seen after 7 days implantation in all samples throughout the thickness of the scaffolds. Collagen III is the first type produced when new ECM is formed during constructive remodelling. Afterwards, this is replaced by collagen I which is more stable (489).

Reassuringly there was no sign of encapsulation observed; a problem that has been seen with chemically cross-linked biological grafts in animals (456) and humans (503).

3 and 7 days time points for subcutaneous implantation in rats were basically selected as being the easiest and cheapest way to assess the host response against our materials. Since this work was a collaborative research between institutions of different countries, involving many people and resources as well as high level of organization; we thought to use first this short-term implantation and cheaper animal model before moving to more complex and expensive long-term models. Alternatively, this was the major limitation of this work since the short-term nature the model cannot be used to assess definitely whether a chronic inflammatory response ensues.

Additionally, implanted cells were not labelled; something that will be necessary in longer-term experiments to provide information on their survival or migration. The immune system of the rats could have eliminated human cells via cellular rejection (504).

Long-term animal experiments will also be required to study the performance of the TERM investigating the development of any chronic immune response, the fate of the ADSCs and the mechanical properties of the TERM after several months of implantation.

Nevertheless, we believe this is the first study that examines the acute host response against a TERM designed for pelvic floor repair, developed from human ADSCs cultured on biodegradable Th-PLA scaffolds.

In addition, although 7 days is too short to test the regenerative potential of the ADSCs, there was no higher immune response against the human cell-seeded scaffolds compared to the other groups of implants. All groups were well integrated into host tissues with an acute response suggesting the potential for production of neo-tissue formation by host cell infiltration and new blood vessels formation; all early indicators of constructive remodelling and promising for long-term integration.

## **Chapter 7**

### **MECHANICAL PROPERTIES OF THE TERMS**

## 7.1 Introduction

There are no standardised protocols for testing the mechanical properties of pelvic floor tissues or materials used to treat SUI and POP. However, many studies have used uniaxial tensile testing to calculate the stress (force divided by cross sectional area of tissue) versus the strain (change in elongation in relation to initial length) of these tissues/materials, which are described in the introduction of this thesis and summarized in this Chapter.

Therefore, all mechanical data of this thesis is based on this method to measure the breaking load of our materials.

The plot obtained, after uniaxial testing, is normally a non-linear curve and has 3 distinct sections: the initial toe, linear and failure regions (505).

In order to normalize the data from a tensile test of different materials, the volume of the tested material was calculated using contact methods. These, may be less precise than non-contact methods and have the risk of causing weakening (506). Then, we used clamp grips as the method of securing the tissue for uniaxial loading, which may be more accurate than pin grips, for instance, since the clamp can purchase the full width of the tissue and distribute the force more evenly across the tissue. Another variable is the strain rate applied to this test; however, this has not been shown to affect the mechanical properties when studying ligaments and tendons from animals (507, 508).

In addition, studies have looked at the effects of ambient air, storage in saline, temperature, and freezing, when testing mechanical properties (509, 510). Nevertheless, it has been shown that there is no effect on mechanical properties of vaginal tissue when comparing fresh and frozen samples, as well as, comparing samples at room temperature and samples at 37°C. In addition, in the same study, samples soaked in saline remained stable for up to 24 hours and storage in paraffin did not affect the results either (510).

Irrespective of this, every uniaxial testing performed in this thesis to test the mechanical properties of TERMs was done with fresh samples after their culture, taken straight from the incubator.

### **7.1.1 Mechanical properties of the native tissues and of the prostheses used to treat SUI and POP**

Only 3 studies could be found where the mechanical properties of paravaginal tissue were investigated (194, 511, 512). These all looked at women with POP, and no similar studies were found for women with SUI. Furthermore, only one of these studies looked at the mechanical properties of healthy (non-prolapsed) paravaginal tissue (194) from pre and post-menopausal women. These values were used to provide the ranges for native tissues which are used in this thesis when comparing mechanical properties of different materials.

Although all materials used to surgically treat SUI and POP present higher mechanical properties than native tissues, the closest in terms of UTS and Young's modulus are rabbit rectus fascia (494), cross-linked porcine dermis (458) and macroporous monofilament PPL (458). Cadaveric dermis and fenestrated porcine dermis (494) showed greater Young's modulus and UTS than native tissues.

After implantation of these materials, clinical and animal studies have reported different results for alterations in mechanical properties. Whereas PPL become stiffer and UTS was decreased, the mechanical properties of autologous rabbit fascia was unchanged (494, 513), which correlates with a lower host response to the latter, as is also seen in women (514).

Cadaveric tissues undergo the greatest decrease in UTS which correlates with the clinical findings of gross degradation with these tissues (515, 516).

Fenestrated porcine dermis grafts lose strength (UTS) and increase stiffness (Young's modulus), but cross linked porcine dermis does not change a great deal. This may be because encapsulation without remodelling has been observed for the latter material after implantation (514, 517).

### **7.1.2 Correlation between mechanical properties and outcomes of the prosthesis used to treat SUI and POP**

As already described in the introduction Chapter of this thesis, macroporous PPL has been shown to have good success rates for SUI and POP repair, although a greater risk

of erosion is associated with this material (518-521). At 5 year follow up, in a randomised trial, better objective success rate with PPL mesh were described when compared to autologous fascia lata (522).

The success of biological materials, such as cross-linked porcine dermis, is very low but the erosion rate is also low (84). When comparing PPL mesh with fenestrated porcine dermis, an objective cure rate of 71.9% and 56.4% was found but the erosion rate was 6.3% and 0% respectively (523).

Alternatively, cadaveric dermis showed high failure rates of 50% at 6-12 months (79, 524).

From the above evaluation, there was no correlation between changes in mechanical properties and the success and/or erosion rates after the implantation of these materials (378).

PPL presents extremely high Young's modulus, which may explain its greater risk of causing erosion, and although UTS is decreased post implantation it remains higher than for native tissues (458).

Autologous grafts and fenestrated porcine dermis have shown reasonable maintenance of mechanical properties after implantation with UTS higher than native tissues, but slightly lower Young's modulus and this may be associated with the lower success rate of these materials when compared to PPL.

For cadaveric dermis and cadaveric fascia although mechanical properties are highly decreased, these have same Young's modulus and higher UTS than native tissue after implantation, which does not correlate with their clinical findings.

Similarly, cross-linked porcine dermis has very low success rates, even though, its mechanical properties are maintained after implantation with the same Young's modulus and higher UTS than native tissues.

It is likely that factors other than the mechanical properties of the materials will influence the final outcome, as commented on in a previous Chapter. The host response to these materials is very relevant and varies considerably with the different implanted materials.

In response to PPL there is often a fibrotic response followed by some strengthening and particularly increasing the stiffness of the material. On one hand, this seems to be desirable for long-term retention but it is more likely to produce erosion.



In general, a good integration into native tissues by constructive remodelling of the implant, as seen for autologous fascia and fenestrated porcine dermis seems to be necessary for better outcomes, which is also the case in hernia models (492). In addition, although mechanical properties of cadaveric tissues are higher than other materials, the high degradation associated with cadaveric tissues may lead to early failure. Probably, encapsulation is not desirable either, since cross-linked porcine dermis is also related to high failure rates whereas its mechanical properties are maintained after implantation, being stronger than native tissues.

### **7.1.3 Mechanical properties for TERMS**

Mechanical properties of healthy native paravaginal tissue from premenopausal women without SUI or POP were used as a target to aim for based on the assumption that these values are representative of the requirements for physiological load bearing. Whether these values are the “ideal” for a TERM is unknown but it seems desirable that an implantable material should have as minimum requirement equivalent values to the native tissue at the time of implantation.

In this thesis, it has been shown that electrospun Th-PLA scaffolds seeded and cultured with ADSCs achieved mechanical properties close to healthy native paravaginal tissue. While the Young’s modulus was slightly lower compared to native tissues, the UTS was higher.

This seems to be desirable since excessively stiff materials may lead to tissue erosion whilst excessively lax materials will fail to provide sufficient support (525). Since PPL shows a high Young’s modulus and this material is associated initially with high success rates, stiffer materials may be desirable (at least initially) for initial support but better long-term outcomes probably require a good host response to the material as well as adequate mechanical properties.

There are also good arguments that perhaps we should aim for an even stronger material in terms of UTS.

Since we are not replacing a native tissue we may aim for a stronger material than these to compensate for global deficiencies in muscular, ligamentous and fascial supports. Indeed, for the current prosthesis these are all stronger than native tissues at the time of

implantation. On the other hand, PLA fibres will degrade over time as previously observed *in vitro*, leading to a weakened TERM, and this may be accelerated *in vivo*. Therefore, starting with a stronger material will theoretically be less likely to result in early failure (figure 7.1.1 and figure 7.1.2).

Nevertheless, questions, such as, how much stronger, *in vivo* degradation rate, and the effect of neo-tissue formation on mechanical properties, will need to be answer with long-term animal experiments.

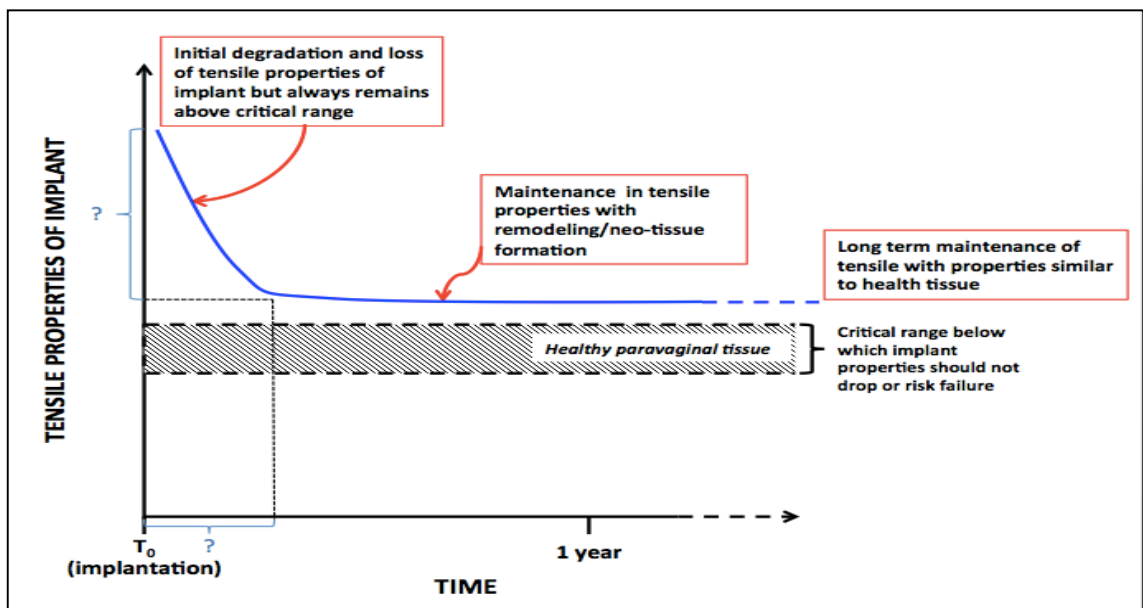


**Figure 7.1.1** The ideal *in vivo* response to a material with optimal tensile properties.

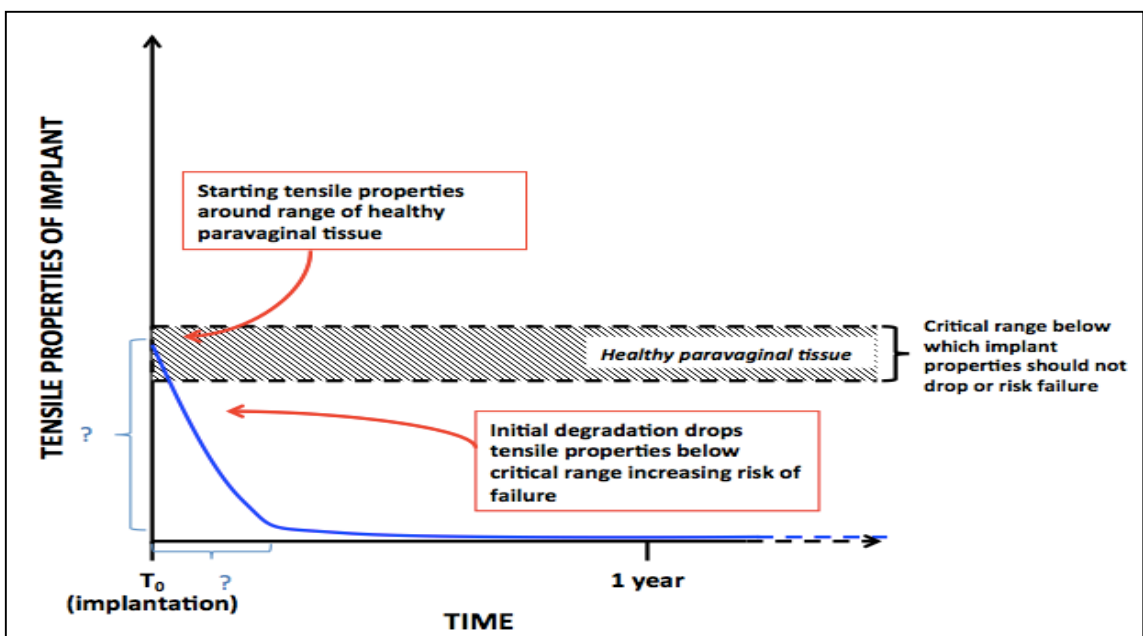


**Figure 7.1.2** Anticipated *in vivo* response to a material leading to early failure.

## 7.2 Increasing mechanical properties of PLA scaffolds

In the previous Chapter of this thesis it was shown that mechanical or chemical stimulation, in terms to increase ECM production, did not have any significant effect on the mechanical properties on the TERMS. In addition, it was demonstrated that, although the culture of cells on scaffolds can increase the values for mechanical properties, the main mechanical properties of a TERM are given by the scaffold.

For this reason in this Chapter we aimed to develop PLA scaffolds designed with different fibre configurations to improve their mechanical properties.

As described in Chapter 3 of this thesis, the electrospinning technique allows the modification of different parameters to produce random or aligned fibres which can affect the mechanical properties of the electrospun scaffolds.

Scaffolds were initially made by aligned fibres to be compared with other scaffolds and we then explored hybrid scaffolds combining aligned and random fibres. Following the setup for the electrospinning rig described in Chapter 2, aligned fibres were produced, based on previous work done in our laboratory, by increasing the speed of the rotation of the collector and reducing the distance between the needles and the collector. It has also been shown in our lab that relatively high voltage reduces the diameter of the fibres which become nanofibres. In addition, reducing the flow rate of the syringe pump reduces the diameter of the fibres too (data not published).

Another issue was getting these aligned fibres all along the width of the collector. The fibres are collected only in a narrow portion of the collector just in front the syringe which has to be very close to the collector.

Therefore, different electrospinning rigs were developed to produce scaffolds made of different combinations of aligned and random PLA fibres as described below:

- PLA random
- Th-PLA random
- Hybrid PLA (280  $\mu\text{m}$ ) (figure 7.2.3)
- Hybrid PLA (150  $\mu\text{m}$ ) (figure 7.2.2)
- PLA mainly aligned (figure 7.2.1)

- PLA aligned

### 7.2.1 Description of the different setups for the electrospinning rig

PLA random and Th-PLA random scaffolds were produced from 16 mL of PLA solution. The electrospinning rig for production of both scaffolds is already described in Chapter 2 and both scaffolds have already been compared in Chapter 3 of this thesis.

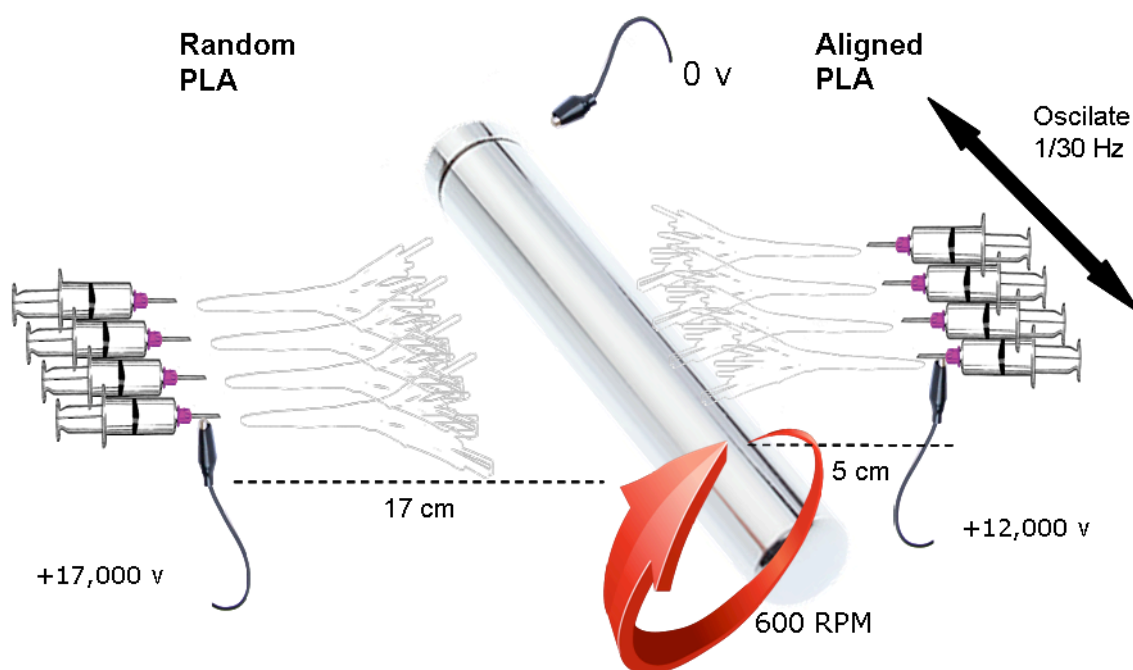


**Figure 7.2.1** Illustration of the electrospinning rig used to produce the mainly aligned PLA scaffolds.

The first rig used to produce hybrid PLA scaffolds is described below which was developed in our lab by PhD student Mr Frazer Bye.

As shown in figure 7.2.1, the left hand setup was adjusted for the formation of randomly oriented fibres, as previously described (8 mL of solution, 4 syringes, 2.4 mL/h, 17 kV, 17 cm from the tip of the needle). The right hand setup was adjusted to favour the formation of aligned fibres (8 mL of solution, 4 syringes, 2.4 mL/h, 12 kV, 5 cm from the tip of the needle). In order to ensure an equal distribution of aligned fibres across the rotating collector, the right hand syringe pump was mounted on a Lego™ robot programmed to reciprocate at 1/30 Hz in front of the collector and its travel set to the collector's width.

Finally, the speed of the rotation of the collector was set to spin at 600 rpm (only one speed setting for both the left and right hand set ups were possible).

A problem not commented before on in this thesis about the electrospinning technique is that, even though the collector is earthed, the fibres are attracted by metals around the rig and it is impossible to work out how much of the initial PLA solution is actually collected on the foil. On the other hand, since syringes for aligned fibres are placed very close to the collector these do not spread out and are mostly collected on the aluminium foil.

Therefore, although we used same amount of polymer solution pumped at the same flow rate, we believe these scaffolds were mainly composed by aligned fibres and that is why these scaffolds were called PLA mainly aligned.

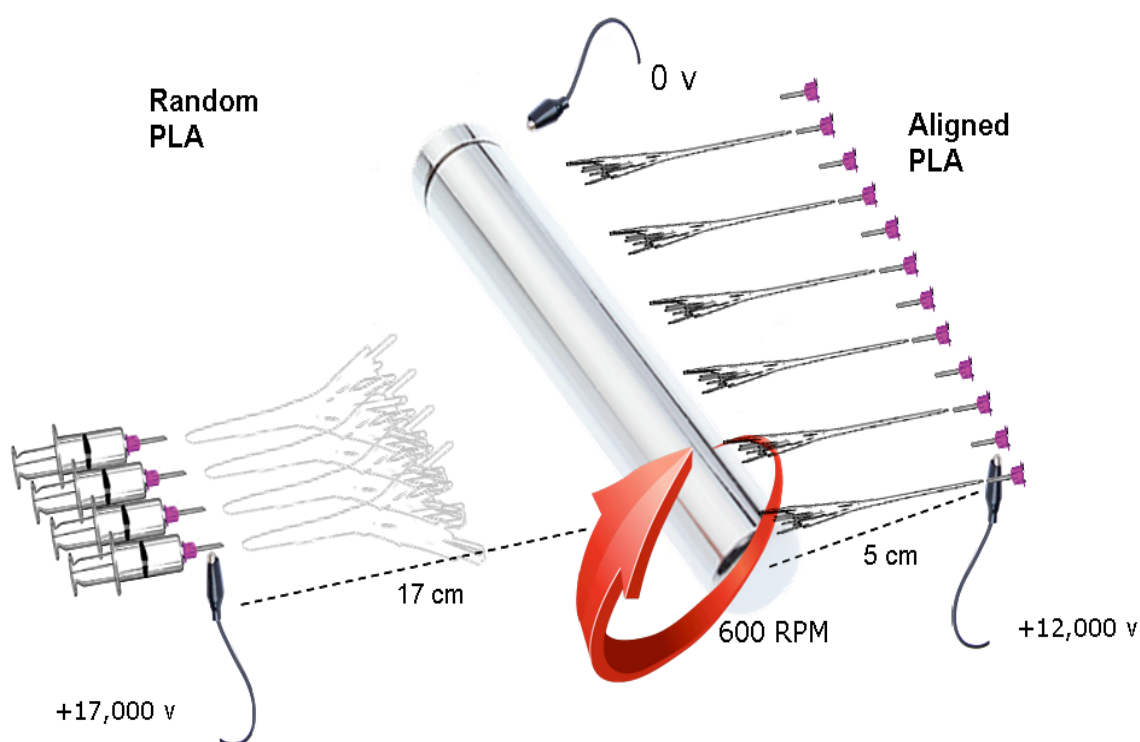


**Figure 7.2.2** Illustration of the electrospinning rig used to produce the hybrid PLA scaffold (150  $\mu\text{m}$ ).

The second electrospinning rig to produce hybrid scaffolds was developed in our lab by Mr Julio Bissoli.

As shown in figure 7.2.2, the left hand setup was adjusted for the formation of randomly oriented fibres, as previously described 20 mL of solution, 4 syringes, 2.4 mL/h, 17 kV,

17 cm from the tip of the needle). The right hand setup was adjusted to favour the formation of aligned fibres using a 50 mL syringe incorporated to a multichannel steel tube (figure 7.2.3) with 12 orifices to incorporate 12 tips; however, 6 of these tips in alternating order were blocked (15 mL of solution, 14.4 mL/h, 12 kV, 5 cm from the tip of the needle). The multichannel needle allowed the homogeneous distribution of the aligned fibres along the width of the collector.

As previously, the speed of the rotation of the collector was set to spin at 600 rpm.

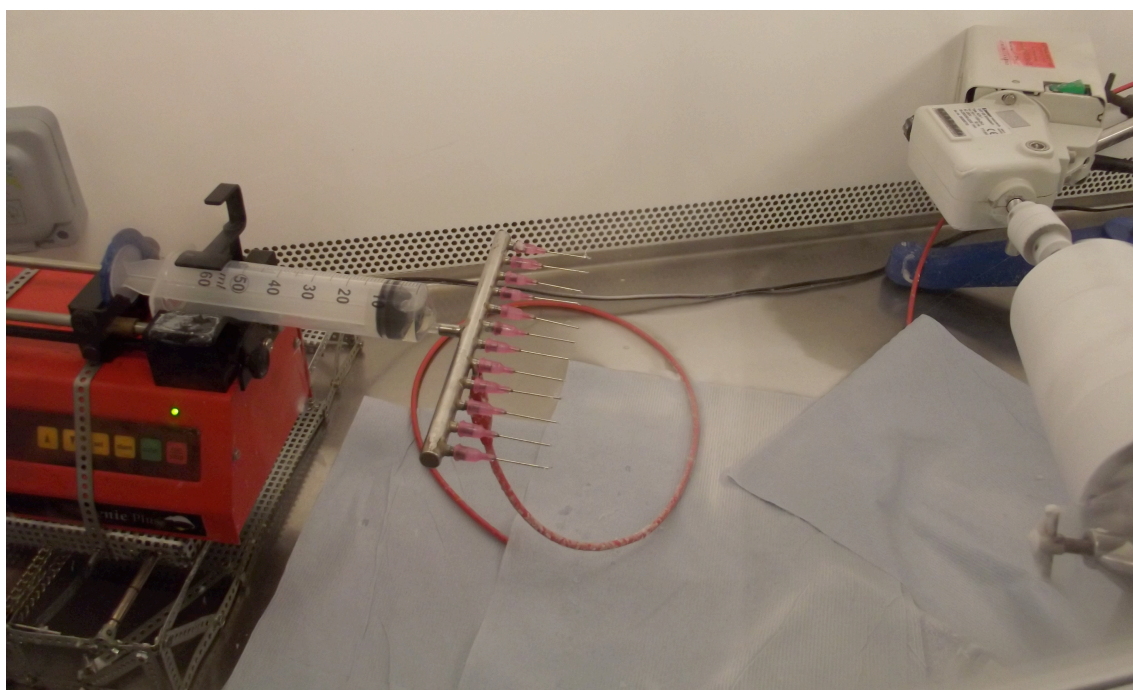


**Figure 7.2.3** Image of the electrospinning rig using the multichannel needle.

Since we had 6 needles working for the multichannel needle the solution was spun in less time. Therefore, we started to spin the random fibres 30 min before the aligned fibres and we finished the electrospinning of the random fibres 30 min later. Nevertheless, again, we believe that more aligned fibres were collected on the foil compared to random fibres. For this reason, we also believe that more random fibres were collected in the aluminium foil compared with PLA mainly aligned scaffolds. Furthermore, the last scaffolds produced were thicker than previous scaffolds (figure 7.2.5a) since we used more polymer solution. These scaffolds were called hybrid PLA (150  $\mu\text{m}$ ).

The last electrospinning rig was developed again by Mr Julio Bissoli aiming for thicker scaffolds with an equal ratio of random and aligned fibres.

As shown in figure 7.2.4, the left hand setup was adjusted for the formation of randomly oriented fibres, now using a multichannel needle (29 mL of solution, 28.8 mL/h, 17 kV, 17 cm from the tip of the needle). The right hand setup was adjusted to form aligned fibres using another multichannel needle (15 mL of solution, 28.8 mL/h, 12 kV, 5 cm from the tip of the needle). Again, the speed of the rotation of the collector was set to spin at 600 rpm.

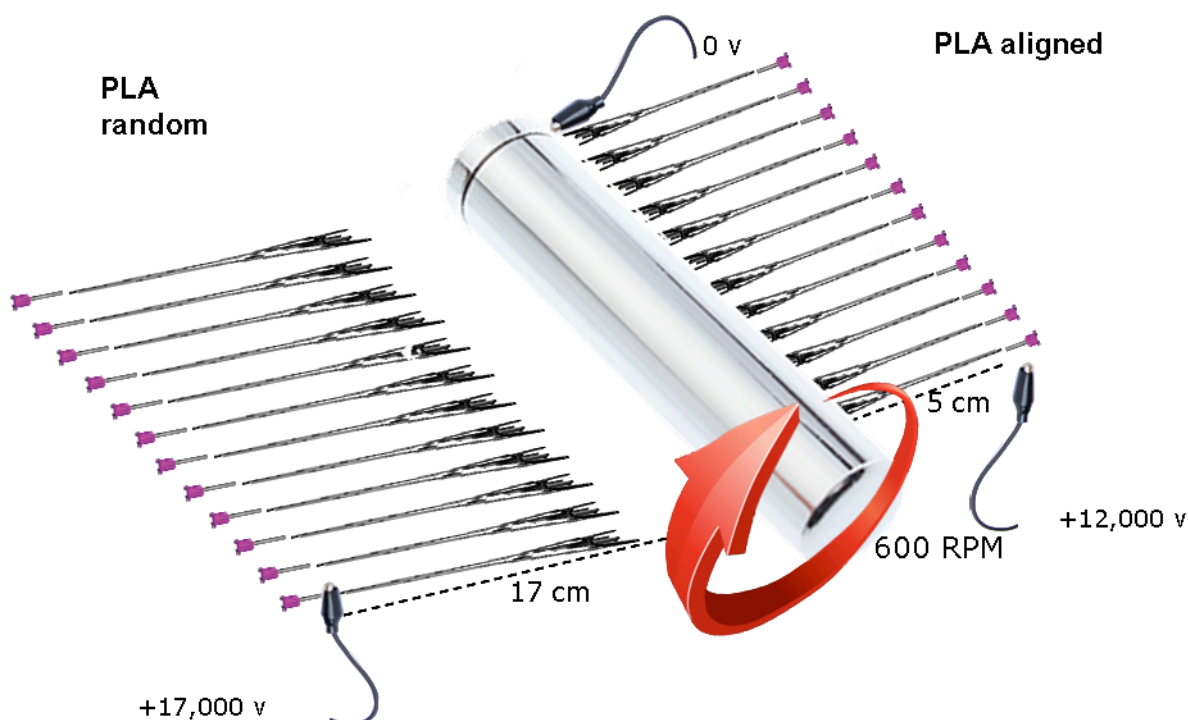


**Figure 7.2.4** Illustration of the electrospinning rig used to produce the hybrid PLA scaffold (280  $\mu\text{m}$ ).

For this rig, both syringes had the same amount of tips and were pumped at the same rate; however, since we had more PLA solution in the multichannel needle for the random fibres these started to be spun 15 min before the aligned fibres and we finished the electrospinning of the random fibres 15 min later.

As above, we could not work out the amount of solution actually spun and collected on the aluminium foil. Again a percentage of the amount of random fibres was lost; however, since we used a higher volume of solution for the random fibres we believe we obtained a more equal ratio of aligned vs random fibres for these last scaffolds

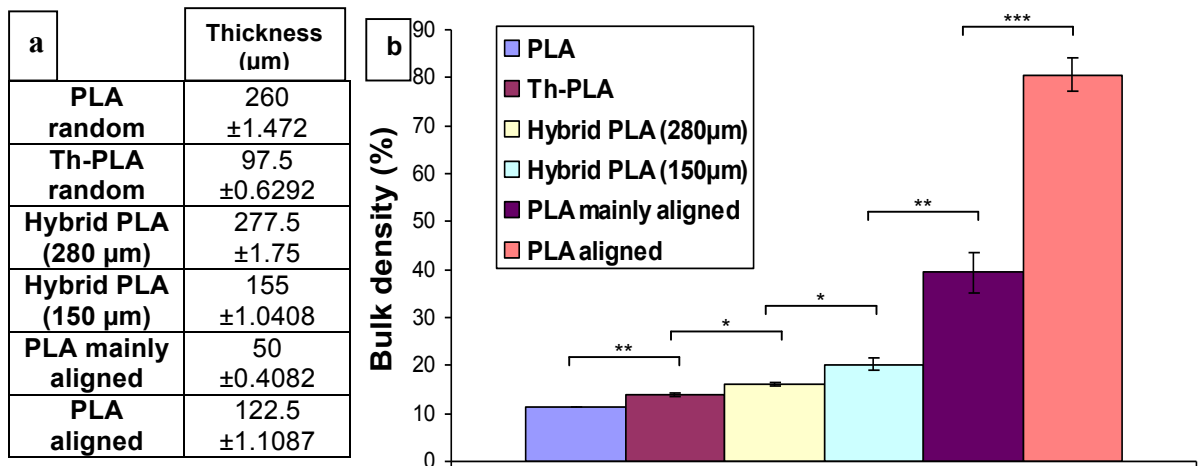


compared with previous scaffolds. In addition, these scaffolds were the thickest (figure 7.2.5a), and therefore, they were called hybrid PLA (280  $\mu\text{m}$ ).

As previously mentioned, we also produced 100% aligned scaffolds made with only one pump syringe and 4 needles with a collector set to spin at 600 rpm (20 mL of solution, 4 needles, 2.4 mL/h, 12 kV, 5 cm from the tip of the needle).

### 7.2.2 Physical and mechanical properties of PLA scaffolds with different fibre configuration

Mechanical properties of all these scaffolds were measured by using a BOSE tensiometer. SEM images and bulk density, calculated as previously described in Chapter 3, were also used for comparison.



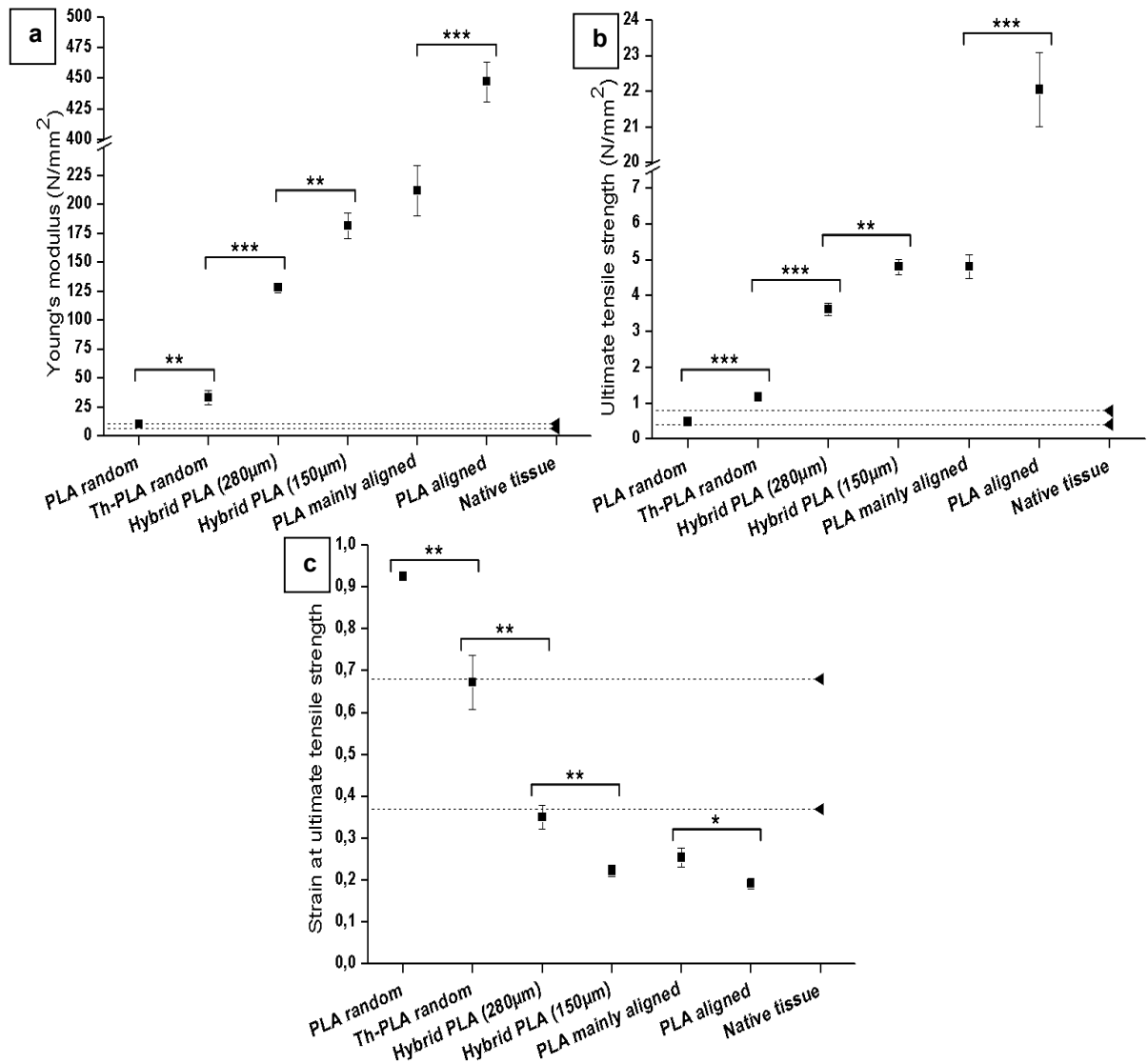
**Figure 7.2.5** (a) Thickness of the 6 different PLA scaffolds, mean $\pm$ SEM ( $n = 3$ ). (b) Bulk density of the 6 different PLA scaffolds, mean $\pm$ SEM ( $n = 3$ ); \* $p < 0.05$ , \*\* $p < 0.005$ , \*\*\* $p < 0.0005$ .

Figure 7.2.5 shows the thickness and bulk density of the PLA scaffolds with 6 different fibre configurations which are presented in the table (figure 7.2.5 a) as the anticipated expectation from higher amount of random fibres to higher amount of aligned fibres, such as described in previous section of this Chapter.

The bulk density was significantly increased from PLA random to PLA aligned scaffolds.



Same kind of correlation was found for mechanical properties of these 6 materials with an increase in Young's modulus and UTS from PLA random to PLA aligned scaffolds, and a decrease in the strain at the UTS from PLA random to PLA aligned scaffolds (figure 7.2.6). In addition, these differences were more significant for the increase of strength (UTS) and stiffness (Young's modulus) than for the decrease of the strain at UTS.



**Figure 7.2.6** Mechanical properties of 6 different PLA fibre configuration scaffolds, mean±SEM (n = 3). The last sample shown is the range for native tissue represented by 2 dashed lines (the range for native healthy paravaginal tissue). (a) YM, \*\*p<0.005; \*\*\*p<0.0001. (b) UTS, \*\*p<0.005; \*\*\*p<0.0005. (c) Strain at UTS, \*p<0.05; \*\*p<0.005.

SEM images confirmed the trend already commented on from random fibres to aligned fibres (figure 7.2.7). Furthermore, scaffolds containing aligned fibres were easier to peel off the aluminium foil and they were flatter scaffolds as can be observed from SEM images too.

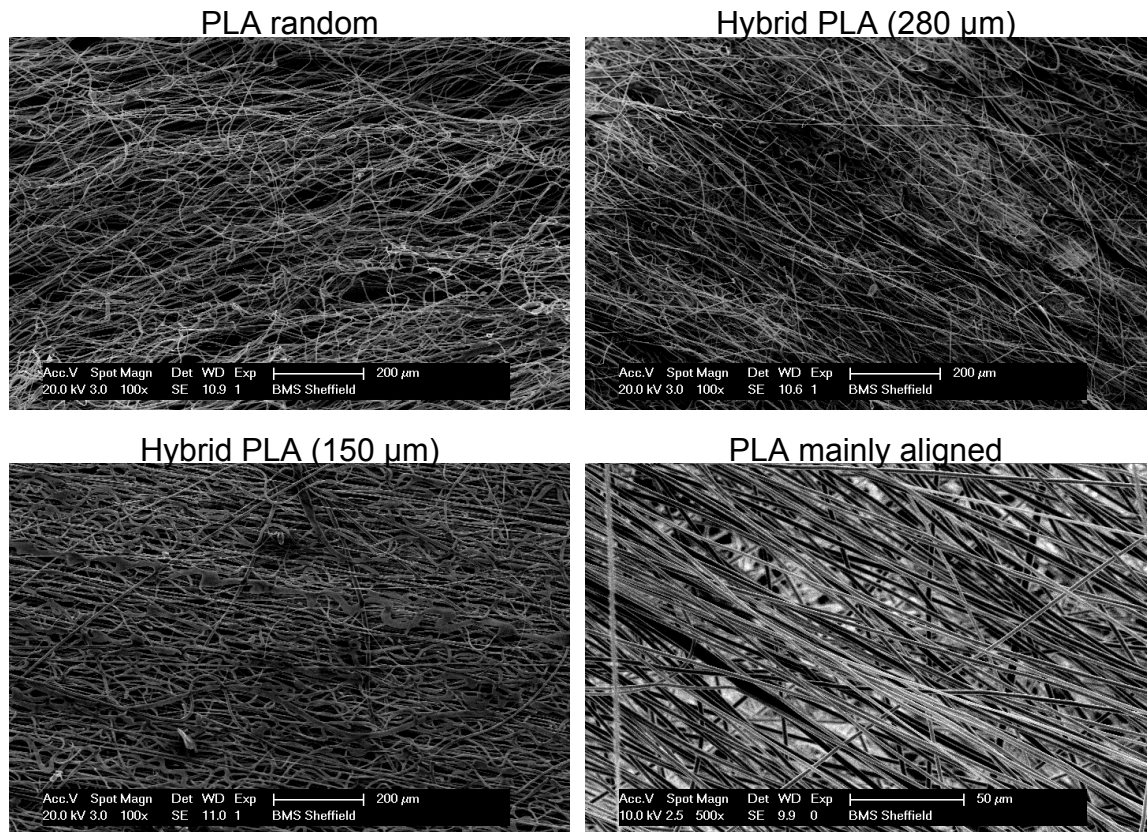


**Figure 7.2.7** Representative SEM images of PLA scaffolds with different fibre configurations.

### 7.3 Effect of different scaffold configurations on cell behaviour

To compare the performance of the cells on scaffolds with different fibre configurations, human ADSCs were seeded on Th-PLA random, hybrid PLA (280 µm) and PLA mainly aligned scaffolds, and were cultured for 2 weeks.

Scaffold preparation was performed as previously described in Chapter 2 of this thesis, but from this point of the project, we used samples of 1.5 x 1.5 cm seeded with  $5 \times 10^5$  ADSCs at passage 6 using metal rings with inner diameter of 1 cm (about  $6.3 \times 10^5$  cells seeded per  $\text{cm}^2$ ).

Metabolic activity of all samples at day 0, 7 and 14 was measured by AlamarBlue<sup>®</sup> staining and, after 14 days, total collagen production using Sirius red staining and mechanical properties using a BOSE tensiometer were also assessed for comparison of these scaffolds.

For PLA mainly aligned scaffolds immunostaining for f-actin, elastin and collagen I and III was performed to assess the distribution of the cells and the ECM components along the PLA fibres.

Metabolic activity was increased for all samples from day 0 to day 14; nevertheless, while cells on Th-PLA random scaffolds had a linear increment, cells on scaffolds containing aligned fibres had a small increment during the first week and a big increment during the second week reaching similar values compared to Th-PLA random scaffolds (figure 7.3.1).

This difference at day 7 was only significant between Th-PLA random and PLA mainly aligned scaffolds.

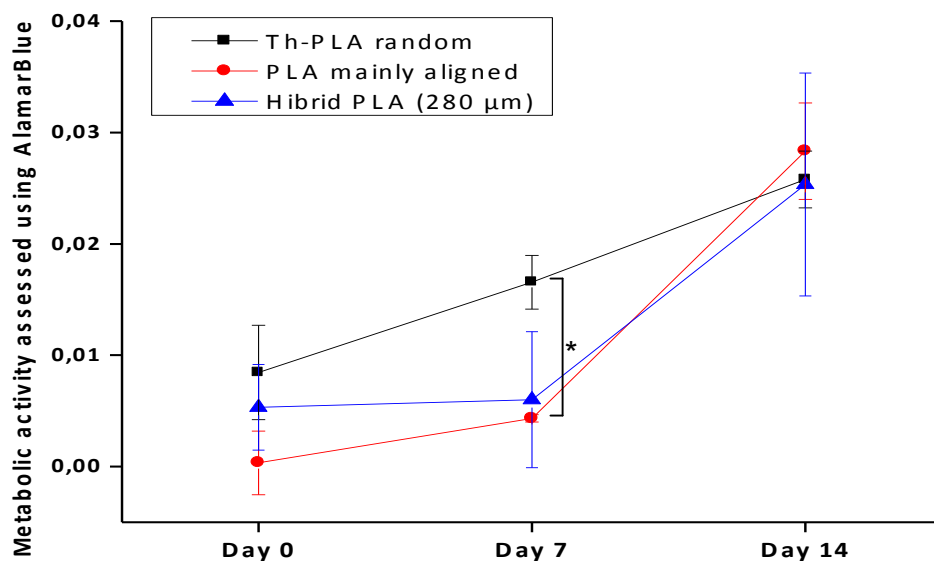


**Figure 7.3.1** AlamarBlue<sup>®</sup> staining for ADSCs on Th-PLA random, hybrid PLA (280 µm) and PLA mainly aligned scaffolds over 2 weeks in culture ( $n=3 \pm \text{SEM}$ ).  $*p < 0.05$ .

Sirius red staining of PLA mainly aligned scaffolds showed significantly higher production of total collagen compared to Th-PLA random scaffolds (figure 7.3.2).

Immunostaining for f-actin, one of the main components of the cytoskeleton, and for the different ECM components demonstrated an aligned distribution of the cells along the fibres of the PLA mainly aligned scaffolds producing the ECM components in an aligned manner too (figure 7.3.3).

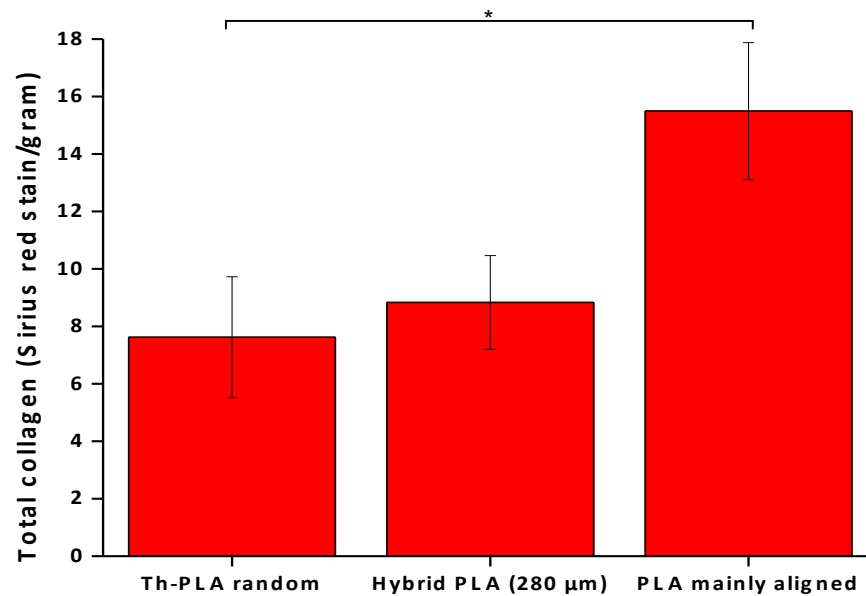


**Figure 7.3.2** Sirius red staining after 14 days of ADSCs cultured on Th-PLA random, hybrid PLA (280 µm) and PLA mainly aligned scaffolds. ( $n=3\pm\text{SEM}$ ).  $*p<0.05$ .

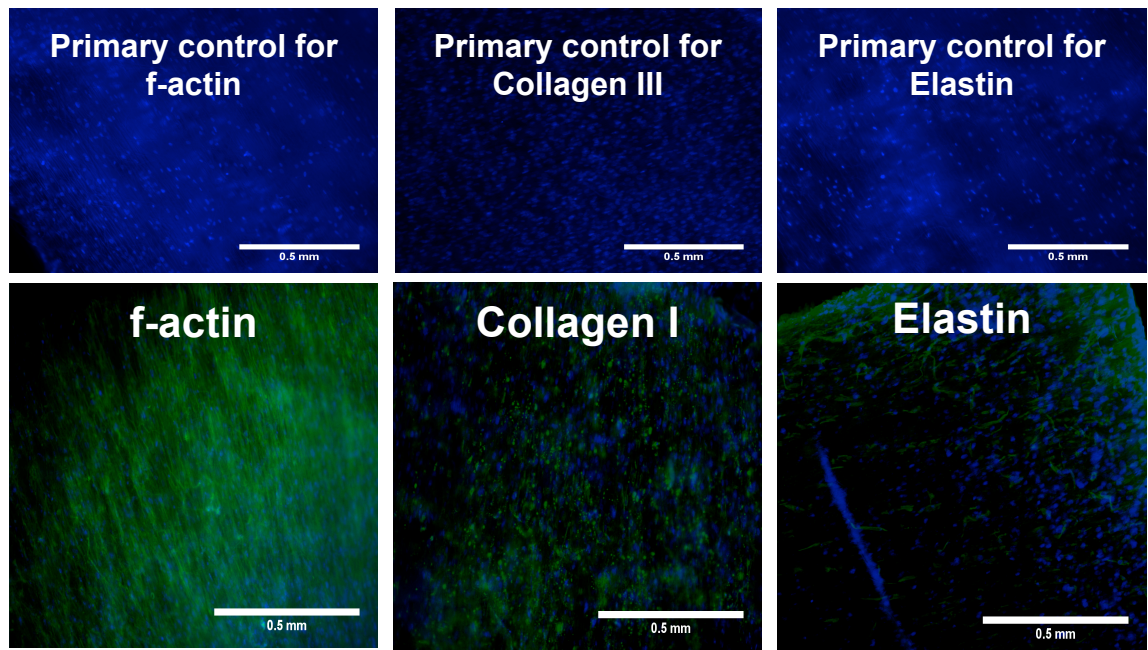


**Figure 7.3.3** Representative images of immunostaining for f-actin, collagen I and elastin of ADSCs cultured on PLA mainly aligned scaffolds for 2 weeks. Scale bar = 0.5 mm.

After 2 weeks in culture with or without ADSCs, mechanical properties of the 3 PLA scaffolds with different fibre configurations showed differences between them as already commented on in the previous section of this Chapter. PLA mainly aligned scaffolds were stiffer and stronger than the others but they snapped very quickly; whereas Th-PLA random scaffolds were the weakest, although they allowed more displacement before they span, and hybrid PLA (280  $\mu\text{m}$ ) scaffolds had values for these 3 mechanical properties between the other 2 materials (figure 7.3.4 and 7.3.5).

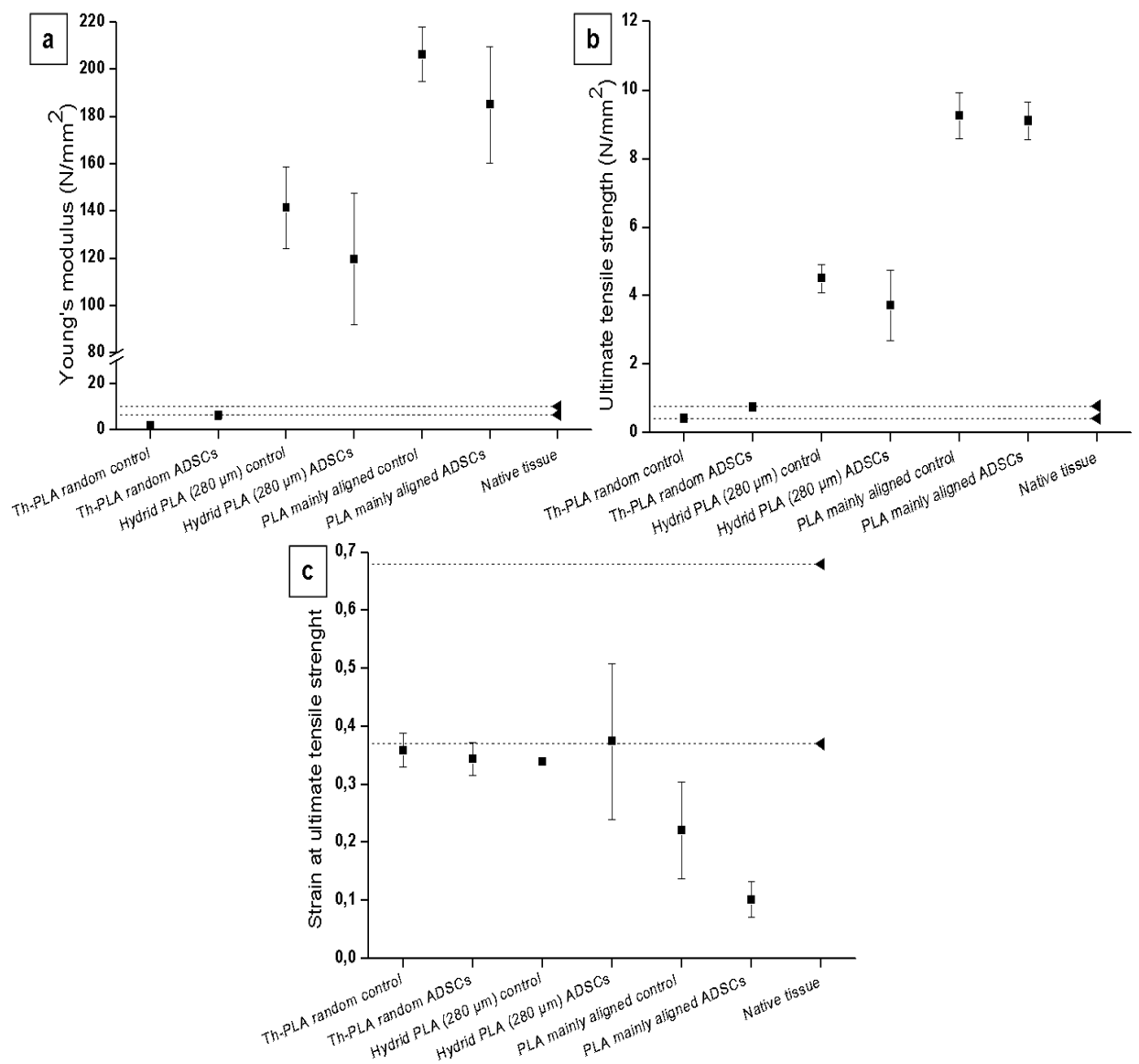


**Figure 7.3.4** Mechanical properties of Th-PLA random, hybrid PLA (280  $\mu\text{m}$ ) and PLA mainly aligned scaffolds cultured with ADSCs for 2 weeks. Results shown are mean $\pm$ SEM, ( $n = 3$ ). The last sample shown is the range for native tissue represented by 2 dashed lines (the range for native healthy paravaginal tissue).

Alternatively, when looking at the effect of the cells on the mechanical properties we can see that cell proliferation and ECM production did not modify the mechanical properties of the hybrid PLA (280  $\mu\text{m}$ ) and PLA mainly aligned scaffolds, compared with their respective controls (scaffolds cultured for 2 weeks in DMEM medium without cells); whereas mechanical properties of Th-PLA random scaffolds were increased after the culture of ADSCs as previously shown in Chapter 4 of this thesis (figure 7.3.4).

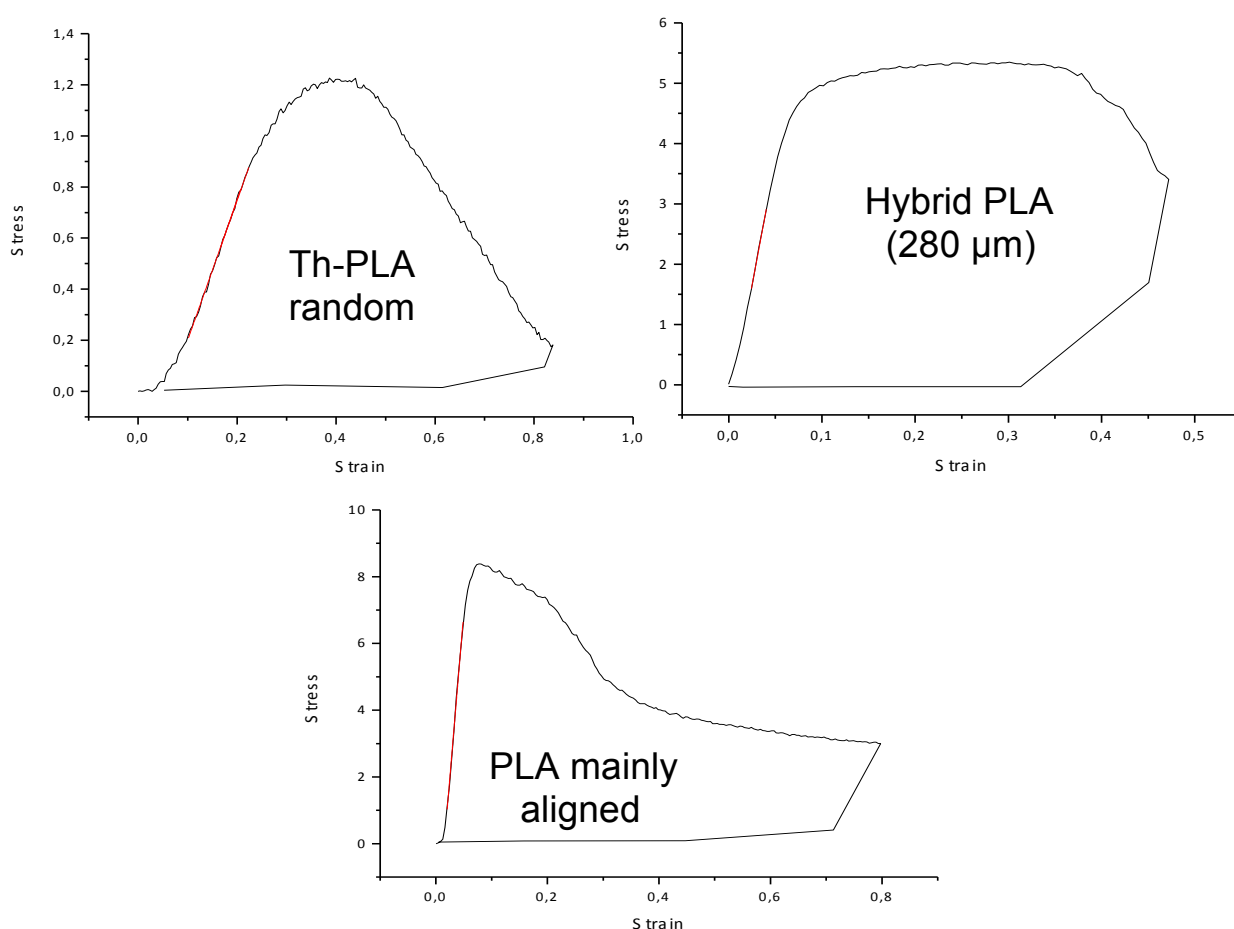


**Figure 7.3.5** Examples of stress-strain plots of Th-PLA random, hybrid PLA (280  $\mu\text{m}$ ) and PLA mainly aligned scaffolds cultured with ADSCs for 2 weeks.

## 7.4 Suture retention test, wettability and degradation

As previously mentioned, suturing PLA scaffolds with aligned fibres, needed for their clinical application, may be an issue.

To study this, a suture retention test using the BOSE tensiometer was performed for 5 of the 6 materials previously assessed in this Chapter.

Each material was cut to a length of 1 cm and a width of 0.5 cm. Then, a stainless steel wire of 0.20 mm of diameter (50 g, Scientific Wire Company, Essex, UK) was passed through a point 0.25 cm away from the top edge in the centre of the scaffold. Finally, each scaffold was clamped from the bottom 0.5 cm away from the edge, and the suture was clamped with the top grid with a gap between the 2 grids of 0.75 cm.

A ramp test of 0.1 mm/sec, same used to assess tensile properties of the scaffolds, was run on the direction of the aligned fibres. Then, the data was normalized by thickness of each scaffold and was plotted below, as N/mm, showing the maximum strength supported by each material before the suture slitted the scaffolds.

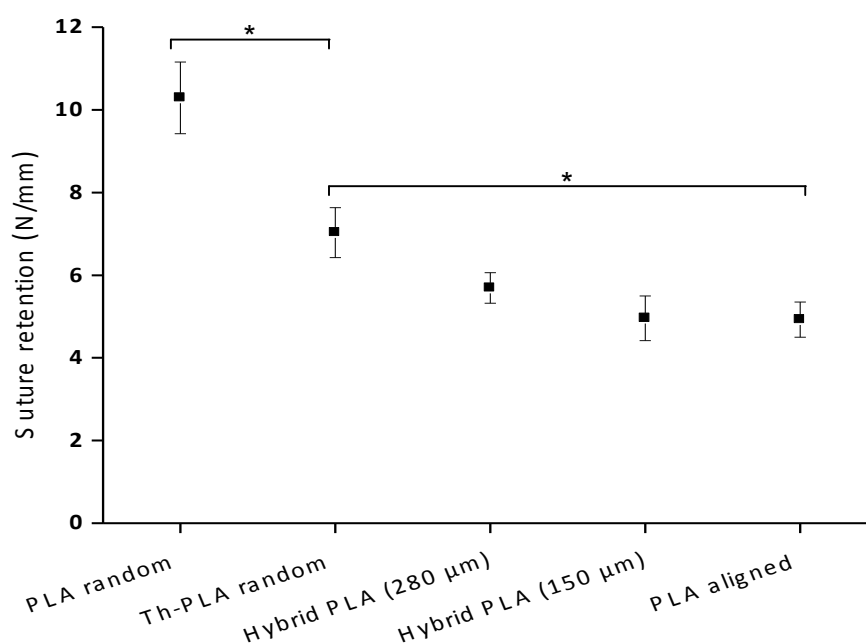


**Figure 7.4.1** Suture retention test of 5 different PLA fibre configuration scaffolds, mean $\pm$ SEM ( $n = 3$ ). \* $p < 0.05$ .

Non-thermoannealed PLA random scaffolds showed the highest strength before the material was slitted by the suture. This was significantly higher than Th-PLA random scaffolds. However, the suture retention strength of the latter was only significantly higher when compared to PLA aligned scaffolds.

Since PLA scaffolds are hydrophobic, we looked at the effects of increasing the wettability of the PLA fibres by using ethanol with the aim to increase the number of cells seeded on our samples.

Hybrid PLA (280  $\mu\text{m}$ ) scaffolds composed of a mixture of random and aligned fibres, were used to study this effect.

One day before cell seeding, half of the scaffolds were soaked in 70% ethanol for 3 seconds. Afterwards, these samples were 3 times washed with PBS and were kept wet until the cell seeding. The rest of the sample preparation and cell seeding was performed as previously described in the second section of this Chapter, obtaining cell-seeded scaffolds and scaffolds without cells (controls) for the non-alcohol treated group and the alcohol treated group, shown as “non-OH treated” and “OH treated” in figures, respectively.

Then, the metabolic activity of all samples from the 2 groups were measured at day 0, 7 and 14 by AlamarBlue<sup>®</sup> staining and, after 14 days, total collagen production using Sirius red staining and mechanical properties using a BOSE tensiometer were also assessed for comparison of these 2 groups.

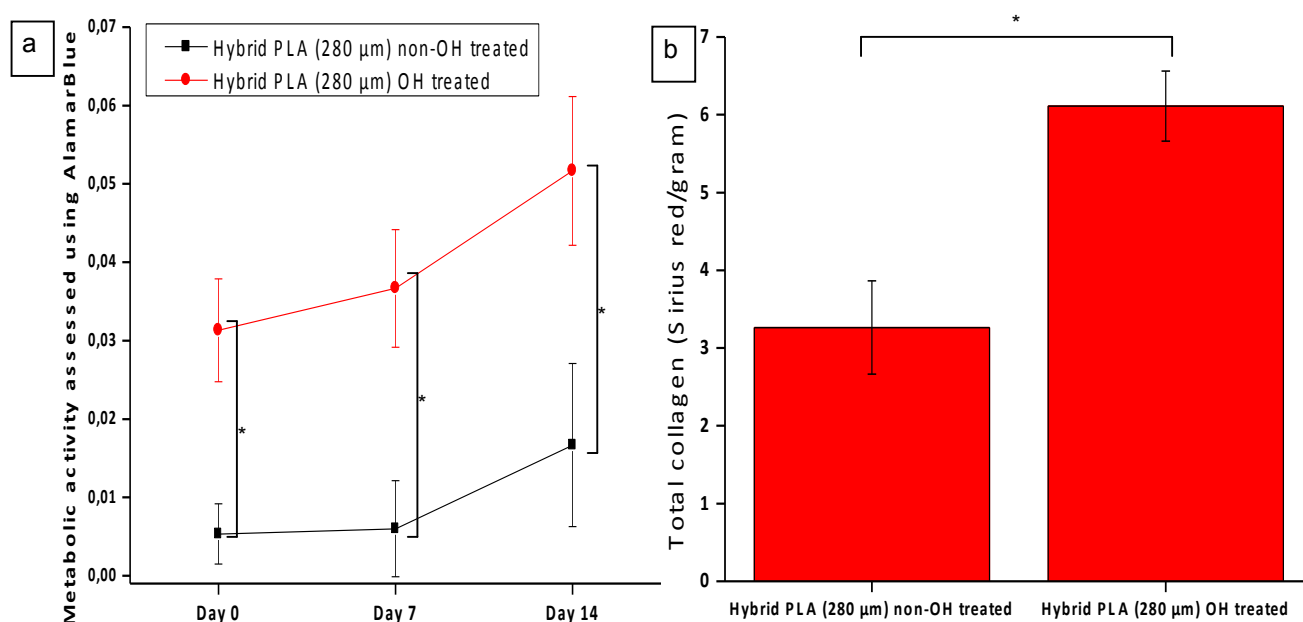


**Figure 7.4.2** (a) AlamarBlue<sup>®</sup> staining for ADSCs on hybrid PLA (280  $\mu\text{m}$ ) scaffolds treated and non-treated with 70% alcohol over 2 weeks in culture ( $n=3\pm\text{SEM}$ ).  $p<0.05$ . (b) Sirius red staining after 14 days of ADSCs cultured on hybrid PLA (280  $\mu\text{m}$ ) scaffolds ( $n=3\pm\text{SEM}$ ).  $*p<0.05$ .



Although ADSCs cultured on hybrid PLA (280  $\mu\text{m}$ ) scaffolds treated or non-treated previously with alcohol similarly increased their metabolic activity from day 0 to day 14 (figure 7.4.2a), the metabolic activity of the cells on the alcohol treated scaffolds was significantly higher from day 0 to day 14.

Total collagen production was also significantly higher for ADSCs cultured on alcohol treated scaffolds compared with the other group (figure 7.4.2b).

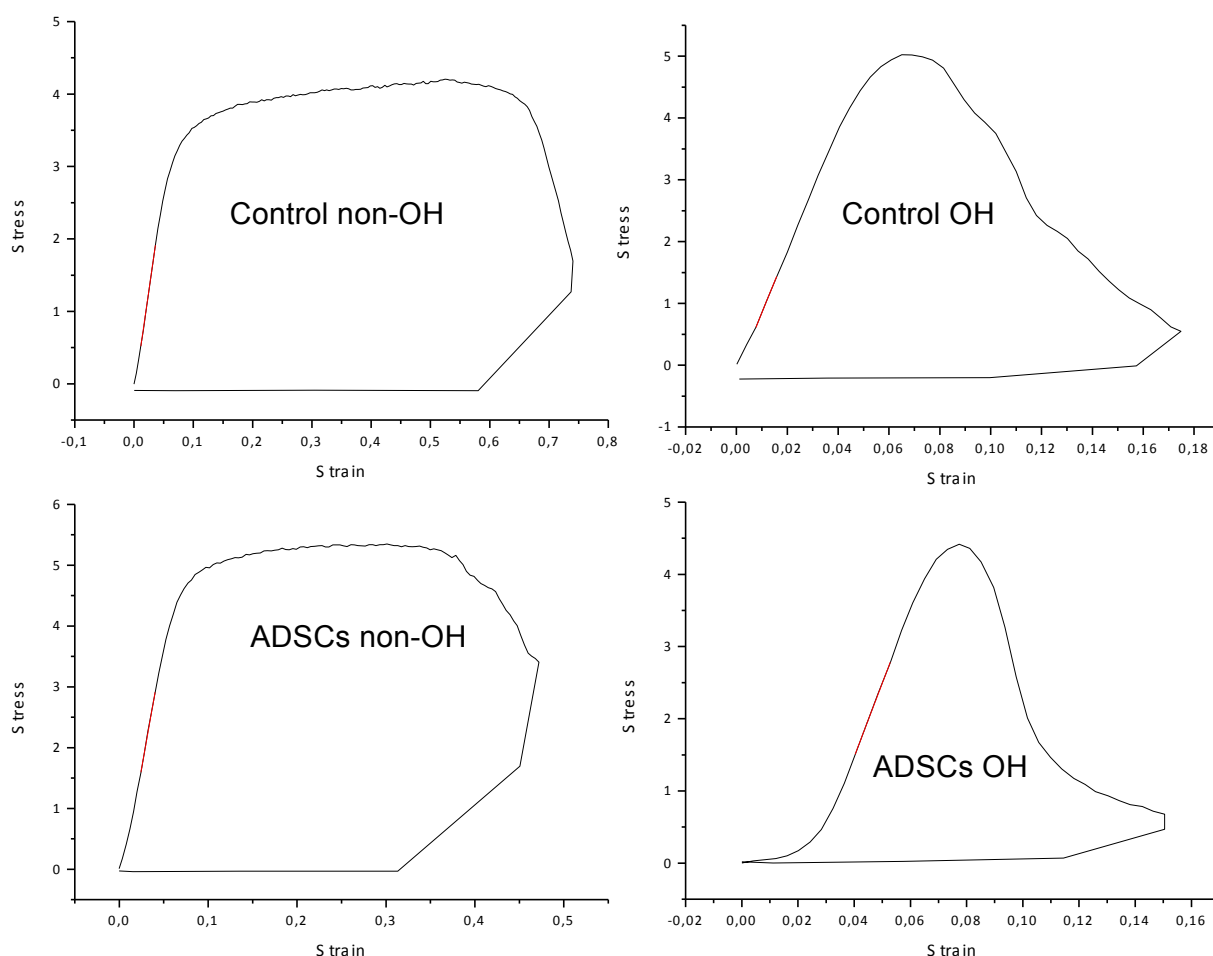


**Figure 7.4.3** Examples of stress-strain plots of hybrid PLA (280  $\mu\text{m}$ ) scaffolds cultured with and without ADSCs for 2 weeks, and previously treated or non-treated with alcohol.

Examples of stress-strain plots of hybrid PLA (280  $\mu\text{m}$ ), alcohol or non-alcohol treated, after 2 weeks in culture with or without ADSCs were next made (figure 7.4.3). There were no differences observed between samples cultured with or without cells. However, treating the scaffolds with alcohol significantly reduced the strain at the UTS compared

with the non-alcohol treated samples, although they maintained similar Young's modulus and the reduction of UTS observed was not significant (figure 7.4.4).

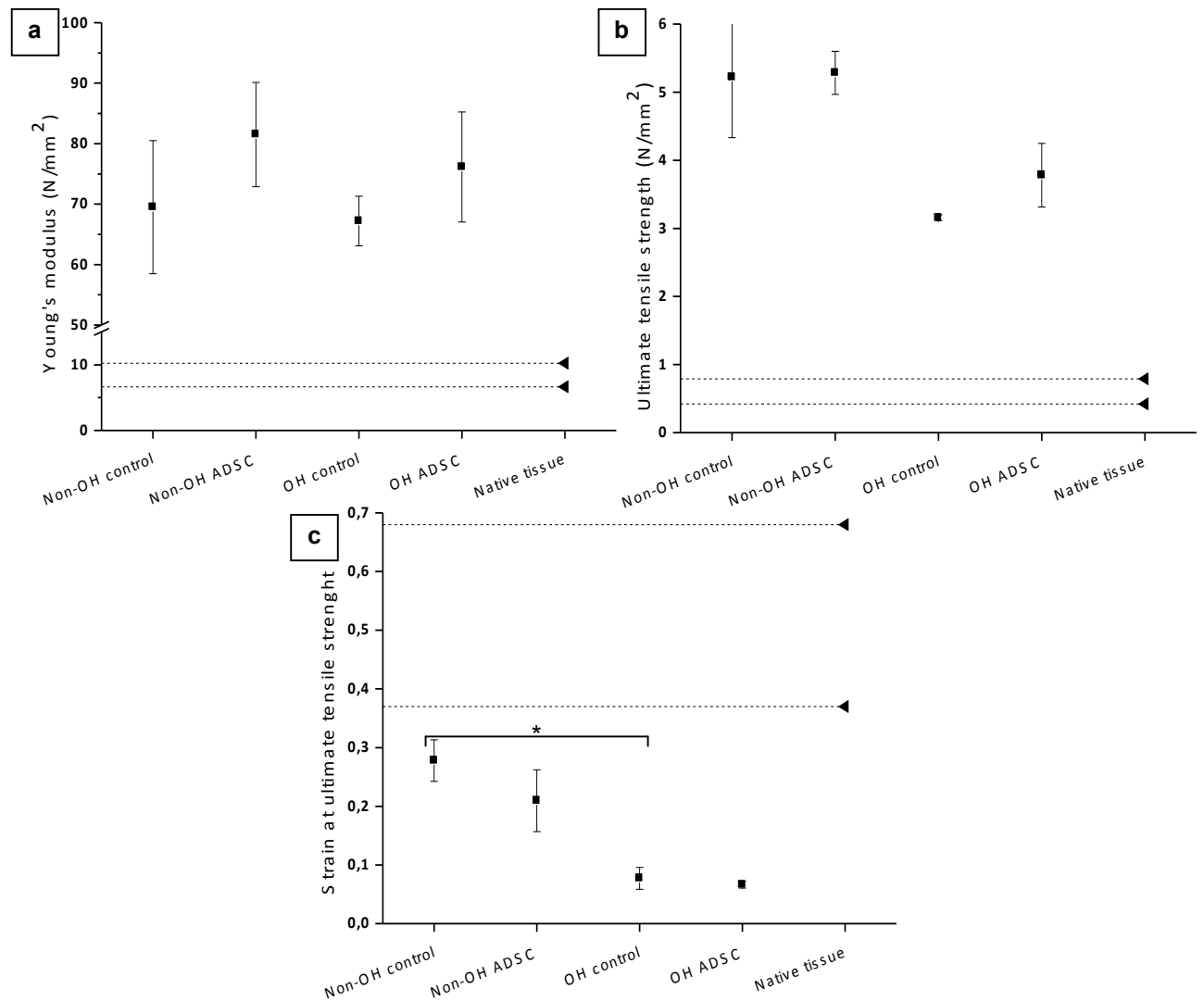


**Figure 7.4.4** Mechanical properties of hybrid PLA (280  $\mu\text{m}$ ) scaffolds cultured with ADSCs for 2 weeks, and previously treated or non-treated with alcohol. Results shown are means  $\pm$ SEM, ( $n = 3$ ). The last sample shown is the range for native tissue represented by 2 dashed lines (the range for native healthy paravaginal tissue). (c) Strain at UTS, \* $p < 0.01$ .

Since PLA scaffolds are degraded by hydrolysis, higher wettability may increase the degradation rate. Therefore, the degradation of scaffolds with different PLA fibre configurations was studied, as well as, the effect of increasing wettability on the degradation of the scaffolds.

To learn about this, Th-PLA random scaffolds and hybrid PLA (150  $\mu\text{m}$ ) scaffolds were cut to 1 cm x 0.5 cm and were soaked in PBS or 70% ethanol for 3 seconds. Then, these samples were kept in DMEM medium inside the incubator at 37°C up to 90 days. Mechanical properties of samples from the 2 different materials, treated and non-treated with alcohol, were tested at day 0, 14, 30 and 90.

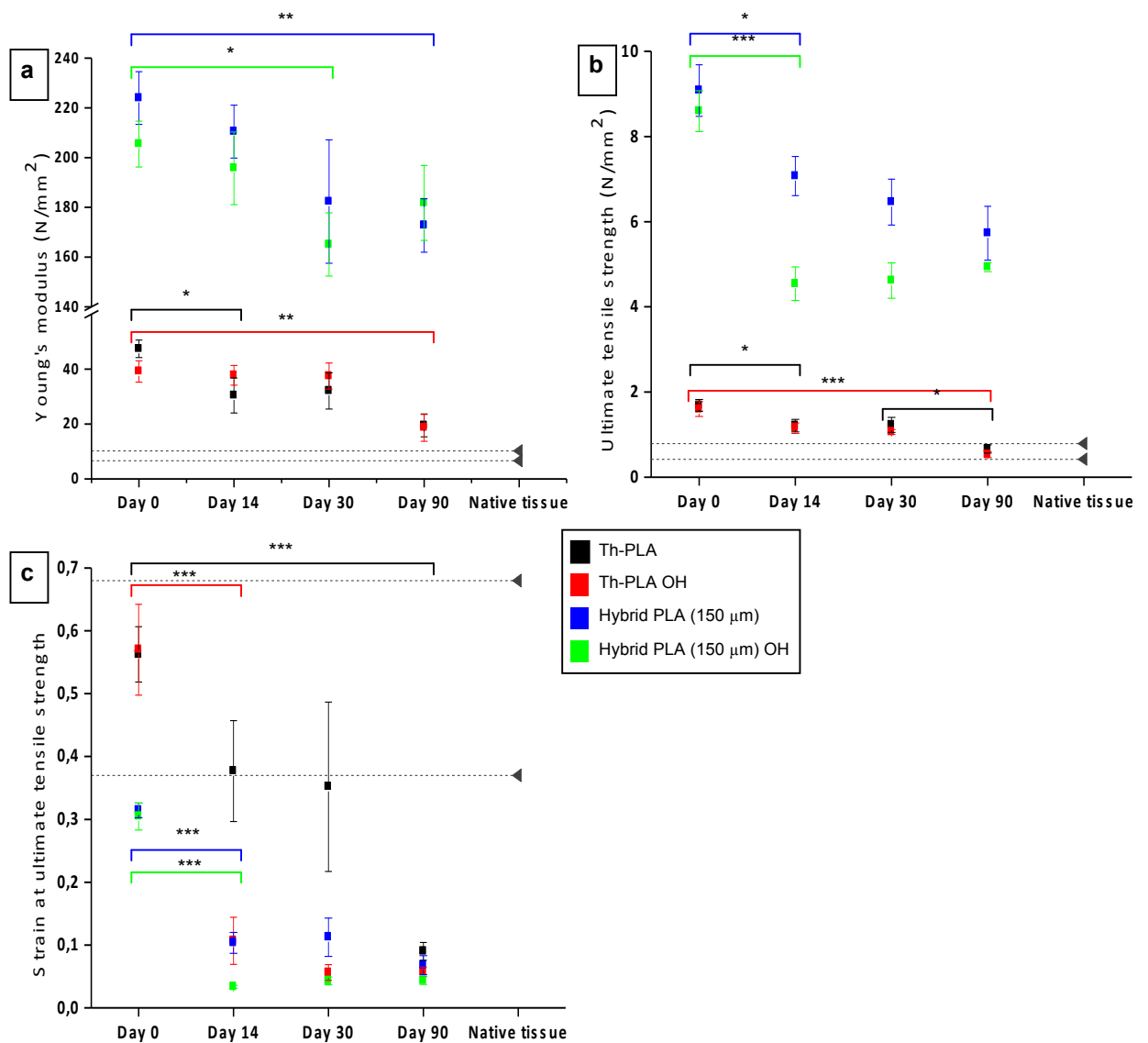


**Figure 7.4.5** Mechanical properties of Th-PLA random and hybrid PLA (150  $\mu\text{m}$ ) scaffolds, previously treated or non-treated with alcohol, at day 0, 14, 30 and 90 cultured in DMEM medium. Results shown are mean $\pm$ SEM, ( $n = 3$ ). The last sample shown is the range for native tissue represented by 2 dashed lines (the range for native healthy paravaginal tissue). (a) YM, \* $p < 0.05$ ; \*\* $p < 0.01$ . (b) UTS, \* $p < 0.05$ ; \*\*\* $p < 0.0005$ . (c) Strain at UTS, \*\*\* $p < 0.0001$ .

As already described in the second section of this Chapter, at day 0 non-alcohol treated scaffolds with a higher aligned fibre content (hybrid PLA (150  $\mu\text{m}$ ) scaffolds) were much stronger (higher UTS) and much stiffer (higher Young's modulus) than Th-PLA random scaffolds. In addition, these values of the mechanical properties of hybrid PLA (150  $\mu\text{m}$ ) scaffolds were also higher than those of native tissues. However, the hybrid scaffold snapped at a lower elongation than the Th-PLA random scaffolds, and values for this mechanical property were also below the values of the native tissues.

Looking at the mechanical properties of the 2 different scaffolds (figure 7.4.5; hybrid PLA (150  $\mu\text{m}$ ) scaffold = blue, and Th-PLA random scaffold = black) there was a small reduction in the UTS of the non-alcohol treated scaffolds by 2 weeks, but then no further reduction in the following 90 days.

The Young's modulus of Th-PLA random scaffolds was significantly reduced at 14 days, but was significantly reduced in hybrid PLA (150  $\mu\text{m}$ ) scaffolds after 30 days in culture. However, after this first small drop, Young's modulus was not significantly reduced any further by up to 90 days. In addition, UTS and Young's modulus for both materials were either above or within the range of values for native tissues for up to 90 days.

On the other hand, the main difference between both materials was in the strain at UTS which decreased significantly after 14 days for hybrid PLA (150  $\mu\text{m}$ ) scaffolds; while for Th-PLA random scaffolds this reduction only became significant at 90 days. After 14 days the hybrid scaffolds snapped with very minor elongation, and being lower than the values for native tissues, whereas this did not happen for the Th-PLA scaffolds until 90 days in culture.

The treatment of Th-PLA scaffolds with ethanol particularly affected the strain at UTS compared to same scaffolds without alcohol treatment. However, only the reduction in Young's modulus for hybrid PLA (150  $\mu\text{m}$ ) alcohol treated scaffolds was similarly affected over time compared with the non-alcohol group. UTS and strain at UTS were significantly reduced after 14 days, although the latter mechanical property was also significantly reduced after 14 days for both groups and under the values for native tissues. In contrast, the UTS of the alcohol treated hybrid PLA (150  $\mu\text{m}$ ) was always above the native tissue values for up to 90 days.

## 7.5 Discussion

We have demonstrated that using the electrospinning technique we can develop a range of materials using one polymer but with different fibre configurations which modulate the mechanical properties of the resulting scaffold, as well as influencing the behaviour of cells cultured on the scaffold.

This was studied in terms of how to modulate the mechanical properties of the scaffolds. We did not compare the mechanical properties of our scaffolds to those of current clinical materials as we previously demonstrated that there is no simple correlation between the mechanical properties and clinical outcome with different materials. Certainly, the host response to the scaffold may be just as important as mechanical properties in determining the clinical success of our materials.

We initially aimed to make a material stronger than native tissue, as a biodegradable scaffold may breakdown and weaken, resulting in early failure of the material

We showed we could make a range of PLA scaffolds made of 100% random fibres to scaffolds with different ratios of random to aligned fibres and to completely aligned PLA scaffolds.

Scaffolds with more random fibres had a lower bulk density due to more porosity within them, whereas, scaffolds with aligned fibres had a higher bulk density as the PLA fibres are organized to more efficiently occupy space, leaving less space between fibres.

The effect on mechanical properties was very clear, leading to scaffolds that were very strong and stiff when a higher content of aligned fibres was present but, on the other hand, scaffolds with a higher content of random fibres allowed more elongation before snapping.

Therefore, weak materials may fail due to elevated forces applied in the pelvic floor while strong, stiff materials such as the current non-degradable clinical material PPL may not snap, but they may lead to a chronic inflammatory response, pain and/or erosion through the vaginal tissues.

It is known that scaffold porosity and pore size plays a significant role in allowing cell infiltration and nutrient diffusion (526). We showed that ADSCs grew well on scaffolds with aligned fibres which influenced the distribution of the cells on the fibres and the

ECM produced. In addition, cells on aligned scaffolds produced greater amounts of total collagen. Collagen is strong under tension and its organisation ultimately determines the mechanical properties of the native tissue.

It has been shown previously that the alignment of fibroblasts controls the orientation of the collagen produced (527). Other groups have shown that elongated human ligament fibroblasts seeded on aligned nanofibres were orientated in the fibre direction (528). These cells also produced significantly more collagen (orientated in the fibre direction) compared to cells on random fibres.

However, this increased production and orientation of the ECM observed in our PLA mainly aligned scaffolds did not have any noticeable effect on the mechanical properties of scaffolds which were already very strong and stiff. Collagen production did slightly increase the mechanical properties of Th-PLA random scaffolds but it was shown that most of the mechanical properties were attributable to the material itself.

Finally, we looked at other important issues such as suture retention, wettability of the scaffolds, and their degradation rate *in vitro*.

Tension-free sutureless suburethral slings were introduced for the treatment of SUI based on their good results in hernia repair (529). This approach showed better outcomes than suturing the same materials since they avoid complications such as voiding obstruction (530). These slings allow an initial small degree of movement to be achieved avoiding excessive suburethral support/pressure. The whole sling is ultimately fibrosed being integrated into native tissues, a fact that makes difficult to remove these slings if a second surgical procedure is needed, due to recurrence of SUI, worsening the situation by further damage of supportive tissues.

After this surgical procedure, patients may resume most normal activities within 1 to 2 weeks and are advised to refrain from driving for 2 weeks, and from sexual intercourse and other strenuous activities for 6 weeks. For POP reconstruction however, sutures are needed for these much bigger meshes.

There are no standardized protocols in the literature for performing a suture retention test; however, we believe that the method used here proved that PLA-random scaffolds had higher strength in retaining a suture compared to aligned scaffolds. On the other hand, this difference was only slightly significant when comparing Th-PLA random and aligned PLA scaffolds.

As expected, we showed that increasing the wettability of the PLA fibres by pre-soaking fibres in alcohol (ethanol) increased the number of seeded ADSCs which attached to hybrid PLA (280  $\mu\text{m}$ ) scaffolds, shown by a higher metabolic activity measurement, and higher collagen production after 14 days culture. However, ethanol pre-treatment also increases the *in vitro* degradation rate of the scaffolds. In addition, previous work (385) and these experiments (as discussed shortly) show that ethanol pre-treatment adversely affects the mechanical properties of the scaffolds.

Th-PLA random scaffolds were chosen as a representative material made by random fibres, while, hybrid PLA (150  $\mu\text{m}$ ) scaffolds were representative of scaffolds with a higher content of aligned fibres.

*In vitro* degradation experiments with these 2 materials showed a reduction of all mechanical properties after 90 days, although this was principally observed for the strain at UTS. Furthermore, this drop appeared to be accelerated in scaffolds with a high content of aligned fibres. Young's modulus and UTS of both materials were reduced after 90 days of culture but were always above the range of values for native tissues.

Alcohol treatment accelerated the reduction of the strain at UTS for both materials, and accelerated up the decrease of UTS of scaffolds with a higher content of aligned fibres; alternatively, the UTS of these scaffolds treated with alcohol were always above the values for native tissues.

From cell testing experiments, hybrid PLA (280  $\mu\text{m}$ ) scaffolds did not show any reduction in mechanical properties from day 0 (figure 7.2.6) to day 14 (figure 7.4.4). Only after alcohol treatment was the strain at UTS of this scaffold reduced at 14 days and being lower than values for native tissues (figure 7.4.4). Since mechanical properties of hybrid PLA (280  $\mu\text{m}$ ) scaffolds, treated with and without alcohol, were similarly affected over the time in culture than Th-PLA random scaffolds, theoretically, this hybrid scaffold may be composed by higher amount of random fibres.

Living tissues have the ability to retain stretch with repetitive strain. An elastic material can return to its original shape when a force or load is removed. However, if residual deformation is present then it is recognised as plasticity. Most biologic materials will exhibit a mixture of these properties (512), which are determined by the interactions between collagen, elastin, proteoglycans, and water within the tissue. Therefore, while after an initial force the material is able to return to its original size, after a higher

amount of force the material starts to be plastically deformed and will not return to its original shape.

These behaviours are important to adapt mechanical properties to different biological situations such as during parturition when the pelvic stretch ratio in the pelvic muscles can reach 3.26 (436).

Women with POP have been shown to have less elastic tissue which snaps at lower stress and strain than those without POP. In addition, while UTS was reduced in vaginal tissues of women with prolapse and in postmenopausal women too, the Young's modulus was increased.

A variety of tests can be performed (531) to test the viscoelasticity of the material such as cyclical loading. The extent of stress supported by the pelvic floor is an important issue to consider (436). As already described in Chapter 5, since the average area of the female pelvis was found to be 94 cm<sup>2</sup> (435), the load on the pelvis was measured as being 19N in the supine position, which rises to 37N in the standing position and reaches 129N on coughing. Therefore testing to failure, usually to a level much higher than this, is thought not to be required, and more importantly should not be used for comparison between tissues. In addition, at present there is still data lacking on the uniaxial testing properties of vaginal tissue and on more complicated biaxial testing which may need to be developed later, as well as, cyclical loading.

Similarly, the strains that the different tissues of the pelvic floor undergo have not been well studied and established. In addition, these strains can be much higher or lower in different situations such as during bowel opening, voiding, intercourse and pregnancy. Therefore, we do not know which strains our material needs to cope with.

In conclusion, we do not know which scaffold with a particular PLA fibre configuration may be the most appropriate to develop our best TERM candidate.

We can develop weaker materials allowing some degree of elastic deformation (PLA and Th-PLA random scaffolds) or we can make very strong and stiff materials which do not allow any elastic deformation.

An intermediate material, such as a hybrid PLA (280 µm) scaffold, which has shown good results for metabolic activity and collagen production may be our anticipated candidate. However, only long-term animal experiments will determine how *in vivo*



degradation and neo-tissue formation affect the mechanical properties of these materials for a long-term repair of the pelvic floor tissues when treating SUI or POP.

## **Chapter 8**

# **EXPLORING METHODOLOGIES OF EXTRACTING AND CULTURING ADSCs**

## 8.1 Introduction

Human MSCs have been shown to have limited proliferative potential *in vitro* due to replicative senescence (532, 533). This is a problem with practical implications since cells need to be expanded for a tissue engineering approach. In addition, these cells in culture can lose their phenotypic characteristics and differentiation potential, which, at the same time, can be slightly different between patients (534, 535). Also, different subpopulations of MSCs isolated from the same tissue can present heterogeneity (536).

The number of passages and the age of the donor have been shown to affect the differentiation potential of BMDSCs leading to donor variability (537, 538). However, other groups have shown that these cells can be cryopreserved and retain differentiation potential after being resurrected up to 15 passages (539).

On the other hand, ADSCs and MSCs isolated from the umbilical cord present higher proliferative ability and differentiation potential than BMDSCs when evaluating their senescence, although both have similar phenotypes and gene expression profiles compared to BMDSCs (540, 541). Donor age and the number of passages also have an effect on the “stemness” of these cells too (542).

It has been suggested that the “stemness” of MSCs can be maintained *in vitro* for long-term when these cells are cultured from explants of the tissues containing these cells, suggesting that the corresponding tissue provides a microenvironment which is essential for keeping MSCs in a stem cell-like state (543).

Other people have also shown the relevance of other conditions such as the culture medium and culture parameters during the isolation of MSCs for better preservation of the proliferative ability and “stemness” (544, 545). It has been shown that initial seeding at very low density of these cells may decrease their proliferative kinetics; although, it does not affect their differentiation potential. On the other hand, it is reported that it is better to passage these cells before they reach a high confluence to keep a high proliferative capacity (546).

To avoid the issues related to senescence and loss of “stemness” of these cells when expanding them, we used new technology from Miltenyi Biotech Company to purify

and enrich ADSCs isolated from fat tissue. This includes faster disaggregation of the tissue and rapid separation of the desired cell population. The devices could be installed inside the theatre to isolate the patient's cells under sterile conditions. This procedure offers the potential to extract ADSCs from lipoaspirate to provide clinically relevant numbers of cells ready to be seeded on the scaffolds and implanted in the patient during the same operation or on the same day. In addition, this approach may avoid some of the regulations concerning the use of cultured cells since these rapidly extracted cells do not need to leave the theatre.

For all these reasons, we decided to compare in this Chapter the potential of ADSCs from different donors and at different passages to develop our TERMS.

We also compared the ability of the cells isolated with this new technology to proliferate and their differentiation potential. We also compared them to cells isolated using the conventional method for their potential to develop a TERM.

Finally, we also looked at the potential of seeding the SVF isolated from adipose tissue directly onto the scaffolds. As previously described, the SVF contain other cell types such as fibroblasts and endothelial cells, which actually may be useful for developing a TERM, as an autologous approach.

## **8.2 Donor variability**

ADSCs were isolated as described in Chapter 2 of this thesis from 3 different donors. These cells were expanded and their differentiation potential was assessed after culture in adipogenic and osteogenic medium, as described in Chapter 2. Batches of cells 1 and 3 were tested at passage 6 and batch 2 was assessed at passage 3.

ADSCs from the 3 batches were positively stained for Oil red O (specific for lipid vesicles) and Alizarin red (specific for calcium deposition) after being cultured for 3 weeks with adipogenic and osteogenic medium respectively (figure 8.2.1). All cells cultured with DMEM medium were slightly stained for Alizarin red, being lower for cells at passage 3 (batch 2); however, the stain of ADSCs cultured with osteogenic medium was similar for all batches and much higher than the controls.

More ADSCs at passage 3 (batch 2) were clearly differentiated into adipocytes by lipid vesicle formation compared with cells at passage 6 (batches 1 and 3).

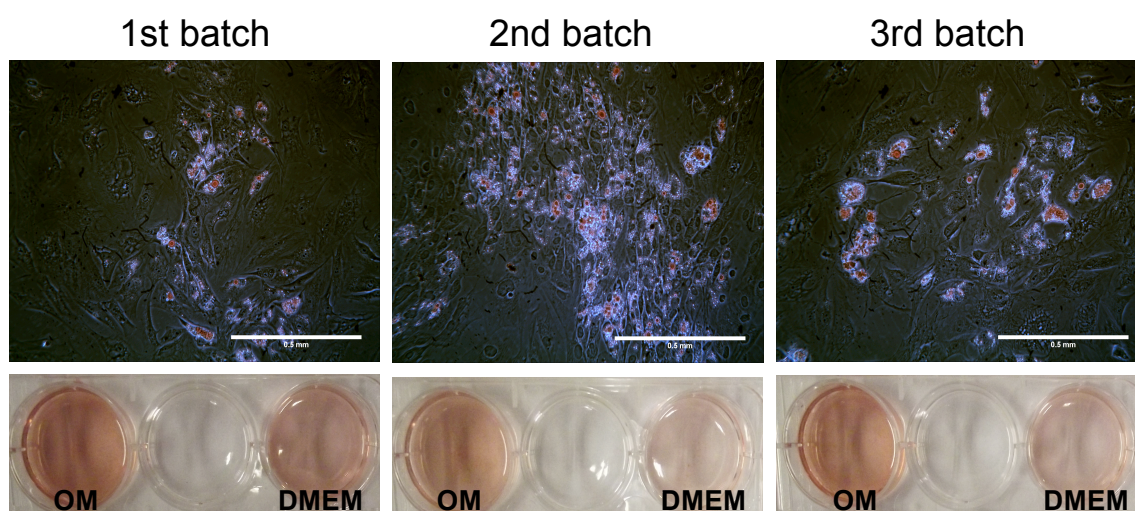


**Figure 8.2.1** Top images: Human ADSCs isolated from 3 donors cultured for 3 weeks with adipogenic medium and stained with 0.3% Oil Red O. Scale bar = 0.5 mm. Bottom images: Human ADSCs isolated from 3 donors cultured for 3 weeks with osteogenic medium (OM) or DMEM medium (for controls) and stained with 5% Alizarin red.

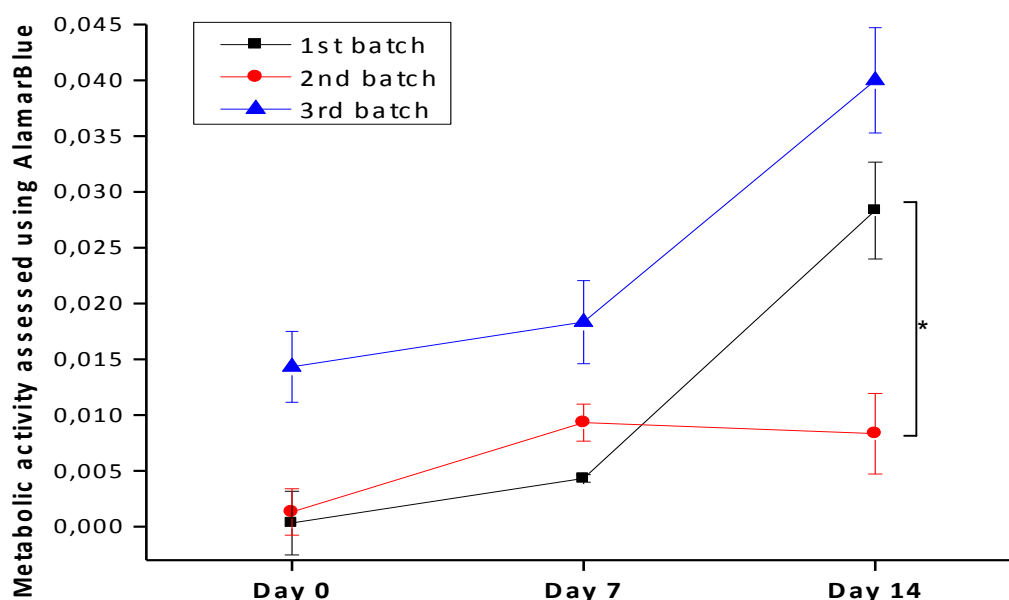


**Figure 8.2.2** AlamarBlue® staining for ADSCs isolated from 3 donors on PLA mainly aligned scaffolds over 2 weeks in culture ( $n=3\pm SEM$ ).  $*p<0.05$ .

Thereafter, the cells from the 3 batches were seeded in different scaffolds. For this, PLA aligned samples were prepared as previously described in a previous Chapter of this

thesis, and  $5 \times 10^5$  ADSCs from each batch were seeded on 1.5 x 1.5 cm scaffolds using metal rings with an internal diameter of 1 cm. In addition, these cells were seeded at passage 6 for batches 1 and 3, and at passage 3 for batch 2. All samples were then cultured for 2 weeks with DMEM medium.

Metabolic activity of all samples was measured at day 0, 7 and 14 by AlamarBlue<sup>®</sup> staining. After 14 days, samples were stained with DAPI to look at the cell density, and total collagen production was measured using Sirius red staining for comparison of the 3 different batches of ADSCs. Furthermore, for scaffolds seeded with cells from batch 2, immunostaining for collagen I and III, and elastin was performed to assess the potential of ADSCs at passage 3 to produce the different ECM components.

Metabolic activity measured by AlamarBlue<sup>®</sup> staining showed a very similar behaviour of cells at passage 6 without differences between the 2 batches, increasing their metabolic activity from day 0 to day 14 (figure 8.2.2). However, ADSCs at passage 3 did not increase their metabolic activity after the first week showing a significant difference in their metabolic activity at day 14 compared with the other 2 batches.

Looking at DAPI staining after 2 weeks culture, all samples were populated in a confluent manner by cells from the 3 different batches, without any visible difference between them (figure 8.2.3).

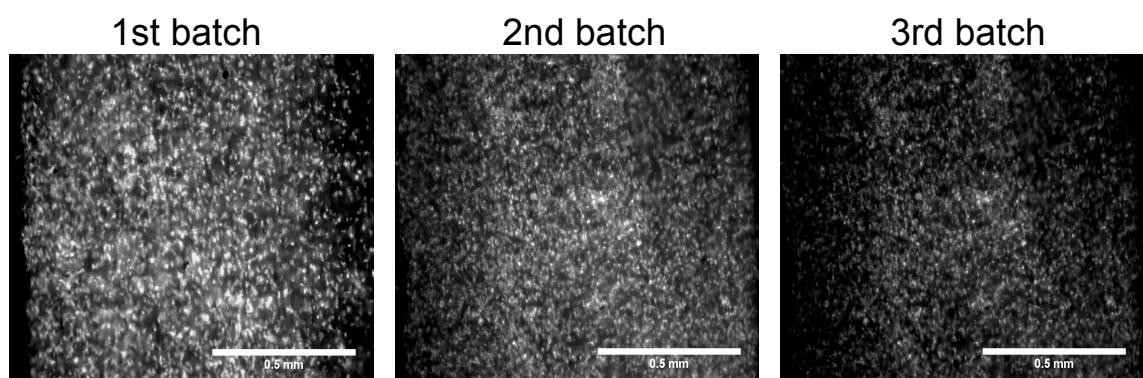


**Figure 8.2.3** Representative images of DAPI staining for PLA aligned samples cultured with ADSCs from 3 different donors for 2 weeks. Scale bar = 0.5 mm.

Sirius red staining did not show any difference in terms of total collagen production between the 3 batches of cells and, therefore, without differences in total collagen

production between ADSCs at passage 3 and 6 when cultured on PLA scaffolds (figure 8.2.4).

Furthermore, as seen by immunostaining (figure 8.2.5), ADSCs at passage 3 were able to produce the different ECM components which have been already shown in this thesis to be produced by ADSCs at passage 6.

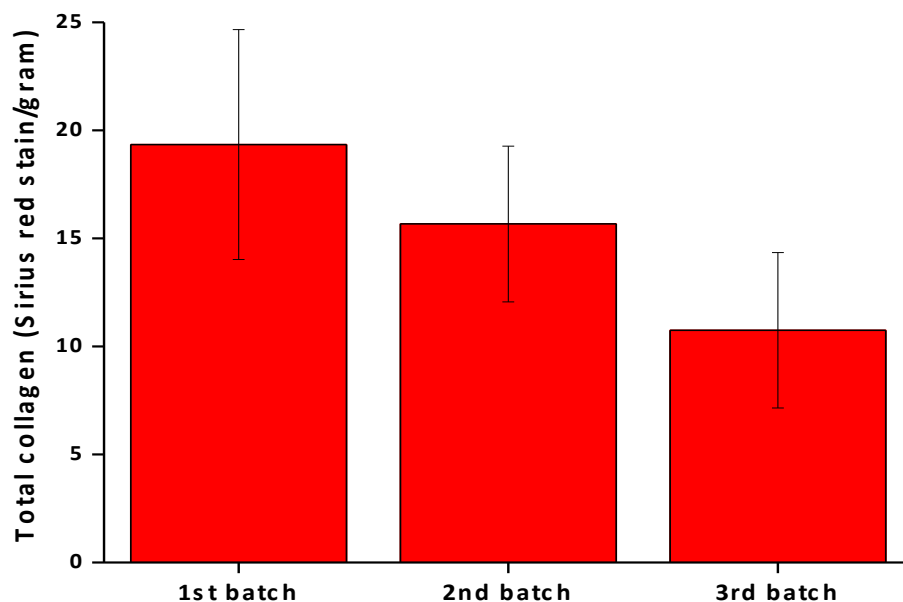


**Figure 8.2.4** Sirius red staining after 14 days of ADSCs from 3 donors cultured on PLA mainly aligned scaffolds. ( $n=3 \pm \text{SEM}$ ).

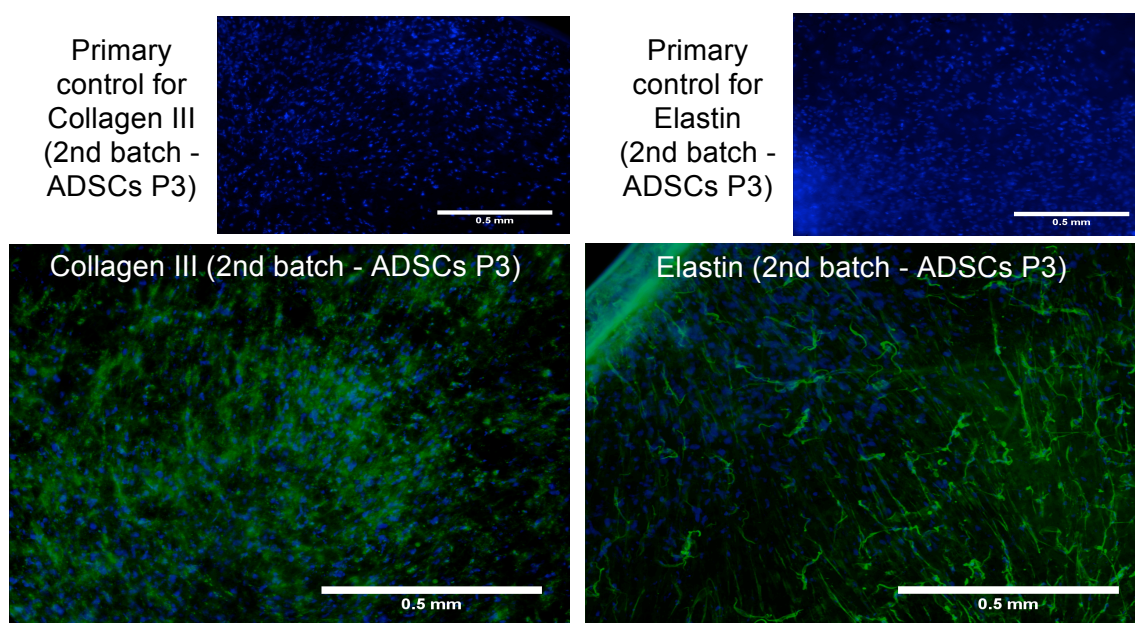


**Figure 8.2.5** Representative images of immunostaining for collagen III and elastin of ADSCs at passage 3 cultured on PLA mainly aligned scaffolds for 2 weeks. Scale bar = 0.5 mm.

### **8.3 One stage “in theatre” approach**

New technology developed by Miltenyi Biotech was assessed for rapid separation of a clinical relevant number of ADSCs which could be seeded on a scaffold and implanted in a one day operation. Similarly, the SVF isolated from adipose tissue was seeded on scaffolds with the aim of developing a TERM avoiding cell expansion.

#### **8.3.1 Rapid ADSCs isolation**

ADSCs were isolated using a GentleMACS<sup>®</sup> Dissociator from Miltenyi Biotech, as described in Chapter 2 of this thesis, and using 2 different speeds (defined GentleMACS Programs which were called “gentle” and “high” speed). ADSCs were also isolated from the same donor using the conventional method (termed as “hand minced”), also described in the second Chapter, for comparison.

We also studied the need for using collagenase and the period of incubation with this enzyme to isolate ADSCs; therefore, we had the following groups:

- High speed, 0.1% collagenase, 45 min incubation.
- High speed, 0.1% collagenase, 15 min incubation.
- High speed, 0.05% collagenase, 45 min incubation.
- High speed, 0.05% collagenase, 15 min incubation.
- High speed, no collagenase.
- Gentle speed, 0.1% collagenase, 45 min incubation.
- Gentle speed, 0.1% collagenase, 15 min incubation.
- Gentle speed, 0.05% collagenase, 45 min incubation.
- Gentle speed, 0.05% collagenase, 15 min incubation.
- Gentle speed, no collagenase.
- Hand minced, 0.1% collagenase, 45 min incubation.
- Hand minced, 0.1% collagenase, 15 min incubation.
- Hand minced, 0.05% collagenase, 45 min incubation.
- Hand minced, 0.05% collagenase, 15 min incubation.
- Hand minced, no collagenase.



10 mL of subcutaneous fat, the same amount previously used for all ADSC isolations in this project, were used for each one of the groups above to isolate ADSCs. All extracted cells from different groups were seeded in individual T25 plastic culture flasks.

When collagenase was not used no cells attached to the flask. Some cells were attached for all of the other groups; however, only from 3 groups were there enough cells to proliferate to confluence for a first passage (figure 8.3.1).

The gentle speed did not work for any group. For high speed and hand minced, only when using 0.1% of collagenase incubated with the fat tissue for 45 min could we expand cells and obtain a confluent population of cells after 1 week from a T25 flask, as previously seen.

Cells isolated using the hand minced procedure, using 0.05% collagenase for 45 min incubation, achieved a confluent population after more than 2 weeks in culture. However, these cells were not used for further experiments as they may have lost proliferative potential due to their length of culture at low density.

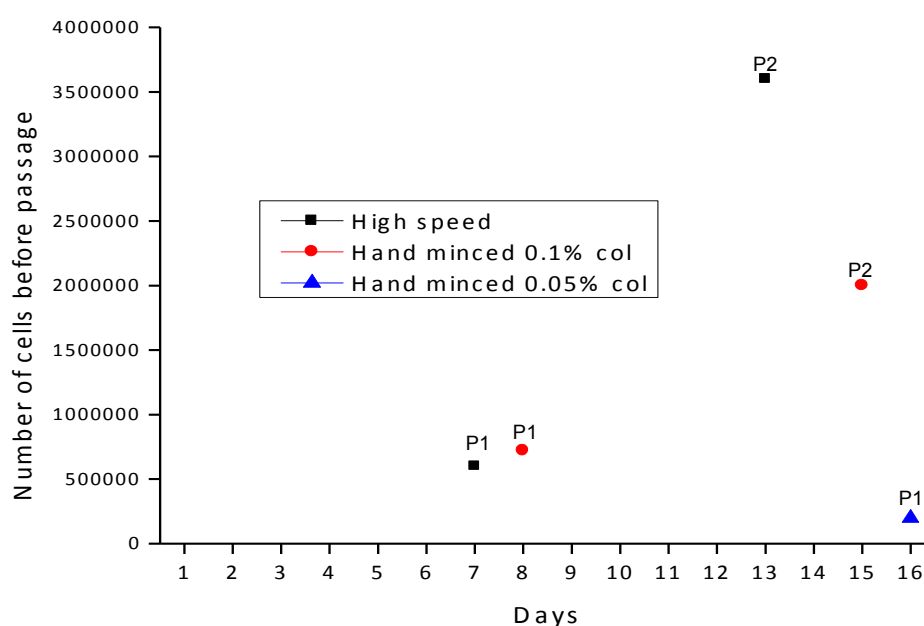


**Figure 8.3.1** Day of passage and number of cells counted in each passage since the isolation of ADSCs using high speed (0.1% collagenase, 45 min incubation) and hand minced (0.1% and 0.05% collagenase, 45 min incubation) methods. P1 = passage 1; P2 = passage 2; col = collagenase.

At passage 3 and 6, ADSCs isolated by high speed and hand minced methods (0.1% collagenase, 45 min incubation) were assessed for differentiation assays by culture of these cells in adipogenic and osteogenic medium.

ADSCs isolated by both methods, and at passage 3 and 6, were positively stained for Oil red O (specific for lipid vesicles) and Alizarin red (specific for calcium deposition) after being cultured for 3 weeks with adipogenic and osteogenic medium respectively (figure 8.3.2). All controls, cells cultured with DMEM medium, stained slightly for Alizarin red; however, the stain of ADSCs isolated by both methods and cultured with osteogenic medium was much higher than the controls, particularly at passage 3.

Similarly, cells at passage 3 isolated by both methods had higher potential to differentiate into adipocytes with more cells showing lipid vesicles formation compared with cells at passage 6.

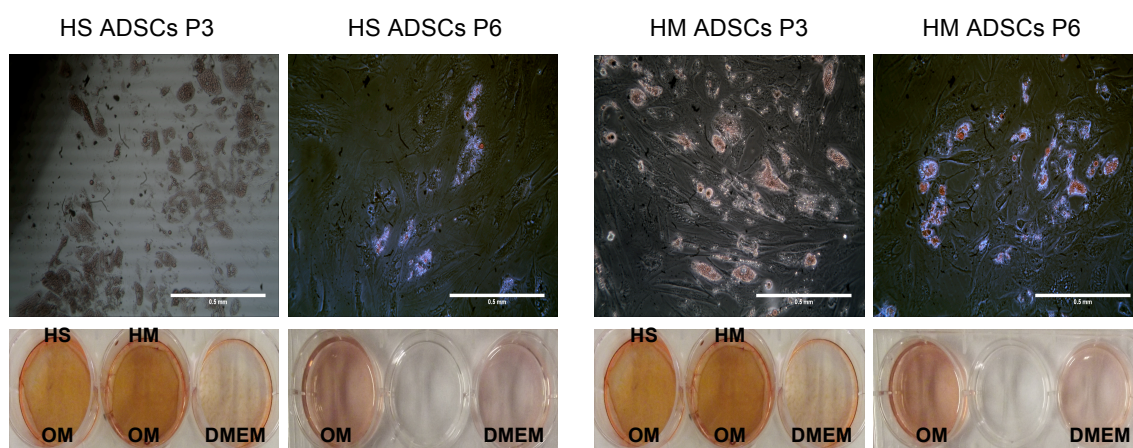


**Figure 8.3.2** Top images: Human ADSCs isolated using high speed and hand minced methods (0.1% collagenase, 45 min incubation) cultured for 3 weeks with adipogenic medium and stained with 0.3% Oil Red O. Scale bar = 0.5 mm. Bottom images: Human ADSCs isolated using high speed and hand minced methods (0.1% collagenase, 45 min incubation) cultured for 3 weeks with osteogenic medium (OM) or DMEM medium (for controls) and stained with 5% Alizarin red. HS = High speed; HM = Hand minced.

Thereafter, cells isolated using high speed and hand minced methods (0.1% collagenase, 45 min incubation) were seeded in scaffolds. For this, hybrid PLA (280  $\mu$ m) samples were prepared as previously described in a previous Chapter of this thesis, and  $5 \times 10^5$  ADSCs at passage 6 from each isolation method were seeded on 1.5 x 1.5 cm scaffolds using metal rings with an internal diameter of 1 cm. All samples were then cultured for 2 weeks with DMEM medium.

Metabolic activity of samples from both groups was measured at day 0, 7 and 14 by AlamarBlue® staining. In addition, after 14 days, total collagen production of both groups was measured using Sirius red staining.

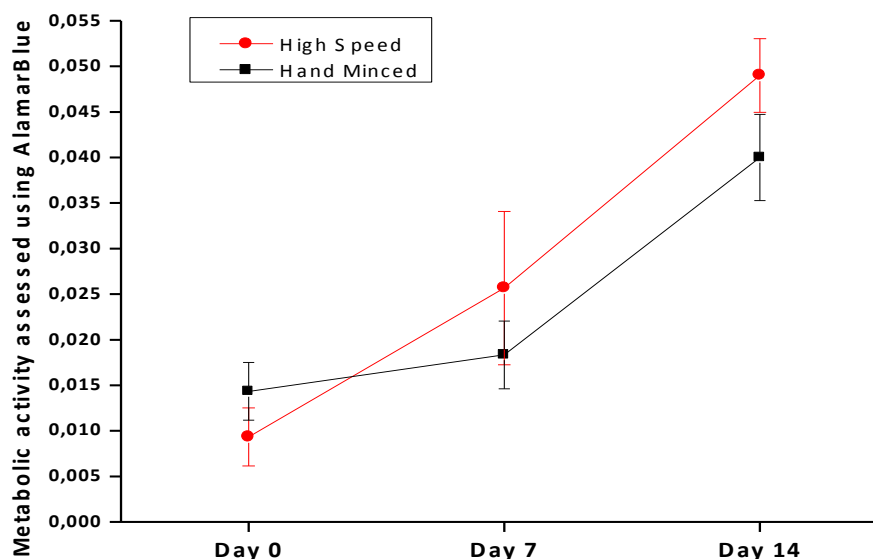


**Figure 8.3.3** AlamarBlue® staining for ADSCs isolated using high speed and hand minced methods (0.1% collagenase, 45 min incubation) on hybrid PLA (280  $\mu$ m) scaffolds over 2 weeks in culture ( $n=3\pm$ SEM).

Metabolic activity was increased over 2 weeks of culture of ADSCs isolated by both high speed and hand minced methods (0.1% collagenase, 45 min incubation), without significant differences between the 2 groups (figure 8.3.3).

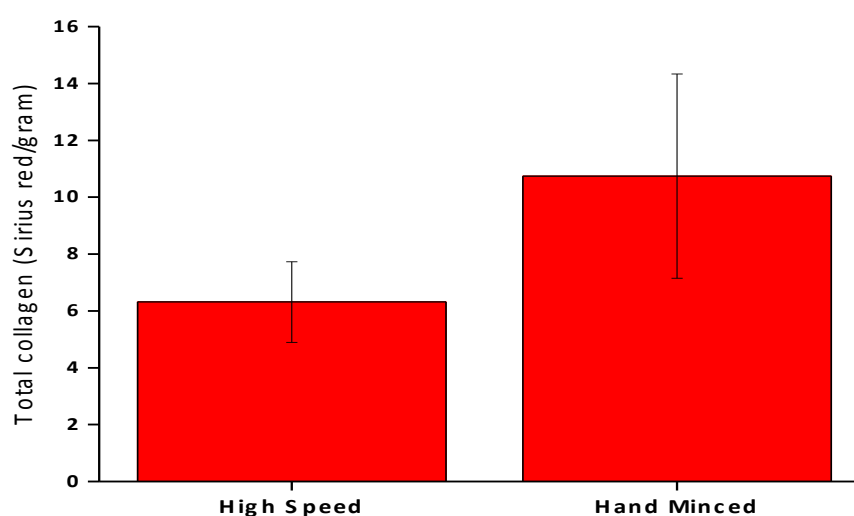


**Figure 8.3.4** Sirius red staining after 14 days of ADSCs isolated using high speed and hand minced methods (0.1% collagenase, 45 min incubation) cultured on hybrid PLA (280  $\mu$ m) scaffolds. ( $n=3\pm$ SEM).

Similarly, by Sirius red staining, the total collagen produced by these cells from the 2 groups did not show significant differences (figure 8.3.4).

### 8.3.2 Seeding the stromal vascular fraction (SVF) on PLA scaffolds

The SVF isolated from 10 mL of fat, as previously described in the second Chapter of this thesis, which is normally seeded into a T25 tissue culture flask for ADSCs isolation, was seeded directly onto hybrid PLA (280  $\mu$ m) scaffolds to assess the potential of the mixture of cells from this stromal fraction to develop a TERM. These cells were compared to same scaffolds seeded with  $5 \times 10^5$  ADSCs at passage 6 (results from Chapter 7).

All samples were cultured for 2 weeks in DMEM medium and metabolic activity was measured at day 0, 7 and 14 by AlamarBlue<sup>®</sup> staining. In addition, after 14 days, total collagen production of both groups was measured using Sirius red staining.

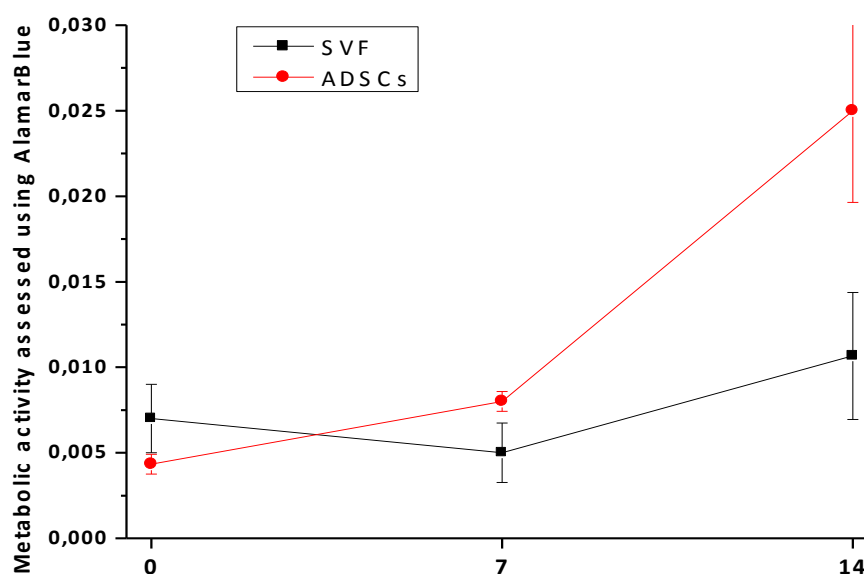


**Figure 8.3.5** AlamarBlue<sup>®</sup> staining of hybrid PLA (280  $\mu$ m) scaffolds seeded with the SVF and ADSCs over 2 weeks in culture ( $n=3 \pm \text{SEM}$ ).

Although there were no significant differences between the 2 groups for metabolic activity at any day over 2 weeks culture on PLA scaffolds, ADSCs at passage 6 clearly showed greater metabolic activity by day 14 and the SVF did not show any significant increase from day 0 to day 14 (figure 8.3.5).

Total collagen production was also significantly greater for ADSCs at passage 6, after 2 weeks culture on PLA scaffolds, compared to the SVF cells seeded and cultured on same scaffolds (figure 8.3.6).

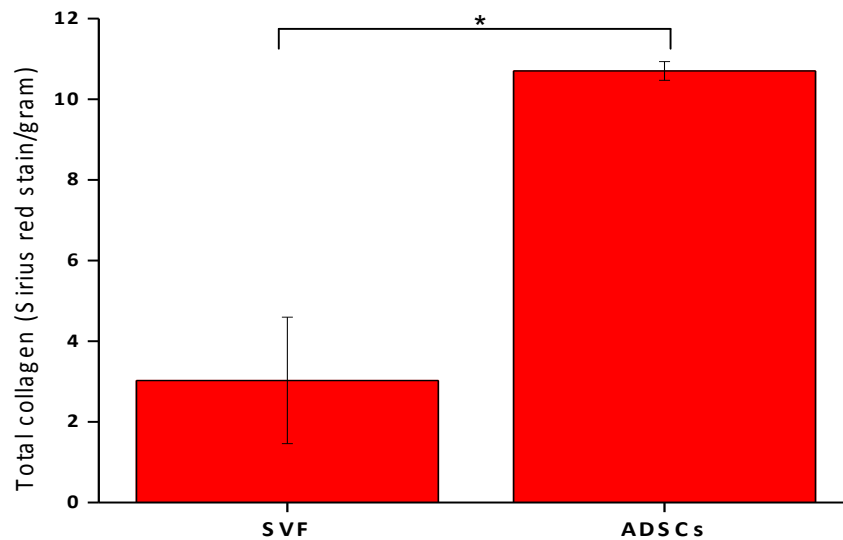


**Figure 8.3.6** *Sirius red staining after 14 days of hybrid PLA (280  $\mu$ m) scaffolds cultured with the SVF and ADSCs. ( $n=3\pm$ SEM). \* $p<0.05$ .*

## 8.5 Discussion

Although, as expected, small variations between ADSCs from different donors were found, different batches of cells did not show significant differences in differentiation and proliferation potential, as well as in their ability to develop a TERM using PLA scaffolds.

Also as expected, these cells showed higher potential to differentiate into adipocytes and osteocytes at lower passage number. Interestingly, ADSCs at both passage 3 and 6 were able to develop a TERM.

Only the metabolic activity showed any differences, which was lower for cells at passage 3 compared to the same cells at passage 6 when cultured on PLA scaffolds. This is difficult to explain since it has been demonstrated that these cells have higher proliferative ability in 2D culture at lower passages (533). In addition, after 14 days culture, DAPI staining showed similar confluent populations of cells in the scaffolds between groups, as well as, similar total collagen production. Also immunostaining

demonstrated a similar ability of ADSCs at passage 3 and passage 6 to produce some of the specific components of the ECM, such as collagen III and elastin.

Using the Milteniy Biotech technology to rapidly isolate ADSCs did not affect the potential of these cells to differentiate or proliferate compared to ADSCs isolated from the same patient using the conventional method. Slight variations were seen when looking at the proliferative rate up to the second passage of both groups; however, this may be affected by the number of cells isolated/seeded at day 0 rather than the method used.

Again these cells showed higher potential to differentiate into adipocytes and osteocytes at lower passage. Both groups of cells similarly increased their metabolic activity over 2 weeks of culture when seeded on PLA scaffolds and produced the same amounts of total collagen.

As described in Chapter 2 of this thesis, we also tested the MACS<sup>®</sup> Separation technology using antibodies magnetically labeled to separate the relevant population of cells from the SVF. This was used to avoid contamination of other cells types, as well as, to know how many of the desired cells are actually isolated from a particular amount of fat. For this, we used an antibody against CD271, a marker which has been used to isolate a subset of multipotent stromal cells from bone marrow (547).

Unfortunately, this antibody did not label any cells from the SVF isolated from subcutaneous fat tissue as all cells were washed out at the end of the protocol. Also, this marker did not show good results for the isolation of multipotent stromal cells from umbilical cord (548).

Alternatively, CD271 together with CD34 have been shown to be expressed in perivascular ADSCs (549-551). These cells have been described to be multipotent stem cells with more regenerative potential, while other subsets of ADSCs would be more committed to differentiate into adult cells from the tissue/organ itself (552).

The literature so far shows only one study where CD271 was used for immunomagnetic separation of ADSCs and they did not find differences compared to cells isolated by the conventional method in terms of gene expression and differentiation potential and lower cell yields were isolated (553).

At this point in this project we do not know whether a particular subset of ADSCs may be more desirable to develop a TERM for the pelvic floor with higher regenerative potential or, in contrast, we actually need to look for another marker to isolate as many ADSCs as possible, since the number of cells isolated by “one stage” in theatre approach may be very relevant.

For these reason, we investigated the potential of seeding the whole SVF on PLA scaffolds using as many cells as possible from this stromal fraction to develop a TERM. As above, since the final clinical approach involves an autologous implantation, other cells types found in this SVF, such as fibroblasts and endothelial cells, may be desirable for this too.

We found promising results since these cells from the SVF were able to seed the scaffolds and produced small amounts of total collagen after 2 weeks culture on PLA scaffolds, although the latter values were significantly lower than seeding elevated number of ADSCs.

However, there are still many issues to look at, such as characterising the actual cells attached to the PLA scaffolds from this fraction and which type of tissue they develop. Also, the main cell type found in this fraction is erythrocytes which are not able to attach the plastic culture flask. Therefore, looking at the use of lysis buffer for erythrocytes may be interesting to help the adherent cells to attach more efficiently the scaffolds as well as, to work out the actual number of the adherent cells isolated from the SVF and found in a specific amount of fat.

Around 2 million ADSCs can be isolated from 250 mL of fat routinely obtained from a low invasive liposuction (554). If we obtained the same number of cells, we should have isolated about 80,000 cells from 10 mL of fat.

However, we may have isolated about 20,000 cells explained by the increase in cell number after 1 week in culture (figure 8.3.1). These cells present growth curves with an initial lag phase of 2 days and then a log phase at exponential growth rate from 3 to 5 days with a doubling time of 24 hours, and has been similar found for ADSCs from passage 3 through to passage 12 (555).

Finally, it has been shown that these cells can be isolated from a fraction called blood and saline fraction of a liposuction (554). For a clinical approach of isolating and using the cells on the day of operation, ADSCs isolated from this fraction would appear to be

ideal since the use of animal derived enzymes for chemical disaggregation of the tissue would also be avoided. This method has been demonstrated to isolate a yield of 250,000 ADSCs from 250 mL of subcutaneous fat. However, whether this number is enough and whether these cells have the potential to develop the final clinical TERM will need to be determined with further studies.



## **Chapter 9**

### **CONCLUSIONS AND FUTURE DIRECTIONS**

Urinary incontinence is a major public health issue, affecting 40% (6 million) of women over 40 in the UK (556). When leakage of urine occurs on coughing or movement it is termed SUI. POP is a related disorder where the pelvic organs bulge into the vagina, and similarly affects half of women over 40. Although not life threatening, these conditions significantly impair physical, social and psychological wellbeing. Over the next 30 years the proportion of women over the age of 75 is estimated to double emphasising the need for durable surgical options without causing complications.

Essentially, POP and SUI occur due to a combination of age and the consequences of pregnancy related weakening of the pelvic floor structures.

SUI is developed by intrinsic sphincter weakness and/or para-urethral tissue weakness leading to urethral hypermobility, which may co-exist to some degree (20). Similarly, weakness in the supportive connective tissues of the vagina, which have been described by Delancey in 3 levels (134), leads to herniation of the underlying tissues into the vagina, and consequently, the prolapse of female pelvic organs.

Both conditions are related to weakness of the pelvic floor tissues by 2 different mechanisms, and are due to different risk factors (16). While, in elderly women, the quality of the ECM of pelvic floor tissues decreases, as well as neurogenic defects can both lead to sphincter dysfunction; a traumatic process in young women such as vaginal delivery, can lead to damage of these tissues (16).

As the etiologies can be so different it is difficult to study the alterations in the ECM in the different conditions. Thus it is not established whether the poor quality of the tissue is due to abnormal synthesis of structural proteins (195-197, 199-202) or an imbalance between the activity of the major proteolytic enzymes that degrade them (203-205) and the inhibitors of proteolysis (206-208).

Similarly, imaging studies do not agree on anatomical alterations at the different levels of the supportive connective tissues analyzed in patients with POP and/or SUI (125, 126, 129, 130).

In the UK one in ten women will need primary surgery for SUI or POP, and 20% of these will require a repeat procedure (557) with over 40,000 operations performed annually in England and Wales alone.

Currently, the best chance of cure is the use of prostheses using either synthetic or biological grafts to reinforce supportive pelvic floor tissues.

Fascial grafts taken from the patient's thigh or abdominal wall, long used as slings to support the urethra in SUI, introduce a risk of complications (e.g. wound infection or hernia) which precludes obtaining larger grafts for the repair of POP.

In the mid 1990's PPL mesh slings were introduced to repair SUI. Mesh is placed through the vagina in a simpler, quicker, less invasive technique, which became rapidly adopted. Soon a plethora of mesh "kits" were marketed, gaining clearance on the basis of their similarity to mesh for abdominal wall hernias, being approved for POP surgery as well to reinforce fascial defects where native tissue repair techniques fail which they do in 20-30% of cases. In the absence of robust long-term safety and efficacy data, this is now considered to have been premature (286).

Alarming reports of debilitating complications of vaginal non-degradable synthetic mesh implantation have since emerged including vaginal wall erosion (0-25.6%) chronic pain (0-5.5%) and sexual problems (1.9-17%). These meshes can become encased in scar tissue, and it is near impossible to safely remove them from the surrounding tissue often requiring multiple operations with no guarantee of resolution. Recently, warning alerts were issued by UK and US regulators whilst in 2013 class action lawsuits against manufacturers by patients led to withdrawal of these synthetic meshes in the USA (286).

Experts agree complications are more likely when surgeons lack sufficient experience and training (286). However, it has been previously described in this thesis that the immune responses against each material are important and may determine the outcome of different materials (558).

A chronic inflammatory response occurring after implantation is likely to be implicated in mesh exposure. As above, PPL implants cannot be remodelled and they can induce the release of a pro-inflammatory cytokine; therefore, some patients respond to them with chronic inflammation leading to excessive fibrosis and encapsulation (488). Alternatively, a range of acellular biological grafts have also been trailed in small studies, but the main problem encountered was a vigorous host response leading to rapid degradation, and consequently, to high failure rates (267).

Therefore, we aimed to develop a tissue engineered alternative material for the treatment of SUI and POP. We hypothesize that a TERM developed from a scaffold designed to degrade slowly may lead to better outcomes than current materials, whilst

the introduction of autologous cells will produce new ECM for long-term support of the patient's pelvic floor. An absorbable material is less likely to result in exposure due to the lack of persisting foreign material in the host tissues and together with the autologous cells component may lead to better integration into host tissues.

To assess this, the main objectives of this project were to identify the best scaffold and cell candidates cultured under optimal conditions to develop a TERM designed for pelvic floor repair. Then, this material was tested in animals to characterize the host response against it. In addition, we explored the possibility of producing a range of architectures of this degradable scaffold with different mechanical properties. Finally, the potential of the chosen cells from different donors was assessed, as well as, some preliminary exploration of how to achieve rapid extraction of cells from fat.

## **9.1 Scaffold candidates**

Th-PLA scaffolds, produced under sterile manner in our clean room by electrospinning technique, were shown to be easy to handle with mechanical properties close to native tissues and with an appropriate pore size to avoid risk of infection (267).

As above, we aimed for a slow rate of biodegradation, and it was shown *in vitro* that this material retained its mechanical strength for at least 90 days achieving values around those of native tissues.

For this thesis, this material was chosen from previous work in our group where this scaffold was compared to 6 other candidate materials used to treat SUI and POP, including PPL, and PLA scaffolds showed better results for cell attachment and ECM production (346). It was hypothesized that good cell attachment would be desirable for better integration into the host tissues to hopefully avoid fibrous encapsulation and/or erosion.

## **9.2 Cell candidates**

Vaginal fibroblasts would intuitively appear to be the most appropriate cell type for developing a TERM designed for pelvic floor repair. However, as an autologous

approach, the isolation of these cells requires invasive methods which may worsen the clinical condition, as well as, these cells have been shown to have altered synthesis of ECM structural components in women with POP (236).

Accordingly, OFs and ADSCs were compared for developing a TERM cultured on Th-PLA scaffolds as both are accessible and are used clinically in tissue engineering applications. In general there were no significant differences identified between these cells since both led to cell proliferation and production of the key ECM components.

OFs can be extracted from small buccal mucosal biopsy taken under local anesthetic, and have been used for urethroplasty (385). Nevertheless, ADSCs were selected for further investigation as these have been found to have considerable potential for regeneration and revascularization in a number of studies (400). Large numbers of these cells can also be quickly isolated using a minimally invasive liposuction in humans (400). ADSCs do not differentiate when cultured in basic DMEM medium displaying fibroblastic behavior, and they produce an endogenous ECM (341); additionally they have been shown to release a growth factor to stimulate fibroblast proliferation with the potential to regenerate connective tissues (343). Furthermore, ADSCs have the potential to inhibit inflammatory responses by secretion of the inhibitor of  $\text{TNF}\alpha$  (343), and a sub-population of ADSCs express an endothelial surface antigen (CD34) which can promote neo-vascularization (559). Taken together these become the most attractive candidate for clinical use for tissue regeneration.

### **9.3 Culture conditions**

We optimized the number of ADSCs and the period of culture of cells on Th-PLA scaffolds to develop a TERM.

We also looked at the effect of different mechanical forces applied to the scaffolds to study how these may affect the survival and behavior of the cells in a dynamic environment such as the pelvic floor. However, these experiments did not show any effect on the tissue produced when these samples were cultured under different mechanical conditions. The methods of mechanically loading the tissues were very basic and may be insufficient to answer the question.

Other experiments have shown that cells on scaffolds subjected to dynamic loading did lead to elastin production which is important in the elastic recoil of an engineered biomaterial (560). Accordingly, this area should be investigated further using a better equipment to subject cells to dynamic loading.

## **9.4 Host response to TERM**

It has been reported that the amount of host tissue infiltration is dependent upon mesh composition, pore size and configuration which will, in turn, influence mesh integration and new ECM production. Interstices of multifilaments bigger than 75  $\mu\text{m}$  may allow the passage of leukocytes increasing resistance to infection, as well as allowing good cell proliferation and blood vessel formation (561).

An acute macrophage response against the Th-PLA scaffolds led to new blood vessels and neo-tissue formation after the host cell infiltration which was promising for long-term integration into the native tissues and would act to tackle infection. This also suggested a quick remodelling by collagen formation for long-term retention of the mechanical properties. In addition, there was no encapsulation which has been described for other biological materials implanted leading to a chronic inflammatory response (324, 456).

On the other hand, from these results we could not attribute any beneficial effect made by the ADSCs in the cell-seeded group of implants and these cells were not tracked in these experiments (attempts to do so by using a cell tracker failed). Therefore, future experiments in animals will need to determine the fate of these cells to assess any regenerative effect made by the ADSCs and a collaboration has been established to obtain GFP transfected ADSCs for future longer term animal experiments.

## **9.5 Mechanical properties of the TERM**

Only long-term animal experiments will establish how the host response against PLA scaffolds will affect the mechanical properties of our TERM. Therefore, although PLA

scaffolds have shown a good retention of the mechanical properties when long-term cultured *in vitro*, a higher degradation rate which may well occur *in vivo* may lead to early failure. On the other hand, a highly fibrotic process may lead to an elevated increase in the stiffness and strength of these TERMS leading to the sort of complications reported for non-degradable synthetic materials.

We proved we can produce a range of PLA scaffolds with different mechanical properties made by different fibre configuration using the electrospinning technique, which can retain their tensile properties. *In vitro* experiments showed a dramatic reduction in the elongation of the scaffolds before they snapped, but this was only seen at 90 days. All of these scaffolds showed good cell attachment and proliferation; in addition, fibre alignment stimulated higher production of total collagen. It has already been shown that the fibre configuration of scaffolds can affect the shape of the cells, their migration, and the organization of the ECM produced (528, 562). Furthermore, this cell organization determines the particular adhesion between cells and between the cells and the scaffolds which can lead to tensile forces applied to the cells stimulating production of the ECM components and MSCs differentiation (563, 564).

## **9.6 Potential of ADSCs**

MSCs have been reported to show variability between donors (534, 535); however, we demonstrated that ADSCs from 3 different donors all developed a TERM using PLA scaffolds, and encouragingly these cells showed the same ability for this over a range of cell passages.

Next the rapid isolation of these cells was assessed using new technology which can be installed in the theatre, as an enclosed system, to achieve a rapid isolation from lipoaspirate of a clinically relevant number of cells which can be implanted into the same patient that day. ADSCs isolated using these devices showed the same proliferative and differentiation potential than the same cells isolated through conventional methods. In addition, cells isolated by both routes did not show significant differences when developing a TERM from PLA scaffolds.

On the other hand, there are other issues to consider in the future. The cells tested in our laboratory were obtained from patients under an anonymous basis; therefore, it will be necessary to test the potential of these cells from elderly women since these patients are more likely to undergo surgery for SUI or POP. Another issue will be to establish the number of these cells which are actually needed and which can be isolated from a patient. As previously mentioned, around 2 million cells can be separated from 250 mL obtained from a routine minimally invasive liposuction. However, the number of ADSCs with potential for this clinical purpose can vary between young and old women, as well as, in lean patients the amount of fat obtained can be much lower. Thus more work is required in this area which nevertheless looks very promising.

<b>SUMMARY OF THESIS RESULTS</b>	
<b>Scaffold candidates</b>	<ul style="list-style-type: none"> <li>- Development and characterization of PLA electrospun scaffolds.</li> <li>- PLA scaffolds were more biocompatible <i>in vitro</i> than 6 clinical materials with mechanical properties close to native tissues of the pelvic floor.</li> </ul>
<b>Cell candidates</b>	<ul style="list-style-type: none"> <li>- <i>In vitro</i>, good cell attachment and proliferation of well characterized OFs and ADSCs with production of ECM.</li> </ul>
<b>Culture conditions</b>	<ul style="list-style-type: none"> <li>- Identification of optimal culture conditions <i>in vitro</i> including number of cells seeded and period of culture.</li> </ul>
<b>Host response</b>	<ul style="list-style-type: none"> <li>- In a rat model, an acute macrophage response against the implanted scaffolds seeded with and without cells led to new blood vessels and neo-tissue formation after the host cell infiltration being all this promising for long-term integration into the native tissues.</li> </ul>
<b>Mechanical properties</b>	<ul style="list-style-type: none"> <li>- Production of electrospun PLA scaffolds from mechanically softer to stronger due to different fibre configuration.</li> <li>- Cells performed similarly well on the different scaffolds.</li> <li>- Degradation studies <i>in vitro</i> showed minimal effects on mechanical properties. These were only relevantly dropped at 90 days for stronger scaffolds.</li> </ul>
<b>Potential of ADSCs</b>	<ul style="list-style-type: none"> <li>- ADSCs did not show variations between donors in culture (2D, 3D).</li> <li>- With translational clinical value, early data showed the potential of culturing ADSCs on PLA scaffolds quickly isolated with new technology or by using the SVF.</li> </ul>

**Table 10** Summary of the results of the thesis.

## 9.7 Future work

At this point of this project, we came up with more possibilities which may need to be considered in the future for the final clinical product. Therefore, a future plan may



involve the production of 2 different materials for pelvic floor surgery that are more suited for purpose than current mesh.

For SUI, since the material implanted can cover relatively small area, we may produce a biocompatible material, which may be non-degradable, with sufficient strength and stiffness to support the urethra and withstand repetitive strain by elastic recoil as the most relevant property for the treatment of this condition. PPL is highly deformed during cycling loading (565); therefore, the implantation of this material can lead to voiding obstruction due to high strength and stiffness, but it can also lead to failure due to plastic deformation after distension. In addition, PPL presents rough edges and rigid forms which are a mismatch with the supple and mobile vaginal tissues in which they are placed.

For POP, fascial defects require much larger meshes and this may have contributed to a higher complication rate, particularly erosion (<15%) (566). To overcome this we propose to stick to the development of the TERM combining a bioresorbable scaffold with autologous ADSCs aiming for a constructive remodelling process that result in a long-term repair of this condition. The next challenge is to also introduce some degree of elasticity into this material too.

Although autologous fascia has success rates of 70-90% in SUI and it does not erode or cause chronic pain (567), it is not considered for POP, and even for SUI it is usually avoided due to the donor site co-morbidities already described. Nevertheless, fascia is a logical tissue to emulate and use as a guide for the design of new materials. Accordingly the mechanical behaviour and properties of rectus fascia will need to be established, since it has been shown in this thesis that there is little data about it in the literature. This can be used along with data on the forces encountered in the pelvic floor to build a profile of the mechanical criteria to be considered for the design of future materials.

As previously described, electrospinning technology allows co-spinning of two polymers in random or aligned orientations which may be used for the scaffold fabrication. For SUI, the desired strength and elasticity may be achieved by interweaving variable proportions of electrospun fibres of non-degradable polyurethanes, capable of stretch and elastic recoil into a sling akin to autologous fascia in mechanical behaviour. For POP, the introduction of biodegradable polyurethane interwoven with the PLA fibres may provide the desired physical support until the native tissue has remodelled.

These materials will require a comprehensive *in vitro* analysis of mechanical behaviour and properties (both with and without cells). Uniaxial tensiometry could be performed before and after a cyclical loading (uniaxial strain) regime in a bioreactor lasting several weeks. A new Ebers bioreactor acquired in our lab may allow a useful testing regime to be introduced into the development of materials based loosely on our current understanding of the forces experienced in the pelvic floor.

The successful outcome of implantation of large scale engineered tissues also depends on how well a vascular network is formed for nutrient diffusion and gas exchange into the centre of the scaffold. It has been shown that MSCs seeded with endothelial cells on scaffolds have potential for angiogenic differentiation using suitable growth factors to guide these cells toward the centre of the scaffold to induce a vascular network (568).

Therefore, another possibility during the scaffold manufacture is the production of a pro-angiogenic material. This would involve different coatings of the scaffolds to positively charge them for heparin binding. Our group has already shown the potential to produce hydrogels with these properties which can bind and release bioactive vascular endothelial growth factor to stimulate endothelial cells proliferation (569). Other approaches to coat scaffolds using the technique of plasma polymerisation to develop a layer by layer electrostatic coating are underway within the group.

As a final clinical product many other aspects will need to be considered for clinical translation such as scaffold production under Good Manufacturing Practice conditions.

As part of this, cleanroom production facilities will be needed and gamma irradiation and e-beam sterilisation may be compared to investigate the extent to which these will affect the properties of the materials. Also, every aspect of the choice of solvents, protocols for the removal and measurement of residual solvent, packaging and storage of the products under vacuum and labelling will need to be considered.

Also as we were not able to separate the desired MSC cell population by using CD271 Ab with Miltenyi Biotech technology, this will need to be further studied which may include the comparison of other CD45 negative perivascular ADSCs subpopulations such as the CD34-CD146+ pericytes and CD34+CD146- adventitial cells (570). To determine their clinical potential, the selected cell preparation will have to be characterised for their phenotype, colony-forming unit content, and their trilineage

adipogenic, chondrogenic and osteogenic potential, as well as, the potential to promote vessel formation, secretome fingerprints, senescence markers and karyotype will need to be assessed as previously described (571-573).

Finally, the most important work will be the implantation in animals of these materials which, ultimately, will determine their long-term performance and outcomes. This will investigate the development of any chronic immune response, the fate of the ADSCs and the mechanical properties of the TERM after several months of implantation. This will be particularly important for establishing the *in vivo* degradation of these scaffolds and establishing the desirable mechanical properties of these materials at time of implantation. As above, the capability to track the implanted ADSCs from the explants after sacrifice will be very relevant to determine survival and migration of these cells, which, in turn, will be necessary to attribute any regenerative contribution of these cells for better outcomes of the TERM.

For this we propose an immunocompetent rabbit model as the animal's size allows simultaneous testing of several large implants (allowing biaxial biomechanical testing). In addition, our collaborators in Leuven from previous animal work have extensive experience with this model, and the outcome measurements (456). For each animal, four full thickness abdominal wall defects can be induced, primarily repaired, and overlaid with experimental or control meshes. For each animal 2 of the 4 defects would be assigned to experimental implants, whereas the 2 other sites will be sham operated (primarily sutured closure, no implant) or overlaid with PPL for comparison.

In conclusion, this thesis answers many questions about cell type and culture on scaffolds for the production of TERM for the pelvic floor but as it is evident from the above these are early steps in this journey.

## References

1. Norton P, Brubaker L. Urinary incontinence in women. *Lancet*. 2006;367(9504):57-67.
2. Ko Y, Lin SJ, Salmon JW, Bron MS. The impact of urinary incontinence on quality of life of the elderly. *The American journal of managed care*. 2005;11(4 Suppl):S103-11.
3. Abrams P, Cardozo L, Fall M, Griffiths D, Rosier P, Ulmsten U, et al. The standardisation of terminology of lower urinary tract function: report from the Standardisation Sub-committee of the International Continence Society. *Neurourology and urodynamics*. 2002;21(2):167-78.
4. Hannestad YS, Rortveit G, Sandvik H, Hunskaar S, Norwegian EsEoIitCoN-T. A community-based epidemiological survey of female urinary incontinence: the Norwegian EPINCONT study. *Epidemiology of Incontinence in the County of Nord-Trondelag. Journal of clinical epidemiology*. 2000;53(11):1150-7.
5. Abrams P, Cardozo L, Fall M, Griffiths D, Rosier P, Ulmsten U, et al. The standardisation of terminology in lower urinary tract function: report from the standardisation sub-committee of the International Continence Society. *Urology*. 2003;61(1):37-49.
6. Stewart WF, Van Rooyen JB, Cundiff GW, Abrams P, Herzog AR, Corey R, et al. Prevalence and burden of overactive bladder in the United States. *World journal of urology*. 2003;20(6):327-36.
7. Hampel C, Wienhold D, Benken N, Eggersmann C, Thuroff JW. Definition of overactive bladder and epidemiology of urinary incontinence. *Urology*. 1997;50(6A Suppl):4-14; discussion 5-7.
8. Subak LL, Waetjen LE, van den Eeden S, Thom DH, Vittinghoff E, Brown JS. Cost of pelvic organ prolapse surgery in the United States. *Obstetrics and gynecology*. 2001;98(4):646-51.
9. Hu TW, Wagner TH, Bentkover JD, Leblanc K, Zhou SZ, Hunt T. Costs of urinary incontinence and overactive bladder in the United States: a comparative study. *Urology*. 2004;63(3):461-5.
10. Wallner LP, Porten S, Meenan RT, O'Keefe Rosetti MC, Calhoun EA, Sarma AV, et al. Prevalence and severity of undiagnosed urinary incontinence in women. *The American journal of medicine*. 2009;122(11):1037-42.
11. Stamey TA, Schaeffer AJ, Condy M. Clinical and roentgenographic evaluation of endoscopic suspension of the vesical neck for urinary incontinence. *Surgery, gynecology & obstetrics*. 1975;140(3):355-60.
12. Shumaker SA, Wyman JF, Uebersax JS, McClish D, Fantl JA. Health-related quality of life measures for women with urinary incontinence: the Incontinence Impact Questionnaire and the Urogenital Distress Inventory. Continence Program in Women (CPW) Research Group. *Quality of life research : an international journal of quality of life aspects of treatment, care and rehabilitation*. 1994;3(5):291-306.
13. Sandvik H, Seim A, Vanvik A, Hunskaar S. A severity index for epidemiological surveys of female urinary incontinence: comparison with 48-hour pad-weighing tests. *Neurourology and urodynamics*. 2000;19(2):137-45.
14. Espuna-Pons M, Dilla T, Castro D, Carbonell C, Casariego J, Puig-Clota M. Analysis of the value of the ICIQ-UI SF questionnaire and stress test in the differential diagnosis of the type of urinary incontinence. *Neurourology and urodynamics*. 2007;26(6):836-41.

15. Klovning A, Avery K, Sandvik H, Hunskaar S. Comparison of two questionnaires for assessing the severity of urinary incontinence: The ICIQ-UI SF versus the incontinence severity index. *Neurourology and urodynamics*. 2009;28(5):411-5.
16. Delancey JO. Why do women have stress urinary incontinence? *Neurourology and urodynamics*. 2010;29 Suppl 1:S13-7.
17. Rud T, Andersson KE, Asmussen M, Hunting A, Ulmsten U. Factors maintaining the intraurethral pressure in women. *Investigative urology*. 1980;17(4):343-7.
18. Abrams P, Andersson KE, Birder L, Brubaker L, Cardozo L, Chapple C, et al. Fourth International Consultation on Incontinence Recommendations of the International Scientific Committee: Evaluation and treatment of urinary incontinence, pelvic organ prolapse, and fecal incontinence. *Neurourology and urodynamics*. 2010;29(1):213-40.
19. Petros PE, Ulmsten UI. An integral theory of female urinary incontinence. Experimental and clinical considerations. *Acta obstetricia et gynecologica Scandinavica Supplement*. 1990;153:7-31.
20. Kayigil O, Iftikhar Ahmed S, Metin A. The coexistence of intrinsic sphincter deficiency with type II stress incontinence. *The Journal of urology*. 1999;162(4):1365-6.
21. DeLancey JO. Structural support of the urethra as it relates to stress urinary incontinence: the hammock hypothesis. *American journal of obstetrics and gynecology*. 1994;170(6):1713-20; discussion 20-3.
22. DeLancey JO. Structural aspects of the extrinsic continence mechanism. *Obstetrics and gynecology*. 1988;72(3 Pt 1):296-301.
23. Yang A, Mostwin JL, Rosenshein NB, Zerhouni EA. Pelvic floor descent in women: dynamic evaluation with fast MR imaging and cinematic display. *Radiology*. 1991;179(1):25-33.
24. Mostwin JL, Yang A, Sanders R, Genadry R. Radiography, sonography, and magnetic resonance imaging for stress incontinence. Contributions, uses, and limitations. *The Urologic clinics of North America*. 1995;22(3):539-49.
25. Jeffcoate TN, Roberts H. Observations on stress incontinence of urine. *American journal of obstetrics and gynecology*. 1952;64(4):721-38.
26. Ball TL, Douglas G, Fulkerson LL. Topographic urethrography. *American journal of obstetrics and gynecology*. 1950;59(6):1252-9.
27. Macura KJ, Genadry RR. Female urinary incontinence: pathophysiology, methods of evaluation and role of MR imaging. *Abdominal imaging*. 2008;33(3):371-80.
28. McGuire EJ, Fitzpatrick CC, Wan J, Bloom D, Sanvordenker J, Ritchey M, et al. Clinical assessment of urethral sphincter function. *The Journal of urology*. 1993;150(5 Pt 1):1452-4.
29. Pajoncini C, Costantini E, Guercini F, Bini V, Porena M. Clinical and urodynamic features of intrinsic sphincter deficiency. *Neurourology and urodynamics*. 2003;22(4):264-8.
30. Resnick NM. Geriatric incontinence. *The Urologic clinics of North America*. 1996;23(1):55-74.
31. Lifford KL, Curhan GC, Hu FB, Barbieri RL, Grodstein F. Type 2 diabetes mellitus and risk of developing urinary incontinence. *Journal of the American Geriatrics Society*. 2005;53(11):1851-7.
32. Maggi S, Minicuci N, Langlois J, Pavan M, Enzi G, Crepaldi G. Prevalence rate of urinary incontinence in community-dwelling elderly individuals: the Veneto study.

The journals of gerontology Series A, Biological sciences and medical sciences. 2001;56(1):M14-8.

33. Carley ME, Schaffer J. Urinary incontinence and pelvic organ prolapse in women with Marfan or Ehlers Danlos syndrome. *American journal of obstetrics and gynecology*. 2000;182(5):1021-3.

34. Rortveit G, Daltveit AK, Hannestad YS, Hunskaar S, Norwegian ES. Urinary incontinence after vaginal delivery or cesarean section. *The New England journal of medicine*. 2003;348(10):900-7.

35. Nitti VW. The prevalence of urinary incontinence. *Reviews in urology*. 2001;3 Suppl 1:S2-6.

36. Nygaard I, Barber MD, Burgio KL, Kenton K, Meikle S, Schaffer J, et al. Prevalence of symptomatic pelvic floor disorders in US women. *JAMA : the journal of the American Medical Association*. 2008;300(11):1311-6.

37. Swithinbank LV, Donovan JL, du Heaume JC, Rogers CA, James MC, Yang Q, et al. Urinary symptoms and incontinence in women: relationships between occurrence, age, and perceived impact. *The British journal of general practice : the journal of the Royal College of General Practitioners*. 1999;49(448):897-900.

38. Sommer P, Bauer T, Nielsen KK, Kristensen ES, Hermann GG, Steven K, et al. Voiding patterns and prevalence of incontinence in women. A questionnaire survey. *British journal of urology*. 1990;66(1):12-5.

39. Brown JS, Grady D, Ouslander JG, Herzog AR, Varner RE, Posner SF. Prevalence of urinary incontinence and associated risk factors in postmenopausal women. Heart & Estrogen/Progestin Replacement Study (HERS) Research Group. *Obstetrics and gynecology*. 1999;94(1):66-70.

40. Steinauer JE, Waetjen LE, Vittinghoff E, Subak LL, Hulley SB, Grady D, et al. Postmenopausal hormone therapy: does it cause incontinence? *Obstetrics and gynecology*. 2005;106(5 Pt 1):940-5.

41. Hendrix SL, Cochrane BB, Nygaard IE, Handa VL, Barnabei VM, Iglesia C, et al. Effects of estrogen with and without progestin on urinary incontinence. *JAMA : the journal of the American Medical Association*. 2005;293(8):935-48.

42. Hannestad YS, Rortveit G, Daltveit AK, Hunskaar S. Are smoking and other lifestyle factors associated with female urinary incontinence? The Norwegian EPINCONT Study. *BJOG : an international journal of obstetrics and gynaecology*. 2003;110(3):247-54.

43. Swash M, Snooks SJ, Henry MM. Unifying concept of pelvic floor disorders and incontinence. *Journal of the Royal Society of Medicine*. 1985;78(11):906-11.

44. Snooks SJ, Swash M, Henry MM, Setchell M. Risk factors in childbirth causing damage to the pelvic floor innervation. *International journal of colorectal disease*. 1986;1(1):20-4.

45. Press JZ, Klein MC, Kaczorowski J, Liston RM, von Dadelszen P. Does cesarean section reduce postpartum urinary incontinence? A systematic review. *Birth*. 2007;34(3):228-37.

46. Deng DY. Urinary incontinence in women. *The Medical clinics of North America*. 2011;95(1):101-9.

47. Brown JS, Wing R, Barrett-Connor E, Nyberg LM, Kusek JW, Orchard TJ, et al. Lifestyle intervention is associated with lower prevalence of urinary incontinence: the Diabetes Prevention Program. *Diabetes care*. 2006;29(2):385-90.

48. Castro RA, Arruda RM, Zanetti MR, Santos PD, Sartori MG, Girao MJ. Single-blind, randomized, controlled trial of pelvic floor muscle training, electrical stimulation,

- vaginal cones, and no active treatment in the management of stress urinary incontinence. *Clinics*. 2008;63(4):465-72.
49. Hendriksson L, Andersson KE, Ulmsten U. The urethral pressure profiles in continent and stress-incontinent women. *Scandinavian journal of urology and nephrology*. 1979;13(1):5-10.
  50. Hilton P, Stanton SL. Urethral pressure measurement by microtransducer: the results in symptom-free women and in those with genuine stress incontinence. *British journal of obstetrics and gynaecology*. 1983;90(10):919-33.
  51. Anderson KE. Pharmacology of lower urinary tract smooth muscles and penile erectile tissues. *Pharmacological reviews*. 1993;45(3):253-308.
  52. Alhasso A, Glazener CM, Pickard R, N'Dow J. Adrenergic drugs for urinary incontinence in adults. *The Cochrane database of systematic reviews*. 2005(3):CD001842.
  53. Kaisary AV. Beta adrenoceptor blockade in the treatment of female urinary stress incontinence. *Journal d'urologie*. 1984;90(5):351-3.
  54. Michel MC, Peters SL. Role of serotonin and noradrenaline in stress urinary incontinence. *BJU international*. 2004;94 Suppl 1:23-30.
  55. Espey MJ, Downie JW, Fine A. Effect of 5-HT receptor and adrenoceptor antagonists on micturition in conscious cats. *European journal of pharmacology*. 1992;221(1):167-70.
  56. Norton PA, Zinner NR, Yalcin I, Bump RC, Duloxetine Urinary Incontinence Study G. Duloxetine versus placebo in the treatment of stress urinary incontinence. *American journal of obstetrics and gynecology*. 2002;187(1):40-8.
  57. Dmochowski RR, Miklos JR, Norton PA, Zinner NR, Yalcin I, Bump RC, et al. Duloxetine versus placebo for the treatment of North American women with stress urinary incontinence. *The Journal of urology*. 2003;170(4 Pt 1):1259-63.
  58. van Kerrebroeck P, Abrams P, Lange R, Slack M, Wyndaele JJ, Yalcin I, et al. Duloxetine versus placebo in the treatment of European and Canadian women with stress urinary incontinence. *BJOG : an international journal of obstetrics and gynaecology*. 2004;111(3):249-57.
  59. Millard RJ, Moore K, Rencken R, Yalcin I, Bump RC, Duloxetine UISG. Duloxetine vs placebo in the treatment of stress urinary incontinence: a four-continent randomized clinical trial. *BJU international*. 2004;93(3):311-8.
  60. Gilja I, Radej M, Kovacic M, Parazajder J. Conservative treatment of female stress incontinence with imipramine. *The Journal of urology*. 1984;132(5):909-11.
  61. Urinary Incontinence: The Management of Urinary Incontinence in Women. National Institute for Health and Clinical Excellence: Guidance. London 2006.
  62. Clark AL, Slayden OD, Hettrich K, Brenner RM. Estrogen increases collagen I and III mRNA expression in the pelvic support tissues of the rhesus macaque. *American journal of obstetrics and gynecology*. 2005;192(5):1523-9.
  63. Falconer C, Ekman-Ordeberg G, Ulmsten U, Westergren-Thorsson G, Barchan K, Malmstrom A. Changes in paraurethral connective tissue at menopause are counteracted by estrogen. *Maturitas*. 1996;24(3):197-204.
  64. Rizk DE, Hassan HA, Al-Marzouqi AH, Ramadan GA, Al-Kedrah SS, Daoud SA, et al. Combined estrogen and ghrelin administration restores number of blood vessels and collagen type I/III ratio in the urethral and anal canal submucosa of old ovariectomized rats. *International urogynecology journal and pelvic floor dysfunction*. 2008;19(4):547-52.
  65. Falconer C, Ekman-Ordeberg G, Blomgren B, Johansson O, Ulmsten U, Westergren-Thorsson G, et al. Paraurethral connective tissue in stress-incontinent

- women after menopause. *Acta obstetricia et gynecologica Scandinavica*. 1998;77(1):95-100.
66. Cody JD, Richardson K, Moehrer B, Hextall A, Glazener CM. Oestrogen therapy for urinary incontinence in post-menopausal women. *The Cochrane database of systematic reviews*. 2009(4):CD001405.
  67. Pickard R, Reaper J, Wyness L, Cody DJ, McClinton S, N'Dow J. Periurethral injection therapy for urinary incontinence in women. *The Cochrane database of systematic reviews*. 2003(2):CD003881.
  68. Corcos J, Collet JP, Shapiro S, Herschorn S, Radomski SB, Schick E, et al. Multicenter randomized clinical trial comparing surgery and collagen injections for treatment of female stress urinary incontinence. *Urology*. 2005;65(5):898-904.
  69. Isom-Batz G, Zimmern PE. Collagen injection for female urinary incontinence after urethral or periurethral surgery. *The Journal of urology*. 2009;181(2):701-4.
  70. Oremus M, Collet JP, Shapiro SH, Penrod J, Corcos J. Surgery versus collagen for female stress urinary incontinence: economic assessment in Ontario and Quebec. *The Canadian journal of urology*. 2003;10(4):1934-44.
  71. Tamanini JT, D'Ancona CA, Tadini V, Netto NR, Jr. Macroplastique implantation system for the treatment of female stress urinary incontinence. *The Journal of urology*. 2003;169(6):2229-33.
  72. Ghoniem G, Corcos J, Comiter C, Bernhard P, Westney OL, Herschorn S. Cross-linked polydimethylsiloxane injection for female stress urinary incontinence: results of a multicenter, randomized, controlled, single-blind study. *The Journal of urology*. 2009;181(1):204-10.
  73. Fernando RJ, Thakar R, Sultan AH, Shah SM, Jones PW. Effect of vaginal pessaries on symptoms associated with pelvic organ prolapse. *Obstetrics and gynecology*. 2006;108(1):93-9.
  74. Jarvis GJ. Surgery for genuine stress incontinence. *British journal of obstetrics and gynaecology*. 1994;101(5):371-4.
  75. Bergman A, Elia G. Three surgical procedures for genuine stress incontinence: five-year follow-up of a prospective randomized study. *American journal of obstetrics and gynecology*. 1995;173(1):66-71.
  76. Sivaslioglu AA, Caliskan E, Dolen I, Haberal A. A randomized comparison of transobturator tape and Burch colposuspension in the treatment of female stress urinary incontinence. *International urogynecology journal and pelvic floor dysfunction*. 2007;18(9):1015-9.
  77. Manca A, Sculpher MJ, Ward K, Hilton P. A cost-utility analysis of tension-free vaginal tape versus colposuspension for primary urodynamic stress incontinence. *BJOG : an international journal of obstetrics and gynaecology*. 2003;110(3):255-62.
  78. Karram MM, Angel O, Koonings P, Tabor B, Bergman A, Bhatia N. The modified Pereyra procedure: a clinical and urodynamic review. *British journal of obstetrics and gynaecology*. 1992;99(8):655-8.
  79. FitzGerald MP, Edwards SR, Fenner D. Medium-term follow-up on use of freeze-dried, irradiated donor fascia for sacrocolpopexy and sling procedures. *International urogynecology journal and pelvic floor dysfunction*. 2004;15(4):238-42.
  80. Amundsen CL, Visco AG, Ruiz H, Webster GD. Outcome in 104 pubovaginal slings using freeze-dried allograft fascia lata from a single tissue bank. *Urology*. 2000;56(6 Suppl 1):2-8.
  81. Walsh IK, Nambirajan T, Donellan SM, Mahendra V, Stone AR. Cadaveric fascia lata pubovaginal slings: early results on safety, efficacy and patient satisfaction. *BJU international*. 2002;90(4):415-9.



82. Sharifiaghdas F, Mortazavi N. Tension-free vaginal tape and autologous rectus fascia pubovaginal sling for the treatment of urinary stress incontinence: a medium-term follow-up. *Medical principles and practice : international journal of the Kuwait University, Health Science Centre*. 2008;17(3):209-14.
83. Mitsui T, Tanaka H, Moriya K, Kakizaki H, Nonomura K. Clinical and urodynamic outcomes of pubovaginal sling procedure with autologous rectus fascia for stress urinary incontinence. *International journal of urology : official journal of the Japanese Urological Association*. 2007;14(12):1076-9.
84. Giri SK, Hickey JP, Sil D, Mabadeje O, Shaikh FM, Narasimhulu G, et al. The long-term results of pubovaginal sling surgery using acellular cross-linked porcine dermis in the treatment of urodynamic stress incontinence. *The Journal of urology*. 2006;175(5):1788-92; discussion 93.
85. Novara G, Artibani W, Barber MD, Chapple CR, Costantini E, Ficarra V, et al. Updated systematic review and meta-analysis of the comparative data on colposuspensions, pubovaginal slings, and midurethral tapes in the surgical treatment of female stress urinary incontinence. *European urology*. 2010;58(2):218-38.
86. Ward KL, Hilton P, Uk, Ireland TVTTG. A prospective multicenter randomized trial of tension-free vaginal tape and colposuspension for primary urodynamic stress incontinence: two-year follow-up. *American journal of obstetrics and gynecology*. 2004;190(2):324-31.
87. Abdel-Fattah M, Barrington JW, Arunkalaivanan AS. Pelvicol pubovaginal sling versus tension-free vaginal tape for treatment of urodynamic stress incontinence: a prospective randomized three-year follow-up study. *European urology*. 2004;46(5):629-35.
88. Haab F, Trockman BA, Zimmern PE, Leach GE. Quality of life and continence assessment of the artificial urinary sphincter in men with minimum 3.5 years of followup. *The Journal of urology*. 1997;158(2):435-9.
89. Venn SN, Greenwell TJ, Mundy AR. The long-term outcome of artificial urinary sphincters. *The Journal of urology*. 2000;164(3 Pt 1):702-6; discussion 6-7.
90. Albo ME, Richter HE, Brubaker L, Norton P, Kraus SR, Zimmern PE, et al. Burch colposuspension versus fascial sling to reduce urinary stress incontinence. *The New England journal of medicine*. 2007;356(21):2143-55.
91. Hodroff MA, Sutherland SE, Kesha JB, Siegel SW. Treatment of stress incontinence with the SPARC sling: intraoperative and early complications of 445 patients. *Urology*. 2005;66(4):760-2.
92. Vervest HA, Bongers MY, van der Wurff AA. Nerve injury: an exceptional cause of pain after TVT. *International urogynecology journal and pelvic floor dysfunction*. 2006;17(6):665-7.
93. Karram MM, Segal JL, Vassallo BJ, Kleeman SD. Complications and untoward effects of the tension-free vaginal tape procedure. *Obstetrics and gynecology*. 2003;101(5 Pt 1):929-32.
94. Leach GE, Dmochowski RR, Appell RA, Blaivas JG, Hadley HR, Lubner KM, et al. Female Stress Urinary Incontinence Clinical Guidelines Panel summary report on surgical management of female stress urinary incontinence. *The American Urological Association. The Journal of urology*. 1997;158(3 Pt 1):875-80.
95. Tamussino KF, Hanzal E, Kolle D, Ralph G, Riss PA, Austrian Urogynecology Working G. Tension-free vaginal tape operation: results of the Austrian registry. *Obstetrics and gynecology*. 2001;98(5 Pt 1):732-6.
96. Meschia M, Pifarotti P, Bernasconi F, Magatti F, Vigano R, Bertozzi R, et al. Tension-free vaginal tape (TVT) and intravaginal slingplasty (IVS) for stress urinary

incontinence: a multicenter randomized trial. *American journal of obstetrics and gynecology*. 2006;195(5):1338-42.

97. Delorme E. [Transobturator urethral suspension: mini-invasive procedure in the treatment of stress urinary incontinence in women]. *Progres en urologie : journal de l'Association francaise d'urologie et de la Societe francaise d'urologie*. 2001;11(6):1306-13.

98. Schraffordt Koops SE, Bisseling TM, Heintz AP, Vervest HA. Prospective analysis of complications of tension-free vaginal tape from The Netherlands Tension-free Vaginal Tape study. *American journal of obstetrics and gynecology*. 2005;193(1):45-52.

99. Hammad FT, Kennedy-Smith A, Robinson RG. Erosions and urinary retention following polypropylene synthetic sling: Australasian survey. *European urology*. 2005;47(5):641-6; discussion 6-7.

100. Kuuva N, Nilsson CG. A nationwide analysis of complications associated with the tension-free vaginal tape (TVT) procedure. *Acta obstetrica et gynecologica Scandinavica*. 2002;81(1):72-7.

101. Benassi G, Marconi L, Accorsi F, Angeloni M, Benassi L. Abscess formation at the ischiorectal fossa 7 months after the application of a synthetic transobturator sling for stress urinary incontinence in a type II diabetic woman. *International urogynecology journal and pelvic floor dysfunction*. 2007;18(6):697-9.

102. Busby G, Broome J. Necrotising fasciitis following unrecognised bladder injury during transobturator sling procedure. *BJOG : an international journal of obstetrics and gynaecology*. 2007;114(1):111-2.

103. Deffieux X, Donnadieu AC, Mordefroid M, Levante S, Frydman R, Fernandez H. Prepubic and thigh abscess after successive placement of two suburethral slings. *International urogynecology journal and pelvic floor dysfunction*. 2007;18(5):571-4.

104. Zumbe J, Porres D, Degiorgis PL, Wyler S. Obturator and thigh abscess after transobturator tape implantation for stress urinary incontinence. *Urologia internationalis*. 2008;81(4):483-5.

105. Goldman HB. Large thigh abscess after placement of synthetic transobturator sling. *International urogynecology journal and pelvic floor dysfunction*. 2006;17(3):295-6.

106. Cardozo LD, Stanton SL. Genuine stress incontinence and detrusor instability--a review of 200 patients. *British journal of obstetrics and gynaecology*. 1980;87(3):184-90.

107. Azam U, Frazer MI, Kozman EL, Ward K, Hilton P, Rane A. The tension-free vaginal tape procedure in women with previous failed stress incontinence surgery. *The Journal of urology*. 2001;166(2):554-6.

108. Yalcin I, Versi E, Benson JT, Schafer W, Bump RC. Validation of a clinical algorithm to diagnose stress urinary incontinence for large studies. *The Journal of urology*. 2004;171(6 Pt 1):2321-5.

109. Matharu GS, Assassa RP, Williams KS, Donaldson M, Matthews R, Tincello DG, et al. Objective assessment of urinary incontinence in women: comparison of the one-hour and 24-hour pad tests. *European urology*. 2004;45(2):208-12.

110. Jorgensen L, Lose G, Andersen JT. One-hour pad-weighing test for objective assessment of female urinary incontinence. *Obstetrics and gynecology*. 1987;69(1):39-42.

111. Karantanis E, Allen W, Stevermuer TL, Simons AM, O'Sullivan R, Moore KH. The repeatability of the 24-hour pad test. *International urogynecology journal and pelvic floor dysfunction*. 2005;16(1):63-8; discussion 8.

112. Wyman JF, Choi SC, Harkins SW, Wilson MS, Fantl JA. The urinary diary in evaluation of incontinent women: a test-retest analysis. *Obstetrics and gynecology*. 1988;71(6 Pt 1):812-7.
113. de Boer TA, Salvatore S, Cardozo L, Chapple C, Kelleher C, van Kerrebroeck P, et al. Pelvic organ prolapse and overactive bladder. *Neurourology and urodynamics*. 2010;29(1):30-9.
114. Mant J, Painter R, Vessey M. Epidemiology of genital prolapse: observations from the Oxford Family Planning Association Study. *British journal of obstetrics and gynaecology*. 1997;104(5):579-85.
115. Bland DR, Earle BB, Vitolins MZ, Burke G. Use of the Pelvic Organ Prolapse staging system of the International Continence Society, American Urogynecologic Society, and Society of Gynecologic Surgeons in perimenopausal women. *American journal of obstetrics and gynecology*. 1999;181(6):1324-7; discussion 7-8.
116. Versi E, Harvey MA, Cardozo L, Brincat M, Studd JW. Urogenital prolapse and atrophy at menopause: a prevalence study. *International urogynecology journal and pelvic floor dysfunction*. 2001;12(2):107-10.
117. Swift SE. The distribution of pelvic organ support in a population of female subjects seen for routine gynecologic health care. *American journal of obstetrics and gynecology*. 2000;183(2):277-85.
118. Samuelsson EC, Victor FT, Tibblin G, Svardsudd KF. Signs of genital prolapse in a Swedish population of women 20 to 59 years of age and possible related factors. *American journal of obstetrics and gynecology*. 1999;180(2 Pt 1):299-305.
119. Fritel X, Varnoux N, Zins M, Breart G, Ringa V. Symptomatic pelvic organ prolapse at midlife, quality of life, and risk factors. *Obstetrics and gynecology*. 2009;113(3):609-16.
120. Slieker-ten Hove MC, Pool-Goudzwaard AL, Eijkemans MJ, Steegers-Theunissen RP, Burger CW, Vierhout ME. Symptomatic pelvic organ prolapse and possible risk factors in a general population. *American journal of obstetrics and gynecology*. 2009;200(2):184 e1-7.
121. Smith FJ, Holman CD, Moorin RE, Tsokos N. Lifetime risk of undergoing surgery for pelvic organ prolapse. *Obstetrics and gynecology*. 2010;116(5):1096-100.
122. Brown JS, Waetjen LE, Subak LL, Thom DH, Van den Eeden S, Vittinghoff E. Pelvic organ prolapse surgery in the United States, 1997. *American journal of obstetrics and gynecology*. 2002;186(4):712-6.
123. DeLancey JO. Anatomic aspects of vaginal eversion after hysterectomy. *American journal of obstetrics and gynecology*. 1992;166(6 Pt 1):1717-24; discussion 24-8.
124. Kerkhof MH, Hendriks L, Brolmann HA. Changes in connective tissue in patients with pelvic organ prolapse--a review of the current literature. *International urogynecology journal and pelvic floor dysfunction*. 2009;20(4):461-74.
125. Santoro GA, Wiczorek AP, Stankiewicz A, Wozniak MM, Bogusiewicz M, Rechberger T. High-resolution three-dimensional endovaginal ultrasonography in the assessment of pelvic floor anatomy: a preliminary study. *International urogynecology journal and pelvic floor dysfunction*. 2009;20(10):1213-22.
126. Majida M, Braekken IH, Umek W, Bo K, Saltyte Benth J, Ellstrom Engh M. Interobserver repeatability of three- and four-dimensional transperineal ultrasound assessment of pelvic floor muscle anatomy and function. *Ultrasound in obstetrics & gynecology : the official journal of the International Society of Ultrasound in Obstetrics and Gynecology*. 2009;33(5):567-73.

127. Broekhuis SR, Futterer JJ, Barentsz JO, Vierhout ME, Kluivers KB. A systematic review of clinical studies on dynamic magnetic resonance imaging of pelvic organ prolapse: the use of reference lines and anatomical landmarks. *International urogynecology journal and pelvic floor dysfunction*. 2009;20(6):721-9.
128. Makinen J, Soderstrom KO, Kiilholma P, Hirvonen T. Histological changes in the vaginal connective tissue of patients with and without uterine prolapse. *Archives of gynecology*. 1986;239(1):17-20.
129. Lewicky-Gaupp C, Yousuf A, Larson KA, Fenner DE, Delancey JO. Structural position of the posterior vagina and pelvic floor in women with and without posterior vaginal prolapse. *American journal of obstetrics and gynecology*. 2010;202(5):497 e1-6.
130. Hjartardottir S, Nilsson J, Petersen C, Lingman G. The female pelvic floor: a dome--not a basin. *Acta obstetrica et gynecologica Scandinavica*. 1997;76(6):567-71.
131. Silva-Filho AL, Saleme CS, Roza T, Martins PA, Parente MM, Pinotti M, et al. Evaluation of pelvic floor muscle cross-sectional area using a 3D computer model based on MRI in women with and without prolapse. *European journal of obstetrics, gynecology, and reproductive biology*. 2010;153(1):110-1.
132. DeLancey JO, Morgan DM, Fenner DE, Kearney R, Guire K, Miller JM, et al. Comparison of levator ani muscle defects and function in women with and without pelvic organ prolapse. *Obstetrics and gynecology*. 2007;109(2 Pt 1):295-302.
133. Hoyte L, Schierlitz L, Zou K, Flesh G, Fielding JR. Two- and 3-dimensional MRI comparison of levator ani structure, volume, and integrity in women with stress incontinence and prolapse. *American journal of obstetrics and gynecology*. 2001;185(1):11-9.
134. DeLancey JO. Anatomy and biomechanics of genital prolapse. *Clinical obstetrics and gynecology*. 1993;36(4):897-909.
135. Handa VL, Garrett E, Hendrix S, Gold E, Robbins J. Progression and remission of pelvic organ prolapse: a longitudinal study of menopausal women. *American journal of obstetrics and gynecology*. 2004;190(1):27-32.
136. Nygaard I, Bradley C, Brandt D, Women's Health I. Pelvic organ prolapse in older women: prevalence and risk factors. *Obstetrics and gynecology*. 2004;104(3):489-97.
137. Lukacz ES, Lawrence JM, Contreras R, Nager CW, Lubner KM. Parity, mode of delivery, and pelvic floor disorders. *Obstetrics and gynecology*. 2006;107(6):1253-60.
138. Rortveit G, Brown JS, Thom DH, Van Den Eeden SK, Creasman JM, Subak LL. Symptomatic pelvic organ prolapse: prevalence and risk factors in a population-based, racially diverse cohort. *Obstetrics and gynecology*. 2007;109(6):1396-403.
139. Zhu L, Bian XM, Long Y, Lang JH. Role of different childbirth strategies on pelvic organ prolapse and stress urinary incontinence: a prospective study. *Chinese medical journal*. 2008;121(3):213-5.
140. Swift S, Woodman P, O'Boyle A, Kahn M, Valley M, Bland D, et al. Pelvic Organ Support Study (POSST): the distribution, clinical definition, and epidemiologic condition of pelvic organ support defects. *American journal of obstetrics and gynecology*. 2005;192(3):795-806.
141. Miedel A, Tegerstedt G, Maehle-Schmidt M, Nyren O, Hammarstrom M. Nonobstetric risk factors for symptomatic pelvic organ prolapse. *Obstetrics and gynecology*. 2009;113(5):1089-97.
142. Kudish BI, Iglesia CB, Sokol RJ, Cochrane B, Richter HE, Larson J, et al. Effect of weight change on natural history of pelvic organ prolapse. *Obstetrics and gynecology*. 2009;113(1):81-8.

143. McLennan MT, Harris JK, Kariuki B, Meyer S. Family history as a risk factor for pelvic organ prolapse. *International urogynecology journal and pelvic floor dysfunction*. 2008;19(8):1063-9.
144. Rinne KM, Kirkinen PP. What predisposes young women to genital prolapse? *European journal of obstetrics, gynecology, and reproductive biology*. 1999;84(1):23-5.
145. Nikolova G, Lee H, Berkovitz S, Nelson S, Sinsheimer J, Vilain E, et al. Sequence variant in the laminin gamma1 (LAMC1) gene associated with familial pelvic organ prolapse. *Human genetics*. 2007;120(6):847-56.
146. Strohbehn K, Jakary JA, Delancey JO. Pelvic organ prolapse in young women. *Obstetrics and gynecology*. 1997;90(1):33-6.
147. Moen MD, Noone MB, Vassallo BJ, Elser DM, Urogynecology N. Pelvic floor muscle function in women presenting with pelvic floor disorders. *International urogynecology journal and pelvic floor dysfunction*. 2009;20(7):843-6.
148. Hagen S, Stark D, Maher C, Adams E. Conservative management of pelvic organ prolapse in women. *The Cochrane database of systematic reviews*. 2006(4):CD003882.
149. Hagen S, Stark D, Glazener C, Sinclair L, Ramsay I. A randomized controlled trial of pelvic floor muscle training for stages I and II pelvic organ prolapse. *International urogynecology journal and pelvic floor dysfunction*. 2009;20(1):45-51.
150. Pott-Grinstein E, Newcomer JR. Gynecologists' patterns of prescribing pessaries. *The Journal of reproductive medicine*. 2001;46(3):205-8.
151. Handa VL, Jones M. Do pessaries prevent the progression of pelvic organ prolapse? *International urogynecology journal and pelvic floor dysfunction*. 2002;13(6):349-51; discussion 52.
152. Jia X, Glazener C, Mowatt G, MacLennan G, Bain C, Fraser C, et al. Efficacy and safety of using mesh or grafts in surgery for anterior and/or posterior vaginal wall prolapse: systematic review and meta-analysis. *BJOG : an international journal of obstetrics and gynaecology*. 2008;115(11):1350-61.
153. Foon R, Tooze-Hobson P, Latthe PM. Adjuvant materials in anterior vaginal wall prolapse surgery: a systematic review of effectiveness and complications. *International urogynecology journal and pelvic floor dysfunction*. 2008;19(12):1697-706.
154. Gauruder-Burmester A, Koutouzidou P, Rohne J, Gronewold M, Tunn R. Follow-up after polypropylene mesh repair of anterior and posterior compartments in patients with recurrent prolapse. *International urogynecology journal and pelvic floor dysfunction*. 2007;18(9):1059-64.
155. Mushinski M. Hysterectomy charges: geographic variations United States, 1994. *Statistical bulletin*. 1996;77(1):2-12.
156. Richter K. [The surgical anatomy of the vaginaefixatio sacrospinalis vaginalis. A contribution to the surgical treatment of vaginal blind pouch prolapse]. *Geburtshilfe und Frauenheilkunde*. 1968;28(4):321-7.
157. Cruikshank SH. Sacrospinous fixation--should this be performed at the time of vaginal hysterectomy? *American journal of obstetrics and gynecology*. 1991;164(4):1072-6.
158. Sand PK, Koduri S, Lobel RW, Winkler HA, Tomezsko J, Culligan PJ, et al. Prospective randomized trial of polyglactin 910 mesh to prevent recurrence of cystoceles and rectoceles. *American journal of obstetrics and gynecology*. 2001;184(7):1357-62; discussion 62-4.
159. Roovers JP, van der Vaart CH, van der Bom JG, van Leeuwen JH, Scholten PC, Heintz AP. A randomised controlled trial comparing abdominal and vaginal prolapse

- surgery: effects on urogenital function. *BJOG : an international journal of obstetrics and gynaecology*. 2004;111(1):50-6.
160. Maher C, Baessler K, Glazener CM, Adams EJ, Hagen S. Surgical management of pelvic organ prolapse in women: a short version Cochrane review. *Neurourology and urodynamics*. 2008;27(1):3-12.
  161. Culligan PJ, Blackwell L, Goldsmith LJ, Graham CA, Rogers A, Heit MH. A randomized controlled trial comparing fascia lata and synthetic mesh for sacral colpopexy. *Obstetrics and gynecology*. 2005;106(1):29-37.
  162. Nygaard IE, McCreery R, Brubaker L, Connolly A, Cundiff G, Weber AM, et al. Abdominal sacrocolpopexy: a comprehensive review. *Obstetrics and gynecology*. 2004;104(4):805-23.
  163. Flynn MK, Webster GD, Amundsen CL. Abdominal sacral colpopexy with allograft fascia lata: one-year outcomes. *American journal of obstetrics and gynecology*. 2005;192(5):1496-500.
  164. Leventoglu S, Menten BB, Akin M, Karen M, Karamercan A, Oguz M. Transperineal rectocele repair with polyglycolic acid mesh: a case series. *Diseases of the colon and rectum*. 2007;50(12):2085-92; discussion 92-5.
  165. de Tayrac R, Picone O, Chauveaud-Lambling A, Fernandez H. A 2-year anatomical and functional assessment of transvaginal rectocele repair using a polypropylene mesh. *International urogynecology journal and pelvic floor dysfunction*. 2006;17(2):100-5.
  166. de Tayrac R, Devoldere G, Renaudie J, Villard P, Guilbaud O, Eglin G, et al. Prolapse repair by vaginal route using a new protected low-weight polypropylene mesh: 1-year functional and anatomical outcome in a prospective multicentre study. *International urogynecology journal and pelvic floor dysfunction*. 2007;18(3):251-6.
  167. Kleeman S, Vassallo B, Segal J, Hungler M, Karram M. The ability of history and a negative cough stress test to detect occult stress incontinence in patients undergoing surgical repair of advanced pelvic organ prolapse. *International urogynecology journal and pelvic floor dysfunction*. 2006;17(1):27-9.
  168. Burgio KL, Nygaard IE, Richter HE, Brubaker L, Gutman RE, Leng W, et al. Bladder symptoms 1 year after abdominal sacrocolpopexy with and without Burch colposuspension in women without preoperative stress incontinence symptoms. *American journal of obstetrics and gynecology*. 2007;197(6):647 e1-6.
  169. Brubaker L, Nygaard I, Richter HE, Visco A, Weber AM, Cundiff GW, et al. Two-year outcomes after sacrocolpopexy with and without burch to prevent stress urinary incontinence. *Obstetrics and gynecology*. 2008;112(1):49-55.
  170. Whitehead WE, Bradley CS, Brown MB, Brubaker L, Gutman RE, Varner RE, et al. Gastrointestinal complications following abdominal sacrocolpopexy for advanced pelvic organ prolapse. *American journal of obstetrics and gynecology*. 2007;197(1):78 e1-7.
  171. Burrows LJ, Meyn LA, Walters MD, Weber AM. Pelvic symptoms in women with pelvic organ prolapse. *Obstetrics and gynecology*. 2004;104(5 Pt 1):982-8.
  172. Olsen AL, Smith VJ, Bergstrom JO, Colling JC, Clark AL. Epidemiology of surgically managed pelvic organ prolapse and urinary incontinence. *Obstetrics and gynecology*. 1997;89(4):501-6.
  173. Fialkow MF, Newton KM, Lentz GM, Weiss NS. Lifetime risk of surgical management for pelvic organ prolapse or urinary incontinence. *International urogynecology journal and pelvic floor dysfunction*. 2008;19(3):437-40.
  174. Nichols DH. What is new in vaginal surgery? *International urogynecology journal and pelvic floor dysfunction*. 1996;7(3):115-6.

175. Morgan DM, Cardoza P, Guire K, Fenner DE, DeLancey JO. Levator ani defect status and lower urinary tract symptoms in women with pelvic organ prolapse. *International urogynecology journal*. 2010;21(1):47-52.
176. Dietz HP, Lanzarone V. Levator trauma after vaginal delivery. *Obstetrics and gynecology*. 2005;106(4):707-12.
177. DeLancey JO, Trowbridge ER, Miller JM, Morgan DM, Guire K, Fenner DE, et al. Stress urinary incontinence: relative importance of urethral support and urethral closure pressure. *The Journal of urology*. 2008;179(6):2286-90; discussion 90.
178. Dietz HP, Steensma AB. The prevalence of major abnormalities of the levator ani in urogynaecological patients. *BJOG : an international journal of obstetrics and gynaecology*. 2006;113(2):225-30.
179. DeLancey JO, Miller JM, Kearney R, Howard D, Reddy P, Umek W, et al. Vaginal birth and de novo stress incontinence: relative contributions of urethral dysfunction and mobility. *Obstetrics and gynecology*. 2007;110(2 Pt 1):354-62.
180. Clobes A, DeLancey JO, Morgan DM. Urethral circular smooth muscle in young and old women. *American journal of obstetrics and gynecology*. 2008;198(5):587 e1-5.
181. Rud T. Urethral pressure profile in continent women from childhood to old age. *Acta obstetrica et gynecologica Scandinavica*. 1980;59(4):331-5.
182. Goh JT. Biomechanical and biochemical assessments for pelvic organ prolapse. *Current opinion in obstetrics & gynecology*. 2003;15(5):391-4.
183. Salman MC, Ozyuncu O, Sargon MF, Kucukali T, Durukan T. Light and electron microscopic evaluation of cardinal ligaments in women with or without uterine prolapse. *International urogynecology journal*. 2010;21(2):235-9.
184. Chin HY, Changchien E, Chiang CH, Yang HP. Extraordinary muscular structure leads to urethral injury after vaginal delivery in animal study. *International urogynecology journal*. 2010;21(10):1231-6.
185. Ramachandran GN, Kartha G. Structure of collagen. *Nature*. 1955;176(4482):593-5.
186. Birk DE. Type V collagen: heterotypic type I/V collagen interactions in the regulation of fibril assembly. *Micron*. 2001;32(3):223-37.
187. Birk DE, Fitch JM, Babiarz JP, Doane KJ, Linsenmayer TF. Collagen fibrillogenesis in vitro: interaction of types I and V collagen regulates fibril diameter. *Journal of cell science*. 1990;95 ( Pt 4):649-57.
188. Bailey AJ, Paul RG, Knott L. Mechanisms of maturation and ageing of collagen. *Mechanisms of ageing and development*. 1998;106(1-2):1-56.
189. Paul RG, Bailey AJ. Glycation of collagen: the basis of its central role in the late complications of ageing and diabetes. *The international journal of biochemistry & cell biology*. 1996;28(12):1297-310.
190. Mott JD, Werb Z. Regulation of matrix biology by matrix metalloproteinases. *Current opinion in cell biology*. 2004;16(5):558-64.
191. Gomez DE, Alonso DF, Yoshiji H, Thorgeirsson UP. Tissue inhibitors of metalloproteinases: structure, regulation and biological functions. *European journal of cell biology*. 1997;74(2):111-22.
192. Kremer EA, Chen Y, Suzuki K, Nagase H, Gorski JP. Hydroxyapatite induces autolytic degradation and inactivation of matrix metalloproteinase-1 and -3. *Journal of bone and mineral research : the official journal of the American Society for Bone and Mineral Research*. 1998;13(12):1890-902.
193. Reay Jones NH, Healy JC, King LJ, Saini S, Shousha S, Allen-Mersh TG. Pelvic connective tissue resilience decreases with vaginal delivery, menopause and uterine prolapse. *The British journal of surgery*. 2003;90(4):466-72.

194. Lei L, Song Y, Chen R. Biomechanical properties of prolapsed vaginal tissue in pre- and postmenopausal women. *International urogynecology journal and pelvic floor dysfunction*. 2007;18(6):603-7.
195. Kokcu A, Yanik F, Cetinkaya M, Alper T, Kandemir B, Malatyalioglu E. Histopathological evaluation of the connective tissue of the vaginal fascia and the uterine ligaments in women with and without pelvic relaxation. *Archives of gynecology and obstetrics*. 2002;266(2):75-8.
196. Liapis A, Bakas P, Pafiti A, Frangos-Plemenos M, Arnoyannaki N, Creatsas G. Changes of collagen type III in female patients with genuine stress incontinence and pelvic floor prolapse. *European journal of obstetrics, gynecology, and reproductive biology*. 2001;97(1):76-9.
197. Vulic M, Strinic T, Tomic S, Capkun V, Jakus IA, Ivica S. Difference in expression of collagen type I and matrix metalloproteinase-1 in uterosacral ligaments of women with and without pelvic organ prolapse. *European journal of obstetrics, gynecology, and reproductive biology*. 2011;155(2):225-8.
198. Ewies AA, Al-Azzawi F, Thompson J. Changes in extracellular matrix proteins in the cardinal ligaments of post-menopausal women with or without prolapse: a computerized immunohistomorphometric analysis. *Human reproduction*. 2003;18(10):2189-95.
199. Moalli PA, Talarico LC, Sung VW, Klingensmith WL, Shand SH, Meyn LA, et al. Impact of menopause on collagen subtypes in the arcus tendineous fasciae pelvis. *American journal of obstetrics and gynecology*. 2004;190(3):620-7.
200. Soderberg MW, Falconer C, Bystrom B, Malmstrom A, Ekman G. Young women with genital prolapse have a low collagen concentration. *Acta obstetrica et gynecologica Scandinavica*. 2004;83(12):1193-8.
201. Goepel C, Hefler L, Methfessel HD, Koelbl H. Periurethral connective tissue status of postmenopausal women with genital prolapse with and without stress incontinence. *Acta obstetrica et gynecologica Scandinavica*. 2003;82(7):659-64.
202. Trabucco E, Soderberg M, Cobellis L, Torella M, Bystrom B, Ekman-Ordeberg G, et al. Role of proteoglycans in the organization of periurethral connective tissue in women with stress urinary incontinence. *Maturitas*. 2007;58(4):395-405.
203. Dviri M, Leron E, Dreihier J, Mazor M, Shaco-Levy R. Increased matrix metalloproteinases-1,-9 in the uterosacral ligaments and vaginal tissue from women with pelvic organ prolapse. *European journal of obstetrics, gynecology, and reproductive biology*. 2011;156(1):113-7.
204. Strinic T, Vulic M, Tomic S, Capkun V, Stipic I, Alujevic I. Matrix metalloproteinases-1, -2 expression in uterosacral ligaments from women with pelvic organ prolapse. *Maturitas*. 2009;64(2):132-5.
205. Gabriel B, Watermann D, Hancke K, Gitsch G, Werner M, Tempfer C, et al. Increased expression of matrix metalloproteinase 2 in uterosacral ligaments is associated with pelvic organ prolapse. *International urogynecology journal and pelvic floor dysfunction*. 2006;17(5):478-82.
206. Phillips CH, Anthony F, Benyon C, Monga AK. Collagen metabolism in the uterosacral ligaments and vaginal skin of women with uterine prolapse. *BJOG : an international journal of obstetrics and gynaecology*. 2006;113(1):39-46.
207. Jackson SR, Avery NC, Tarlton JF, Eckford SD, Abrams P, Bailey AJ. Changes in metabolism of collagen in genitourinary prolapse. *Lancet*. 1996;347(9016):1658-61.
208. Chen BH, Wen Y, Li H, Polan ML. Collagen metabolism and turnover in women with stress urinary incontinence and pelvic prolapse. *International urogynecology journal and pelvic floor dysfunction*. 2002;13(2):80-7; discussion 7.



209. Ritz-Timme S, Laumeier I, Collins MJ. Aspartic acid racemization: evidence for marked longevity of elastin in human skin. *The British journal of dermatology*. 2003;149(5):951-9.
210. Liu X, Zhao Y, Pawlyk B, Damaser M, Li T. Failure of elastic fiber homeostasis leads to pelvic floor disorders. *The American journal of pathology*. 2006;168(2):519-28.
211. Nakamura T, Lozano PR, Ikeda Y, Iwanaga Y, Hinek A, Minamisawa S, et al. Fibulin-5/DANCE is essential for elastogenesis in vivo. *Nature*. 2002;415(6868):171-5.
212. Alperin M, Debes K, Abramowitch S, Meyn L, Moalli PA. LOXL1 deficiency negatively impacts the biomechanical properties of the mouse vagina and supportive tissues. *International urogynecology journal and pelvic floor dysfunction*. 2008;19(7):977-86.
213. Soderberg MW, Bystrom B, Kalamajski S, Malmstrom A, Ekman-Ordeberg G. Gene expressions of small leucine-rich repeat proteoglycans and fibulin-5 are decreased in pelvic organ prolapse. *Molecular human reproduction*. 2009;15(4):251-7.
214. Takacs P, Gualtieri M, Nassiri M, Candiotti K, Fornoni A, Medina CA. Differential expression of smooth muscle regulatory proteins in the uterosacral ligaments of women with uterine prolapse. *American journal of obstetrics and gynecology*. 2010;202(6):620 e1-5.
215. Takacs P, Nassiri M, Vician A, Candiotti K, Fornoni A, Medina CA. Fibulin-5 expression is decreased in women with anterior vaginal wall prolapse. *International urogynecology journal and pelvic floor dysfunction*. 2009;20(2):207-11.
216. Jung HJ, Jeon MJ, Yim GW, Kim SK, Choi JR, Bai SW. Changes in expression of fibulin-5 and lysyl oxidase-like 1 associated with pelvic organ prolapse. *European journal of obstetrics, gynecology, and reproductive biology*. 2009;145(1):117-22.
217. Kuang PP, Goldstein RH, Liu Y, Rishikof DC, Jean JC, Joyce-Brady M. Coordinate expression of fibulin-5/DANCE and elastin during lung injury repair. *American journal of physiology Lung cellular and molecular physiology*. 2003;285(5):L1147-52.
218. Yamamoto K, Yamamoto M, Akazawa K, Tajima S, Wakimoto H, Aoyagi M. Decrease in elastin gene expression and protein synthesis in fibroblasts derived from cardinal ligaments of patients with prolapsus uteri. *Cell biology international*. 1997;21(9):605-11.
219. Goepel C. Differential elastin and tenascin immunolabeling in the uterosacral ligaments in postmenopausal women with and without pelvic organ prolapse. *Acta histochemica*. 2008;110(3):204-9.
220. Karam JA, Vazquez DV, Lin VK, Zimmern PE. Elastin expression and elastic fibre width in the anterior vaginal wall of postmenopausal women with and without prolapse. *BJU international*. 2007;100(2):346-50.
221. Lin SY, Tee YT, Ng SC, Chang H, Lin P, Chen GD. Changes in the extracellular matrix in the anterior vagina of women with or without prolapse. *International urogynecology journal and pelvic floor dysfunction*. 2007;18(1):43-8.
222. Chen B, Wen Y, Polan ML. Elastolytic activity in women with stress urinary incontinence and pelvic organ prolapse. *Neurourology and urodynamics*. 2004;23(2):119-26.
223. Chen B, Wen Y, Yu X, Polan ML. The role of neutrophil elastase in elastin metabolism of pelvic tissues from women with stress urinary incontinence. *Neurourology and urodynamics*. 2007;26(2):274-9.
224. Poncet S, Meyer S, Richard C, Aubert JD, Juillerat-Jeanneret L. The expression and function of the endothelin system in contractile properties of vaginal myofibroblasts

- of women with uterovaginal prolapse. *American journal of obstetrics and gynecology*. 2005;192(2):426-32.
225. Meyer S, Achtari C, Hohlfeld P, Juillerat-Jeanneret L. The contractile properties of vaginal myofibroblasts: is the myofibroblasts contraction force test a valuable indication of future prolapse development? *International urogynecology journal and pelvic floor dysfunction*. 2008;19(10):1399-403.
  226. Ewies AA, Elshafie M, Li J, Stanley A, Thompson J, Styles J, et al. Changes in transcription profile and cytoskeleton morphology in pelvic ligament fibroblasts in response to stretch: the effects of estradiol and levormeloxifene. *Molecular human reproduction*. 2008;14(2):127-35.
  227. Wen Y, Zhao YY, Polan ML, Chen B. Effect of relaxin on TGF-beta1 expression in cultured vaginal fibroblasts from women with stress urinary incontinence. *Reproductive sciences*. 2008;15(3):312-20.
  228. Makinen J, Kahari VM, Soderstrom KO, Vuorio E, Hirvonen T. Collagen synthesis in the vaginal connective tissue of patients with and without uterine prolapse. *European journal of obstetrics, gynecology, and reproductive biology*. 1987;24(4):319-25.
  229. Moehrer B, Hextall A, Jackson S. Oestrogens for urinary incontinence in women. *The Cochrane database of systematic reviews*. 2003(2):CD001405.
  230. Savvas M, Bishop J, Laurent G, Watson N, Studd J. Type III collagen content in the skin of postmenopausal women receiving oestradiol and testosterone implants. *British journal of obstetrics and gynaecology*. 1993;100(2):154-6.
  231. Brincat M, Moniz CF, Kabalan S, Versi E, O'Dowd T, Magos AL, et al. Decline in skin collagen content and metacarpal index after the menopause and its prevention with sex hormone replacement. *British journal of obstetrics and gynaecology*. 1987;94(2):126-9.
  232. Brincat M, Kabalan S, Studd JW, Moniz CF, de Trafford J, Montgomery J. A study of the decrease of skin collagen content, skin thickness, and bone mass in the postmenopausal woman. *Obstetrics and gynecology*. 1987;70(6):840-5.
  233. Bai SW, Chung DJ, Yoon JM, Shin JS, Kim SK, Park KH. Roles of estrogen receptor, progesterone receptor, p53 and p21 in pathogenesis of pelvic organ prolapse. *International urogynecology journal and pelvic floor dysfunction*. 2005;16(6):492-6.
  234. Lang JH, Zhu L, Sun ZJ, Chen J. Estrogen levels and estrogen receptors in patients with stress urinary incontinence and pelvic organ prolapse. *International journal of gynaecology and obstetrics: the official organ of the International Federation of Gynaecology and Obstetrics*. 2003;80(1):35-9.
  235. Ewies AA, Thompson J, Al-Azzawi F. Changes in gonadal steroid receptors in the cardinal ligaments of prolapsed uteri: immunohistomorphometric data. *Human reproduction*. 2004;19(7):1622-8.
  236. Chen B, Wen Y, Wang H, Polan ML. Differences in estrogen modulation of tissue inhibitor of matrix metalloproteinase-1 and matrix metalloproteinase-1 expression in cultured fibroblasts from continent and incontinent women. *American journal of obstetrics and gynecology*. 2003;189(1):59-65.
  237. Wen Y, Polan ML, Chen B. Do extracellular matrix protein expressions change with cyclic reproductive hormones in pelvic connective tissue from women with stress urinary incontinence? *Human reproduction*. 2006;21(5):1266-73.
  238. Zong W, Zyczynski HM, Meyn LA, Gordy SC, Moalli PA. Regulation of MMP-1 by sex steroid hormones in fibroblasts derived from the female pelvic floor. *American journal of obstetrics and gynecology*. 2007;196(4):349 e1-11.

239. Zong W, Meyn LA, Moalli PA. The amount and activity of active matrix metalloproteinase 13 is suppressed by estradiol and progesterone in human pelvic floor fibroblasts. *Biology of reproduction*. 2009;80(2):367-74.
240. Ahn KH, Kim T, Hur JY, Kim SH, Lee KW, Kim YT. Relationship between serum estradiol and follicle-stimulating hormone levels and urodynamic results in women with stress urinary incontinence. *International urogynecology journal*. 2011;22(6):731-7.
241. DeLancey JO, Starr RA. Histology of the connection between the vagina and levator ani muscles. Implications for urinary tract function. *The Journal of reproductive medicine*. 1990;35(8):765-71.
242. Badiou W, Granier G, Bousquet PJ, Monrozies X, Mares P, de Tayrac R. Comparative histological analysis of anterior vaginal wall in women with pelvic organ prolapse or control subjects. A pilot study. *International urogynecology journal and pelvic floor dysfunction*. 2008;19(5):723-9.
243. Ford LE, Seow CY, Pratusевич VR. Plasticity in smooth muscle, a hypothesis. *Canadian journal of physiology and pharmacology*. 1994;72(11):1320-4.
244. Ueki N, Sobue K, Kanda K, Hada T, Higashino K. Expression of high and low molecular weight caldesmons during phenotypic modulation of smooth muscle cells. *Proceedings of the National Academy of Sciences of the United States of America*. 1987;84(24):9049-53.
245. Payne AM, Yue P, Pritchard K, Marston SB. Caldesmon mRNA splicing and isoform expression in mammalian smooth-muscle and non-muscle tissues. *The Biochemical journal*. 1995;305 ( Pt 2):445-50.
246. Takacs P, Nassiri M, Gualtieri M, Candiotti K, Medina CA. Uterosacral ligament smooth muscle cell apoptosis is increased in women with uterine prolapse. *Reproductive sciences*. 2009;16(5):447-52.
247. Gunst SJ, Fredberg JJ. The first three minutes: smooth muscle contraction, cytoskeletal events, and soft glasses. *Journal of applied physiology*. 2003;95(1):413-25.
248. Katsuyama H, Wang CL, Morgan KG. Regulation of vascular smooth muscle tone by caldesmon. *The Journal of biological chemistry*. 1992;267(21):14555-8.
249. Ansari S, Alahyan M, Marston SB, El-Mezgueldi M. Role of caldesmon in the Ca<sup>2+</sup> regulation of smooth muscle thin filaments: evidence for a cooperative switching mechanism. *The Journal of biological chemistry*. 2008;283(1):47-56.
250. Li Y, Lin JL, Reiter RS, Daniels K, Soll DR, Lin JJ. Caldesmon mutant defective in Ca(2+)-calmodulin binding interferes with assembly of stress fibers and affects cell morphology, growth and motility. *Journal of cell science*. 2004;117(Pt 16):3593-604.
251. Boreham MK, Miller RT, Schaffer JJ, Word RA. Smooth muscle myosin heavy chain and caldesmon expression in the anterior vaginal wall of women with and without pelvic organ prolapse. *American journal of obstetrics and gynecology*. 2001;185(4):944-52.
252. Northington GM, Basha M, Arya LA, Wein AJ, Chacko S. Contractile response of human anterior vaginal muscularis in women with and without pelvic organ prolapse. *Reproductive sciences*. 2011;18(3):296-303.
253. Sun MJ, Cheng WL, Wei YH, Kuo CL, Sun S, Tsai HD, et al. Low copy number and high 4977 deletion of mitochondrial DNA in uterosacral ligaments are associated with pelvic organ prolapse progression. *International urogynecology journal and pelvic floor dysfunction*. 2009;20(7):867-72.

254. Yiou R, Authier FJ, Gherardi R, Abbou C. Evidence of mitochondrial damage in the levator ani muscle of women with pelvic organ prolapse. *European urology*. 2009;55(5):1241-3.
255. Helt M, Benson JT, Russell B, Brubaker L. Levator ani muscle in women with genitourinary prolapse: indirect assessment by muscle histopathology. *Neurourology and urodynamics*. 1996;15(1):17-29.
256. Dimpfl T, Jaeger C, Mueller-Felber W, Anthuber C, Hirsch A, Brandmaier R, et al. Myogenic changes of the levator ani muscle in premenopausal women: the impact of vaginal delivery and age. *Neurourology and urodynamics*. 1998;17(3):197-205.
257. Connell KA, Guess MK, Chen H, Andikyan V, Bercik R, Taylor HS. HOXA11 is critical for development and maintenance of uterosacral ligaments and deficient in pelvic prolapse. *The Journal of clinical investigation*. 2008;118(3):1050-5.
258. Ulmsten U, Petros P. Intravaginal slingplasty (IVS): an ambulatory surgical procedure for treatment of female urinary incontinence. *Scandinavian journal of urology and nephrology*. 1995;29(1):75-82.
259. Julian TM. The efficacy of Marlex mesh in the repair of severe, recurrent vaginal prolapse of the anterior midvaginal wall. *American journal of obstetrics and gynecology*. 1996;175(6):1472-5.
260. Hinoul P, Roovers JP, Ombelet W, Vanspauwen R. Surgical management of urinary stress incontinence in women: a historical and clinical overview. *European journal of obstetrics, gynecology, and reproductive biology*. 2009;145(2):219-25.
261. Tommaso Falcone HPL, Marjorie Shulman, Mary Beth Ritchey, Nancy Pressly, Colin Anderson-Smits, Jill Brown, Julia Corrado, Cara Krulewitch, Shanika Craig. FDA Commissioned Meeting Materials of the Obstetrics and Gynecology Devices Panel. <http://www.fda.gov/AdvisoryCommittees/CommitteesMeetingMaterials/MedicalDevices/MedicalDevicesAdvisoryCommittee/ObstetricsandGynecologyDevices/ucm262488.htm>: 2011 September 8-9, 2011. Report No.
262. Jha S, Moran P. The UK national prolapse survey: 5 years on. *International urogynecology journal*. 2011;22(5):517-28.
263. Vanspauwen R, Seman E, Dwyer P. Survey of current management of prolapse in Australia and New Zealand. *The Australian & New Zealand journal of obstetrics & gynaecology*. 2010;50(3):262-7.
264. Schultz DG. FDA Public Health Notification: Serious Complications Associated with Transvaginal Placement of Surgical Mesh in Repair of Pelvic Organ Prolapse and Stress Urinary Incontinence 2008 [cited 2013 19th July].
265. Schraffordt Koops SE, Bisseling TM, Heintz APM, Vervest HAM. Prospective analysis of complications of tension-free vaginal tape from The Netherlands Tension-free Vaginal Tape study. *American journal of obstetrics and gynecology*. 2005;193(1):45-52.
266. Bako A, Dhar R. Review of synthetic mesh-related complications in pelvic floor reconstructive surgery. *International urogynecology journal*. 2009;20(1):103-11.
267. Birch C. The use of prosthetics in pelvic reconstructive surgery. *Best Practice & Research in Clinical Obstetrics & Gynaecology*. 2005;19(6):979-91.
268. Deprest J, Claerhout F, Zheng F, Konstantinovic M, Spelzini F, Guelinckx I, et al. Synthetic and biodegradable prostheses in pelvic floor surgery. In: Slager EFBVHBHVH, editor. *Gynaecology, Obstetrics, and Reproductive Medicine in Daily Practice*. International Congress Series. 12792005. p. 387-97.
269. Bafghi A, Benizri EI, Trastour C, Benizri EJ, Michiels JF, Bongain A. Multifilament polypropylene mesh for urinary incontinence: 10 cases of infections

- requiring removal of the sling. *Bjog-an International Journal of Obstetrics and Gynaecology*. 2005;112(3):376-8.
270. Melman L, Jenkins ED, Hamilton NA, Bender LC, Brodt MD, Deeken CR, et al. Histologic and biomechanical evaluation of a novel macroporous polytetrafluoroethylene knit mesh compared to lightweight and heavyweight polypropylene mesh in a porcine model of ventral incisional hernia repair. *Hernia*. 2011;15(4):423-31.
271. Spiess PE, Rabah D, Herrera C, Singh G, Moore R, Corcos J. The tensile properties of tension-free vaginal tape and cadaveric fascia lata in an in vivo rat model. *BJU international*. 2004;93(1):171-3.
272. Zorn KC, Spiess PE, Singh G, Orvieto MA, Moore B, Corcos J. Long-term tensile properties of tension-free vaginal tape, suprapubic arc sling system and urethral sling in an in vivo rat model. *J Urol*. 2007;177(3):1195-8.
273. Jones KA, Feola A, Meyn L, Abramowitch SD, Moalli PA. Tensile properties of commonly used prolapse meshes. *International urogynecology journal*. 2009;20(7):847-53.
274. Dietz HP, Vancaillie P, Svehla M, Walsh W, Steensma AB, Vancaillie TG. Mechanical properties of urogynecologic implant materials. *International urogynecology journal and pelvic floor dysfunction*. 2003;14(4):239-43.
275. Afonso JS, Martins PALS, Girao MJBC, Jorge RMN, Ferreira AJM, Mascarenhas T, et al. Mechanical properties of polypropylene mesh used in pelvic floor repair. *International urogynecology journal*. 2008;19(3):375-80.
276. Govier FE, Kobashi KC, Comiter C, Jones P, Dakil SE, James R, et al. Multi-center prospective study of the long-term effectiveness of a silicone coated synthetic mesh sling. *J Urol*. 2004;171(4):92-3.
277. Rabah DM, Begin LR, Zahran A, Corcos J. Tissue reactions of the rabbit urinary bladder to cadaveric human fascia lata and polypropylene surgical mesh. *The Canadian journal of urology*. 2004;11(4):2344-9.
278. Wang AC, Lee LY, Lin CT, Chen JR. A histologic and immunohistochemical analysis of defective vaginal healing after continence taping procedures: A prospective case-controlled pilot study. *Am J Obstet Gynecol*. 2004;191(6):1868-74.
279. Bogusiewicz M, Wrobel A, Jankiewicz K, Adamiak A, Skorupski P, Tomaszewski J, et al. Collagen deposition around polypropylene tapes implanted in the rectus fascia of female rats. *European Journal of Obstetrics Gynecology and Reproductive Biology*. 2006;124(1):106-9.
280. Bazi TM, Hamade RF, Hussein IAH, Nader KA, Jurjus A. Polypropylene midurethral tapes do not have similar biologic and biomechanical performance in the rat. *Eur Urol*. 2007;51(5):1364-75.
281. Maia de Almeida SH, Freitas Rodrigues MA, Gregorio E, Crespigio J, Moreira HA. Influence of sling material on inflammation and collagen deposit in an animal model. *International Journal of Urology*. 2007;14(11):1040-3.
282. Huffaker RK, Muir TW, Rao A, Baumann SS, Kuehl TJ, Pierce LM. Histologic response of porcine collagen-coated and uncoated polypropylene grafts in a rabbit vagina model. *Am J Obstet Gynecol*. 2008;198(5):7.
283. Woodruff AJ, Cole EE, Dmochowski RR, Scarpero HM, Beckman EN, Winters JC. Histologic comparison of pubovaginal sling graft materials: A comparative study. *Urology*. 2008;72(1):85-9.
284. Elmer C, Blomgren B, Falconer C, Zhang A, Altman D. Histological Inflammatory Response to Transvaginal Polypropylene Mesh for Pelvic Reconstructive Surgery. *J Urol*. 2009;181(3):1189-95.

285. Pierce LM, Grunlan MA, Hou Y, Baumann SS, Kuehl TJ, Muir TW. Biomechanical properties of synthetic and biologic graft materials following long-term implantation in the rabbit abdomen and vagina. *Am J Obstet Gynecol.* 2009;200(5).
286. Chapple CR, Raz S, Brubaker L, Zimmern PE. Mesh sling in an era of uncertainty: lessons learned and the way forward. *European urology.* 2013;64(4):525-9.
287. Cosson M, Debodinance P, Boukerrou M, Chauvet MP, Lobry P, Crepin G, et al. Mechanical properties of synthetic implants used in the repair of prolapse and urinary incontinence in women: which is the ideal material? *International urogynecology journal and pelvic floor dysfunction.* 2003;14(3):169-78; discussion 78.
288. Weber AM, Walters MD, Piedmonte MR, Ballard LA. Anterior colporrhaphy: a randomized trial of three surgical techniques. *American journal of obstetrics and gynecology.* 2001;185(6):1299-304; discussion 304-6.
289. Fianu S, Soderberg G. Absorbable polyglactin mesh for retropubic sling operations in female urinary stress incontinence. *Gynecologic and obstetric investigation.* 1983;16(1):45-50.
290. Birch C, Fynes MM. The role of synthetic and biological prostheses in reconstructive pelvic floor surgery. *Current opinion in obstetrics & gynecology.* 2002;14(5):527-35.
291. Choe JM, Kothandapani R, James L, Bowling D. Autologous, cadaveric, and synthetic materials used in sling surgery: Comparative biomechanical analysis. *Urology.* 2001;58(3):482-6.
292. Dora CD, Dimarco DS, Zobitz ME, Elliott DS. Time dependent variations in biomechanical properties of cadaveric fascia, porcine dermis, porcine small intestine submucosa, polypropylene mesh and autologous fascia in the rabbit model: Implications for sling surgery. *J Urol.* 2004;171(5):1970-3.
293. Hilger WS, Walter A, Zobitz ME, Leslie KO, Magtibay P, Cornella J. Histological and biomechanical evaluation of implanted graft materials in a rabbit vaginal and abdominal model. *Am J Obstet Gynecol.* 2006;195(6):1826-31.
294. Jeong S, Ma YR, Park YG. Histopathological study of frontalis suspension materials. *Japanese Journal of Ophthalmology.* 2000;44(2):171-4.
295. Pinna BdR, Stavale JN, de Lima Pontes PA, Campones do Brasil OdO. Histological analysis of autologous fascia graft implantation into the rabbit voice muscle. *Brazilian Journal of Otorhinolaryngology.* 2011;77(2):185-90.
296. Fitzgerald MP, Mollenhauer J, Brubaker L. The fate of rectus fascia suburethral slings. *Am J Obstet Gynecol.* 2000;183(4):964-6.
297. Vangsness CT, Garcia IA, Mills CR, Kainer MA, Roberts MR, Moore TM. Allograft transplantation in the knee: Tissue regulation, procurement, processing, and sterilization. *American Journal of Sports Medicine.* 2003;31(3):474-81.
298. Walter AJ, Morse AN, Leslie KO, Zobitz ME, Hentz JG, Cornella JL. Changes in tensile strength of cadaveric human fascia lata after implantation in a rabbit vagina model. *J Urol.* 2003;169(5):1907-10.
299. Sclafani AP, Romo T, 3rd, Jacono AA, McCormick S, Cocker R, Parker A. Evaluation of acellular dermal graft in sheet (AlloDerm) and injectable (micronized AlloDerm) forms for soft tissue augmentation. Clinical observations and histological analysis. *Archives of facial plastic surgery.* 2000;2(2):130-6.
300. Yildirim A, Basok EK, Gulpinar T, Gurbuz C, Zemheri E, Tokuc R. Tissue reactions of 5 sling materials and tissue material detachment strength of 4 synthetic mesh materials in a rabbit model. *J Urol.* 2005;174(5):2037-40.

301. Richters CD, Pirayesh A, Hoeksema H, Kamperdijk EWA, Kreis RW, Dutrieux RP, et al. Development of a dermal matrix from glycerol preserved allogeneic skin. *Cell and Tissue Banking*. 2008;9(4):309-15.
302. Rice RD, Ayubi FS, Shaub ZJ, Parker DM, Armstrong PJ, Tsai JW. Comparison of Surgisis(A (R)), AlloDerm(A (R)), and Vicryl Woven Mesh(A (R)) Grafts for Abdominal Wall Defect Repair in an Animal Model. *Aesthetic Plastic Surgery*. 2010;34(3):290-6.
303. Kolb CM, Pierce LM, Rooft SB. Biocompatibility comparison of novel soft tissue implants vs commonly used biomaterials in a pig model. *Otolaryngology--head and neck surgery : official journal of American Academy of Otolaryngology-Head and Neck Surgery*. 2012;147(3):456-61.
304. Krambeck AE, Dora CD, Sebo TJ, Rohlinger AL, DiMarco DS, Elliott DS. Time-dependent variations in inflammation and scar formation of six different pubovaginal sling materials in the rabbit model. *Urology*. 2006;67(5):1105-10.
305. VandeVord PJ, Broadrick KM, Krishnamurthy B, Singla AK. A Comparative Study Evaluating the In Vivo Incorporation of Biological Sling Materials. *Urology*. 2010;75(5):1228-33.
306. Carbone JM, Kavalier E, Hu JC, Raz S. Pubovaginal sling using cadaveric fascia and bone anchors: Disappointing early results. *Journal of Urology*. 2001;165(5):1605-10.
307. Freytes DO, Tullius RS, Badylak SF. Effect of storage upon material properties of lyophilized porcine extracellular matrix derived from the urinary bladder. *Journal of Biomedical Materials Research Part B-Applied Biomaterials*. 2006;78B(2):327-33.
308. Macleod TM, Williams G, Sanders R, Green CJ. Histological evaluation of Permacol (TM) as a subcutaneous implant over a 20-week period in the rat model. *British Journal of Plastic Surgery*. 2005;58(4):518-32.
309. Pierce LM, Rao A, Baumann SS, Glassberg JE, Kuehl TJ, Muir TW. Long-term histologic response to synthetic and biologic graft materials implanted in the vagina and abdomen of a rabbit model. *Am J Obstet Gynecol*. 2009;200(5).
310. Sandor M, Xu H, Connor J, Lombardi J, Harper JR, Silverman RP, et al. Host Response to Implanted Porcine-Derived Biologic Materials in a Primate Model of Abdominal Wall Repair. *Tissue Engineering Part A*. 2008;14(12):2021-31.
311. Badylak S, Kokini K, Tullius B, Simmons-Byrd A, Morff R. Morphologic study of small intestinal submucosa as a body wall repair device. *Journal of Surgical Research*. 2002;103(2):190-202.
312. Zhang F, Zhang J, Lin SY, Oswald T, Sones W, Cai ZW, et al. Small intestinal submucosa in abdominal wall repair after TRAM flap harvesting in a rat model. *Plastic and Reconstructive Surgery*. 2003;112(2):565-70.
313. Konstantinovic ML, Lagae P, Zheng F, Verbeken EK, De Ridder D, Deprest JA. Comparison of host response to polypropylene and non-cross-linked porcine small intestine serosal-derived collagen implants in a rat model. *Bjog-an International Journal of Obstetrics and Gynaecology*. 2005;112(11):1554-60.
314. Poulouse BK, Scholz S, Moore DE, Schmidt CR, Grogan EL, Lao OB, et al. Physiologic properties of small intestine submucosa. *Journal of Surgical Research*. 2005;123(2):262-7.
315. Ko R, Kazacos EA, Snyder S, Ernst DMJ, Lantz GC. Tensile strength comparison of small intestinal submucosa body wall repair. *Journal of Surgical Research*. 2006;135(1):9-17.

316. Rauth TP, Poulouse BK, Nanney LB, Holzman MD. A comparative analysis of expanded polytetrafluoroethylene and small intestinal submucosa - Implications for patch repair in ventral herniorrhaphy. *Journal of Surgical Research*. 2007;143(1):43-9.
317. Liu Z, Tang R, Zhou Z, Song Z, Wang H, Gu Y. Comparison of two porcine-derived materials for repairing abdominal wall defects in rats. *PloS one*. 2011;6(5):e20520-e.
318. Badylak S, Kokini M, Tullius B, Whitson B. Strength over time of a resorbable bioscaffold for body wall repair in a dog model. *Journal of Surgical Research*. 2001;99(2):282-7.
319. Thiel M, Palma PCR, Riccetto CLZ, Dambros M, Netto NR. A stereological analysis of fibrosis and inflammatory reaction induced by four different synthetic slings. *BJU international*. 2005;95(6):833-7.
320. Suckow MA, Wolter WR, Fecteau C, LaBadie-Suckow SM, Johnson C. Bupivacaine-enhanced small intestinal submucosa biomaterial as a hernia repair device. *Journal of Biomaterials Applications*. 2012;27(2):231-7.
321. Feldner PC, Jr., Castro RA, Cipolotti LA, Delroy CA, Ferreira Sartori MG, Batista Castello Girao MJ. Anterior vaginal wall prolapse: a randomized controlled trial of SIS graft versus traditional colporrhaphy. *International urogynecology journal*. 2010;21(9):1057-63.
322. Cole E, Gomelsky A, Dmochowski RR. Encapsulation of a porcine dermis pubovaginal sling. *J Urol*. 2003;170(5):1950-.
323. Wiedemann A, Otto M. Small intestinal submucosa for pubourethral sling suspension for the treatment of stress incontinence: First histopathological results in humans. *J Urol*. 2004;172(1):215-8.
324. Deprest J, Klosterhalfen B, Schreurs A, Verguts J, De Ridder D, Claerhout F. Clinicopathological Study of Patients Requiring Reintervention After Sacrocolpopexy With Xenogenic Acellular Collagen Grafts. *J Urol*. 2010;183(6):2249-55.
325. Langer R, Vacanti JP. Tissue engineering. *Science*. 1993;260(5110):920-6.
326. Atala A, Bauer SB, Soker S, Yoo JJ, Retik AB. Tissue-engineered autologous bladders for patients needing cystoplasty. *Lancet*. 2006;367(9518):1241-6.
327. Jack GS, Zhang R, Lee M, Xu Y, Wu BM, Rodriguez LV. Urinary bladder smooth muscle engineered from adipose stem cells and a three dimensional synthetic composite. *Biomaterials*. 2009;30(19):3259-70.
328. Sharma AK, Fuller NJ, Sullivan RR, Fulton N, Hota PV, Harrington DA, et al. Defined populations of bone marrow derived mesenchymal stem and endothelial progenitor cells for bladder regeneration. *The Journal of urology*. 2009;182(4 Suppl):1898-905.
329. Drewa T. Using hair-follicle stem cells for urinary bladder-wall regeneration. *Regenerative medicine*. 2008;3(6):939-44.
330. Zhang Y, McNeill E, Tian H, Soker S, Andersson KE, Yoo JJ, et al. Urine derived cells are a potential source for urological tissue reconstruction. *The Journal of urology*. 2008;180(5):2226-33.
331. Weiser AC, Franco I, Herz DB, Silver RI, Reda EF. Single layered small intestinal submucosa in the repair of severe chordee and complicated hypospadias. *The Journal of urology*. 2003;170(4 Pt 2):1593-5; discussion 5.
332. Bhargava S, Patterson JM, Inman RD, MacNeil S, Chapple CR. Tissue-engineered buccal mucosa urethroplasty-clinical outcomes. *European urology*. 2008;53(6):1263-9.



333. De Filippo RE, Kornitzer BS, Yoo JJ, Atala A. Penile urethra replacement with autologous cell-seeded tubularized collagen matrices. *Journal of tissue engineering and regenerative medicine*. 2012.
334. De Filippo RE, Yoo JJ, Atala A. Engineering of vaginal tissue in vivo. *Tissue engineering*. 2003;9(2):301-6.
335. Ho MH, Heydarkhan S, Vernet D, Kovanecz I, Ferrini MG, Bhatia NN, et al. Stimulating vaginal repair in rats through skeletal muscle-derived stem cells seeded on small intestinal submucosal scaffolds. *Obstetrics and gynecology*. 2009;114(2 Pt 1):300-9.
336. Hung MJ, Wen MC, Hung CN, Ho ES, Chen GD, Yang VC. Tissue-engineered fascia from vaginal fibroblasts for patients needing reconstructive pelvic surgery. *International urogynecology journal*. 2010;21(9):1085-93.
337. Raya-Rivera AM, Esquiliano D, Fierro-Pastrana R, Lopez-Bayghen E, Valencia P, Ordorica-Flores R, et al. Tissue-engineered autologous vaginal organs in patients: a pilot cohort study. *Lancet*. 2014;384(9940):329-36.
338. Cannon TW, Sweeney DD, Conway DA, Kamo I, Yoshimura N, Sacks M, et al. A tissue-engineered suburethral sling in an animal model of stress urinary incontinence. *BJU international*. 2005;96(4):664-9.
339. Zou XH, Zhi YL, Chen X, Jin HM, Wang LL, Jiang YZ, et al. Mesenchymal stem cell seeded knitted silk sling for the treatment of stress urinary incontinence. *Biomaterials*. 2010;31(18):4872-9.
340. Martinez-Climent JA, Andreu EJ, Prosper F. Somatic stem cells and the origin of cancer. *Clinical & translational oncology : official publication of the Federation of Spanish Oncology Societies and of the National Cancer Institute of Mexico*. 2006;8(9):647-63.
341. Kang JW, Kang KS, Koo HC, Park JR, Choi EW, Park YH. Soluble factors-mediated immunomodulatory effects of canine adipose tissue-derived mesenchymal stem cells. *Stem cells and development*. 2008;17(4):681-93.
342. Shi LB, Cai HX, Chen LK, Wu Y, Zhu SA, Gong XN, et al. Tissue engineered bulking agent with adipose-derived stem cells and silk fibroin microspheres for the treatment of intrinsic urethral sphincter deficiency. *Biomaterials*. 2014;35(5):1519-30.
343. Vermette M, Trottier V, Menard V, Saint-Pierre L, Roy A, Fradette J. Production of a new tissue-engineered adipose substitute from human adipose-derived stromal cells. *Biomaterials*. 2007;28(18):2850-60.
344. Hu R, Ling W, Xu W, Han D. Fibroblast-like cells differentiated from adipose-derived mesenchymal stem cells for vocal fold wound healing. *PLoS One*. 2014;9(3):e92676.
345. Mangera A, Bullock AJ, Chapple CR, MacNeil S. Are biomechanical properties predictive of the success of prostheses used in stress urinary incontinence and pelvic organ prolapse? A systematic review. *Neurourology and urodynamics*. 2012;31(1):13-21.
346. Mangera A, Bullock AJ, Roman S, Chapple CR, MacNeil S. Comparison of candidate scaffolds for tissue engineering for stress urinary incontinence and pelvic organ prolapse repair. *BJU international*. 2013;112(5):674-85.
347. Kulkarni RK, Pani KC, Neuman C, Leonard F. Polylactic acid for surgical implants. *Archives of surgery*. 1966;93(5):839-43.
348. Tsuji H, Ikarashi K. In vitro hydrolysis of poly(L-lactide) crystalline residues as extended-chain crystallites. Part I: long-term hydrolysis in phosphate-buffered solution at 37 degrees C. *Biomaterials*. 2004;25(24):5449-55.

349. Ceonzo K, Gaynor A, Shaffer L, Kojima K, Vacanti CA, Stahl GL. Polyglycolic acid-induced inflammation: role of hydrolysis and resulting complement activation. *Tissue engineering*. 2006;12(2):301-8.
350. Gasparini G, Kosvintsev SR, Stillwell MT, Holdich RG. Preparation and characterization of PLGA particles for subcutaneous controlled drug release by membrane emulsification. *Colloids and surfaces B, Biointerfaces*. 2008;61(2):199-207.
351. Kumbar SG, Nukavarapu SP, James R, Nair LS, Laurencin CT. Electrospun poly(lactic acid-co-glycolic acid) scaffolds for skin tissue engineering. *Biomaterials*. 2008;29(30):4100-7.
352. Mikos AG, Bao Y, Cima LG, Ingber DE, Vacanti JP, Langer R. Preparation of poly(glycolic acid) bonded fiber structures for cell attachment and transplantation. *Journal of biomedical materials research*. 1993;27(2):183-9.
353. Mikos AG, Sarakinos G, Leite SM, Vacanti JP, Langer R. Laminated three-dimensional biodegradable foams for use in tissue engineering. *Biomaterials*. 1993;14(5):323-30.
354. Nam YS, Park TG. Biodegradable polymeric microcellular foams by modified thermally induced phase separation method. *Biomaterials*. 1999;20(19):1783-90.
355. Schugens C, Maquet V, Grandfils C, Jerome R, Teyssie P. Polylactide macroporous biodegradable implants for cell transplantation. II. Preparation of polylactide foams by liquid-liquid phase separation. *Journal of biomedical materials research*. 1996;30(4):449-61.
356. Hollister SJ, Maddox RD, Taboas JM. Optimal design and fabrication of scaffolds to mimic tissue properties and satisfy biological constraints. *Biomaterials*. 2002;23(20):4095-103.
357. Vitte J, Benoliel AM, Pierres A, Bongrand P. Is there a predictable relationship between surface physical-chemical properties and cell behaviour at the interface? *European cells & materials*. 2004;7:52-63; discussion
358. Newton D, Mahajan R, Ayres C, Bowman JR, Bowlin GL, Simpson DG. Regulation of material properties in electrospun scaffolds: Role of cross-linking and fiber tertiary structure. *Acta biomaterialia*. 2009;5(1):518-29.
359. Deshpande P, McKean R, Blackwood KA, Senior RA, Ogunbanjo A, Ryan AJ, et al. Using poly(lactide-co-glycolide) electrospun scaffolds to deliver cultured epithelial cells to the cornea. *Regenerative medicine*. 2010;5(3):395-401.
360. Tan EP, Lim CT. Effects of annealing on the structural and mechanical properties of electrospun polymeric nanofibres. *Nanotechnology*. 2006;17(10):2649-54.
361. Buchko CJ, Kozloff KM, Martin DC. Surface characterization of porous, biocompatible protein polymer thin films. *Biomaterials*. 2001;22(11):1289-300.
362. Ma PX, Choi JW. Biodegradable polymer scaffolds with well-defined interconnected spherical pore network. *Tissue engineering*. 2001;7(1):23-33.
363. Chen G, Sato T, Ohgushi H, Ushida T, Tateishi T, Tanaka J. Culturing of skin fibroblasts in a thin PLGA-collagen hybrid mesh. *Biomaterials*. 2005;26(15):2559-66.
364. Pattison M, Webster TJ, Leslie J, Kaefer M, Haberstroh KM. Evaluating the in vitro and in vivo efficacy of nano-structured polymers for bladder tissue replacement applications. *Macromolecular bioscience*. 2007;7(5):690-700.
365. Bini TB, Gao S, Xu X, Wang S, Ramakrishna S, Leong KW. Peripheral nerve regeneration by microbraided poly(L-lactide-co-glycolide) biodegradable polymer fibers. *Journal of biomedical materials research Part A*. 2004;68(2):286-95.
366. Patrick CW, Jr., Chauvin PB, Hobley J, Reece GP. Preadipocyte seeded PLGA scaffolds for adipose tissue engineering. *Tissue engineering*. 1999;5(2):139-51.

367. Park SS, Ward MJ. Tissue-engineered cartilage for implantation and grafting. *Facial plastic surgery : FPS*. 1995;11(4):278-83.
368. Yang F, Murugan R, Wang S, Ramakrishna S. Electrospinning of nano/micro scale poly(L-lactic acid) aligned fibers and their potential in neural tissue engineering. *Biomaterials*. 2005;26(15):2603-10.
369. Corey JM, Gertz CC, Wang BS, Birrell LK, Johnson SL, Martin DC, et al. The design of electrospun PLLA nanofiber scaffolds compatible with serum-free growth of primary motor and sensory neurons. *Acta biomaterialia*. 2008;4(4):863-75.
370. Murray-Dunning C, McArthur SL, Sun T, McKean R, Ryan AJ, Haycock JW. Three-dimensional alignment of schwann cells using hydrolysable microfiber scaffolds: strategies for peripheral nerve repair. *Methods in molecular biology*. 2011;695:155-66.
371. Inoguchi H, Kwon IK, Inoue E, Takamizawa K, Maehara Y, Matsuda T. Mechanical responses of a compliant electrospun poly(L-lactide-co-epsilon-caprolactone) small-diameter vascular graft. *Biomaterials*. 2006;27(8):1470-8.
372. Paletta JR, Mack F, Schenderlein H, Theisen C, Schmitt J, Wendorff JH, et al. Incorporation of osteoblasts (MG63) into 3D nanofibre matrices by simultaneous electrospinning and spraying in bone tissue engineering. *European cells & materials*. 2011;21:384-95.
373. de Tayrac R, Chentouf S, Garreau H, Braud C, Guiraud I, Boudeville P, et al. In vitro degradation and in vivo biocompatibility of poly(lactic acid) mesh for soft tissue reinforcement in vaginal surgery. *Journal of biomedical materials research Part B, Applied biomaterials*. 2008;85(2):529-36.
374. de Tayrac R, Letouzey V, Garreau H, Guiraud I, Vert M, Mares P. Tissue healing during degradation of a long-lasting bioresorbable gamma-ray-sterilised poly(lactic acid) mesh in the rat: a 12-month study. *European surgical research Europäische chirurgische Forschung Recherches chirurgicales europeennes*. 2010;44(2):102-10.
375. Mathe ML, Lavigne JP, Oliva-Lauraire MC, Guiraud I, Mares P, de Tayrac R. [Comparison of different biomaterials for vaginal surgery using an in vivo model of meshes infection in rats]. *Gynecologie, obstetrique & fertilite*. 2007;35(5):398-405.
376. Birch C. The use of prosthetics in pelvic reconstructive surgery. *Best practice & research Clinical obstetrics & gynaecology*. 2005;19(6):979-91.
377. Costolo MA, Lennhoff JD, Pawle R, Rietman EA, Stevens AE. A nonlinear system model for electrospinning sub-100 nm polyacrylonitrile fibres. *Nanotechnology*. 2008;19(3):035707.
378. Mangera A, Bullock AJ, Chapple CR, Macneil S. Are biomechanical properties predictive of the success of prostheses used in stress urinary incontinence and pelvic organ prolapse? A systematic review. *Neurourology and urodynamics*. 2012;31(1):13-21.
379. Skala CE, Petry IB, Gebhard S, Hengstler JG, Albrich SB, Maltaris T, et al. Isolation of fibroblasts for coating of meshes for reconstructive surgery: differences between mesh types. *Regenerative medicine*. 2009;4(2):197-204.
380. Tomaszewski J, Adamiak-Godlewska A, Bogusiewicz M, Brzana W, Juszcak M, Rzeski W, et al. [Collagen type III biosynthesis by cultured pubocervical fascia fibroblasts surrounding mono and multifilament polypropylene mesh after estrogens and tamoxifen treatment]. *Ginekologia polska*. 2010;81(7):493-500.
381. Levine LA, Strom KH, Lux MM. Buccal mucosa graft urethroplasty for anterior urethral stricture repair: evaluation of the impact of stricture location and lichen sclerosus on surgical outcome. *The Journal of urology*. 2007;178(5):2011-5.

382. Nahoum A. One-stage operation for correction of mild hypospadias with chordee. *The Journal of urology*. 1947;58(1):74-7.
383. Dubey D, Kumar A, Mandhani A, Srivastava A, Kapoor R, Bhandari M. Buccal mucosal urethroplasty: a versatile technique for all urethral segments. *BJU international*. 2005;95(4):625-9.
384. Bhargava S, Chapple CR, Bullock AJ, Layton C, MacNeil S. Tissue-engineered buccal mucosa for substitution urethroplasty. *BJU international*. 2004;93(6):807-11.
385. Selim M, Bullock AJ, Blackwood KA, Chapple CR, MacNeil S. Developing biodegradable scaffolds for tissue engineering of the urethra. *BJU international*. 2011;107(2):296-302.
386. Peran M, Marchal JA, Lopez E, Jimenez-Navarro M, Boulaiz H, Rodriguez-Serrano F, et al. Human cardiac tissue induces transdifferentiation of adult stem cells towards cardiomyocytes. *Cytotherapy*. 2010;12(3):332-7.
387. Pedemonte E, Benvenuto F, Casazza S, Mancardi G, Oksenberg JR, Uccelli A, et al. The molecular signature of therapeutic mesenchymal stem cells exposes the architecture of the hematopoietic stem cell niche synapse. *BMC genomics*. 2007;8:65.
388. Wislet-Gendebien S, Wautier F, Leprince P, Rogister B. Astrocytic and neuronal fate of mesenchymal stem cells expressing nestin. *Brain research bulletin*. 2005;68(1-2):95-102.
389. Krampera M, Marconi S, Pasini A, Galie M, Rigotti G, Mosna F, et al. Induction of neural-like differentiation in human mesenchymal stem cells derived from bone marrow, fat, spleen and thymus. *Bone*. 2007;40(2):382-90.
390. Keating A. Mesenchymal stromal cells. *Current opinion in hematology*. 2006;13(6):419-25.
391. Wu Y, Chen L, Scott PG, Tredget EE. Mesenchymal stem cells enhance wound healing through differentiation and angiogenesis. *Stem cells*. 2007;25(10):2648-59.
392. Drost AC, Weng S, Feil G, Schafer J, Baumann S, Kanz L, et al. In vitro myogenic differentiation of human bone marrow-derived mesenchymal stem cells as a potential treatment for urethral sphincter muscle repair. *Annals of the New York Academy of Sciences*. 2009;1176:135-43.
393. Kinebuchi Y, Aizawa N, Imamura T, Ishizuka O, Igawa Y, Nishizawa O. Autologous bone-marrow-derived mesenchymal stem cell transplantation into injured rat urethral sphincter. *International journal of urology : official journal of the Japanese Urological Association*. 2010;17(4):359-68.
394. Corcos J, Loutochin O, Campeau L, Eliopoulos N, Bouchentouf M, Blok B, et al. Bone marrow mesenchymal stromal cell therapy for external urethral sphincter restoration in a rat model of stress urinary incontinence. *Neurourology and urodynamics*. 2011;30(3):447-55.
395. Pittenger MF, Mackay AM, Beck SC, Jaiswal RK, Douglas R, Mosca JD, et al. Multilineage potential of adult human mesenchymal stem cells. *Science*. 1999;284(5411):143-7.
396. Oshima H, Payne TR, Urish KL, Sakai T, Ling Y, Gharaibeh B, et al. Differential myocardial infarct repair with muscle stem cells compared to myoblasts. *Molecular therapy : the journal of the American Society of Gene Therapy*. 2005;12(6):1130-41.
397. Lee JY, Qu-Petersen Z, Cao B, Kimura S, Jankowski R, Cummins J, et al. Clonal isolation of muscle-derived cells capable of enhancing muscle regeneration and bone healing. *The Journal of cell biology*. 2000;150(5):1085-100.

398. Qu-Petersen Z, Deasy B, Jankowski R, Ikezawa M, Cummins J, Pruchnic R, et al. Identification of a novel population of muscle stem cells in mice: potential for muscle regeneration. *The Journal of cell biology*. 2002;157(5):851-64.
399. Kwon D, Kim Y, Pruchnic R, Jankowski R, Usiene I, de Miguel F, et al. Periurethral cellular injection: comparison of muscle-derived progenitor cells and fibroblasts with regard to efficacy and tissue contractility in an animal model of stress urinary incontinence. *Urology*. 2006;68(2):449-54.
400. Roche R, Festy F, Fritel X. Stem cells for stress urinary incontinence: the adipose promise. *Journal of cellular and molecular medicine*. 2010;14(1-2):135-42.
401. Zuk PA, Zhu M, Mizuno H, Huang J, Futrell JW, Katz AJ, et al. Multilineage cells from human adipose tissue: implications for cell-based therapies. *Tissue engineering*. 2001;7(2):211-28.
402. Ning H, Lin G, Lue TF, Lin CS. Neuron-like differentiation of adipose tissue-derived stromal cells and vascular smooth muscle cells. *Differentiation; research in biological diversity*. 2006;74(9-10):510-8.
403. Miranville A, Heeschen C, Sengenès C, Curat CA, Busse R, Bouloumie A. Improvement of postnatal neovascularization by human adipose tissue-derived stem cells. *Circulation*. 2004;110(3):349-55.
404. Miyahara Y, Nagaya N, Kataoka M, Yanagawa B, Tanaka K, Hao H, et al. Monolayered mesenchymal stem cells repair scarred myocardium after myocardial infarction. *Nature medicine*. 2006;12(4):459-65.
405. Rodríguez LV, Alfonso Z, Zhang R, Leung J, Wu B, Ignarro LJ. Clonogenic multipotent stem cells in human adipose tissue differentiate into functional smooth muscle cells. *Proceedings of the National Academy of Sciences of the United States of America*. 2006;103(32):12167-72.
406. Bacou F, el Andaloussi RB, Daussin PA, Micallef JP, Levin JM, Chammas M, et al. Transplantation of adipose tissue-derived stromal cells increases mass and functional capacity of damaged skeletal muscle. *Cell transplantation*. 2004;13(2):103-11.
407. Safford KM, Hicok KC, Safford SD, Halvorsen YD, Wilkison WO, Gimble JM, et al. Neurogenic differentiation of murine and human adipose-derived stromal cells. *Biochemical and biophysical research communications*. 2002;294(2):371-9.
408. Arrigoni E, Lopa S, de Girolamo L, Stanco D, Brini AT. Isolation, characterization and osteogenic differentiation of adipose-derived stem cells: from small to large animal models. *Cell and tissue research*. 2009;338(3):401-11.
409. Kozak LP, Anunciado-Koza R. UCP1: its involvement and utility in obesity. *Int J Obes (Lond)*. 2008;32 Suppl 7:S32-8.
410. Zhang J, Wu L, Qu JM. Inhibited proliferation of human lung fibroblasts by LPS is through IL-6 and IL-8 release. *Cytokine*. 2011;54(3):289-95.
411. Wiegand C, Hipler UC. Methods for the measurement of cell and tissue compatibility including tissue regeneration processes. *GMS Krankenhaushygiene interdisziplinär*. 2008;3(1):Doc12.
412. Junqueira LC, Bignolas G, Brentani RR. Picrosirius staining plus polarization microscopy, a specific method for collagen detection in tissue sections. *The Histochemical journal*. 1979;11(4):447-55.
413. Mitterberger M, Marksteiner R, Margreiter E, Pinggera GM, Colleselli D, Frauscher F, et al. Autologous myoblasts and fibroblasts for female stress incontinence: a 1-year follow-up in 123 patients. *BJU international*. 2007;100(5):1081-5.
414. Almeida FG, Nobre YT, Leite KR, Bruschini H. Autologous transplantation of adult adipose derived stem cells into rabbit urethral wall. *International urogynecology journal*. 2010;21(6):743-8.

415. De Filippo RE, Yoo JJ, Atala A. Urethral replacement using cell seeded tubularized collagen matrices. *The Journal of urology*. 2002;168(4 Pt 2):1789-92; discussion 92-3.
416. MacNeil S. Progress and opportunities for tissue-engineered skin. *Nature*. 2007;445(7130):874-80.
417. Eyckmans J, Boudou T, Yu X, Chen CS. A hitchhiker's guide to mechanobiology. *Developmental cell*. 2011;21(1):35-47.
418. Lee WC, Maul TM, Vorp DA, Rubin JP, Marra KG. Effects of uniaxial cyclic strain on adipose-derived stem cell morphology, proliferation, and differentiation. *Biomechanics and modeling in mechanobiology*. 2007;6(4):265-73.
419. Riehl BD, Park JH, Kwon IK, Lim JY. Mechanical Stretching for Tissue Engineering: Two-Dimensional and Three-Dimensional Constructs. *Tissue engineering Part B, Reviews*. 2012.
420. Pioletti DP. Biomechanics and tissue engineering. *Osteoporosis international : a journal established as result of cooperation between the European Foundation for Osteoporosis and the National Osteoporosis Foundation of the USA*. 2011;22(6):2027-31.
421. Ingber DE. Mechanobiology and diseases of mechanotransduction. *Annals of medicine*. 2003;35(8):564-77.
422. Benhardt HA, Cosgriff-Hernandez EM. The role of mechanical loading in ligament tissue engineering. *Tissue engineering Part B, Reviews*. 2009;15(4):467-75.
423. Szczesny SE, Lee CS, Soslowsky LJ. Remodeling and repair of orthopedic tissue: role of mechanical loading and biologics. *Am J Orthop (Belle Mead NJ)*. 2010;39(11):525-30.
424. Brown TD. Techniques for mechanical stimulation of cells in vitro: a review. *Journal of biomechanics*. 2000;33(1):3-14.
425. Carpentier B, Layrolle P, Legallais C. Bioreactors for bone tissue engineering. *The International journal of artificial organs*. 2011;34(3):259-70.
426. Shi ZD, Tarbell JM. Fluid flow mechanotransduction in vascular smooth muscle cells and fibroblasts. *Annals of biomedical engineering*. 2011;39(6):1608-19.
427. Kreja L, Liedert A, Schlenker H, Brenner RE, Fiedler J, Friemert B, et al. Effects of mechanical strain on human mesenchymal stem cells and ligament fibroblasts in a textured poly(L-lactide) scaffold for ligament tissue engineering. *Journal of materials science Materials in medicine*. 2012.
428. Gould RA, Chin K, Santisakultarm TP, Dropkin A, Richards JM, Schaffer CB, et al. Cyclic strain anisotropy regulates valvular interstitial cell phenotype and tissue remodeling in three-dimensional culture. *Acta biomaterialia*. 2012;8(5):1710-9.
429. Waldman SD, Couto DC, Gryn timer MD, Pilliar RM, Kandel RA. Multi-axial mechanical stimulation of tissue engineered cartilage: review. *European cells & materials*. 2007;13:66-73; discussion -4.
430. Waldman SD, Spiteri CG, Gryn timer MD, Pilliar RM, Kandel RA. Long-term intermittent compressive stimulation improves the composition and mechanical properties of tissue-engineered cartilage. *Tissue engineering*. 2004;10(9-10):1323-31.
431. Correia C, Pereira AL, Duarte AR, Frias AM, Pedro AJ, Oliveira JT, et al. Dynamic Culturing of Cartilage Tissue: The Significance of Hydrostatic Pressure. *Tissue engineering Part A*. 2012.
432. Martinez H, Brackmann C, Enejder A, Gatenholm P. Mechanical stimulation of fibroblasts in micro-channeled bacterial cellulose scaffolds enhances production of oriented collagen fibers. *Journal of biomedical materials research Part A*. 2012;100(4):948-57.

433. Altman GH, Horan RL, Martin I, Farhadi J, Stark PR, Volloch V, et al. Cell differentiation by mechanical stress. *FASEB journal : official publication of the Federation of American Societies for Experimental Biology*. 2002;16(2):270-2.
434. Gauvin R, Parenteau-Bareil R, Larouche D, Marcoux H, Bisson F, Bonnet A, et al. Dynamic mechanical stimulations induce anisotropy and improve the tensile properties of engineered tissues produced without exogenous scaffolding. *Acta biomaterialia*. 2011;7(9):3294-301.
435. Baragi RV, Delancey JO, Caspari R, Howard DH, Ashton-Miller JA. Differences in pelvic floor area between African American and European American women. *American journal of obstetrics and gynecology*. 2002;187(1):111-5.
436. Ashton-Miller JA, Delancey JO. On the biomechanics of vaginal birth and common sequelae. *Annual review of biomedical engineering*. 2009;11:163-76.
437. Danisovic L, Varga I, Zamborsky R, Bohmer D. The tissue engineering of articular cartilage: cells, scaffolds and stimulating factors. *Exp Biol Med (Maywood)*. 2012;237(1):10-7.
438. Jenner JM, van Eijk F, Saris DB, Willems WJ, Dhert WJ, Creemers LB. Effect of transforming growth factor-beta and growth differentiation factor-5 on proliferation and matrix production by human bone marrow stromal cells cultured on braided poly lactic-co-glycolic acid scaffolds for ligament tissue engineering. *Tissue engineering*. 2007;13(7):1573-82.
439. Hagerty P, Lee A, Calve S, Lee CA, Vidal M, Baar K. The effect of growth factors on both collagen synthesis and tensile strength of engineered human ligaments. *Biomaterials*. 2012;33(27):6355-61.
440. Fu P, Sodian R, Luders C, Lemke T, Kraemer L, Hubler M, et al. Effects of basic fibroblast growth factor and transforming growth factor-beta on maturation of human pediatric aortic cell culture for tissue engineering of cardiovascular structures. *ASAIO J*. 2004;50(1):9-14.
441. Kavitha O, Thampan RV. Factors influencing collagen biosynthesis. *Journal of cellular biochemistry*. 2008;104(4):1150-60.
442. Jeffrey JJ, Martin GR. The role of ascorbic acid in the biosynthesis of collagen. I. Ascorbic acid requirement by embryonic chick tibia in tissue culture. *Biochimica et biophysica acta*. 1966;121(2):269-80.
443. Ghosh AK. Factors involved in the regulation of type I collagen gene expression: implication in fibrosis. *Exp Biol Med (Maywood)*. 2002;227(5):301-14.
444. Boyera N, Galey I, Bernard BA. Effect of vitamin C and its derivatives on collagen synthesis and cross-linking by normal human fibroblasts. *International journal of cosmetic science*. 1998;20(3):151-8.
445. Murad S, Grove D, Lindberg KA, Reynolds G, Sivarajah A, Pinnell SR. Regulation of collagen synthesis by ascorbic acid. *Proceedings of the National Academy of Sciences of the United States of America*. 1981;78(5):2879-82.
446. Russell SB, Russell JD, Trupin KM. Collagen synthesis in human fibroblasts: effects of ascorbic acid and regulation by hydrocortisone. *Journal of cellular physiology*. 1981;109(1):121-31.
447. Bean AC, Almarza AJ, Athanasiou KA. Effects of ascorbic acid concentration on the tissue engineering of the temporomandibular joint disc. *Proceedings of the Institution of Mechanical Engineers Part H, Journal of engineering in medicine*. 2006;220(3):439-47.
448. Cimini M, Boughner DR, Ronald JA, Johnston DE, Rogers KA. Dermal fibroblasts cultured on small intestinal submucosa: Conditions for the formation of a neotissue. *Journal of biomedical materials research Part A*. 2005;75(4):895-906.

449. Yoshida H, Matsusaki M, Akashi M. Development of thick and highly cell-incorporated engineered tissues by hydrogel template approach with basic fibroblast growth factor or ascorbic acid. *Journal of biomaterials science Polymer edition*. 2010;21(4):415-28.
450. Fan JC, Waldman SD. The effect of intermittent static biaxial tensile strains on tissue engineered cartilage. *Annals of biomedical engineering*. 2010;38(4):1672-82.
451. Moalli PA, Howden NS, Lowder JL, Navarro J, Debes KM, Abramowitch SD, et al. A rat model to study the structural properties of the vagina and its supportive tissues. *American journal of obstetrics and gynecology*. 2005;192(1):80-8.
452. Wittman AB, Wall LL. The evolutionary origins of obstructed labor: bipedalism, encephalization, and the human obstetric dilemma. *Obstetrical & gynecological survey*. 2007;62(11):739-48.
453. Schimpf M, Tulikangas P. Evolution of the female pelvis and relationships to pelvic organ prolapse. *International urogynecology journal and pelvic floor dysfunction*. 2005;16(4):315-20.
454. Liu G, Daneshgari F, Li M, Lin D, Lee U, Li T, et al. Bladder and urethral function in pelvic organ prolapsed lysyl oxidase like-1 knockout mice. *BJU international*. 2007;100(2):414-8.
455. Lee UJ, Gustilo-Ashby AM, Daneshgari F, Kuang M, Vurbic D, Lin DL, et al. Lower urogenital tract anatomical and functional phenotype in lysyl oxidase like-1 knockout mice resembles female pelvic floor dysfunction in humans. *American journal of physiology Renal physiology*. 2008;295(2):F545-55.
456. Claerhout F, Verbist G, Verbeken E, Konstantinovic M, De Ridder D, Deprest J. Fate of collagen-based implants used in pelvic floor surgery: a 2-year follow-up study in a rabbit model. *American journal of obstetrics and gynecology*. 2008;198(1):94 e1-6.
457. Pierce LM, Rao A, Baumann SS, Glassberg JE, Kuehl TJ, Muir TW. Long-term histologic response to synthetic and biologic graft materials implanted in the vagina and abdomen of a rabbit model. *American journal of obstetrics and gynecology*. 2009;200(5):546 e1-8.
458. Pierce LM, Grunlan MA, Hou Y, Baumann SS, Kuehl TJ, Muir TW. Biomechanical properties of synthetic and biologic graft materials following long-term implantation in the rabbit abdomen and vagina. *American journal of obstetrics and gynecology*. 2009;200(5):549 e1-8.
459. Huffaker RK, Muir TW, Rao A, Baumann SS, Kuehl TJ, Pierce LM. Histologic response of porcine collagen-coated and uncoated polypropylene grafts in a rabbit vagina model. *American journal of obstetrics and gynecology*. 2008;198(5):582 e1-7.
460. Higgins EW, Rao A, Baumann SS, James RL, Kuehl TJ, Muir TW, et al. Effect of estrogen replacement on the histologic response to polypropylene mesh implanted in the rabbit vagina model. *American journal of obstetrics and gynecology*. 2009;201(5):505 e1-9.
461. Walter AJ, Morse AN, Leslie KO, Hentz JG, Cornella JL. Histologic evaluation of human cadaveric fascia lata in a rabbit vagina model. *International urogynecology journal and pelvic floor dysfunction*. 2006;17(2):136-42.
462. Abramov Y, Webb AR, Miller JJ, Alshahrour A, Botros SM, Goldberg RP, et al. Biomechanical characterization of vaginal versus abdominal surgical wound healing in the rabbit. *American journal of obstetrics and gynecology*. 2006;194(5):1472-7.
463. Shepherd PR. Vaginal prolapse in ewes. *The Veterinary record*. 1992;130(25):564.
464. Low JC, Sutherland HK. A census of the prevalence of vaginal prolapse in sheep flocks in the Borders region of Scotland. *The Veterinary record*. 1987;120(24):571-5.



465. Davies FG. The occurrence of vaginal eversion and allied disorders in fat ewes. *Research in veterinary science*. 1970;11(1):86-90.
466. Ayen E, Noakes DE. Displacement of the tubular genital tract of the ewe during pregnancy. *The Veterinary record*. 1997;141(20):509-12.
467. Otto LN, Slayden OD, Clark AL, Brenner RM. The rhesus macaque as an animal model for pelvic organ prolapse. *American journal of obstetrics and gynecology*. 2002;186(3):416-21.
468. Coates KW, Galan HL, Shull BL, Kuehl TJ. The squirrel monkey: an animal model of pelvic relaxation. *American journal of obstetrics and gynecology*. 1995;172(2 Pt 1):588-93.
469. Moalli PA, Shand SH, Zyczynski HM, Gordy SC, Meyn LA. Remodeling of vaginal connective tissue in patients with prolapse. *Obstetrics and gynecology*. 2005;106(5 Pt 1):953-63.
470. Kaiho Y, Kamo I, Chancellor MB, Arai Y, de Groat WC, Yoshimura N. Role of noradrenergic pathways in sneeze-induced urethral continence reflex in rats. *American journal of physiology Renal physiology*. 2007;292(2):F639-46.
471. Conway DA, Kamo I, Yoshimura N, Chancellor MB, Cannon TW. Comparison of leak point pressure methods in an animal model of stress urinary incontinence. *International urogynecology journal and pelvic floor dysfunction*. 2005;16(5):359-63.
472. Kamo I, Hashimoto T. Involvement of reflex urethral closure mechanisms in urethral resistance under momentary stress condition induced by electrical stimulation of rat abdomen. *American journal of physiology Renal physiology*. 2007;293(3):F920-6.
473. Wood HM, Kuang M, Woo L, Hijaz A, Butler RS, Penn M, et al. Cytokine expression after vaginal distention of different durations in virgin Sprague-Dawley rats. *The Journal of urology*. 2008;180(2):753-9.
474. Woo LL, Hijaz A, Kuang M, Penn MS, Damaser MS, Rackley RR. Over expression of stem cell homing cytokines in urogenital organs following vaginal distention. *The Journal of urology*. 2007;177(4):1568-72.
475. Lin AS, Carrier S, Morgan DM, Lue TF. Effect of simulated birth trauma on the urinary continence mechanism in the rat. *Urology*. 1998;52(1):143-51.
476. Damaser MS, Whitbeck C, Chichester P, Levin RM. Effect of vaginal distension on blood flow and hypoxia of urogenital organs of the female rat. *J Appl Physiol* (1985). 2005;98(5):1884-90.
477. Cannon TW, Wojcik EM, Ferguson CL, Saraga S, Thomas C, Damaser MS. Effects of vaginal distension on urethral anatomy and function. *BJU international*. 2002;90(4):403-7.
478. Rodriguez LV, Chen S, Jack GS, de Almeida F, Lee KW, Zhang R. New objective measures to quantify stress urinary incontinence in a novel durable animal model of intrinsic sphincter deficiency. *American journal of physiology Regulatory, integrative and comparative physiology*. 2005;288(5):R1332-8.
479. Pauwels E, De Wachter S, Wyndaele JJ. Evaluation of different techniques to create chronic urinary incontinence in the rat. *BJU international*. 2009;103(6):782-5; discussion 5-6.
480. Petros PE. The pubourethral ligaments--an anatomical and histological study in the live patient. *International urogynecology journal and pelvic floor dysfunction*. 1998;9(3):154-7.
481. Chermansky CJ, Cannon TW, Torimoto K, Fraser MO, Yoshimura N, de Groat WC, et al. A model of intrinsic sphincteric deficiency in the rat: electrocauterization. *Neurourology and urodynamics*. 2004;23(2):166-71.

482. Eberli D, Andersson KE, Yoo JJ, Atala A. A canine model of irreversible urethral sphincter insufficiency. *BJU international*. 2009;103(2):248-53.
483. Takahashi S, Chen Q, Ogushi T, Fujimura T, Kumagai J, Matsumoto S, et al. Periurethral injection of sustained release basic fibroblast growth factor improves sphincteric contractility of the rat urethra denervated by botulinum-a toxin. *The Journal of urology*. 2006;176(2):819-23.
484. Peng CW, Chen JJ, Chang HY, de Groat WC, Cheng CL. External urethral sphincter activity in a rat model of pudendal nerve injury. *Neurourology and urodynamics*. 2006;25(4):388-96.
485. Jiang HH, Pan HQ, Gustilo-Ashby MA, Gill B, Glaab J, Zaszczurynski P, et al. Dual simulated childbirth injuries result in slowed recovery of pudendal nerve and urethral function. *Neurourology and urodynamics*. 2009;28(3):229-35.
486. Hijaz A, Daneshgari F, Cannon T, Damaser M. Efficacy of a vaginal sling procedure in a rat model of stress urinary incontinence. *The Journal of urology*. 2004;172(5 Pt 1):2065-8.
487. Chapple CR, Raz S, Brubaker L, Zimmern PE. Mesh Sling in an Era of Uncertainty: Lessons Learned and the Way Forward. *European urology*. 2013.
488. Zheng F, Xu L, Verbiest L, Verbeken E, De Ridder D, Deprest J. Cytokine production following experimental implantation of xenogenic dermal collagen and polypropylene grafts in mice. *Neurourology and urodynamics*. 2007;26(2):280-9.
489. Badylak SF, Valentin JE, Ravindra AK, McCabe GP, Stewart-Akers AM. Macrophage phenotype as a determinant of biologic scaffold remodeling. *Tissue engineering Part A*. 2008;14(11):1835-42.
490. Thiel M, Rodrigues Palma PC, Riccetto CL, Dambros M, Netto NR, Jr. A stereological analysis of fibrosis and inflammatory reaction induced by four different synthetic slings. *BJU international*. 2005;95(6):833-7.
491. Bazi TM, Hamade RF, Abdallah Hajj Hussein I, Abi Nader K, Jurjus A. Polypropylene midurethral tapes do not have similar biologic and biomechanical performance in the rat. *European urology*. 2007;51(5):1364-73; discussion 73-5.
492. Jenkins ED, Melman L, Deeken CR, Greco SC, Frisella MM, Matthews BD. Biomechanical and histologic evaluation of fenestrated and nonfenestrated biologic mesh in a porcine model of ventral hernia repair. *Journal of the American College of Surgeons*. 2011;212(3):327-39.
493. Yildirim A, Basok EK, Gulpinar T, Gurbuz C, Zemheri E, Tokuc R. Tissue reactions of 5 sling materials and tissue material detachment strength of 4 synthetic mesh materials in a rabbit model. *The Journal of urology*. 2005;174(5):2037-40.
494. Hilger WS, Walter A, Zobitz ME, Leslie KO, Magtibay P, Cornella J. Histological and biomechanical evaluation of implanted graft materials in a rabbit vaginal and abdominal model. *American journal of obstetrics and gynecology*. 2006;195(6):1826-31.
495. Atmaca AF, Serefoglu EC, Eroglu M, Gurdal M, Metin A, Kayigil O. Time-dependent changes in biomechanical properties of four different synthetic materials in a rabbit model and the importance in respect to sling surgery. *Urologia internationalis*. 2008;81(4):456-61.
496. Manodoro S, Endo M, Uvin P, Albersen M, Vlacil J, Engels A, et al. Graft-related complications and biaxial tensiometry following experimental vaginal implantation of flat mesh of variable dimensions. *BJOG : an international journal of obstetrics and gynaecology*. 2013;120(2):244-50.
497. Karlovsky ME, Kushner L, Badlani GH. Synthetic biomaterials for pelvic floor reconstruction. *Current urology reports*. 2005;6(5):376-84.

498. Keys T, Badlani G. The scientific rationale for using biomaterials in stress urinary incontinence and pelvic organ prolapse. *Current urology reports*. 2011;12(6):393-5.
499. Mantovani A, Sica A, Locati M. Macrophage polarization comes of age. *Immunity*. 2005;23(4):344-6.
500. Hung MJ, Wen MC, Huang YT, Chen GD, Chou MM, Yang VC. Fascia tissue engineering with human adipose-derived stem cells in a murine model: Implications for pelvic floor reconstruction. *Journal of the Formosan Medical Association = Taiwan yi zhi*. 2013.
501. Blackwood KA, McKean R, Canton I, Freeman CO, Franklin KL, Cole D, et al. Development of biodegradable electrospun scaffolds for dermal replacement. *Biomaterials*. 2008;29(21):3091-104.
502. Ulrich D, Edwards SL, White JF, Supit T, Ramshaw JA, Lo C, et al. A preclinical evaluation of alternative synthetic biomaterials for fascial defect repair using a rat abdominal hernia model. *PLoS One*. 2012;7(11):e50044.
503. Deprest J, Klosterhalfen B, Schreurs A, Verguts J, De Ridder D, Claerhout F. Clinicopathological study of patients requiring reintervention after sacrocolpopexy with xenogenic acellular collagen grafts. *The Journal of urology*. 2010;183(6):2249-55.
504. Sadek HA, Garry DJ. Letter by Sadek and Garry regarding article, "Iron-oxide labeling and outcome of transplanted mesenchymal stem cells in the infarcted myocardium". *Circulation*. 2008;117(14):e306; author reply e7.
505. Abramowitch SD, Feola A, Jallah Z, Moalli PA. Tissue mechanics, animal models, and pelvic organ prolapse: a review. *European journal of obstetrics, gynecology, and reproductive biology*. 2009;144 Suppl 1:S146-58.
506. Lee TQ, Woo SL. A new method for determining cross-sectional shape and area of soft tissues. *Journal of biomechanical engineering*. 1988;110(2):110-4.
507. Lanir Y, Fung YC. Two-dimensional mechanical properties of rabbit skin. II. Experimental results. *Journal of biomechanics*. 1974;7(2):171-82.
508. Yin FC, Fung YC. Mechanical properties of isolated mammalian ureteral segments. *The American journal of physiology*. 1971;221(5):1484-93.
509. Moon DK, Woo SL, Takakura Y, Gabriel MT, Abramowitch SD. The effects of refreezing on the viscoelastic and tensile properties of ligaments. *Journal of biomechanics*. 2006;39(6):1153-7.
510. Rubod C, Boukerrou M, Brieu M, Dubois P, Cosson M. Biomechanical properties of vaginal tissue. Part 1: new experimental protocol. *The Journal of urology*. 2007;178(1):320-5; discussion 5.
511. Cosson M, Lambaudie E, Boukerrou M, Lobry P, Crepin G, Ego A. A biomechanical study of the strength of vaginal tissues. Results on 16 post-menopausal patients presenting with genital prolapse. *European journal of obstetrics, gynecology, and reproductive biology*. 2004;112(2):201-5.
512. Goh JT. Biomechanical properties of prolapsed vaginal tissue in pre- and postmenopausal women. *International urogynecology journal and pelvic floor dysfunction*. 2002;13(2):76-9; discussion 9.
513. Dora CD, Dimarco DS, Zobitz ME, Elliott DS. Time dependent variations in biomechanical properties of cadaveric fascia, porcine dermis, porcine small intestine submucosa, polypropylene mesh and autologous fascia in the rabbit model: implications for sling surgery. *The Journal of urology*. 2004;171(5):1970-3.
514. Woodruff AJ, Cole EE, Dmochowski RR, Scarpero HM, Beckman EN, Winters JC. Histologic comparison of pubovaginal sling graft materials: a comparative study. *Urology*. 2008;72(1):85-9.

515. Carbone JM, Kavalier E, Hu JC, Raz S. Pubovaginal sling using cadaveric fascia and bone anchors: disappointing early results. *The Journal of urology*. 2001;165(5):1605-11.
516. FitzGerald MP, Mollenhauer J, Brubaker L. The fate of rectus fascia suburethral slings. *American journal of obstetrics and gynecology*. 2000;183(4):964-6.
517. Gandhi S, Kubba LM, Abramov Y, Botros SM, Goldberg RP, Victor TA, et al. Histopathologic changes of porcine dermis xenografts for transvaginal suburethral slings. *American journal of obstetrics and gynecology*. 2005;192(5):1643-8.
518. Argirovic RB, Gudovic AM, Babovic IR, Berisavac MV. Transvaginal repair of genital prolapse with polypropylene mesh using a tension-free technique. *European journal of obstetrics, gynecology, and reproductive biology*. 2010;153(1):104-7.
519. de Tayrac R, Gervaise A, Chauveaud A, Fernandez H. Tension-free polypropylene mesh for vaginal repair of anterior vaginal wall prolapse. *The Journal of reproductive medicine*. 2005;50(2):75-80.
520. Iglesia CB, Sokol AI, Sokol ER, Kudish BI, Gutman RE, Peterson JL, et al. Vaginal mesh for prolapse: a randomized controlled trial. *Obstetrics and gynecology*. 2010;116(2 Pt 1):293-303.
521. Winckler JA, Ramos JG, Dalmolin BM, Winckler DC, Doring M. Comparative study of polypropylene and aponeurotic slings in the treatment of female urinary incontinence. *International braz j urol : official journal of the Brazilian Society of Urology*. 2010;36(3):339-47.
522. Tate SB, Blackwell L, Lorenz DJ, Steptoe MM, Culligan PJ. Randomized trial of fascia lata and polypropylene mesh for abdominal sacrocolpopexy: 5-year follow-up. *International urogynecology journal*. 2011;22(2):137-43.
523. Natale F, La Penna C, Padoa A, Agostini M, De Simone E, Cervigni M. A prospective, randomized, controlled study comparing Gynemesh, a synthetic mesh, and Pelvicol, a biologic graft, in the surgical treatment of recurrent cystocele. *International urogynecology journal and pelvic floor dysfunction*. 2009;20(1):75-81.
524. VandeVord PJ, Broadrick KM, Krishnamurthy B, Singla AK. A comparative study evaluating the in vivo incorporation of biological sling materials. *Urology*. 2010;75(5):1228-33.
525. Chen HY, Ho M, Hung YC, Huang LC. Analysis of risk factors associated with vaginal erosion after synthetic sling procedures for stress urinary incontinence. *International urogynecology journal and pelvic floor dysfunction*. 2008;19(1):117-21.
526. Karageorgiou V, Kaplan D. Porosity of 3D biomaterial scaffolds and osteogenesis. *Biomaterials*. 2005;26(27):5474-91.
527. Wang JHC, Jia F, Gilbert TW, Woo SL. Cell orientation determines the alignment of cell-produced collagenous matrix. *Journal of biomechanics*. 2003;36(1):97-102.
528. Lee CH, Shin HJ, Cho IH, Kang YM, Kim IA, Park KD, et al. Nanofiber alignment and direction of mechanical strain affect the ECM production of human ACL fibroblast. *Biomaterials*. 2005;26(11):1261-70.
529. Witkowski P, Abbonante F, Fedorov I, Sledzinski Z, Pejcić V, Slavin L, et al. Are mesh anchoring sutures necessary in ventral hernioplasty? Multicenter study. *Hernia*. 2007;11(6):501-8.
530. Ogah J, Cody JD, Rogerson L. Minimally invasive synthetic suburethral sling operations for stress urinary incontinence in women. *The Cochrane database of systematic reviews*. 2009(4):CD006375.
531. Woo SL, Debski RE, Withrow JD, Janaushek MA. Biomechanics of knee ligaments. *The American journal of sports medicine*. 1999;27(4):533-43.

532. Bertolo A, Mehr M, Janner-Jametti T, Graumann U, Aebli N, Baur M, et al. An in vitro expansion score for tissue-engineering applications with human bone marrow-derived mesenchymal stem cells. *Journal of tissue engineering and regenerative medicine*. 2013.
533. Bernardo ME, Zaffaroni N, Novara F, Cometa AM, Avanzini MA, Moretta A, et al. Human bone marrow derived mesenchymal stem cells do not undergo transformation after long-term in vitro culture and do not exhibit telomere maintenance mechanisms. *Cancer research*. 2007;67(19):9142-9.
534. Ferrero I, Mazzini L, Rustichelli D, Gunetti M, Mareschi K, Testa L, et al. Bone marrow mesenchymal stem cells from healthy donors and sporadic amyotrophic lateral sclerosis patients. *Cell transplantation*. 2008;17(3):255-66.
535. Tondreau T, Lagneaux L, Dejeneffe M, Delforge A, Massy M, Mortier C, et al. Isolation of BM mesenchymal stem cells by plastic adhesion or negative selection: phenotype, proliferation kinetics and differentiation potential. *Cytotherapy*. 2004;6(4):372-9.
536. Wagner W, Ho AD, Zenke M. Different facets of aging in human mesenchymal stem cells. *Tissue engineering Part B, Reviews*. 2010;16(4):445-53.
537. Kretlow JD, Jin YQ, Liu W, Zhang WJ, Hong TH, Zhou G, et al. Donor age and cell passage affects differentiation potential of murine bone marrow-derived stem cells. *BMC cell biology*. 2008;9:60.
538. Wagner W, Horn P, Castoldi M, Diehlmann A, Bork S, Saffrich R, et al. Replicative senescence of mesenchymal stem cells: a continuous and organized process. *PLoS One*. 2008;3(5):e2213.
539. Xiang Y, Zheng Q, Jia BB, Huang GP, Xu YL, Wang JF, et al. Ex vivo expansion and pluripotential differentiation of cryopreserved human bone marrow mesenchymal stem cells. *Journal of Zhejiang University Science B*. 2007;8(2):136-46.
540. Lee RH, Kim B, Choi I, Kim H, Choi HS, Suh K, et al. Characterization and expression analysis of mesenchymal stem cells from human bone marrow and adipose tissue. *Cellular physiology and biochemistry : international journal of experimental cellular physiology, biochemistry, and pharmacology*. 2004;14(4-6):311-24.
541. Vidal MA, Walker NJ, Napoli E, Borjesson DL. Evaluation of senescence in mesenchymal stem cells isolated from equine bone marrow, adipose tissue, and umbilical cord tissue. *Stem cells and development*. 2012;21(2):273-83.
542. Guercio A, Di Bella S, Casella S, Di Marco P, Russo C, Piccione G. Canine mesenchymal stem cells (MSCs): characterization in relation to donor age and adipose tissue-harvesting site. *Cell biology international*. 2013;37(8):789-98.
543. Otte A, Bucan V, Reimers K, Hass R. Mesenchymal Stem Cells Maintain Long-Term In Vitro Stemness During Explant Culture. *Tissue engineering Part C, Methods*. 2013.
544. Chen HH, Decot V, Ouyang JP, Stoltz JF, Bensoussan D, de Isla NG. In vitro initial expansion of mesenchymal stem cells is influenced by the culture parameters used in the isolation process. *Bio-medical materials and engineering*. 2009;19(4-5):301-9.
545. Zhu H, Miosge N, Schulz J, Schliephake H. Regulation of multilineage gene expression and apoptosis during in vitro expansion of human bone marrow stromal cells with different cell culture media. *Cells, tissues, organs*. 2010;192(4):211-20.
546. Neuhuber B, Swanger SA, Howard L, Mackay A, Fischer I. Effects of plating density and culture time on bone marrow stromal cell characteristics. *Experimental hematology*. 2008;36(9):1176-85.

547. Kuci S, Kuci Z, Kreyenberg H, Deak E, Putsch K, Huenecke S, et al. CD271 antigen defines a subset of multipotent stromal cells with immunosuppressive and lymphohematopoietic engraftment-promoting properties. *Haematologica*. 2010;95(4):651-9.
548. Attar A, Ghalyanchi Langeroudi A, Vassaghi A, Ahrari I, Maharlooee MK, Monabati A. Role of CD271 enrichment in the isolation of mesenchymal stromal cells from umbilical cord blood. *Cell biology international*. 2013;37(9):1010-5.
549. Erdman CP, Dosier CR, Olivares-Navarrete R, Baile C, Guldborg RE, Schwartz Z, et al. Effects of resveratrol on enrichment of adipose-derived stem cells and their differentiation to osteoblasts in two-and three-dimensional cultures. *Journal of tissue engineering and regenerative medicine*. 2012;6 Suppl 3:s34-46.
550. Xiao J, Yang X, Jing W, Guo W, Sun Q, Lin Y, et al. Adipogenic and osteogenic differentiation of Lin(-)CD271(+)Sca-1(+) adipose-derived stem cells. *Molecular and cellular biochemistry*. 2013;377(1-2):107-19.
551. Yang S, Eto H, Kato H, Doi K, Kuno S, Kinoshita K, et al. Comparative Characterization of Stromal Vascular Cells Derived from Three Types of Vascular Wall and Adipose Tissue. *Tissue engineering Part A*. 2013.
552. Crisan M, Yap S, Casteilla L, Chen CW, Corselli M, Park TS, et al. A perivascular origin for mesenchymal stem cells in multiple human organs. *Cell stem cell*. 2008;3(3):301-13.
553. Griesche N, Luttmann W, Luttmann A, Stammermann T, Geiger H, Baer PC. A simple modification of the separation method reduces heterogeneity of adipose-derived stem cells. *Cells, tissues, organs*. 2010;192(2):106-15.
554. Francis MP, Sachs PC, Elmore LW, Holt SE. Isolating adipose-derived mesenchymal stem cells from lipoaspirate blood and saline fraction. *Organogenesis*. 2010;6(1):11-4.
555. Yang XF, He X, He J, Zhang LH, Su XJ, Dong ZY, et al. High efficient isolation and systematic identification of human adipose-derived mesenchymal stem cells. *Journal of biomedical science*. 2011;18:59.
556. Perry S, Shaw C, Assassa P, Dallosso H, Williams K, Brittain KR, et al. An epidemiological study to establish the prevalence of urinary symptoms and felt need in the community: the Leicestershire MRC Incontinence Study. Leicestershire MRC Incontinence Study Team. *Journal of public health medicine*. 2000;22(3):427-34.
557. Abdel-Fattah M, Familusi A, Fielding S, Ford J, Bhattacharya S. Primary and repeat surgical treatment for female pelvic organ prolapse and incontinence in parous women in the UK: a register linkage study. *BMJ open*. 2011;1(2):e000206.
558. Rechberger T, Jankiewicz K, Adamiak A, Miotla P, Chrobak A, Jerzak M. Do preoperative cytokine levels offer a prognostic factor for polypropylene mesh erosion after suburethral sling surgery for stress urinary incontinence? *International urogynecology journal and pelvic floor dysfunction*. 2009;20(1):69-74.
559. Traktuev DO, Merfeld-Clauss S, Li J, Kolonin M, Arap W, Pasqualini R, et al. A population of multipotent CD34-positive adipose stromal cells share pericyte and mesenchymal surface markers, reside in a periendothelial location, and stabilize endothelial networks. *Circulation research*. 2008;102(1):77-85.
560. Bye FJ, Wang L, Bullock AJ, Blackwood KA, Ryan AJ, MacNeil S. Postproduction processing of electrospun fibres for tissue engineering. *Journal of visualized experiments : JoVE*. 2012(66).
561. Brun JL, Bordenave L, Lefebvre F, Bareille R, Barbie C, Rouais F, et al. Physical and biological characteristics of the main biomaterials used in pelvic surgery. *Bio-medical materials and engineering*. 1992;2(4):203-25.

562. Wang JH, Jia F, Gilbert TW, Woo SL. Cell orientation determines the alignment of cell-produced collagenous matrix. *Journal of biomechanics*. 2003;36(1):97-102.
563. Engler AJ, Sen S, Sweeney HL, Discher DE. Matrix elasticity directs stem cell lineage specification. *Cell*. 2006;126(4):677-89.
564. Rowlands AS, George PA, Cooper-White JJ. Directing osteogenic and myogenic differentiation of MSCs: interplay of stiffness and adhesive ligand presentation. *American journal of physiology Cell physiology*. 2008;295(4):C1037-44.
565. Velayudhan S, Martin D, Cooper-White J. Evaluation of dynamic creep properties of surgical mesh prostheses--uniaxial fatigue. *Journal of biomedical materials research Part B, Applied biomaterials*. 2009;91(1):287-96.
566. Committee on Gynecologic P. Vaginal placement of synthetic mesh for pelvic organ prolapse. *Female pelvic medicine & reconstructive surgery*. 2012;18(1):5-9.
567. Zimmern PE. Surgical treatment for stress urinary incontinence in women: novelties, concerns and ethics. *Women's health*. 2012;8(1):31-3.
568. McCoy RJ, O'Brien FJ. Influence of shear stress in perfusion bioreactor cultures for the development of three-dimensional bone tissue constructs: a review. *Tissue engineering Part B, Reviews*. 2010;16(6):587-601.
569. Gilmore L, Rimmer S, McArthur SL, Mittar S, Sun D, MacNeil S. Arginine functionalization of hydrogels for heparin binding--a supramolecular approach to developing a pro-angiogenic biomaterial. *Biotechnology and bioengineering*. 2013;110(1):296-317.
570. James AW, Zara JN, Corselli M, Askarinam A, Zhou AM, Hourfar A, et al. An abundant perivascular source of stem cells for bone tissue engineering. *Stem cells translational medicine*. 2012;1(9):673-84.
571. Roubelakis MG, Tsaknakis G, Pappa KI, Anagnostou NP, Watt SM. Spindle shaped human mesenchymal stem/stromal cells from amniotic fluid promote neovascularization. *PLoS One*. 2013;8(1):e54747.
572. Watt SM, Gullo F, van der Garde M, Markeson D, Camicia R, Khoo CP, et al. The angiogenic properties of mesenchymal stem/stromal cells and their therapeutic potential. *British medical bulletin*. 2013;108:25-53.
573. Zhou B, Tsaknakis G, Coldwell KE, Khoo CP, Roubelakis MG, Chang CH, et al. A novel function for the haemopoietic supportive murine bone marrow MS-5 mesenchymal stromal cell line in promoting human vasculogenesis and angiogenesis. *British journal of haematology*. 2012;157(3):299-311.
574. Falconer C, Soderberg M, Blomgren B, Ulmsten U. Influence of different sling materials on connective tissue metabolism in stress urinary incontinent women. *International urogynecology journal and pelvic floor dysfunction*. 2001;12:S19-S23.
575. Klinge U, Klosterhalfen B, Birkenhauer V, Junge K, Conze J, Schumpelick V. Impact of polymer pore size on the interface scar formation in a rat model. *Journal of Surgical Research*. 2002;103(2):208-14.
576. Boulanger L, Boukerrou M, Lambaudie E, Defossez A, Cosson M. Tissue integration and tolerance to meshes used in gynecologic surgery: An experimental study. *European Journal of Obstetrics Gynecology and Reproductive Biology*. 2006;125(1):103-8.
577. Spelzini F, Konstantinovic ML, Guelinckx I, Verbist G, Verbeken E, De Ridder D, et al. Tensile strength and host response towards silk and type I polypropylene implants used for augmentation of fascial repair in a rat model. *Gynecologic and Obstetric Investigation*. 2007;63(3):155-62.

578. Krause H, Bennett M, Forwood M, Goh J. Biomechanical properties of raw meshes used in pelvic floor reconstruction. *International urogynecology journal*. 2008;19(12):1677-81.
579. Jenkins ED, Melman L, Deeken CR, Greco SC, Frisella MM, Matthews BD. Biomechanical and Histologic Evaluation of Fenestrated and Nonfenestrated Biologic Mesh in a Porcine Model of Ventral Hernia Repair. *Journal of the American College of Surgeons*. 2011;212(3):327-39.
580. Chancellor MB, Yokoyama T, Tirney S, Mattes CE, Ozawa H, Yoshimura N, et al. Preliminary results of myoblast injection into the urethra and bladder wall: a possible method for the treatment of stress urinary incontinence and impaired detrusor contractility. *Neurourology and urodynamics*. 2000;19(3):279-87.
581. Yokoyama T, Huard J, Pruchnic R, Yoshimura N, Qu Z, Cao B, et al. Muscle-derived cell transplantation and differentiation into lower urinary tract smooth muscle. *Urology*. 2001;57(4):826-31.
582. Lee JY, Cannon TW, Pruchnic R, Fraser MO, Huard J, Chancellor MB. The effects of periurethral muscle-derived stem cell injection on leak point pressure in a rat model of stress urinary incontinence. *International urogynecology journal and pelvic floor dysfunction*. 2003;14(1):31-7; discussion 7.
583. Cannon TW, Lee JY, Somogyi G, Pruchnic R, Smith CP, Huard J, et al. Improved sphincter contractility after allogenic muscle-derived progenitor cell injection into the denervated rat urethra. *Urology*. 2003;62(5):958-63.
584. Lee JY, Paik SY, Yuk SH, Lee JH, Ghil SH, Lee SS. Long term effects of muscle-derived stem cells on leak point pressure and closing pressure in rats with transected pudendal nerves. *Molecules and cells*. 2004;18(3):309-13.
585. Chermansky CJ, Tarin T, Kwon DD, Jankowski RJ, Cannon TW, de Groat WC, et al. Intraurethral muscle-derived cell injections increase leak point pressure in a rat model of intrinsic sphincter deficiency. *Urology*. 2004;63(4):780-5.
586. Tamaki T, Uchiyama Y, Okada Y, Ishikawa T, Sato M, Akatsuka A, et al. Functional recovery of damaged skeletal muscle through synchronized vasculogenesis, myogenesis, and neurogenesis by muscle-derived stem cells. *Circulation*. 2005;112(18):2857-66.
587. Kwon D, Minnery B, Kim Y, Kim JH, de Miguel F, Yoshimura N, et al. Neurologic recovery and improved detrusor contractility using muscle-derived cells in rat model of unilateral pelvic nerve transection. *Urology*. 2005;65(6):1249-53.
588. Strasser H, Marksteiner R, Margreiter E, Pinggera GM, Mitterberger M, Frauscher F, et al. Autologous myoblasts and fibroblasts versus collagen for treatment of stress urinary incontinence in women: a randomised controlled trial. *Lancet*. 2007;369(9580):2179-86.
589. Carr LK, Steele D, Steele S, Wagner D, Pruchnic R, Jankowski R, et al. 1-year follow-up of autologous muscle-derived stem cell injection pilot study to treat stress urinary incontinence. *International urogynecology journal and pelvic floor dysfunction*. 2008;19(6):881-3.
590. Nitta M, Tamaki T, Tono K, Okada Y, Masuda M, Akatsuka A, et al. Reconstitution of experimental neurogenic bladder dysfunction using skeletal muscle-derived multipotent stem cells. *Transplantation*. 2010;89(9):1043-9.
591. Jack GS, Almeida FG, Zhang R, Alfonso ZC, Zuk PA, Rodriguez LV. Processed lipoaspirate cells for tissue engineering of the lower urinary tract: implications for the treatment of stress urinary incontinence and bladder reconstruction. *The Journal of urology*. 2005;174(5):2041-5.



592. Fu Q, Song XF, Liao GL, Deng CL, Cui L. Myoblasts differentiated from adipose-derived stem cells to treat stress urinary incontinence. *Urology*. 2010;75(3):718-23.
593. Lin G, Wang G, Banie L, Ning H, Shindel AW, Fandel TM, et al. Treatment of stress urinary incontinence with adipose tissue-derived stem cells. *Cytotherapy*. 2010;12(1):88-95.
594. Yamamoto T, Gotoh M, Hattori R, Toriyama K, Kamei Y, Iwaguro H, et al. Periurethral injection of autologous adipose-derived stem cells for the treatment of stress urinary incontinence in patients undergoing radical prostatectomy: report of two initial cases. *International journal of urology : official journal of the Japanese Urological Association*. 2010;17(1):75-82.

## APPENDIX

**Table 3** Mechanical properties and host response against synthetic materials implanted in animals and humans:

Author	Sample	Mechanical Properties	Host Response
Falconer et al. 2001 (574)	Mersilene - Prolene		Mersilene induce a higher inflammatory response than Prolene. Mersilene is easier to extract than Prolene.
Klinge et al. 2002 (575)	heavy weight monofilament (HWM) and low weight multifilament (LWM) on the posterior abdominal wall		HWM: intense inflammation, embedded in connective tissue. LWM: less pronounced inflammatory response and fibrotic capsule, collagen distributed within the mesh.
Dietz et al. 2003 (274)	Prolene – Mersilene – TVT – IVS tape – SPARC tape – GoreTex Micromesh – GoreTex Soft Tissue Patch	TVT has the lowest initial stiffness.	
Spiess et al. 2004 (271)	Polypropylene TVT Cadaveric fascia lata (CFL)	TVT has the greater break load and the maximum average load compared to CFL.	
Rabah et al. 2004 (277)	Polypropylene mesh		Inflammation localized in the graft.
Wang et al. 2004 (278)	Polypropylene TVT – Polypropylene SPARC		Pronounced fibrosis around the fibres, it might correlate with erosion.
Govier et al. 2004 (276)	Polypropylene mesh vs. Silicone-coated mesh		Polypropylene mesh allows a dense tissue ingrowth
Thiel et al. 2005 (319)	Polypropylene mesh		- Mild inflammatory response. - Mild collagen formation.
Yildirim et al. 2005 (300)	Gynecare TVT – SPARC™ - polypropylene mesh -		Inflammation and fibrosis are decreased in large pores meshes.
Konstantinovic et al. 2005 (313)	Marlex into the anterior abdominal wall		Pronounced inflammatory reaction and vascularization throughout the graft
Krambeck et al. 2006 (304)	Polypropylene mesh		- Great scar formation. - Mild inflammatory response.
Boulanger et al. 2006 (576)	Vicryl – Vypro – Prolene – Prolene Soft - Mersuture		Vicryl: low level of inflammation and completely absorbed. Vypro: intense inflammation and strong fibrotic response. Prolene and Prolene Soft: well integrated, weak inflammatory response. Mersuture: no good integration.
Bogusiewicz et al. 2006	Macroporous TVT – Microporous IVS		- Both induced production of similar amount of

(279)			collagen. - Differences in the arrangement of collagen and inflammation intensity.
Bazi et al. 2007 (280)	Polypropylene IVS – polypropylene SPARC™ - polypropylene TVT	They all show similar mechanical properties after removal.	They induce different host responses due to different porosity.
Zorn et al. 2007 (272)	SPARC – TVT – Stratisis	TVT has tensile properties similar to SPARC and They are superior to Stratisis.	
Spelzini et al. 2007 (577)	Polypropylene type I mesh vs. A macroporous silk construct		Polypropylene meshes induce a moderate inflammatory response and not architectural degradation.
Woodruff et al. 2008 (283)	Polypropylene mesh		- No evidences of degradation or encapsulation, abundant host infiltration. - Neovascularisation was visible.
Krause et al. 2008 (578)	Atrium (x4), Dexon (x4), Gynemesh (x5), IVS (x5), Prolene (x4), SPARC (x5), TVT (x5), Vypro II (x5) and 3 controls.	Mechanical properties are variables across many polypropylene meshes. IVS and Vypro: high level of stress-shielding. Dexon, SPARC, TVT and Vypro III compliant at low loads. Gynemesh, prolene and Atrium have intermediate properties.	Type I meshes (monofilamentous): small tissue fibrosis, minimal giant cells or histiocytes Type III meshes: moderate fibrotic reaction, highest proportion of giant cells.
Huffaker et al. 2008 (282)	Pelvitex (Collagen-coated) and Gynemesh (uncoated Polypropylene meshes)		Both materials induce a mild foreign body reaction with minimal fibrosis.
Alfonso et al. 2008 (275)	Aris – TVTO – Uretex – Avaulta – Auto Suture	Polypropylene filament thickness influence mechanical properties. TVT has the lowest tensile strength.	
Pierce et al. 2009 (285)	Polypropylene mesh	Polypropylene have similar mechanical properties to the native tissues in terms of ultimate tensile strength and Young's modulus.	- Mild inflammatory reaction for long term. - Good host tissue incorporation.
Jones et al. 2009 (273)	Tension Free Gynecare PS®	New generations of polypropylene meshes are less stiff.	
Elmer et al. 2009 (284)	PROLIFT®		- Increase in macrophages and mast cells count. - Mild but persistent foreign body response.
Melman et al. 2011 (270)	Bard® mesh (HWPP) - Ultrapro® (LWPP) - GORE®Infinet mesh (ePTFE)	Their maximum tensile strength decreases over time for all of them.	- Inflammation decreases with time. - Cell infiltration increases with time.

**Table 4** Mechanical properties and host response against autologous grafts implanted in animals and humans:

Author	Sample	Mechanical Properties	Host Response
FitzGerald et al. 2000 (296)	Autologous rectus fascia implanted in 5 patients suffering SUI. Samples obtained, respectively, from transvaginal revision after 3, 5, 8 and 17 weeks, and from replacement after 4 years.		<ul style="list-style-type: none"> <li>- Moderate and uniform infiltration of host fibroblasts and neovascularization after 5 and 8 weeks implantation.</li> <li>- After 4 years implantation, no evidence of inflammatory cell infiltrate or foreign body reaction, and collagen remodelling by connective tissue organized longitudinally.</li> </ul>
Jeong et al. 2000 (294)	Autologous lata fascia implanted in 16 rabbits randomized into 4 survival groups (1, 2, 4 and 8 weeks). Implantation into upper eyelids.		<ul style="list-style-type: none"> <li>- Low inflammatory cells infiltration.</li> <li>- Fibroblast infiltration and collagen remodelling.</li> </ul>
Dora et al. 2004 (292)	Autologous rectus fascia implanted in 15 rabbits randomized into 3 survival groups (2, 6 and 12 weeks). Implantation on the anterior rectus fascia.	No significant decrease of biomechanical properties after 12 weeks implantation.	<ul style="list-style-type: none"> <li>- 50% decrease of surface area.</li> </ul>
Hilger et al. 2006 (293)	Autologous rectus fascia implanted in 20 rabbits randomized into 2 survival groups (6 and 12 weeks). Half implanted on the rectus fascia and half on the posterior vagina fascia.	No significant decrease of biomechanical properties after 12 weeks implantation.	<ul style="list-style-type: none"> <li>- Collagen remodelling by moderate collagen infiltration but encapsulation as well.</li> <li>- Minimal inflammatory response.</li> <li>- Minimal neovascularization.</li> </ul>
Krambeck et al. 2006 (304)	Autologous rectus fascia implanted subcutaneously on the anterior rectus fascia of 10 rabbits randomized into 2 survival groups (6 and 12 weeks).		<ul style="list-style-type: none"> <li>- Moderate fibrosis.</li> <li>- High degree of scar.</li> <li>- High degree of inflammatory infiltrate.</li> </ul>
Woodruff et al. 2008 (283)	Autologous fascia grafts explanted after sling revision from 5 women, due to different complications, between 2-65 months after implantation.		<ul style="list-style-type: none"> <li>- Moderate and uniform infiltration of host fibroblasts and few neovascularization.</li> <li>- Collagen remodelling by new collagen fibres organized longitudinally.</li> <li>- No evidence of encapsulation or gross infection.</li> <li>- Moderate degradation.</li> </ul>
Pinna et al. 2011 (295)	Autologous fascia lata implanted 14 rabbits randomized into 2 survival groups (30 and 60 days). Implantation into the right voice muscle.		<ul style="list-style-type: none"> <li>- No significant inflammatory reaction.</li> <li>- No significant fibrosis or scarring.</li> </ul>

**Table 5** Mechanical properties and host response against allografts implanted in animals and humans:

Author	Sample	Mechanical Properties	Host Response
Sclafani et al. 2000 (299)	Human cadaveric dermis (AlloDerm®) disk implanted subdermally behind a patient's ear. Micronized human cadaveric dermis (AlloDerm®) injected intradermally and subdermally in 2 different locations behind a patient's ear. Both implants examined 3 and 1 month after implantation, respectively.		<ul style="list-style-type: none"> <li>- Both materials extensively invaded by host fibroblasts.</li> <li>- Both materials present new collagen in-growth.</li> </ul>
Walter et al. 2003 (298)	Freeze-dried and gamma-irradiated human cadaveric lata fascia implanted in 18 rabbits and excised 12 weeks after implantation.	Significant decrease of biomechanical properties after 12 weeks implantation.	
Spiess et al. 2004 (271)	Human cadaveric fascia lata implanted subcutaneously on the abdominal wall of 20 rats randomized into 2 survival groups (6 and 12 weeks).	No significant decrease of tensile strength with time.	
Yildirim et al. 2005 (300)	Human cadaveric lata fascia implanted in 20 rabbits randomized into 4 survival groups (2, 7, 15 and 30 days). Implantation subcutaneously on the abdominal wall.		<ul style="list-style-type: none"> <li>- Acute inflammation by high cell infiltration predominantly of polymorphous granulocytes.</li> <li>- Integration in host tissue by moderate fibrotic process and muscle infiltration on day 30, with persistent inflammatory response.</li> </ul>
Krambeck et al. 2006 (304)	Cadaveric fascia lata implanted subcutaneously on the anterior rectus fascia of 10 rabbits randomized into 2 survival groups (6 and 12 weeks).		<ul style="list-style-type: none"> <li>- Moderate to high focal fibrosis.</li> <li>- Minimal to moderate degree of scar.</li> <li>- High degree of inflammatory infiltrate.</li> </ul>
Hilger et al. 2006 (293)	Human cadaveric dermis and lata fascia implanted in 20 rabbits randomized into 2 survival groups (6 and 12 weeks). Half implanted on the rectus fascia and half on the posterior vagina fascia.	Very significant decrease of biomechanical properties after 12 weeks implantation.	<ul style="list-style-type: none"> <li>- 2 missing or fragmented materials implanted on the vagina after 12 weeks.</li> <li>- Moderate inflammatory response.</li> <li>- Minimal neovascularization.</li> <li>- Minimal collagen ingrowth without significant cell infiltration.</li> </ul>
Richtes et al. 2008 (301)	Human cadaveric dermis subcutaneously implanted in 16 rats randomized into 4 groups (materials descellularized with NaOH after 4 different periods). All animals sacrificed after 4 weeks.		<ul style="list-style-type: none"> <li>- No degradation and good integration with the surrounding tissues.</li> <li>- Higher inflammatory response for samples descellularized for shorter periods, and associated to more vessels formation.</li> <li>- Fibrovascular in-growth</li> </ul>

			with better collagen organization for same samples.
Woodruff et al. 2008 (283)	Human cadaveric dermis slings explanted after revision from 2 women, due to different complications, between 2-65 months after implantation.		<ul style="list-style-type: none"> <li>- Moderate levels of encapsulation.</li> <li>- High levels of degradation.</li> <li>- Peripheries of the grafts invaded by fibroblasts but central portions remained acellular.</li> </ul>
VandeVord et al. 2010 (305)	Human cadaveric dermis and fascia lata implanted in 16 rats, respectively, and both randomized into 4 survival groups (2, 4, 8, 12 weeks). Implantation around the bladder neck, anchored to the surrounding tissues.		<ul style="list-style-type: none"> <li>- Thin fibrous capsule formation.</li> <li>- Moderate cell infiltration and angiogenesis.</li> </ul>
Rice et al. 2010 (302)	Human cadaveric dermis (AlloDerm®) implanted in 18 rats randomized into 2 survival groups (30 and 60 days). Implantation subcutaneously on abdominis rectus muscle defect.	Increase of tensile strength after 30 days and, again, increase of tensile strength after 60 days respectively to 30 days.	<ul style="list-style-type: none"> <li>- Moderate amounts of collagen deposition well organized.</li> <li>- Abundant revascularization.</li> </ul>
Kolb et al. 2012 (303)	Human cadaveric dermis (AlloDerm®) implanted subcutaneously in 5 pigs randomized into 4 survival groups (7, 21, 90 and 180 days).		<ul style="list-style-type: none"> <li>- Robust inflammatory response after 7 days implantation, which achieved maximal level at 21 days, with formation of granulomas and areas of necrosis noted within the graft.</li> <li>- Moderate fibroblast infiltration, collagen in-growth and neovascularisation.</li> <li>- Moderate levels of encapsulation.</li> </ul>

**Table 6** Mechanical properties and host response against xenografts implanted in animals and humans:

Author	Sample	Mechanical Properties	Host Response
Badylak et al. 2001 (318)	Abdominal wall defect repaired with SIS in 40 dogs randomized into 8 survival groups (1, 4, 7, and 10 days; and 1, 3, 6, and 24 months).	Strength was decreased from day 1 to day 10 after implantation, followed by a progressive increase, until double of the original strength 24 months after implantation.	- Rapid degradation with associated and subsequent host remodelling.
Zhang et al. 2002 (312)	Abdominal wall defect repaired with SIS in 52 rats randomized into 4 survival groups (3 days, 2 weeks, 1 and 2 months).	No significant changes of biomechanical properties from 2 weeks to 1 month after implantation.	- Moderately organized collagenous connective tissue. - Mild lymphocyte infiltration and fibroblast proliferation. - Inflammatory response decreased after 1 month and connective tissue becomes more organized and incorporate into the native surrounding tissues.
Badylak et al. 2002 (311)	Abdominal wall defect repaired with SIS in 10 dogs and 30 rats, both, randomized into 4 survival groups (1 week, 1 month, 3 months, 6 months, and 2 years).		- No shrinkage or expansion of the graft site over the 2-year period of the study. - 1 week after implantation, abundant levels of polymorphonuclear leukocytes diminished to negligible after 1 month. - Moderate neovascularization. - By 3 months, graft material was not recognizable and was replaced by moderately well organized host tissues including collagenous connective tissue, adipose tissue, and skeletal muscle.
Cole et al. 2003 (322)	SIS removed from a 42-years-old female patient 4 months after puvovaginal implantation of the sling due to severe obstruction.		- Completely intact acellular sling. - Well define fibrous capsule. - Chronic inflammatory response.
Wiedemann et al. 2004 (323)	Biopsies taken from the implantation site of the SIS band under the vaginal mucosa from 3 patients during reoperation, at a mean of 12.7 months, after pubourethral sling procedures due to recurrent urinary stress incontinence.		- Focal residues of SIS implant. - No evidence of a specific tissue reaction that might point to a foreign body reaction. - No evidence of any significant immunological reaction and in particular no evidence of any chronic inflammatory reaction.
Konstantinovic	Abdominal wall defect	Significant increase of	- Moderate acute

et al. 2005 (313)	repaired with SIS in 24 Wistar rats randomized into 4 survival groups (7, 14, 30 and 90 days).	biomechanical properties after 90 days implantation.	inflammatory response at day 7, decreased to minimal after 90 days. - Moderate neovascularization. - Abundant collagen deposition well organized after 90 days.
Macleod et al. 2005 (308)	SIS and porcine dermis (Permacol®) implanted subcutaneously on the anterior rectus fascia of 18 rats each randomized into 5 survival groups (1, 2, 4, 10, and 20 weeks).		For both grafts: - Absent acute inflammatory response. - From moderate chronic inflammation after 1 week implantation to minimal after 20 weeks. - Absent eosinophilic infiltration and stromal fibroblastic reaction over the entire implantation. - From moderate fibrosis and vascularity around the grafts after 1 week implantation to minimal after 20 weeks.
Puolose et al. 2005 (314)	Perforated vs. nonperforated SIS implanted on the peritoneal surface of the abdominal wall of 12 pigs randomized into 2 survival groups (2 and 8 weeks).		- Both type of SIS contracted 50% from their original surface area. - Sever and moderate collagen deposition and neovascularization, respectively, which was slightly higher for perforated SIS.
Thiel et al. 2005 (319)	SIS implanted subcutaneously on the abdominal wall of 30 rats randomized into 3 survival groups (7, 30 and 90 days).		- Moderate inflammatory reaction increased to severe after 90 days. - 86% of the graft replaced by new collagen fibres.
Krambeck et al. 2006 (304)	SIS and porcine dermis implanted subcutaneously on the anterior rectus fascia of 10 rabbits randomized into 2 survival groups (6 and 12 weeks).		- Procine dermis presented moderate fibrosis which was minimal for SIS. - Minimal degree of scar for both grafts and high degree of inflammatory infiltrate.
Ko et al. 2006 (315)	Abdominal wall defect repaired with 8-layer SIS in 20 domestic pigs randomized into 2 survival groups (1 and 4 months).	No significant changes of biomechanical properties after 4 months implantation.	- Dense fibrous connective tissue ingrowth. - Minimal to mild mononuclear inflammatory cell infiltrate throughout the connective tissue.
Hilger et al. 2006 (293)	Porcine dermis implanted in 20 rabbits randomized into 2 survival groups (6 and 12 weeks). Half implanted on the rectus fascia and half on the posterior vagina fascia.	Very significant decrease of biomechanical properties after 12 weeks implantation.	- 2 missing or fragmented materials 12 weeks after being implanted on the vagina. - Moderate to strong inflammatory response. - Minimal collagen ingrowth without



			significant cell infiltration. - Minimal neovascularization.
Rauth et al. 2007 (316)	SIS implanted on the peritoneal surface of the abdominal wall of 6 pigs sacrificed 8 weeks after implantation.		- 80% of contraction from original surface area. - Moderate neovascularization. - Densely populated by host cells with moderate amounts of new disorganized collagen deposition.
Woodruff et al. 2008 (283)	Porcine dermis slings explanted after revision from 4 women, due to different complications, between 2-65 months after implantation.		- Severe encapsulation. - None degradation. - None fibroblasts infiltration and neovascularization.
Sandor et al. 2008 (310)	Abdominal wall defect repaired with SIS and porcine dermis (Permacol®) in 33 primates randomized into 3 survival groups (1, 3 and 6 months).	No changes of healing strength from 1 to 6 months. High variation for SIS samples after 6 months implantation indicating scarring.	- Considerable contraction after 1 month for both materials, but not significant change over the next 5 months. - Better integration of both materials at late stage by scar formation. - Inflammatory cells infiltration 3 months after implantation for SIS and associated to formation of few blood vessels. - Acellular porcine dermis over the entire course implantation with substantial inflammation surrounding their perimeter. - Partial resorption for both materials after 6 months.
Price et al. 2009 (285)	Cross-linked porcine dermis implanted on the abdominal wall and posterior vagina of 18 rabbits sacrificed 9 months after implantation.	11 grafts remained intact without significant changes of biomechanical properties compared to the baseline values. They just were thicker and tolerated less elongation at failure. 7 grafts were partially degraded but thicker again and with significant decrease of all biomechanical properties.	- Host connective tissue incorporation between fibres. - Intense foreign body reaction in degraded grafts which may be expedited in vaginal environment.
Price et al. 2009 (309)	Cross-linked porcine dermis implanted on the abdominal wall and posterior vagina of 22 rabbits sacrificed 9 months after implantation.		- Samples from vagina presented moderate inflammation, mild neovascularization and minimal fibroblast proliferation. - Samples from abdomen presented mild inflammation, minimal neovascularization and mild

			<p>fibroblast proliferation.</p> <ul style="list-style-type: none"> <li>- 37% of abdominal implants partly degraded or missing, and 70% of the vaginal implants. While few grafts were encapsulated without host cell infiltration, degraded grafts were replaced by host collagen.</li> </ul>
VandeVord et al. 2010 (305)	<p>SIS and porcine dermis implanted in 16 rats, respectively, and both randomized into 4 survival groups (2, 4, 8, 12 weeks). Implantation around the bladder neck, anchored to the surrounding tissues.</p>		<ul style="list-style-type: none"> <li>- Thin fibrous capsule formation.</li> <li>- Moderate cell infiltration and angiogenesis for SIS and minimal for porcine dermis.</li> </ul>
Rice et al. 2010 (302)	<p>Abdominal wall defect repair with SIS (Surgisis®) in 18 rats randomized into 2 survival groups (30 and 60 days).</p>	<p>Increase of tensile strength after 30 days and, again, increase of tensile strength after 60 days respectively to 30 days.</p>	<ul style="list-style-type: none"> <li>- Moderate amounts of collagen deposition well organized.</li> <li>- Abundant revascularization.</li> </ul>
Deprest et al. 2010 (324)	<p>13 patients underwent secondary sacrocolpopexy because of failure or vaginal revision because of a graft related complication after the initial sacrocolpopexy with porcine dermal collagen (Pelvicol®) (9) or SIS (Surgisis®) (4).</p>		<ul style="list-style-type: none"> <li>- Pelvicol presented high degradation rates associated with no body foreign reaction.</li> <li>- Pelvicol remnants were integrated into collagen rich connective tissue with limited neovascularization (scar host tissue).</li> <li>- No significant body foreign reaction to Surgisis grafts.</li> <li>- Surgisis no longer recognizable replaced by irregularly organized connective tissue and fat tissue.</li> </ul>
Liu et al. 2011 (317)	<p>Abdominal wall defect repaired with SIS and acellular porcine dermal matrix in 50 Sprague Dawley rats randomized into 5 survival groups (1, 2, 4, 8 and 12 weeks).</p>	<p>After initial decrease of biomechanical properties at week 2, these were increased over the next 10 weeks reaching similar values from week 1.</p>	<ul style="list-style-type: none"> <li>- Pronounced inflammatory response 1 to 4 weeks after implantation for SIS compared with porcine dermal, but fell to similar negligible values for both after 12 weeks.</li> <li>- Large neovascularization and collagen deposition, which was higher for SIS group.</li> <li>- SIS implants degraded more quickly and were almost totally replaced by organized collagenous tissues.</li> <li>- Contraction at first weeks leading to significant lower</li> </ul>

			surface area in both materials.
Jenkins et al. 2011 (579)	Abdominal wall defect repaired with porcine dermal matrix in 24 Yucatan minipigs randomized into 2 survival groups (1 and 6 months).	Significantly greater incorporation strengths after 6 months compared with 1 month.	<ul style="list-style-type: none"> <li>- Moderate cell infiltration.</li> <li>- Moderate extracellular matrix deposition.</li> <li>- Moderate neovascularisation.</li> <li>- Partial degradation and from widely to mild fibrous encapsulation.</li> </ul>
Suckow et al. 2012 (320)	Abdominal wall defect repaired with SIS in 12 rats sacrificed 1 month after implantation.		<ul style="list-style-type: none"> <li>- Small amount of residual SIS remained were surrounded by mild to moderate chronic inflammation.</li> </ul>
Kolb et al. 2012 (303)	Cross-linked porcine dermis (Permacol®) implanted subcutaneously in 5 pigs randomized into 4 survival groups (7, 21, 90 and 180 days).		<ul style="list-style-type: none"> <li>- Mild inflammatory response decreased to minimal from day 7 to day 180 after implantation.</li> <li>- None to minimal neovascularization after 180 days.</li> <li>- Moderate levels of encapsulation.</li> </ul>

**Table 7** Engineered tissues for pelvic floor repair:

Author	Engineered construct	Model	Implantation	Improvements
De Filippo et al. 2003 (334)	Vaginal epithelial and smooth muscle cells seeded on polyglycolic acid scaffolds	Nude mice	Implanted subcutaneously	Multilayered tissue strips of both cell types and penetrating native vasculature after 1 week. Increased organization of the smooth muscle and epithelial tissue by 4 weeks. Contractile properties of the tissue-engineered vaginal constructs similar to those of normal vaginal tissue
Cannon et al. 2005 (338)	MDSC seeded on small intestinal submucosa (SIS)	Rats with bilateral proximal sciatic nerve transaction	Implanted suburethrally and sutured to the pubic bone	Improved leak point pressure, but not significant differences were showed with only the SIS sling implantation
Atala et al. 2006 (326)	Autologous urothelial and muscle cells seeded and cultured in composites of collagen or polyglycolic acid scaffolds	Seven patients with myelomeningocele (aged 4-19 years)	Constructs implanted as cystoplasty for bladder reconstruction	46 months post-operatively, the mean bladder leak point pressure decreased at capacity, and the volume and compliance increased. Recovery of bowel function
Bhargava et al. 2008 (384)	Autologous buccal keratinocytes and fibroblasts seeded and cultured in acellular donor de-epidermised dermis	5 patients with urethral stricture secondary to lichen sclerosis	Uretroplasty	After 3 years follow-up, one patient had complete excision of the grafted urethra and one required partial graft excision, for fibrosis and hyperproliferation of tissue, respectively. Three patients have a patent urethra with the engineered tissue <i>in situ</i> .
Drewa et al. 2008 (329)	Rat hair follicle stem cell seeded onto bladder acellular matrices cultured for one week	Rats with surgically created defect within the anterior bladder wall	Cell-seeded group and matrices group were implanted on the defect of the anterior bladder wall	Two animals died in the acellular group, the other develop stone disease. Muscle layer regeneration was better in the cell-seeded group
Jack et al. 2009 (327)	Human-ADSCs cultured in 85:15 poly-lactic-glycolic acid scaffolds and under smooth muscle inductive medium	Nude rats underwent removal of half their bladders	Bladder repair by augmentation with the ADSCs engineered construct, with acellular composite or by suture closure	After 12 weeks, only the engineered construct group maintained bladder capacity and compliance, and increased smooth muscle mass and its contraction
Ho et al. 2009 (335)	MDSCs cultured in small intestinal submucosa	Rats with hysterectomy and partial vaginectomy	Vaginal implantation	Stimulated vaginal tissue repair, including keratin-5 positive epithelium formation and prevented

	(acellular matrix)			fibrosis at 4 and 8 weeks
Hung et al 2010 (336)	Human vaginal fibroblasts cultured in biodegradable poly-DL-lactic-glycolic acid mesh coated with collagen	Nude mice	Subcutaneous implantation	A well-organized neofascia formation was traced up to 12 weeks, without rejection or inflammatory reaction
Zou et al. 2010 (339)	Bone marrow derived mesenchymal stem cell seeded degradable silk scaffold	Sprague-Dawley rats with bilateral proximal sciatic nerve transaction leading to confirmed SUI	Implanted via trans-abdominal and sutured to abdominal wall	Same leak point pressure improvement compare with sling implantation without cells. However, sling plus cells showed higher collagen production and ultimate tensile strength, as ligament-like tissue formation was determined, suggesting long-term retention

**Table 8** Injection of MDSCs for the treatment of SUI:

Author	Cell type	Model	Implantation	Improvements
Chancellor et al. 2000 (580)	Labelled myoblasts	Mice	Injected periurethrally and into the bladder wall	After 3-4 days formation of myotubes and myofibres in the smooth muscle layers of the urethra and bladder wall
Yokoyama et al. 2001 (581)	Labelled MDSCs	Mice	Injected into the bladder wall	After 5, 35, and 70, long term survival and differentiation into myofibres
Lee et al. 2003 (582)	MDSCs	Rats with sciatic nerve transected	Periurethral injection	Increased leak point pressure after 4 weeks
Cannon et al. 2003 (583)	MDSCs	6-week-old Sprague-Dawley rats sciatic nerve transected	Periurethral injection	Muscular urethral contraction restored after 2 weeks
Lee et al. 2004 (584)	MDSC and bovine Collagen	Rats with denervation of the pudendal nerve	Periurethral injection	Increased leak point pressure and closing pressure after 4 and 12 weeks
Chermansky et al. 2004 (585)	MDSCs	Sprague-Dawley rats by cauterizing tissues lateral to the mid-urethra	Intraurethral injection	After 2, 4 and 6 weeks increased leak point pressure and number of nerves in the striated muscle
Tamaki et al. 2005 (586)	MDSCs	Severe-damage model of mouse tibialis anterior muscle	Injection in the tibialis anterior muscle	Myogenesis, neurogenesis and vasculogenesis in striated muscle
Kwon et al. 2005 (587)	MDSCs, fibroblasts and mixture of both	Rat with unilateral pelvic nerve transection	Injection in the sphincteric urethral unit	No differences between cell types; only fibroblast improved leak point pressure because obstruction
Mitterberger et al. 2007 (413)	Autologous myoblasts and fibroblasts	123 women with SUI	Fibroblast plus small amount of collagen implanted into the urethral submucosa and myoblasts injected into the rhabdosphincter	After 1 year 79% completely continent and improvement of the thickness and contractibility of the rhabdosphincter
Strasser et al. 2007 (588)	Autologous myoblasts, fibroblasts and collagen	63 women with SUI	Injection into the rhabdosphincter and the urethra	Improvement of the rhabdosphincter thickness and contractibility after 1 year
Carr et al. 2008 (589)	Autologous MDSCs	8 women with SUI	Periurethral injection	Continent recover in 5 women after 10 months
Nitta et al. 2010 (590)	MDSCs	Nude rat with damage on the bladder branch of the pelvic plexus	Injection into the bladder branch of the pelvic plexus	Differentiation into Schwann cells, perineural cells, vascular smooth muscle cells, pericytes and fibroblasts

**Table 9** Injection of ADSCs for the treatment of SUI:

Author	Cell type	Model	Implantation site	Improvements
Jack et al. 2005 (591)	ADSCs from human lipoaspirate	Immuno-competent incontinent rat model of SUI	Cells injected into the bladder and the urethra labelled with fluorescent marker	After 12 weeks, cells were positively analyzed for smooth muscle morphology and alpha-actin phenotype
Fu et al. 2010 (592)	Endogenous rat ADSCs	Vaginal balloon dilatation method in female Sprague-Dawley rats inducing SUI	Cells injected into the posterior urethral muscularis in the bladder neck after myoblastic differentiation with 5-azacitidine	After 3 months leak point pressure and bladder capacity increased, such as increased number of myoblasts with $\alpha$ -smooth muscle actin expression under the mucosa
Lin et al. 2010 (593)	Rat ADSCs isolated from the peri-ovary fat	Rats induced to develop SUI by postpartum vaginal balloon dilation and bilateral ovariectomy	Urethral injection of the cells labelled with thymidine analogue BrdU or EdU	Normal-voiding with significantly higher smooth muscle content
Almeida et al. 2010 (414)	Rabbit ADSCs isolated from inguinal fat pad	New Zealand adult female rabbits	Cells labelled with DiI marker and injected into the urethra wall	After 2 weeks, cells formed a dense nodule in the submucosa, but after 4 weeks, cells dispersed uniformly in the whole extension of the urethra wall
Yamamoto et al. 2010 (594)	Human ADSCs from abdomen liposuction	2 women with moderate SUI after radical prostatectomy	Cells were transurethrally injected into the rhabdosphincter and submucosa of the urethra	During 12 weeks follow-up were positively tested for 24-h pad test, a validated patient questionnaire, urethral pressure profile, transrectal ultrasonography, and magnetic resonance imaging

